

Investigating the treatment optimisation of a pilot-scale Anaerobic Sequencing Batch Reactor (AnSBR) and partial characterisation of the winery wastewater using Near-infrared (NIR) spectroscopy

by

Richard Frederick Edwards



*Thesis presented in partial fulfilment of the requirements for the degree of
Master of Science (Food Science)
in the Faculty of AgriSciences
at
Stellenbosch University*

Supervisor: Prof Gunnar O Sigge

March 2020

Declaration

By submitting this thesis electronically, I declare that the entirety of the work contained therein is my own, original work, that I am the sole author thereof (save to the extent explicitly otherwise stated), that reproduction and publication thereof by Stellenbosch University will not infringe any third party rights and that I have not previously in its entirety or in part submitted it for obtaining any qualification.

Date: March 2020

Abstract

Water is arguably the most vital natural resource on Earth. It is of critical importance to humans, plants, animals, environments as well as ecosystems. Agriculture is estimated to be responsible for the abstraction of approximately 66 – 70 % of the freshwater supply globally, with that number rising to 90 % in some countries. The wine industry in South Africa is responsible for producing large amounts of wastewater with 1.24 billion litres of wastewater generated in 2018. Winery wastewater is challenging to treat due to variable strength and seasonal compositional variation. Biological treatments are very effective for the removal of organic pollutants in winery wastewater. Anaerobic digestion is an example of a biological treatment that has been widely used for the treatment of winery wastewater. Anaerobic sequencing batch reactor (AnSBR) is a viable option for the treatment of winery wastewater. The technology is still under development and has not been used extensively in the wine industry. The advantages of the AnSBR include ease of changing operational parameters, can operate in batch or fed-batch mode; it efficiently removes chemical oxygen demand (COD) and generates biogas with a high methane percentage, that can potentially be reclaimed as a source of heat generation. Knowledge of the optimal conditions for pH, mixing intervals and feeding time of the AnSBR is limited and needs to be investigated. Two important parameters for the overall stability and performance of an AnSBR are COD and total suspended solids (TSS) concentrations. Determination of these parameters are however time-consuming and laborious. Near-infrared (NIR) spectroscopy is a rapid, non-destructive technique which makes use of the wavelength range of 780 – 2 500 nm. The first aim of this study was to investigate potential for the use of NIR to quantify and classify winery wastewater based on the COD and TSS concentration.

Near-infrared spectroscopy was used in combination with multivariate data analysis (MDA) for the classification and quantification of COD and TSS in winery wastewater. Spectra were acquired using a benchtop FT-NIR (Büchi NIR-Flex N500) spectrophotometer with a wavelength range of 1 000 – 2 500 nm and a portable spectrophotometer with a wavelength range of 900 – 1 700 nm.

The concentration of COD could be predicted with a RMSEP value of 893 mg.L⁻¹, an error of 9.9 % compared to the range of the reference values, using PCR along with orthogonal signal correction (OSC). This was achieved using the wavelength range 2 060 – 2 340 nm on the benchtop instrument. The PCR model performed to a satisfactory degree to be used as a screening method to rapidly determine COD concentration of winery wastewater. The concentration of TSS could be predicted with a RMSEP of 136.94 mg.L⁻¹, an error of 5.72 %, using the benchtop instrument. The prediction model for TSS achieved a prediction performance that was almost comparable to the reference method, meaning it is suitable for screening purposes at the very least. Classification accuracies of 90.4 % (COD) & 100 % (TSS), 80.1 % (COD) & 95 % (TSS) could be achieved with the benchtop and handheld instruments respectively. Both the benchtop and the handheld instruments could classify winery wastewater based on their COD or TSS concentrations to a satisfactory degree. The above classification accuracies for the handheld instrument indicates that classification of winery

wastewater, into low or high strength categories, may be possible for in-line monitoring of winery wastewater and screening via class, instead of quantification.

The second aim of this study was to evaluate whether the AnSBR technology could successfully treat winery wastewater of varying quality and determine the optimal operational parameters for the reactor

A pilot-scale AnSBR with a volume of 165 L was operated for 16 cycles treating winery wastewater. The cycle length was 24 h and the hydraulic retention time (HRT) was approximately 1.85 days. The reactor was initially seeded with 22 kg anaerobic granules. A central composite design (CCD) was performed to determine the optimal operational parameters. A mean COD reduction of 68.32 % (mean influent 5 852 mg.L⁻¹) was achieved along with a mean polyphenol reduction of 53.35 % (mean influent 215 mg.L⁻¹)(SAWIS, 2018) and a stable VFA:Alkalinity of 0.23 on average. The AnSBR technology could therefore feasibly be used to treat winery wastewater. The pH, feeding time and mixing interval were selected to determine the optimal operational parameters. The optimal values achieved were determined to be: pH 7.30; feed time 180.91 minutes and a mixing interval of 84.17 minutes. This study confirmed the optimal operational parameters previously obtained for treatment of synthetic winery wastewater with an AnSBR.

Uittreksel

Water is waarskynlik die belangrikste natuurlike hulpbron op aarde. Dit is van kardinale belang vir mense, plante, diere, die omgewing sowel as ekosisteme. Landbou sal na raming verantwoordelik wees vir die onttrekking van ongeveer 66 – 70 % van die varswatertoevoer wêreldwyd, en styg tot 90 % in sommige lande. Die wynbedryf in Suid-Afrika is verantwoordelik vir die vervaardiging van groot hoeveelhede afvalwater, met 1,24 miljard liter afvalwater wat in 2018 gegenereer was. Die afvalwater van die wynmakery is uitdagend om te behandel weens die wisselvallige sterkte en seisoenale samestelling. Biologiese behandelings is baie effektief vir die verwydering van organiese besoedelende stowwe in wynkelderafvalwater. Anaërobiese vertering is 'n voorbeeld van 'n biologiese behandeling wat wyd gebruik word vir die behandeling van afvalwater van die wynmakery. Anaërobiese Opeenvolgende Lot Reaktor (AOLR) is 'n lewensvatbare opsie vir die behandeling van wynkelderafvalwater. Die tegnologie is nog in die ontwikkelings-fase en word nog nie breedvoerig in die wynbedryf gebruik nie. Die voordele van die AOLR sluit in: die gemak om bedryfsparameters moeiteloos te verander, dit kan in 'n lot proses of semi-lot proses werk; dit verwyder chemiese suurstof vereiste (CSV) doeltreffend en genereer biogas met 'n hoë metaanpersentasie, wat moontlik as 'n bron van hitte-generasie herwin kan word. Kennis van die optimale toestande vir pH, meng-intervalle en voedingstyd van die AOLR is beperk en moet ondersoek word. Twee belangrike parameters vir die algehele stabiliteit en werkverrigting van 'n AOLR is, CSV en totale gesuspendeerde vastestowwe (TGV). Die bepaling van hierdie parameters is egter tydrowend en moeisam. Naby-infrarooi (NIR) spektroskopie is 'n vinnige, nie-vernietigende tegniek wat gebruik maak van die golflengte reeks van 780 - 2 500 nm. Die eerste doel van hierdie studie was om die potensiaal vir die gebruik van NIR om wynafvalwater te kwantifiseer en te klassifiseer op grond van die CSV- en TGV-konsentrasie te ondersoek.

Naby-infrarooi (NIR) spektroskopie is gebruik in kombinasie met meerveranderlike data analise (MDA) tegnieke vir die klassifikasie en kwantifisering van CSV en TGV in wynkelderafvalwater. Spektre is verkry met behulp van 'n tafemodel FT-NIR (Büchi NIR-Flex N500) spektrofotometer met 'n golflengte reeks van 1 000 - 2 500 nm en 'n draagbare spektrofotometer met 'n golflengte reeks van 900 - 1 700 nm.

Die CSV-konsentrasie kon voorspel word met 'n RMSEP-waarde van 893 mg.L⁻¹, 'n fout van 9,9 % in vergelyking met die reeks verwysingswaardes, met behulp van PCR saam met ortogonale seinkorreksie (OSK). Dit is bereik met behulp van die 2 060 - 2 340 nm golflengte reeks op die tafemodel instrument. Die PCR-model is bevredigend uitgevoer, om as 'n siftingsmetode gebruik te word, om die CSV-konsentrasie van die wynkelderafvalwater vinnig te bepaal. Die konsentrasie van TGV kon voorspel word met 'n RMSEP van 136,94 mg.L⁻¹, 'n fout van 5,72 %, met behulp van die tafemodel instrument. Die voorspellingsmodel vir TGV het 'n voorspellingsprestasie behaal wat amper vergelykbaar was met die verwysingsmetode, wat beteken dat dit ten minste geskik is vir siftingsdoeleindes. Klassifikasie akkuraatheid van 90.4 % (CSV) en 100 % (TGV), 80.1 % (CSV) en 95 % (TGV) kon onderskeidelik met die tafemodel en die draagbare instrument verkry word.

Beide die tafelmodel en die draagbare instrument kon die wynkelderafvalwater volgens hul CSV- of TGV-konsentrasies in 'n bevredigende wyse klassifiseer. Die bogenoemde klassifikasie-akkuraatheid vir die draagbare instrument dui aan dat die klassifikasie van wynkelderafvalwater, in lae of hoë sterkte kategorieë, moontlik is vir in-lyn monitering en sifting van wynkelderafvalwater in plaas van kwantifisering.

Die tweede doel van hierdie studie was om te evalueer of die AOLR-tegnologie suksesvol wynkelderafvalwater van verskillende gehalte kan behandel en die optimale bedryfsparameters vir die reaktor bepaal.

'n Kleinskaal AOLR met 'n volume van 165 L het vir 16 siklusse gehardloop om die wynkelderafvalwater te behandel. Die sikluslengte was 24 uur en die hidrouliese retensietyd (HRT) was ongeveer 1,85 dae. Die reaktor is aanvanklik met 22 kg anaërobiese korrels gesaai. 'n Sentrale saamgestelde ontwerp (SSO) is uitgevoer om die optimale bedryfsparameters te bepaal. 'n Gemiddelde CSV-vermindering van 68,32 % is behaal, tesame met 'n gemiddelde polifenolvermindering van 53,35 % en 'n stabiele VFA: alkaliniteit van gemiddeld 0.23. Die AOLR-tegnologie kan dus gebruik word vir die behandeling van wynkelderafvalwater. Die pH, voedingstyd en meng-interval is gekies om die optimale bedryfsparameters te bepaal. Daar is bepaal dat die volgende optimale waardes bereik is: pH 7,30; voer-tyd 180,91 minute en 'n meng-interval van 84,17 minute. Hierdie studie het die optimale bedryfsparameters wat voorheen verkry is vir die behandeling van sintetiese wynkelderafvalwater met 'n AOLR bevestig.

Acknowledgements

I would like to acknowledge the following people and institutions for their contribution towards the completion of this study

I would like to thank my supervisor, Prof Gunnar Sigge for giving me the opportunity to pursue postgraduate studies and for the guidance and support throughout the project.

The Department of Process Engineering for helping design and construct the reactor.

The staff and students at the Department of Food Science for all the help no matter how trivial it may have seemed. For all the lunch time discussions in the tea room and the generally friendly environment within the Department.

WineTech for funding this project and for giving me the opportunity to pursue postgraduate studies.

Dr Stefan Hayward for all the help throughout the project, from design ideas, to helping move the reactor and setting up the GC. Thank you for all the help and encouragement

Sebastian Orth for staying late at night when I needed to scan samples in the lab until 2am and for coming with to countless trips to AgriMark for supplies.

A very special thanks to John-Pieter Botha for wiring the PLC and assistance with the set-up on of the reactor on the farm.

Thank you to my parents, Richard, Lieze and my sister Robynne for the continued support throughout. Without their support and encouragement, I would not have been able to complete my studies.

To all of my friends who I may not have mentioned personally, thank you to everyone for being there throughout this journey.

Lastly, I would like to thank my amazing wife Kiah Edwards. Thank you for always being there to help me throughout, from going to buy components for the reactor to helping compile my thesis late at night. Thank you for being there and encouraging me to try just one more time when it felt like nothing was working. Your love and support has been felt throughout and I am forever grateful for having you in my life. I could not have done it without you

Table of Contents

| | |
|--|------|
| Declaration | i |
| Abstract | ii |
| Uittreksel | iv |
| Acknowledgements | vi |
| List of Figures | xiii |
| List of Tables | xvii |
| List of Abbreviations | xix |
| Chapter 1 Introduction | 1 |
| 1.1 References | 5 |
| Chapter 2 Literature Review | 9 |
| 2.1 Introduction | 9 |
| 2.2 Wine industry and winemaking process | 10 |
| 2.2.1 History and statistics | 10 |
| 2.2.2 Winemaking procedure | 11 |
| 2.2.2.1 White wine | 11 |
| 2.2.2.2 Red wine | 11 |
| 2.3 Winery wastewater composition | 14 |
| 2.4 Regulations | 15 |
| 2.5 Current treatment options | 17 |
| 2.5.1 Physical methods | 18 |
| 2.5.2 Physiochemical methods | 18 |
| 2.5.2.1 Iron exchange | 18 |
| 2.5.2.2 Reverse Osmosis | 18 |
| 2.5.2.3 Coagulation & flocculation | 18 |
| 2.5.2.4 Membrane filtration | 19 |
| 2.5.3 Biological treatments | 19 |
| 2.5.3.1 Aerobic processes | 19 |
| | vii |

| | |
|---|----|
| 2.5.3.1.1 Aerobic treatment of winery wastewater: application | 20 |
| 2.5.3.2 Anaerobic processes..... | 23 |
| 2.5.3.2.1 Detailed anaerobic process | 23 |
| 2.5.3.2.2 Anaerobic general..... | 25 |
| 2.5.3.2.3 Applications of anaerobic processes | 26 |
| 2.6 Anaerobic sequencing batch reactor..... | 29 |
| 2.6.1 Feed | 29 |
| 2.6.2 React..... | 29 |
| 2.6.3 Settle..... | 29 |
| 2.6.4 Decant..... | 30 |
| 2.7 Operational conditions that effect performance of the AnSBR | 32 |
| 2.7.1 Temperature..... | 32 |
| 2.7.2 pH and alkalinity | 33 |
| 2.7.3 Volatile fatty acids (VFA's) | 34 |
| 2.7.4 Nutrients..... | 35 |
| 2.7.5 Organic loading rate (OLR)..... | 35 |
| 2.7.6 Mixing regime | 36 |
| 2.7.7 Inhibition and toxicity..... | 38 |
| 2.7.8 HRT..... | 40 |
| 2.8 Chemical quantification methods..... | 41 |
| 2.9 Near-infrared (NIR) spectroscopy..... | 42 |
| 2.10 NIR in literature | 44 |
| 2.11 Conclusion | 47 |
| 2.12 References..... | 48 |
| Chapter 3 Determination of Chemical Oxygen Demand (COD) and Total Suspended Solids (TSS) Using Near-Infrared (NIR) Spectroscopy | 58 |
| Abstract | 58 |
| 3.1 Introduction..... | 58 |

| | |
|---|----|
| 3.2 Materials and methods..... | 60 |
| 3.2.1 Samples..... | 60 |
| 3.2.2 Analytical methods | 60 |
| 3.2.3 NIR instrumentation | 60 |
| 3.2.4 Spectral acquisition..... | 61 |
| 3.2.4.1 Benchtop instrument..... | 61 |
| 3.2.4.2 Handheld instrument..... | 61 |
| 3.2.5 Spectral analysis | 61 |
| 3.2.6 Pre-processing | 62 |
| 3.2.7 Exploratory data analysis (EDA)..... | 62 |
| 3.2.8 Multivariate data analysis..... | 63 |
| 3.2.8.1 Model development | 63 |
| 3.2.8.2 Partial least squares regression (PLSR)..... | 63 |
| 3.2.8.3 Principal component regression (PCR) | 63 |
| 3.2.8.3 Discriminant analysis (DA) | 64 |
| 3.2.9 Performance measures..... | 64 |
| 3.3 Results and discussion | 65 |
| 3.3.1 COD quantification and classification (benchtop) | 65 |
| 3.3.1.1 Spectral analysis | 65 |
| 3.3.1.2 Exploratory data analysis..... | 67 |
| 3.3.1.2.1 Principal component analysis..... | 67 |
| 3.3.1.2.2 Wavelength selection | 70 |
| 3.3.1.3 Multivariate data analysis: Model development (benchtop)..... | 75 |
| 3.3.1.3.1 Principal component regression (PCR) | 75 |
| 3.3.1.3.2 Wavelength selection performance | 77 |
| 3.3.1.3.3 Partial least squares regression (PLS-R)..... | 78 |
| 3.3.1.3.4 Wavelength selection performance | 80 |
| 3.3.1.3.5 Discriminant analysis (DA) | 80 |

| | |
|---|-----|
| 3.3.2 COD quantification and classification (handheld) | 82 |
| 3.3.2.1 Spectral analysis | 82 |
| 3.3.2.2 Exploratory data analysis..... | 84 |
| 3.3.2.2.1 Principal component analysis..... | 84 |
| 3.3.2.3 Multivariate data analysis: Model development (handheld)..... | 86 |
| 3.3.2.3.1 Principal component regression..... | 86 |
| 3.3.2.3.2 Partial least squares regression..... | 88 |
| 3.3.2.3.3 Discriminant analysis | 89 |
| 3.3.3 TSS quantification and classification (benchtop)..... | 92 |
| 3.3.3.1 Spectral analysis | 92 |
| 3.3.3.2 Exploratory data analysis..... | 92 |
| 3.3.3.2.1 Principal component analysis..... | 92 |
| 3.3.3.2.2 Wavelength selection | 94 |
| 3.3.3.3 Multivariate data analysis: Model development (benchtop)..... | 97 |
| 3.3.3.3.1 Principal component regression..... | 97 |
| 3.3.3.3.2 Partial least squares regression..... | 99 |
| 3.3.3.3.3 Wavelength selection performance PCR and PLS-R | 100 |
| 3.3.3.3.4 Discriminant analysis | 101 |
| 3.3.4 TSS quantification and classification (handheld)..... | 103 |
| 3.3.4.1 Spectral analysis | 103 |
| 3.3.4.2 Exploratory data analysis..... | 104 |
| 3.3.4.2.1 Principal component analysis..... | 104 |
| 3.3.4.3 Multivariate data analysis: Model development (handheld)..... | 106 |
| 3.3.4.3.1 Principal component regression..... | 106 |
| 3.3.4.3.2 Partial least squares regression..... | 107 |
| 3.3.4.3.3 Discriminant analysis | 108 |
| 3.4 Conclusion | 110 |
| 3.5 References | 111 |

| | |
|---|-----|
| Chapter 4 Investigating the Performance and Optimisation of pH, Feeding Time and Mixing Intervals of an Anaerobic Sequencing Batch Reactor (AnSBR) for the Treatment of Winery Wastewater | 117 |
| Abstract | 117 |
| 4.1 Introduction | 117 |
| 4.2 Materials and methods..... | 118 |
| 4.2.1 Experimental phases..... | 118 |
| 4.2.2 AnSBR design | 118 |
| 4.2.3 Reactor start-up and operation | 121 |
| 4.2.4 Operational time of the reactor | 122 |
| 4.2.5 Experimental design | 123 |
| 4.2.6 Analytical methods | 125 |
| 4.2.7 Data analysis | 126 |
| 4.3 Results and discussion | 126 |
| 4.3.1 Phase 1..... | 126 |
| 4.3.2 Phase 2..... | 127 |
| 4.3.2.1 COD reduction percentage | 127 |
| 4.3.2.2 Optimisation of control parameters (COD reduction %)..... | 129 |
| 4.3.2.3 Ultimate COD reduction | 132 |
| 4.3.2.4 Optimisation of control parameters (ultimate COD)..... | 134 |
| 4.3.2.5 TSS content..... | 137 |
| 4.3.2.6 Optimisation of control parameters for TSS content | 138 |
| 4.3.2.7 Polyphenol reduction percentage | 141 |
| 4.3.2.8 Optimisation of control parameters for polyphenol reduction percentage | 142 |
| 4.3.2.9 VFA: Alkalinity..... | 144 |
| 4.3.2.10 Methane percentage | 148 |
| 4.3.2.10 Overall optimal conditions | 152 |
| 4.4 Conclusion | 153 |
| 4.5 References | 154 |

| | |
|---|-----|
| Chapter 5 General Discussion and Conclusion | 158 |
| 5.1 Concluding remarks | 162 |
| 5.2 References | 163 |

This thesis is presented in the format prescribed by the Department of Food Science at Stellenbosch University. The language, style and referencing format used are in accordance with the requirements of *the International Journal of Food Science and Technology*. This thesis represents a compilation of manuscripts where each chapter and sub-chapters are individual entities and some repetition between chapters has, therefore, been unavoidable.

List of Figures

| | |
|--|----|
| Figure 2.1 Flow Diagram of Winemaking process. Adapted from (Arvanitoyannis et al., 2006; Devesa-Rey et al., 2011; Ene et al., 2013) | 13 |
| Figure 2.2 Representation of aerobic process. Adapted from (Chetty & Pillay, 2015). | 20 |
| Figure 2.3 Anaerobic Process. Adapted from (Zhang et al., 2014; Show & Lee, 2016). | 24 |
| Figure 2.4 Representation of anaerobic process. Adapted from (Chetty & Pillay, 2015). | 26 |
| Figure 2.5 Illustration of the AnSBR process. | 30 |
| Figure 2.6 Different modes of spectral acquisition; (a) transmittance, (b) transreflectance, (c) diffuse reflectance, (d) interactance, (e) transmittance through scattering media. | 43 |
| Figure 3.1 Diagram illustrating spectral acquisition of samples for the benchtop instrument. One sample was divided into 10 subsamples with each subsample being scanned 5 times. In total 50 spectra obtained per farm per day. | 62 |
| Figure 3. 2 Unprocessed spectra of COD divided into three categories; In (Blue), Warning (Red) and Out (Green)..... | 66 |
| Figure 3. 3 PCA (OSC corrected) analysis of spectral data for three COD categories; In (Blue), Warning (Red) and Out (Green). Separation 100% explained in PC 1..... | 67 |
| Figure 3. 4 PCA loadings line plot for PC1 (100% explained) with interpretable bands at 1 380 -1 500 nm, 1 930 nm and 2 250 - 2 290 nm..... | 68 |
| Figure 3. 5 Correlation loadings plot for PC1 on OSC corrected data showing all wavelengths (1 000 – 2 500 nm) important for separation. | 69 |
| Figure 3. 6 Correlation loadings plot for PC1 on MSC and OSC corrected data illustrating important wavelengths..... | 69 |
| Figure 3. 7 PCA (MSC and Savitzky-Golay second derivative) scores plot (PC1 (94%) vs PC2 (5%)) for COD categories; In (Blue), Warning (Red) and Out (Green). | 70 |
| Figure 3. 8 Correlation loadings plot (PC 1) of data pre-processed with MSC and SGD2 showing prominent wavebands at 1 389 – 1 544 nm (Green), 1 800 -2 000 nm (Orange) and 2 060 – 2 340 nm (Purple). | 71 |
| Figure 3. 9 PLS-R of the data (MSC + SGD2) showing the predicted vs reference values for COD using all wavelengths..... | 73 |
| Figure 3. 10 PLS-R of the data (MSC + SGD2) showing the predicted vs reference values for COD using the wavelengths 2 060 – 2 340 nm..... | 74 |
| Figure 3. 11 PCA scores plot of SNV and detrended data using PCR. Overlap of classes in the centre of the scores plot leads to poor prediction of COD concentration..... | 75 |
| Figure 3. 12 Scores plots of OSC corrected data in PCR showing distinct separation explained by PC 1 for the 3 COD classes..... | 77 |

| | |
|---|-----|
| Figure 3. 13 Unprocessed spectra in wavelength range 908 – 1 651 nm in three categories; In (Blue), Warning (Red) and Out (Green). | 83 |
| Figure 3. 14 PCA of raw spectra (PC1 vs PC2) for the three categories of COD concentration; In (Blue), Warning (Red) and Out (Green). | 84 |
| Figure 3. 15 PCA of OSC processed spectra (PC 1 vs PC 2) for the three COD categories; In (Blue), Warning (red) and Out (Green). | 85 |
| Figure 3. 16 Loadings line plot indicating 3 wavelengths that may explain separation of COD classes at 1 120, 1 162 and 1 378 nm. | 85 |
| Figure 3. 17 Correlation loadings for PC1 to determine important wavelengths in the range 908 – 1 651 nm. All wavelengths were deemed important to explain the separation..... | 86 |
| Figure 3. 18 PCA scores plot for COD concentration on spectra pre-processed with SNV, detrending and SGD2. | 88 |
| Figure 3. 19 Raw spectra for TSS data divided into two categories; Low (Blue) and High (Red). | 92 |
| Figure 3. 20 PCA (OSC corrected) analysis of spectral data for two TSS categories; Low (Blue) and High (Red). Separation 100 % explained in PC1. | 93 |
| Figure 3. 21 Loadings line plot for PC2 (61 % Y-Variance explained) with four wavebands of importance at 1 388 - 1 410, 1 881, 1 904 and 2 200 – 2 400 nm. | 94 |
| Figure 3. 22 Correlation loadings on MSC and SGD2 pre-processed data showing prominent wavebands at 1 378, 1 407, 1 780, 1 839, 1 882, 1 904, 2 045 and 2 394 nm..... | 95 |
| Figure 3. 23 Partial least squares regression on OSC corrected data for prediction of TSS using all wavelengths. RMSECV (Red) of 202.93 mg.L ⁻¹ | 96 |
| Figure 3. 23 Partial least squares regression on OSC corrected data for prediction of TSS using all wavelengths. RMSECV (Red) of 202.93 mg.L ⁻¹ | 96 |
| Figure 3. 24 Partial least squares regression on OSC corrected data for prediction of TSS using reduced wavelengths (1 900 – 2 500 nm). RMSECV (Red) of 216.20 mg.L ⁻¹ | 96 |
| Figure 3. 25 Raw spectra of winery wastewater for the wavelength range 908 – 1 651 nm showing the two categories of TSS: Low (Blue) and High (Red). | 104 |
| Figure 3. 26 PCA scores plot (PC1 vs PC2) for unprocessed data indicating some separation between the two classes; Low (Blue) and High (Red). | 104 |
| Figure 3. 27 PCA scores plot (PC1 vs PC2) for data processed with OSC for the two categories of TSS; Low (Blue) and High (Red). | 105 |
| Figure 3. 28 Loadings line plot of OSC data with perturbations at 1 310 nm and 1 378 nm. | 105 |
| Figure 4.1 Conical base of the AnSBR made from stainless steel. The cone has a diameter of 400 mm and a volume of roughly 16 L. | 119 |
| Figure 4.2 Diagram of the layout of the filter nozzles and the PVC plate. | 120 |

| | |
|--|-----|
| Figure 4. 3 Diagram of the AnSBR. Water flowed from 90 L tank into reactor, into the overflow tank and recirculated in the reactor..... | 121 |
| Figure 4.4 Pareto chart of COD reduction percentage..... | 128 |
| Figure 4.5 Contour plot showing COD reduction percentages for the interaction of pH and feed time..... | 130 |
| Figure 4. 6 Contour plot showing COD reduction percentages for the interaction of pH and mixing frequency. | 131 |
| Figure 4.7 Contour plot showing COD reduction percentage for the parameters of feed time and mixing intervals. | 132 |
| Figure 4.8 Pareto chart for the ultimate COD reduction value. | 133 |
| Figure 4.9 Contour plot showing COD ultimate for the parameter's pH and feed time..... | 135 |
| Figure 4.10 Contour plot showing the optimal parameters for pH and mixing regime to reduce ultimate COD. | 135 |
| Figure 4.11 Contour plot showing the effect of feed time and mixing interval to reduce ultimate COD..... | 136 |
| Figure 4.12 Pareto chart for the effluent TSS content of the winery wastewater..... | 137 |
| Figure 4. 13 Contour plot showing optimal parameters for pH and mixing time to reduce TSS in the effluent. | 139 |
| Figure 4.14 Contour plot showing optimal parameters for pH and mixing intervals related to TSS content of the effluent..... | 139 |
| Figure 4. 15 Contour plot showing optimal parameters for feed time and mixing intervals related to TSS content of the effluent. | 140 |
| Figure 4. 16 Contour plot showing optimal parameters for feed time and mixing intervals related to TSS content of the effluent. | 141 |
| Figure 4. 17 Contour plot showing the optimal parameters of pH and feed time for the removal of polyphenol reduction percentage. | 142 |
| Figure 4. 18 Contour plot showing optimal conditions for pH and mixing interval for removal of polyphenols from winery wastewater. | 143 |
| Figure 4. 19 Contour plot showing optimal conditions for feed time and mixing interval for the removal of polyphenols from winery wastewater..... | 144 |
| Figure 4.20 Pareto chart for the factors influencing VFA:Alkalinity..... | 145 |
| Figure 4.21 Contour plot showing optimal conditions for pH and feed time for VFA:Alkalinity. | 146 |
| Figure 4. 22 Contour plot showing optimal conditions for pH and mixing interval for VFA:Alkalinity. | 147 |
| Figure 4. 23 Contour plot showing optimal conditions for feed time and mixing interval for VFA:Alkalinity.. | 147 |
| Figure 4. 24 Pareto chart for the factors influencing methane percentage. | 149 |

Figure 4. 25 Contour plot showing optimal conditions for pH and feed time for methane percentage.....150

Figure 4. 26 Contour plot showing optimal conditions for pH and mixing interval for methane percentage.
.....151

Figure 4. 27 Contour plot showing optimal conditions for feed time and mixing interval for methane
percentage.....151

List of Tables

| | |
|---|----|
| Table 2.1 Winemaking steps and wastewater generation sources. Adapted from (Woodard, 2001; Vlyssides et al., 2005)..... | 14 |
| Table 2.2 Average composition of winery wastewater..... | 15 |
| Table 2.3 Potential effects of untreated winery wastewater to the environment. Adapted from EPA, (Rengasamy & Marchuk, 2011; Ene et al., 2013; Hirzel et al., 2017). | 16 |
| Table 2.4 South African guidelines for irrigation water up to 2000 m ³ .d ⁻¹ | 17 |
| Table 2.5 South African guidelines for irrigation water of 50 and 200 cubic metres of water per day..... | 17 |
| Table 2.6 Advantages and disadvantages of the various aerobic treatments. | 22 |
| Table 2.7 Comparison of aerobic and anaerobic processes..... | 27 |
| Table 2.8 Advantages and disadvantages of the various anaerobic treatments. | 28 |
| Table 2.9 Differences between the anaerobic sequencing batch reactor and the upflow anaerobic sludge blanket..... | 32 |
| Table 2.10 Optimal temperature range of micro-organisms. | 33 |
| Table 3.1 Principal component regression calibration, cross validation and prediction results of COD concentration for four different pre-processing combinations. 76 | 76 |
| Table 3.2 Principal component regression results for COD concentration prediction using OSC for wavelengths 2 060 – 2 340 nm..... | 78 |
| Table 3.3 Partial least squares regression results for calibration, cross validation and prediction of COD for four different pre-processing combinations. | 78 |
| Table 3.4 Partial least squares regression results for COD concentration prediction using OSC for wavelengths 2 060 – 2 340 nm..... | 80 |
| Table 3.5 DA model results to assess the performance of the different pre-processing along with optimal method (LDA, QDA or Mahalanobis) for COD discrimination. | 81 |
| Table 3.6 Performance measures used to assess the LDA model (5 PCs) with OSC as pre-processing for the classification of COD into three classes..... | 82 |
| Table 3.7 Principal component regression results for calibration, cross-validation and prediction of COD concentration for two different pre-processing combinations..... | 87 |
| Table 3.8 Partial least squares regression results for calibration, cross-validation and prediction for two different pre-processing approaches | 89 |
| Table 3.9 DA model results to assess the performance of the different pre-processing along with optimal method (LDA, QDA or Mahalanobis) for COD discrimination. | 91 |
| Table 3.10 Performance measures used to assess the LDA and QDA models using OSC as pre-processing for the classification of COD into three classes..... | 91 |

| | |
|---|-----|
| Table 3. 11 Principal component regression results for calibration, cross-validation and prediction for four different pre-processing approaches to predict TSS in winery wastewater. | 97 |
| Table 3. 12 Partial least squares regression results for calibration, cross-validation and prediction for four different pre-processing approaches to predict TSS in winery wastewater. | 100 |
| Table 3. 13 Partial least squares regression and principal component regression results for calibration, cross-validation and prediction for OSC pre-processed data to predict TSS in winery wastewater using wavelengths 1 900 – 2 500 nm. | 101 |
| Table 3. 14 DA model results to assess the performance of the different pre-processing along with optimal method (LDA, QDA or Mahalanobis) for TSS discrimination. | 102 |
| Table 3. 15 Performance measures used to assess the LDA model (5 PCs) for the classification of TSS into two classes. | 103 |
| Table 3. 16 Principal component regression results for calibration, cross-validation and prediction of TSS concentration for two different pre-processing combinations. | 107 |
| Table 3. 17 Partial least squares regression results for calibration, cross-validation and prediction for MSC and SGD2 OSC pre-processed data to predict TSS in winery wastewater. | 108 |
| Table 3. 18 Performance measures used to assess LDA models for the classification of TSS into two classes. | 109 |
| Table 3. 19 DA model results to assess the performance of the different pre-processing along with optimal method (LDA, QDA or Mahalanobis) for TSS discrimination. | 109 |
| Table 4. 1 Concentrations of trace elements in the trace element solution fed to the AnSBR. | 122 |
| Table 4. 2 Values for the central composite design for each parameter; pH, Feed time and mixing interval. | 124 |
| Table 4. 3 Calculated values for pH, feed time and mixing intervals used for each run in the central composite design. | 125 |
| Table 4. 4 Optimal operating parameters with regards to COD reduction percentage. | 132 |
| Table 4. 5 Optimal operating parameters with regards to ultimate COD reduction. | 137 |
| Table 4. 6 Optimal operating parameters with regards to TSS of the effluent. | 140 |
| Table 4.7 Optimal operating parameters with regards to polyphenol removal percentage. | 144 |
| Table 4.8 Optimal operating parameters with regards to VFA:Alkalinity. | 148 |
| Table 4.9 Optimal operating parameters with regards to methane percentage. | 152 |
| Table 4. 10 Overall optimal values achieved for all the performance parameters evaluated during the experiment. | 152 |
| Table 4. 11 Optimal values achieved for the three parameters to yield the best results for all performance measure. | 152 |

List of Abbreviations

| | |
|---------|---|
| AD | anaerobic digestion |
| AnSBR | anaerobic sequencing batch reactor |
| BOD | biological oxygen demand |
| C:N | carbon to nitrogen ratio |
| CCD | central composite design |
| COD | chemical oxygen demand |
| COD:N:P | chemical oxygen demand to nitrogen to phosphorous ratio |
| CV | cross-validation |
| DA | discriminant analysis |
| DET | detrend |
| EC | electrical conductivity |
| F:C | feed length to cycle length ratio |
| F:M | substrate to biomass ratio |
| FN | false negative |
| FP | false positive |
| FT | Fourier Transform |
| FT-NIR | Fourier Transform Near-Infrared |
| GC | gas chromatography |
| HDPE | high density polyethylene |
| HRT | hydraulic retention time |
| InGaAs | Indium Gallium Arsenide |
| KOH | potassium hydroxide |
| kW | kilowatt |
| LDA | linear discriminant analysis |
| LED | light emitting diodes |
| LLDPE | linear low density polyethylene |
| LVs | latent variables |
| MDA | multivariate data analysis |
| MF | microfiltration |
| MSC | multiplicative scattering correction |
| MWPLS | moving window partial least squares |
| NF | nanofiltration |
| NIR | near-infrared |
| NTU | nephelometric turbidity unit |

| | |
|----------------|--|
| OLR | organic loading rate |
| OSC | orthogonal signal correction |
| PC | principal component |
| PCA | principal component analysis |
| PCR | principal component regression |
| PCs | principal components |
| PLC | programmable logic controller |
| PLS | partial least squares |
| PLSR | partial least squares regression |
| PP | polyphenols |
| PVC | polyvinyl chloride |
| QDA | quadratic discriminant analysis |
| R ² | coefficient of determination |
| RER | range error ratio |
| RMSECV | root mean square error of cross-validation |
| RMSEP | root mean square error of prediction |
| RSM | response surface methodology |
| SAR | sodium absorption ratio |
| SEL | standard error of laboratory |
| SEP | standard error of prediction |
| SG | Savitzky-Golay |
| SGD2 | Savitzky-Golay second derivative |
| SNV | standard normal variate |
| SS | suspended solids |
| TN | true negative |
| TOC | total organic carbon |
| TP | true positive |
| TSS | total suspended solids |
| UASB | upflow anaerobic sludge blanket |
| UF | ultrafiltration |
| VFA | volatile fatty acids |
| VSS | volatile suspended solids |
| WW | winery wastewater |

Chapter 1

Introduction

Water is arguably the most important natural resource on Earth. It is of vital importance, not only to humans, but to plants, animals, environments and ecosystems (Sivakumar, 2011). Approximately 2.5 % of all the water on Earth is estimated to be freshwater with a further 68.7 % of this water being inaccessible as it is locked in permanent snow cover and glaciers (Carpenter *et al.*, 2011). Current water systems will be affected by an increase in population, climate change, increased industrialisation in cities and transboundary river basins (Sivakumar, 2011; Cooley *et al.*, 2014; Besbes *et al.*, 2019; du Plessis, 2019; McNabb, 2019). Global population is estimated to grow to 8.5 billion by 2030 and this will increase to approximately 9.7 billion by 2050 (Jury & Vaux, 2007; McNabb, 2019). To maintain current per capita food supply, production of food will have to increase by approximately 50 % (Jury & Vaux, 2007). Depending on factors such as actual population growth and income and without improvement in land and water productivity, crop water consumption must increase by 70 – 90 % to meet the demand for food in 2050 (De Fraiture & Wichelns, 2010).

Agriculture is estimated to be responsible for approximately 66 - 70 % of the freshwater abstraction globally, with some countries using up to 90 % of their freshwater resources (UNESCO, 2017; Barbera & Gurnari, 2018). In South Africa water abstraction for agricultural usage is 62.5 % which is lower than the global average, yet still a significant amount of water (FAO, 2016). Industrial water usage accounts for 10.5 % of the freshwater withdrawals in South Africa (FAO, 2016). Industrial wastewater however has a higher strength and therefore has a higher potential for pollution of freshwater (Moharikar *et al.*, 2005).

South Africa is currently the 9th largest producer of wine in the world (OIV, 2019). The South African wine industry is an important revenue generator for farmers with producers' income totalling R6.298 billion (SAWIS, 2018). This is therefore a vital industry for economic growth and job creation. The large scale of the wine industry places strain on the water resources, due to usage of large volumes of freshwater and generation of large volumes of high strength wastewater (Van Schoor, 2005; Mosse *et al.*, 2011).

The wine industry is responsible for the usage of copious amounts of freshwater during the wine-making process. Water usage among Australian wineries found the average water usage to be 2.67 L of freshwater per 1 L of wine produced, with large variation in water usage (1.2 – 14.4 L) in other countries (Kumar *et al.*, 2009; Quinteiro *et al.*, 2014; Angel, 2018; Martins *et al.*, 2018). South African wineries use approximately 2m³ of water per tonne of grapes crushed, resulting in usage of 2.48 billion litres of water for the 2018 harvest season (Howell & Myburgh, 2018; SAWIS, 2018). Winery wastewater generation is estimated to be 50 % of the total water usage in South African wineries, resulting in 1.24 billion litres of wastewater generated per annum (Howell & Myburgh, 2018; SAWIS, 2018). The wastewater is challenging

to treat due to seasonal and compositional variation as well as its high strength in terms of chemical oxygen demand (COD) (Da Ros *et al.*, 2014; Bories & Sire, 2016).

Reported characteristics of winery wastewater include: COD concentration of 800 – 27 200 mg.L⁻¹; pH between 4.0 and 7.1; total suspended solids (TSS) 200 – 1 200 mg.L⁻¹ and volatile suspended solids (VSS) of 130 – 420 mg.L⁻¹ (Petruccioli *et al.*, 2000; Eusebio *et al.*, 2004; Vlyssides *et al.*, 2005; Bories & Sire, 2016). Due to the high strength nature of the wastewater, it must adhere to strict regulations before it can be discharged or utilised for irrigation purposes (RSA, 2013). To comply with these regulations it is often necessary to treat the wastewater using physical, chemical or biological treatments prior to disposal or irrigation (Welz *et al.*, 2016). Re-use of treated industrial wastewater for irrigation could reduce freshwater withdrawals for the agricultural sector (Meneses *et al.*, 2010; Pedrero *et al.*, 2010).

Biological treatments are very effective for the removal of organic compounds in winery wastewater; however the variability of the wastewater presents a potential hindrance to its effectiveness (Mosse *et al.*, 2011). Biological treatments can be divided into aerobic and anaerobic treatment options (Mohana *et al.*, 2009; Ioannou *et al.*, 2015). Anaerobic processes have been shown to have various advantages over aerobic processes. Anaerobic processes have simple designs and the operation is simple (Eleutheria *et al.*, 2016). The operational parameters are not extreme and run at a temperature of 35°C, a pH of 6.8 – 7.2 and are not subjected to extreme pressures (Gerardi, 2003; Eleutheria *et al.*, 2016). There is a low sludge production volume associated with anaerobic processes with only 5 -10 % sludge produced (Andreottola *et al.*, 2009). Anaerobic digestion results in the production of biogas, of which methane is a big contributor, which can be used to generate heat or power for use at the facility (Show & Lee, 2016). Disadvantages of anaerobic processes include long start-up times and increased initial production cost (Parawira, 2004; Show & Lee, 2016).

Anaerobic digestion has been widely used for the treatment of winery wastewater with upflow anaerobic sludge blanket (UASB) and covered aerobic lagoons being utilised often (Keyser *et al.*, 2003; Moletta, 2005; Andreottola *et al.*, 2009). Chemical oxygen demand reduction percentages achieved with these technologies range from 65 – 98 % (Keyser *et al.*, 2003; Moletta, 2005; Andreottola *et al.*, 2009). Anaerobic sequencing batch reactor (AnSBR) is another type of anaerobic reactor that could be utilised to treat winery wastewater. The AnSBR operates on a fill and draw basis and the process can be divided into four steps: feeding; reacting; settling and decanting (Sung & Dague, 1995; Khanal *et al.*, 2017). There are several advantages of the AnSBR technology which include: ease of changing operational parameters such as feeding rate or mixing intervals and can therefore treat a variable range of wastewater quality (Myra *et al.*, 2015); there is no need for an external clarifier as this happens inside the reactor vessel (Al-Rekabi *et al.*, 2007; Gurtekin, 2014); the technology efficiently removes COD and produces biogas with a high methane percentage (Shao *et al.*, 2008; Myra *et al.*, 2015). Anaerobic sequencing batch reactor technology has been used successfully for the treatment of a variety of wastewaters such as: olive mill-; domestic sewage- and brewery-wastewater. There is however limited research performed to evaluate the efficacy of the AnSBR

technology for the treatment of winery wastewater. Research is limited to lab-scale reactors with volumes rarely exceeding 14.7 L. Knowledge of optimal conditions for mixing intervals, feeding strategy and operational pH of the AnSBR is limited and needs to be explored further for the treatment of winery wastewater.

Two important conditions for the overall stability and performance of an AnSBR are COD and TSS concentrations. A high level of these in wastewater may lead to reactor overload, which could lead to failure of the reactor as functional microorganisms may perish. Determination of COD and TSS in influent winery wastewater is therefore very important to avoid reactor failure. The determination of COD and TSS can be a time-consuming task and both methods take approximately 120 – 180 minutes (APHA, 2005). Chemical oxygen demand is generally determined using test kits and involves the chemical reaction with potassium dichromate (Pan *et al.*, 2011). It also requires a digestion step of 120 minutes followed by a cooling step of 30 minutes before COD can be determined (APHA, 2005). Determination of total suspended solids involves filtering and consequent drying of a sample in an oven which may take up to two hours to complete (APHA, 2005). It is therefore important to develop a method that can quantify the COD and TSS concentrations rapidly for screening purposes.

Near-infrared (NIR) spectroscopy is a rapid, non-destructive and accurate technique which makes use of the wavelength range 780 – 2 500 nm and is sometimes referred to as the overtone region (Pasquini, 2003; Ozaki *et al.*, 2006). It is called this as the absorption of polymers originates from the first overtones of N-H, S-H, C-H and O-H bending and stretching vibrations (Ozaki *et al.*, 2006; Huang *et al.*, 2008). This makes NIR spectroscopy useful in the biological and organic fields to reveal information about the samples (Ozaki *et al.*, 2006). The spectral bands obtained in the NIR region are broad with lots of overlap which may make it difficult to determine specific chemical compounds (Workman Jr, 1993). Furthermore, the spectra obtained may be influenced by other chemical or physical variables (Ozaki *et al.*, 2006; Siesler *et al.*, 2008). It is therefore necessary to incorporate multivariate data analysis techniques to extract the necessary information (Pasquini, 2003). Techniques used for quantification include partial least squares regression (PLS-R) (Wold *et al.*, 1983) and principal component regression (PCR) (Massy, 1965). Principal component analysis can be used as an exploratory technique for cluster analysis and linear-, quadratic- and mahalanobis-discriminant analysis is commonly used as classification techniques (Fisher, 1936).

Quantification studies using NIR for the determination of COD and TSS of wastewaters from various sources have been performed. Quantification of COD has been successfully predicted in domestic sewage with prediction error of cross-validated samples under 10 % of the reference range (Yang *et al.*, 2009). This has been achieved without pre-treatment of the water and involved no digestion step. Determination of COD has been successfully predicted for sucrose containing solutions as well as solutions containing bovine-serum albumin (BSA) (Innocent *et al.*, 2007). Ethanol content in a hydrogen bioreactor has previously been predicted using NIR spectroscopy (Zhang *et al.*, 2009a). Near-infrared spectroscopy has been successfully used to

predict TSS in dairy sludge wastewater as well as in urban wastewaters (Páscoa *et al.*, 2008; Melendez-Pastor *et al.*, 2013).

Near-infrared spectroscopy in combination with multivariate data analysis techniques has been used to successfully predict COD and TSS concentrations in a variety of different wastewaters. It is an appropriate alternative technique that is rapid, non-destructive, requires no digestion step and involves no chemicals. There has however not been work undertaken to predict COD and TSS concentrations in winery wastewater and no attempt has been made to classify winery wastewater into different classes based on the concentration of COD or TSS in the wastewater. There is therefore a need to develop a method using NIR spectroscopy to classify and quantify winery wastewater based on the TSS and COD concentrations for screening of wastewater, before treatment of the wastewater proceeds. There is also potential to use portable devices to monitor the concentrations of COD and TSS during a reaction cycle and alert the operator to impending reactor failure.

The first aim of this research was to rapidly quantify and classify winery wastewater, using NIR spectroscopy, from four different farms based on the COD and TSS concentrations of the wastewater. Specific objectives were established to develop models that:

- Enable the prediction of COD and TSS concentrations for winery wastewater using a benchtop FT-NIR spectrophotometer within a 10 % error of the concentration range;
- Determine the COD and TSS of winery wastewater using a portable, handheld NIR spectrophotometer within a 10 % error of the concentration range;
- Classify winery wastewater as high or low strength based on COD and TSS concentrations respectively using a benchtop FT-NIR spectrophotometer and a portable, handheld spectrophotometer.

The second aim of this study was to investigate the performance of a pilot-scale AnSBR to treat winery wastewater and determine the optimal operational parameters. The following objectives were established:

- Design and commissioning of a novel pilot-scale AnSBR;
- Acclimitisation of anaerobic granules to winery wastewater until a COD reduction percentage of 70 % was reached treating wastewater with an initial COD concentration of 8 000 mg.L⁻¹;
- A central composite experiment design (CCD) was used and the regression coefficients for the applicable variables were analysed;
- To determine optimal operational parameters for pH, feeding time and mixing intervals, efficiency parameters such COD, TSS, Volatile fatty acids (VFA):Alkalinity; polyphenol reduction and methane percentage were monitored.

1.1 References

- Al-Rekabi, W.S., Qiang, H. & Qiang, W.W. (2007). Review on sequencing batch reactors. *Pakistan Journal of nutrition*, **6**, 11-19.
- Andreottola, G., Foladori, P. & Ziglio, G. (2009). Biological treatment of winery wastewater: an overview. *Water Science and Technology*, **60**, 1117-1125.
- Angel, H. (2018). Turning water into wine-Exploring approaches for improved water management among five vitivinicultural sustainability programs. *IIIEE Master Thesis*.
- APHA (2005). Standard methods for the examination of water and wastewater. *American Public Health Association (APHA): Washington, DC, USA*.
- Barbera, M. & Gurnari, G. (2018). Water Reuse in the Food Industry: Quality of Original Wastewater Before Treatments. In: *Wastewater Treatment and Reuse in the Food Industry*. Pp. 1-16. Springer.
- Besbes, M., Chahed, J. & Hamdane, A. (2019). The World Water Issues. In: *National Water Security*. Pp. 1-29. Springer.
- Bories, A. & Sire, Y. (2016). Impacts of winemaking methods on wastewaters and their treatment. *South African Journal of Enology and Viticulture*, **31**, 38-44.
- Carpenter, S.R., Stanley, E.H. & Vander Zanden, M.J. (2011). State of the world's freshwater ecosystems: physical, chemical, and biological changes. *Annual review of Environment and Resources*, **36**, 75-99.
- Cooley, H., Ajami, N., Ha, M.-L., Srinivasan, V., Morrison, J., Donnelly, K. & Christian-Smith, J. (2014). Global water governance in the twenty-first century. In: *The world's water*. Pp. 1-18. Springer.
- Da Ros, C., Cavinato, C., Pavan, P. & Bolzonella, D. (2014). Winery waste recycling through anaerobic co-digestion with waste activated sludge. *Waste Management*, **34**, 2028-2035.
- De Fraiture, C. & Wichelns, D. (2010). Satisfying future water demands for agriculture. *Agricultural Water Management*, **97**, 502-511.
- du Plessis, A. (2019). Climate Change and Freshwater Resources: Current Observations, Impacts, Vulnerabilities and Future Risks. In: *Water as an Inescapable Risk*. Pp. 55-78. Springer.
- Eleutheria, N., Maria, I., Vasiliki, T., Alexandros, E., Alexandros, A. & Vasileios, D. (2016). Energy Recovery and Treatment of Winery Wastes by a Compact Anaerobic Digester. *Waste and Biomass Valorization*, **7**, 799-805.
- Eusebio, A., Petruccioli, M., Lageiro, M., Federici, F. & Duarte, J.C. (2004). Microbial characterisation of activated sludge in jet-loop bioreactors treating winery wastewaters. *Journal of Industrial Microbiology and Biotechnology*, **31**, 29-34.
- FAO (2016). South Africa. [WWW document]. http://www.fao.org/nr/water/aquastat/countries_regions/Profile_segments/ZAF-WU_eng.stm. 27/07/2017
- Fisher, R.A. (1936). The use of multiple measurements in taxonomic problems. *Annals of eugenics*, **7**, 179-188.

- Gerardi, M.H. (2003). The microbiology of anaerobic digesters. Pp. 99-103 New Jersey: John Wiley & Sons.
- Gurtekin, E. (2014). Sequencing batch reactor. *Akademik Platform, ISEM2014 Adiyaman–Turkey*.
- Howell, C. & Myburgh, P. (2018). Management of winery wastewater by re-using it for crop irrigation-A review. *South African Journal of Enology and Viticulture*, **39**, 116-131.
- Huang, H., Yu, H., Xu, H. & Ying, Y. (2008). Near infrared spectroscopy for on/in-line monitoring of quality in foods and beverages: A review. *Journal of Food Engineering*, **87**, 303-313.
- Innocent, M.R., Morita, K. & Miyazato, Y. (2007). Rapid Estimation of Chemical Oxygen Demand of some Organic Solutions by using NIR and Chemometrics. *Journal of the Japanese Society of Agricultural Technology Management*, **14**, 107-114.
- Ioannou, L., Puma, G.L. & Fatta-Kassinos, D. (2015). Treatment of winery wastewater by physicochemical, biological and advanced processes: A review. *Journal of hazardous materials*, **286**, 343-368.
- Jury, W.A. & Vaux, H.J. (2007). The emerging global water crisis: managing scarcity and conflict between water users. *Advances in agronomy*, **95**, 1-76.
- Keyser, M., Witthuhn, R., Ronquest, L.-C. & Britz, T. (2003). Treatment of winery effluent with upflow anaerobic sludge blanket (UASB)–granular sludges enriched with *Enterobacter sakazakii*. *Biotechnology letters*, **25**, 1893-1898.
- Khanal, S., Giri, B., Nitayavardhana, S. & Gadhamshetty, V. (2017). Anaerobic bioreactors/digesters: design and development. In: *Current Developments in Biotechnology and Bioengineering*. Pp. 261-279. Elsevier.
- Kumar, A., Frost, P., Correll, R. & Oemcke, D. (2009). Winery wastewater generation, treatment and disposal: A survey of Australian practice. CSIRO Land and Water Report.
- Martins, A.A., Araújo, A.R., Graça, A., Caetano, N.S. & Mata, T.M. (2018). Towards sustainable wine: Comparison of two Portuguese wines. *Journal of Cleaner Production*, **183**, 662-676.
- Massy, W.F. (1965). Principal components regression in exploratory statistical research. *Journal of the American Statistical Association*, **60**, 234-256.
- McNabb, D.E. (2019). The population growth barrier. In: *Global Pathways to Water Sustainability*. Pp. 67-81. Springer.
- Melendez-Pastor, I., Almendro-Candel, M.B., Navarro-Pedreño, J., Gómez, I., Lillo, M.G. & Hernández, E.I. (2013). Monitoring urban wastewaters' characteristics by visible and short wave near-infrared spectroscopy. *Water*, **5**, 2026-2036.
- Meneses, M., Pasqualino, J.C. & Castells, F. (2010). Environmental assessment of urban wastewater reuse: treatment alternatives and applications. *Chemosphere*, **81**, 266-272.
- Mohana, S., Acharya, B.K. & Madamwar, D. (2009). Distillery spent wash: Treatment technologies and potential applications. *Journal of hazardous materials*, **163**, 12-25.
- Moharikar, A., Purohit, H.J. & Kumar, R. (2005). Microbial population dynamics at effluent treatment plants. *Journal of Environmental Monitoring*, **7**, 552-558.

- Moletta, R. (2005). Winery and distillery wastewater treatment by anaerobic digestion. *Water Science and Technology*, **51**, 137-144.
- Mosse, K., Patti, A., Christen, E. & Cavagnaro, T. (2011). Winery wastewater quality and treatment options in Australia. *Australian Journal of Grape and Wine Research*, **17**, 111-122.
- Myra, T., David, H., Judith, T., Marina, Y., Ricky, B.J. & Reynaldo, E. (2015). Biological treatment of meat processing wastewater using anaerobic sequencing batch reactor (ASBR). *International Research Journal of Biological Sciences*, **4**, 66-75.
- OIV (2019). 2019 Statistical report on world vitiviniculture. [WWW document]. <http://www.oiv.int/public/medias/6782/oiv-2019-statistical-report-on-world-vitiviniculture.pdf>.
- Ozaki, Y., McClure, W.F. & Christy, A.A. (2006). *Near-infrared spectroscopy in food science and technology*. John Wiley & Sons.
- Pan, T., Chen, W.W., Chen, Z.H. & Xie, J. (Year). Waveband selection for NIR spectroscopy analysis of wastewater COD. In: *Key Engineering Materials*. Pp. 393-396. Month and 2011
- Parawira, W. (2004). Anaerobic treatment of agricultural residues and wastewater. *University of Lund Department of Biotechnology*.
- Páscoa, R.N., Lopes, J.A. & Lima, J.L. (2008). In situ near infrared monitoring of activated dairy sludge wastewater treatment processes. *Journal of Near Infrared Spectroscopy*, **16**, 409-419.
- Pasquini, C. (2003). Near infrared spectroscopy: fundamentals, practical aspects and analytical applications. *Journal of the Brazilian chemical society*, **14**, 198-219.
- Pedrero, F., Kalavrouziotis, I., Alarcón, J.J., Koukoulakis, P. & Asano, T. (2010). Use of treated municipal wastewater in irrigated agriculture—Review of some practices in Spain and Greece. *Agricultural Water Management*, **97**, 1233-1241.
- Petruccioli, M., Duarte, J. & Federici, F. (2000). High-rate aerobic treatment of winery wastewater using bioreactors with free and immobilized activated sludge. *Journal of bioscience and bioengineering*, **90**, 381-386.
- Quinteiro, P., Dias, A.C., Pina, L., Neto, B., Ridoutt, B.G. & Arroja, L. (2014). Addressing the freshwater use of a Portuguese wine ('vinho verde') using different LCA methods. *Journal of Cleaner Production*, **68**, 46-55.
- RSA (2013). Revision of General Authorisation of Section 39 of the National Water Act,1998 (Act No. 36 of 1998). Pretoria: Government Printer: Government Gazette No. 36820 September 2013.
- SAWIS (2018). SA wine industry 2018 statistics NR 43. [WWW document]. http://www.sawis.co.za/info/download/Book_2018_statistics_year_english_final.pdf.
- Shao, X., Peng, D., Teng, Z. & Ju, X. (2008). Treatment of brewery wastewater using anaerobic sequencing batch reactor (ASBR). *Bioresource technology*, **99**, 3182-3186.
- Show, K. & Lee, D. (2016). Anaerobic Treatment Versus Aerobic Treatment. *Current Developments in Biotechnology and Bioengineering: Biological Treatment of Industrial Effluents*, 205.

- Siesler, H.W., Ozaki, Y., Kawata, S. & Heise, H.M. (2008). *Near-infrared spectroscopy: principles, instruments, applications*. John Wiley & Sons.
- Sivakumar, B. (2011). Water crisis: from conflict to cooperation—an overview. *Hydrological Sciences Journal*, **56**, 531-552.
- Sung, S. & Dague, R.R. (1995). Laboratory studies on the anaerobic sequencing batch reactor. *Water Environment Research*, **67**, 294-301.
- UNESCO (2017). The United Nations World Water Development Report 2017 : Water and Jobs. Pp. 1-12. Italy: United Nations.
- Van Schoor, L. (2005). Guidelines for the management of wastewater and solid waste at existing wineries. *Winetech, PO Box*, **528**.
- Vlyssides, A., Barampouti, E. & Mai, S. (2005). Wastewater characteristics from Greek wineries and distilleries. *Water Science and Technology*, **51**, 53-60.
- Welz, P., Holtman, G., Haldenwang, R. & Le Roes-Hill, M. (2016). Characterisation of winery wastewater from continuous flow settling basins and waste stabilisation ponds over the course of 1 year: implications for biological wastewater treatment and land application. *Water Science and Technology*, **74**, 2036-2050.
- Wold, S., Martens, H. & Wold, H. (1983). The multivariate calibration problem in chemistry solved by the PLS method. In: *Matrix pencils*. Pp. 286-293. Springer.
- Workman Jr, J. (1993). A brief review of the near infrared measurement technique. *NIR news*, **4**, 8-16.
- Yang, Q., Liu, Z. & Yang, J. (2009). Simultaneous determination of chemical oxygen demand (COD) and biological oxygen demand (BOD5) in wastewater by near-infrared spectrometry. *Journal of Water Resource and Protection*, **4**, 286-289.
- Zhang, M.-L., Sheng, G.-P., Mu, Y., Li, W.-H., Yu, H.-Q., Harada, H. & Li, Y.-Y. (2009). Rapid and accurate determination of VFAs and ethanol in the effluent of an anaerobic H₂-producing bioreactor using near-infrared spectroscopy. *Water Research*, **43**, 1823-1830.

Chapter 2

Literature Review

2.1 Introduction

Water is the most important natural resource on Earth and is of vital importance for humans, plants, animals, ecosystems and environments (Sivakumar, 2011). Access to water can be the difference between life and death as well as between wealth and poverty (Sivakumar, 2011; Kondusamy & Kalamdhad, 2014). The availability of water is the largest constraint influencing development in South Africa as practically all the available surface water is currently in use and additional water is imported from neighbouring countries (Scholes, 2001; Blignaut & Van Heerden, 2009). Population growth, shifting from plant based diets to meat based diets, climate change and other challenges will further increase strain on the natural water resources (Cooley *et al.*, 2014). The total amount of water on earth is estimated to be approximately $1.4 \times 10^9 \text{ km}^3$, of which 2.5 % ($35 \times 10^6 \text{ km}^3$) is freshwater (Carpenter *et al.*, 2011). Furthermore, around 68.7 % of freshwater is inaccessible for human use as it is locked in glaciers as well as permanent snow cover in the Arctic and Antarctic regions (Carpenter *et al.*, 2011). The main sources of water that are used for human consumption are acquired from rivers and freshwater lakes and constitute roughly 0.26 % of the total global freshwater resources, which equates to $90 \times 10^3 \text{ km}^3$ (Sivakumar, 2011).

There is a limited amount of available freshwater and this is exacerbated in some regions as water is not evenly distributed around the world, or even in South Africa, with some parts experiencing higher levels of rainfall than other regions (Blignaut & Van Heerden, 2009; Cooley *et al.*, 2014). The human population is estimated to reach 7.9 billion people in the year 2025 and 9.7 billion by the year 2050 (Jury & Vaux, 2007; Sivakumar, 2011; UNESCO, 2017; McNabb, 2019). In order to maintain the current per capita food supply, food production will have to be increased by anything between 50 and 100 % (Jury & Vaux, 2007; Baulcombe *et al.*, 2009; Alexandratos & Bruinsma, 2012). This will put severe strain on the already limited supply of freshwater. The water requirements for food production would therefore increase by $7\,700 \text{ km}^3$ per year by 2050. Improvements in production efficiency and the expansion of agricultural land may only yield 800 km^3 per year. In order for many industries to survive until this period it will be of major importance that they increase their production efficiency and conservation efforts (Jury & Vaux, 2007; Baulcombe *et al.*, 2009)

Water scarcity is defined as access to less than $1\,000 \text{ m}^3$ of water per person annually (UNESCO, 2017). This is not just a potential problem facing the human population in 2050, but has already surfaced across the globe (UNESCO, 2017). Currently around 2.4 billion people worldwide either lack ready access to drinking water or have access to water that is deemed unsafe for human consumption (UNESCO, 2017). Economic water scarcity is when water is available, however is inaccessible due to financial constraints or infrastructure shortages (UN, 2006). The total amount of people living in economic water scarce areas are

approximately 1.6 billion people. This takes the total amount of the world population that has limited access to water to a total of 3.3 billion people (UN, 2006).

Agriculture is responsible for the use of approximately 70% of all the freshwater globally (UNESCO, 2017). Industry is responsible for 19 % of the freshwater use and domestic usage only equals 11 % on a global scale (UNESCO, 2017). The South African landscape differs slightly from the global landscape. Agriculture also uses the most water, but this figure is estimated to be slightly lower at 62.5% (FAO, 2016). The next main user of water is municipalities, which account for 27 % of the freshwater, both in cities and rural areas. Industry is responsible for the remaining 10.5 % of freshwater withdrawals in the country (FAO, 2016). If it is assumed that the South African population will follow the same trend as population growth globally, then there will be significantly more people to feed in South Africa by the year 2050 and this will place increasing strain on the water resources in the country.

Industrial wastewater generation is much less than that of the agricultural sector. However due to the high strength nature of industrial wastewater, it has the potential to pollute water to a much greater degree (Moharikar *et al.*, 2005). By treating the industrial wastewater and subsequently utilising it for irrigation, it would place less strain on the freshwater withdrawal by the agricultural sector. The brewing, winemaking and distillery industries, which are classified as part of the beverage industry, generate large amounts of wastewater. These industries therefore have the potential to reuse large amounts of the wastewater that they generate themselves (Visvanathan & Asano, 2009). Industries which generate large volumes of wastewater, such as the wine industry, can limit some of their costs by implementing wastewater treatment plants at their facility. Water that is used in the production process may be reduced by 50 to 90 % by using internal wastewater recycling (Visvanathan & Asano, 2009). Because the wine industry generates such a large volume of wastewater, there is a lot of research currently being conducted to find new techniques of treating winery wastewater for reuse in the process, or for irrigation of the vineyards.

2.2 Wine industry and winemaking process

2.2.1 History and statistics

The production of wine by humans can be traced back to almost 6 000 years ago. The earliest evidence of winemaking dates back to between 5 400 BC and 5 000 BC (Soleas *et al.*, 1997). Modern winemaking processes seemed to have begun in the 17th century as evidenced by the presence of sulphur in old wine barrels (Soleas *et al.*, 1997). The South African wine industry started in the 1650's and is regarded as one of the oldest wine industries outside of Europe (Bruwer, 2003). In spite of this, countries such as Italy and France dominated the international wine markets until the 1980's (Cusmano *et al.*, 2010). The wine industry in South Africa started to grow in the 1990's as there had been technological advances that have been stimulated by investment as well as research in the field (Cusmano *et al.*, 2010). The wine industry in South Africa plays an important role in job creation, business growth, regional development, corporate investment and tourism (Bruwer, 2003).

The South African wine industry is localised in the Western Cape with 91 415 (96.7 %) hectares of the total vines in the country (SAWIS, 2016). Of the 493 private cellars in the country, 479 are situated in the Western Cape (SAWIS, 2016). Stellenbosch has the highest percentage of total vines in the country with 16.36 % of the vines. The Paarl area has the second highest of 16.17 %. The rest of the wine producing areas in the country are Robertson, Swartland, Bredekloof, Olifants River, Worcester, Northern Cape, Cape South Coast and the Klein Karoo (SAWIS, 2016).

South Africa currently ranks 9th on the list of leading wine producers in the world for the International Organisation of Vine and Wine (OIV) forecasted data for 2019. Italy, France, Spain, United States of America (USA), Argentina, Chile, Australia and Germany are currently ranked above South Africa (OIV, 2019). Of the 267 million hectolitres produced worldwide, South Africa produces 9.60 million hectolitres (SAWIS, 2018). White wines are the most commonly produced wines, accounting for 65 % of the total wine production and thus red wine accounting for 35 % of total wine production in South Africa. Whilst grapes crushed as well as the amount of wine and wine products produced has decreased since 2014, the domestic sales and exports have increased over the same period. The wine producers consequently saw an increase in their income over this period from R4.7 billion to R6.298 billion (SAWIS, 2018). This follows the trend of increased producers' income year on year since 2003, with the producers having increased their income by 190 % over this period (SAWIS, 2016). The state revenue followed the same trend with them generating R7.403 billion (SAWIS, 2018). This is an increase of 230 % since 2003. It can therefore be confirmed that the wine industry in South Africa is very important to the economy of the country, especially the Western Cape.

2.2.2 Winemaking procedure

2.2.2.1 White wine

To produce white wine, the following typical procedure is followed. The grapes that are to be transformed into wine are received in the hopper and subsequently crushed. During this step, the stems are also removed. This results in the production of a mash, to which sulphur dioxide is added to inhibit bacterial growth in the wine (Arvanitoyannis *et al.*, 2006). The mash is then cooled to inhibit micro-organism growth. Grape juice is then extracted by pressing the mash and the juice settles overnight in a settling tank, in order for the sediment to settle (Joshi *et al.*, 2017). The juice is then transferred to a fermentation tank where it is subsequently inoculated with the correct yeast (Woodard, 2001). Once fermentation is complete the wine is drawn to a stainless steel tank for fining to begin (Woodard, 2001). Fining is the process of clarification of the wine using fining agents (Conradie, 2015). The wine is then cooled and bottled. During the bottling stage the wine may possibly be protected from oxidation by bottling in an inert atmosphere (Ene *et al.*, 2013).

2.2.2.2 Red wine

The red wine production procedure differs from that of white wine, although the processes do share similarities. During the production of red wine, the fermentation and maceration step takes place before the

mash is pressed to obtain juice. The second fermentation commences once the pressing has completed. The wine is transferred to barrels or tanks where malolactic acid fermentation may take place if required. Maturation of the wine may take place in tanks or in barrels (Conradie, 2015). Wine ageing is a practice that is used to improve the quality of the wine as well as its organoleptic properties (García-Carpintero *et al.*, 2012). Maturation may modify the characteristics of the wine due to chemical reactions that occur due to oxygen passing through the pores of the wood and due to the compounds that are extracted from the wood (García-Carpintero *et al.*, 2012). The use of barrels is quite expensive to the industry, so by introducing oak chips into stainless steel barrels during fermentation it allows these wines to have characteristics such as those that are fermented solely in barrels (García-Carpintero *et al.*, 2012). Once maturation is complete, the wine is filtered and bottled and ready to be distributed (Joshi *et al.*, 2017). The flow diagram detailing the two separate wine processes as well as steps where wastewater is generated is illustrated in **Figure 2.1**.

The winemaking process, as seen in **Figure 2.1**, generates a large volume of wastewater. For every litre of wine produced, wastewater generation can be in the region of 2 to 14L (Oliveira *et al.*, 2009). The winemaking procedure can be divided into 7 main steps, with each step contributing to wastewater generation (Vlyssides *et al.*, 2005). The steps are as follows;

1. Reception
2. Must Production
3. Fermentation (No Wastewater Production)
4. Decanting
5. Maturation and Stabilisation
6. Filtration
7. Transportation and Disposal

The fermentation process does not contribute to the production of wastewater within the winery. Two processes contribute the most to wastewater production. These processes are must production and filtering (Vlyssides *et al.*, 2005). Wastewater generation in these steps is because of extensive cleaning and pre-cleaning processes in the winery. The volume generated in these steps is dependent on the size of the tanks and can be calculated using the following formula: specific production volume = $71.58 V \times 0.328373$ where V is the tank volume in m³ (Vlyssides *et al.*, 2005). Conversely, the volume of wastewater generation is the least during the period when wine is transported to its destination (Vlyssides *et al.*, 2005). The main steps in the winemaking process that would lead to wastewater generation is illustrated in **Table 2.1**.

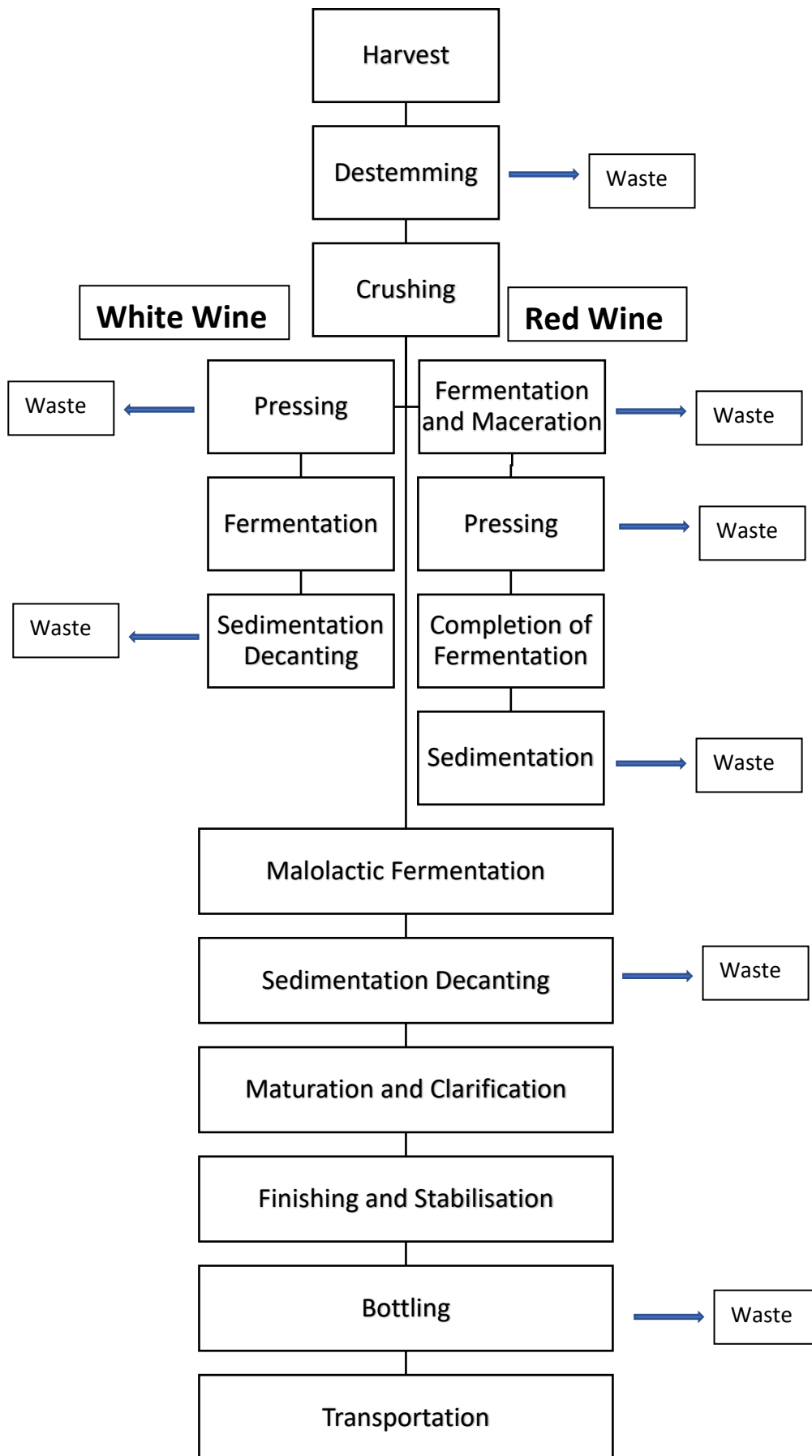


Figure 2.1 Flow Diagram of Winemaking process. Adapted from (Arvanitoyannis *et al.*, 2006; Devesa-Rey *et al.*, 2011; Ene *et al.*, 2013)

Table 2.1 Winemaking steps and wastewater generation sources. Adapted from (Woodard, 2001; Vlyssides *et al.*, 2005).

| Step | Process | Wastewater Generation |
|------|---------------------------------------|---|
| 1 | Reception | Washing of all machinery as well as floors |
| 2 | Must Production | Washing of machinery e.g. pneumatic press Normal plant clean-up waste Waste lees Loss of must when transferred to the fermentation tanks and the pre cleaning of these tanks |
| 3 | Fermentation | Wastewater from normal clean-up practises |
| 4 | Decanting | Normal plant wash down i.e. cleaning of tanks Pre-washing stabilisation tanks Cleaning of decanting pump Wine losses due to decanting |
| 5 | Maturation and Stabilisation | No wastewater production |
| 6 | Filtration | Normal plant clean-up Washing of storage tanks Filter cleaning (Filtering earth residues) Wine losses during transfer Water from the transportation pump |
| 7 | Bottling, Transportation and disposal | Spillage and overfilling in bottling stage Washing of tanks Washing transportation pumps Cleaning of production room |

2.3 Winery wastewater composition

Due to the seasonal nature of the winemaking process, winery wastewater characteristics and composition are variable. Added to this is the fact that each winery must be treated as an individual entity based on the winemaking capacity of the cellar, the types of wines produced, the equipment present at the winery as well as the water management plan of the specific winery (Bories & Sire, 2016).

Winery wastewater is generated internally, by cleaning of the winery production area and tanks (Mosse *et al.*, 2011). The major contributors to the composition of winery wastewater are therefore wine, grape varietal, suspended solids as well as cleaning or sanitising agents used (Vlyssides *et al.*, 2005; Mosse *et al.*, 2011; Ene *et al.*, 2013). Winery wastewater is characterised as a high strength wastewater in terms of

COD (Da Ros *et al.*, 2014). Organic compounds contributing to the high COD are mainly sugars, organic acids, esters and polyphenolic compounds (Mosse *et al.*, 2011). In the early harvest period, sugars are the predominant contributor to COD, however as the end of the harvest season approaches, ethanol becomes the main contributor to the COD of the wastewater, with sugars having a negligible effect (Bories & Sire, 2016). The composition of winery wastewater is summarised in **Table 2.2**.

Table 2.2 Average composition of winery wastewater.

| | Min | Max | Mean |
|--|-------|--------|----------|
| COD (mg.L ⁻¹) | 800 | 27 200 | 8 963.24 |
| BOD (mg.L ⁻¹) | 210 | 8 000 | 2 877.5 |
| pH | 4.0 | 7.1 | 6.31 |
| TSS (mg.L ⁻¹) | 0.2 | 1.3 | 0.54 |
| TOC (ppm) | 1255 | 1 255 | 1 255 |
| TS (mg.L ⁻¹) | 3 900 | 4 100 | 4 000 |
| SS (mg.L ⁻¹) | 0.14 | 0,2 | 0.17 |
| VSS (mg.L ⁻¹) | 0.13 | 0.42 | 0.22 |
| T _{phosphorous} (mg.L ⁻¹) | 0.3 | 65.7 | 21.35 |
| T _{nitrogen} (mg.L ⁻¹) | 21,3 | 71 | 55.825 |
| T _{phenolics} (mg.L ⁻¹) | 2,8 | 1 450 | 270 |

(Petruccioli *et al.*, 2000; Eusebio *et al.*, 2004; Vlyssides *et al.*, 2005; Agustina *et al.*, 2008; Kirzhner *et al.*, 2008; Bories & Sire, 2016; Welz *et al.*, 2016).

Wineries may discharge the wastewater that is generated internally into municipal reticulation systems, or may be irrigated onto land used for agricultural activities (Welz *et al.*, 2016). In South Africa, approximately 95 % of all winery wastewater is irrigated onto land using sprinkler systems (Van Schoor, 2005). The quality of the water may be improved by treating it with physical, chemical or biological treatments prior to disposal of the water (Welz *et al.*, 2016). The enhancement of the water quality is an important step as untreated winery wastewater may present a danger to the environment (Ene *et al.*, 2013). The environmental concerns associated with untreated winery wastewater are illustrated in **Table 2.3**. The untreated wastewater may have debilitating effects on ecosystems. It may cause eutrophication in rivers and it contains some compounds which may be harmful to animals as well as humans.

2.4 Regulations

Any wastewater that is subsequently used for irrigation purposes must adhere to specific guidelines as stipulated in the National Water Act of 1998 that was revised in 2013. The guidelines differ based on the volume of water used for irrigation purposes on any given day. The volumes stipulated in the act vary from

2 000 m³ per day to less than 50 m³ per day. The guidelines for irrigation up are given in **Table 2.4** and **Table 2.5**

Table 2. 3 Potential effects of untreated winery wastewater to the environment. Adapted from EPA, (Rengasamy & Marchuk, 2011; Ene et al., 2013; Hirzel et al., 2017).

| Constituent | Indicators | Impact |
|----------------------|-------------|--|
| Organic Matter | BOD | Depletion of oxygen causing death of plants and fish |
| | COD | Odours if stored in open lagoons or applied to land |
| | TOC | Can contain toxic or carcinogenic compounds, therefore potentially harmful to human health |
| Alkalinity / Acidity | pH | May cause death of aquatic organisms at extreme pH |
| | Calcium | Influence microbial activity |
| | carbonate | Influence solubility, availability and toxicity of heavy metals |
| | | Influences growth of crops |
| Nutrients | Nitrogen | Eutrophication or algal bloom |
| | Phosphorous | Nitrite and nitrate may be toxic to children |
| | Potassium | N is toxic for crops in large quantities |
| | Sulphur | Sodium and potassium may alter soil structure |
| | Sodium | |
| Salinity | EC | Undesirable taste |
| | TDS | Toxic to aquatic organisms, plants animals and humans |
| | Chloride | Water uptake by plants affected |
| Metal Contamination | Chromium | Toxic for plants, animals and humans |
| | Cobalt | Negative effects for ecosystems |
| | Copper | |
| | Nickel | |
| | Zinc | |
| | Lead | |
| | Mercury | |

Table 2. 4 South African guidelines for irrigation of biodegradeable wastewater between 500 and 2 000 m³.d⁻¹.

| Variables | Units | Limits |
|--|--------------------------|---------------------------------------|
| pH | | ≥ 5.5 - ≤ 9.5 |
| Electrical conductivity | mS.m ⁻¹ | ≤ 70 intake to a max of 150 per metre |
| Suspended solids | mg.L ⁻¹ | ≤ 25 |
| Chlorine as free chlorine | mg.L ⁻¹ | ≤ 0.25 |
| Fluoride | mg.L ⁻¹ | ≤ 1 |
| Soap, oil and grease | mg.L ⁻¹ | ≤ 2.5 |
| Chemical oxygen demand (COD) | mg.L ⁻¹ | ≤ 75 |
| Faecal Coliforms | CFU. 100mL ⁻¹ | ≤ 1000 |
| Ammonia (ionised and de-ionised) as Nitrogen | mg.L ⁻¹ | ≤ 3 |
| Nitrate / Nitrite as Nitrogen | mg.L ⁻¹ | ≤ 15 |
| Orthophosphate as phosphorous | mg.L ⁻¹ | ≤ 10 |

Table 2. 5 South African guidelines for irrigation water of biodegradable industrial wastewater.

| Variable | Units | ≤50 m ³ | 50>vol≤500 m ³ |
|-------------------------------|--------------------------|----------------------------|---------------------------|
| pH | | ≥ 6 and ≤ 9 | ≥ 6 and ≤ 9 |
| Electrical conductivity | mS.m ⁻¹ | ≤ 200 | ≤ 200 |
| COD | mg.L ⁻¹ | ≤ 5000 after algae removal | ≤ 400 after algae removal |
| Faecal Coliforms | CFU.100 mL ⁻¹ | ≤ 100 000 | ≤ 100 000 |
| Sodium absorption ratio (SAR) | | ≤ 5 | ≤ 5 |

2.5 Current treatment options

There are many treatment options available to treat wastewater of different composition and strengths. These treatment options include physical, physicochemical and biological treatments (Woodard, 2001; Mosse *et al.*, 2011; Welz *et al.*, 2016). The main aim of these treatment options is to reduce the concentration of the organic matter and solids and in some cases to reduce the inorganic load as well (Quayle *et al.*, 2009).

Determining which treatment options are most suitable for each winery is reliant upon many factors such as maintenance, expertise required and capital investment cost (Mosse *et al.*, 2011).

2.5.1 Physical methods

One of the first wastewater treatment options is physical pre-treatments. Physical methods are therefore also known as primary wastewater treatment methods. One of the main reasons to employ these methods is to protect machinery in the cellar from becoming clogged by solids such as the grape stems, stalks and leaves (Mosse *et al.*, 2011). Screening and settling are examples of primary treatment methods.

2.5.2 Physicochemical methods

Physicochemical methods are frequently employed after primary treatment. The reason for applying these treatments is to further reduce COD, turbidity and colour (Mohana *et al.*, 2009). Not all physicochemical processes are created equal, with each treatment differing with regards to the particle size it can remove (Buys, 2015). Examples of physicochemical methods include: Ion exchange, reverse osmosis, coagulation, flocculation and membrane filtration (Mosse *et al.*, 2011; Ioannou *et al.*, 2015).

2.5.2.1 Ion exchange

The principle of ion exchange is the exchange of ions between immobilised resin and the solution. This method is effective for the removal of ions such as ammonium, chromium and boron from wastewaters (Mosse *et al.*, 2011). This process has a low energy requirement and has the ability to reduce sodium and potassium levels, however this process is only applicable for large scale wineries (Mosse *et al.*, 2011). Ion exchange processes are not commonly used in the treatment of winery wastewater.

2.5.2.2 Reverse Osmosis

Reverse osmosis is very effective as a water purification technique and removes salts very effectively from wastewater. This treatment will usually be used to treat water that is intended for potable reuse (Mosse *et al.*, 2011). This treatment option is also prone to fouling and as such must be combined with a microfiltration step. The addition of this step increases the price of using such a treatment and makes it unviable for small to medium scale wineries. The majority of winery wastewater in South Africa is used for irrigation purposes (Van Schoor, 2005), making reverse osmosis unnecessary in the South African wine industry.

2.5.2.3 Coagulation & flocculation

Coagulation is a primary processing step that is used to accelerate the agglomeration of particles in solution (Betancourt & Rose, 2004). Flocculation follows the coagulation step and the combination of the two treatments result in the solids separating from the liquid. This is used to destabilise colloidal impurities and

in the process, produces large aggregates that are easily removed by addition of a filtration step (Gao *et al.*, 2002). Aluminium salts are commonly used as coagulants in this water treatment (Gao *et al.*, 2002).

2.5.2.4 Membrane filtration

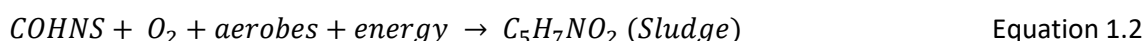
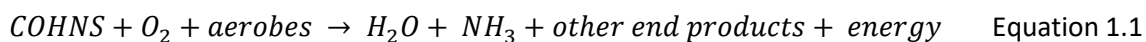
The processes included under this broad category are microfiltration (MF), ultrafiltration (NF) and nanofiltration (NF) (Zularisam *et al.*, 2006). Microparticles and macromolecules, which include organic colloids, microorganisms, inorganic particles and dissolved organic matter are removed using MF and UF (Zularisam *et al.*, 2006; Shivajirao, 2012). Microfiltration reduces the turbidity and colloidal suspensions in water as it acts a porous barrier. UF has a higher removal rate but operates at higher pressures. These processes are adequate for water reclamation as the water is not intended for drinking purposes (Shivajirao, 2012). If the treated water is intended for human consumption, MF and UF could be used alongside NF or reverse osmosis in order to minimise fouling of the membrane (Shivajirao, 2012).

2.5.3 Biological treatments

Biological treatments are very effective at removing organic compounds from winery wastewater as they are readily biodegradable (Mosse *et al.*, 2011). The main difficulty when using biological treatments is that the composition and volume of winery wastewater generated fluctuates (Mosse *et al.*, 2011). Biological treatments can be crudely subdivided into aerobic and anaerobic processes for the treatment of wastewaters (Mohana *et al.*, 2009; Mosse *et al.*, 2011; Ioannou *et al.*, 2015)

2.5.3.1 Aerobic processes

Aerobic treatment technologies are commonly used in the wine industry to treat the incoming wastewater (Sheridan *et al.*, 2014; Ioannou *et al.*, 2015). Aerobic processes are oxidation processes where aerobic bacteria degrade the organic matter in the wastewater in the presence of oxygen (Show & Lee, 2016). Organic carbon is utilised as the energy source for heterotrophic microorganisms and is degraded into biomass, CO₂, ammonia, energy, water as well as other end products (Show & Lee, 2016). The process is illustrated in the following equations



Many aerobic processes have the advantage of being more stable than anaerobic processes (Show & Lee, 2016). Other advantages of the aerobic processes include ease of use, high COD removal efficiency, versatility in the process when modifying the size of the operation and the process is well established, leading

to easier troubleshooting (Mosse et al., 2011; Ioannou et al., 2015). The main disadvantage of aerobic treatment of water is the fact that large quantities of sludge is produced (Mosse et al., 2011). The extent of sludge production is illustrated in **Figure 2.2**.

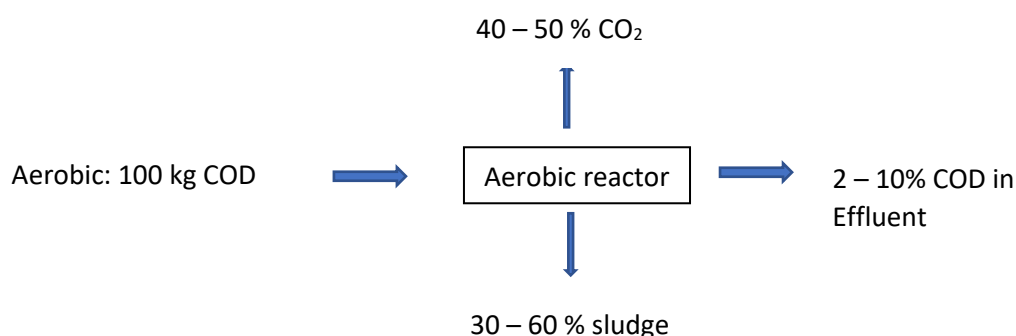


Figure 2.2 Representation of aerobic process. Adapted from (Chetty & Pillay, 2015).

Table 2.6 illustrates the different types of aerobic treatment options available with their respective advantages and disadvantages. The COD removal also illustrates how effective the various treatments are.

2.5.3.1.1 Aerobic treatment of winery wastewater: application

A number of studies have been conducted to assess the remediation of winery effluent (Bruculeri *et al.*, 2005; Bolzonella *et al.*, 2010; Montalvo *et al.*, 2010). A study was conducted on the efficacy of two pilot scale fed-batch aerated lagoons (Montalvo et al., 2010). The wastewater was treated in the larger of the two lagoons for the first 30 days, with the second lagoon in operation from days 31 to 54. The winery wastewater was intermittently fed into the lagoons at set intervals to simulate operational conditions. After 21 days from inception of the experiment the COD reduction percentage reached a maximum of 91 % (influent COD: 8 700 mg.L⁻¹). The COD removal remained constant and stable thereafter, indicating the efficacy of this treatment option (Montalvo et al., 2010).

The co-treatment of municipal wastewater alongside winery wastewater was investigated in a conventional activated sludge process at full scale (Bruculeri et al., 2005). Two different times of the year were identified to represent the wine making procedure accurately. These two periods were described as vintage and non-vintage, where during vintage season, wastewater with a higher COD was fed into the process. The COD removal efficiency of the processes were 90 % (Influent COD: 5 480 kg.d⁻¹) during vintage and 87 % (Influent COD: 2 515 kg.d⁻¹) during non-vintage. High removal efficiencies are thus achievable using this method.

Treatment of winery wastewater using an aerobic sequencing batch reactor was investigated (Brito et al., 2007). COD removal efficiency was above 90 % (Influent COD: 400 – 2 000 mg.L⁻¹) for all times of the year as well as influent COD concentration.

In order to investigate the efficiency of the membrane bioreactor, a full scale membrane bioreactor treated approximately 110 m³.day⁻¹ with COD levels up to 1 600 Kg COD.day⁻¹ (Bolzonella et al., 2010). COD was removed with an average efficiency of 95 % with low sludge yield.

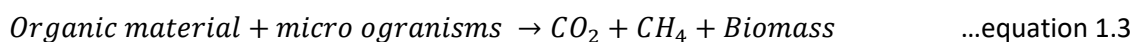
Table 2. 6 Advantages and disadvantages of the various aerobic treatments.

| Treatment | Advantages | Disadvantages | COD Reduction | Reference |
|----------------------------|--|---|---------------|--|
| Aerated lagoons | <ul style="list-style-type: none"> • Easy management | <ul style="list-style-type: none"> • Energy intensive • Works best on small volumes | 91% | (Maynard <i>et al.</i> , 1999; Montalvo <i>et al.</i> , 2010) |
| Activated sludge | <ul style="list-style-type: none"> • Easily managed • High reduction of COD | <ul style="list-style-type: none"> • Uses lots of energy • Requires lots of nutrients (N and P) | 87 – 98% | (Fumi <i>et al.</i> , 1995; Brucculeri <i>et al.</i> , 2005; Andreottola <i>et al.</i> , 2009) |
| Sequencing batch reactor | <ul style="list-style-type: none"> • Automation simple • Low capital investment | <ul style="list-style-type: none"> • Storage tanks required • Difficulties with shock loading | >90% | (Torrijos & Moletta, 1997; Brito <i>et al.</i> , 2007; López-Palau <i>et al.</i> , 2012) |
| Membrane bioreactor | <ul style="list-style-type: none"> • Improved treated water quality • Small footprint • Rapid start-up • Settling not a problem • Low sludge volume | <ul style="list-style-type: none"> • High establishment cost for membrane • Membrane fouling | 95 – 97% | (Artiga <i>et al.</i> , 2005; Bolzonella <i>et al.</i> , 2010) |
| Jet-loop activated sludge | <ul style="list-style-type: none"> • Low energy required • High efficiency | <ul style="list-style-type: none"> • Limited application | 94 – 98% | (Petruccioli <i>et al.</i> , 2002) |
| Air microbubble bioreactor | <ul style="list-style-type: none"> • High biological conversion | <ul style="list-style-type: none"> • Limited applications | 93% | (Petruccioli <i>et al.</i> , 2002; Oliveira <i>et al.</i> , 2009) |

A jet-looped activated sludge reactor that had a 15dm³ working volume was used to treat winery wastewater for a period of just longer than a year (Petruccioli *et al.*, 2002). Wastewater from various farms was used in this study. The wastewater was also collected at different times throughout the year, ensuring varying COD levels. The reactor illustrated its efficacy by having a COD removal efficiency that never dipped below 90 % over the course of the year.

2.5.3.2 Anaerobic processes

Anaerobic digestion is a process that occurs in the absence of oxygen and is a much more complicated process than the aerobic process as there is an abundance of potential pathways for the microbial population to utilise (Arvanitoyannis *et al.*, 2006; Show & Lee, 2016). The anaerobic process can be summarised in the following equation:



It is possible to divide the anaerobic process into two distinct stages, namely acid formation and methane formation (Show & Lee, 2016). However the process is more complicated and is better described by dividing the process into 4 distinct stages (Gallert & Winter, 2008). The stages are hydrolysis, acidogenesis, acetogenesis and methanogenesis (Gallert & Winter, 2008; Kondusamy & Kalamdhad, 2014; Show & Lee, 2016).

2.5.3.2.1 Detailed anaerobic process

As discussed in the previous section, the anaerobic process can be divided into 4 stages. The process is summarised in **Figure 2.3**.

a) Hydrolysis

Hydrolysis converts insoluble organic compounds, such as proteins, carbohydrates and fats, into simpler organic compounds (Kondusamy & Kalamdhad, 2014). Simple organic compounds, which are soluble in water, are then utilised as an energy source. It is important for the simple compounds to be soluble in water and of a low molecular mass so that the compounds can be utilised by the microorganisms (Gallert & Winter, 2008). Hydrolysis is catalysed by extracellular hydrolytic enzymes (Kondusamy & Kalamdhad, 2014).

Hydrolysis can be further classified depending on the reaction that they catalyse. For example, lipases produce glycerol and fatty acids when the ester bonds of lipids are hydrolysed. Other extracellular enzymes include, protease, cellulase, amylase and pectinase (Kondusamy & Kalamdhad, 2014; Show & Lee, 2016). Hydrolysis of complex organic matter is a slow process and is the limiting factor of the anaerobic digestion process (Kondusamy & Kalamdhad, 2014; Zhang *et al.*, 2014; Eleutheria *et al.*, 2016).

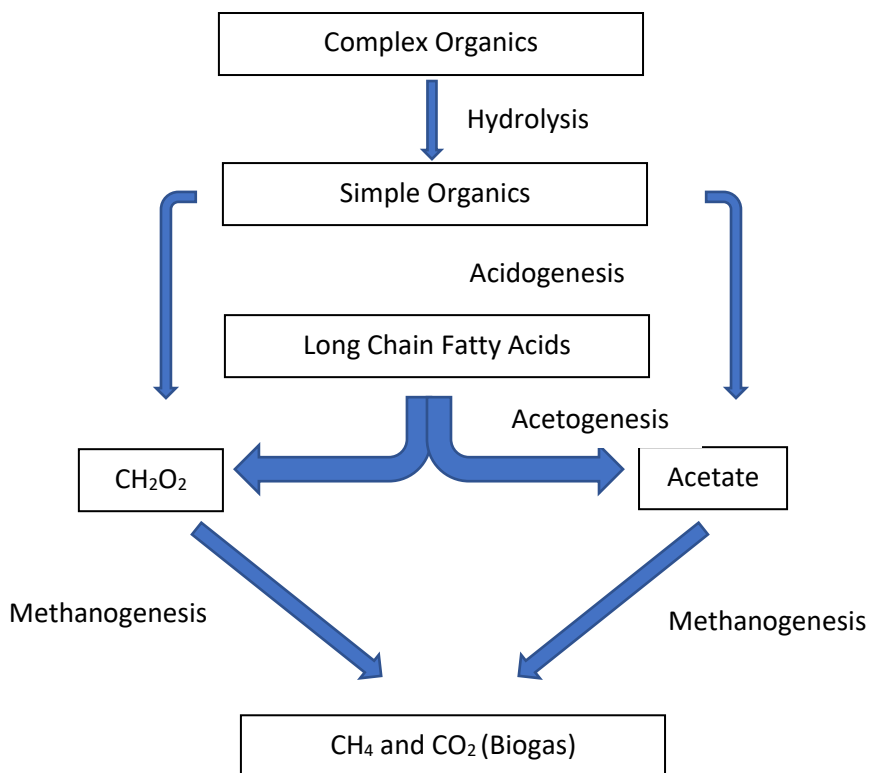


Figure 2.3 Anaerobic Process. Adapted from (Zhang *et al.*, 2014; Show & Lee, 2016).

b) Acidogenesis

This is the second step in the anaerobic digestion process. Acidogenesis is responsible for the conversion of the hydrolysed products into even simpler molecules with a lower molecular weight (Kondusamy & Kalamdhad, 2014).

Volatile fatty acids (VFA) are simple molecules and include acetic, propionic and butyric acid (Parawira, 2004; Kondusamy & Kalamdhad, 2014). The specific proportions of VFA's produced during this stage are important in the functioning of anaerobic digestion. Acetic acid and butyric acid are the precursors that are preferred in the formation of methane (Parawira, 2004). Other products produced during this stage include alcohols, aldehydes, hydrogen ammonia and carbon dioxide (Show & Lee, 2016). Of the by-products of acidogenesis, acetate is considered to be the most important of the intermediates (Show & Lee, 2016).

A great diversity of bacteria are responsible for the acidification, with most of the bacteria being anaerobic. The acidogenic bacteria can metabolise products at very low pH (Kondusamy & Kalamdhad, 2014). The acidogenic step is the fastest step in the anaerobic process (Parawira, 2004; Kondusamy & Kalamdhad, 2014).

c) Acetogenesis

During acetogenesis the products from acidification are converted into acetic acids, carbon dioxide and hydrogen by acetogenic bacteria (Kondusamy & Kalamdhad, 2014). Acetogenesis has two groups of active

bacteria. These two groups are hydrogen-producing acetogens and homoacetogens (Show & Lee, 2016). Homoacetogens however only contribute to roughly 2 % of acetate formation. Hydrogen-producing acetogens on the other hand catabolise organic acids, alcohols and other compounds to form acetate as well as CO₂ (Show & Lee, 2016). Homoacetogens do have a very important role in anaerobic digestion, even though they produce low levels of acetate. The homoacetogens utilise some of the hydrogen that is produced by the hydrogen-producing acetogens and in so doing decreases the total hydrogen in the system. Methanogens that utilise hydrogen have a higher affinity for hydrogen than homoacetogens, with both contributing to lower levels of hydrogen in the process (Show & Lee, 2016) This is very important as hydrogen is a growth inhibitor for hydrogen-producing acetogens (Buys, 2015). Hydrogen has some positive effects on the process with carbon dioxide being reduced to acetate in the presence of hydrogen (Show & Lee, 2016). There is therefore a very fine equilibrium that needs to be maintained with regards to hydrogen concentration, hydrogen producing acetogens and homoacetogens.

d) Methanogenesis

The final step in the anaerobic process is methanogenesis. During this stage methanogens utilise acetic acid, carbon dioxide and hydrogen. The result of this is ultimately the formation of methane as well as carbon dioxide (Kalyuzhnyi *et al.*, 2000).

Methanogens belong to the phylum Archaea. Two groups of methanogens have currently been identified (Show & Lee, 2016). The first group has 33 species and they reduce carbon dioxide and hydrogen to produce methane (Show & Lee, 2016). They also have the ability to utilise formate to produce methane. The 2nd group only has 14 species and these species utilise methanol, acetate and / or methylamines (Kondusamy & Kalamdhad, 2014; Show & Lee, 2016).

Around 70 % of the methane that is produced is from acetate with the remaining 30 % from the reduction of carbon dioxide to methane (Solera *et al.*, 2002). The growth rate of methanogenic bacteria is slow and grows at a similar rate to acetogenic bacteria, making this a possible rate limiting step (Solera *et al.*, 2002). Hydrolysis is only the rate limiting step during the breakdown of polymers and fats. If the reaction rate drops there is a possibility of acetic acid accumulating to toxic levels (Show & Lee, 2016). The methanogens are most active in the pH range 6.6 – 7.3 (Demirel & Scherer, 2008). At a pH below 6.2, it is possible for the methanogens to be inhibited (Demirel & Scherer, 2008). The accumulation of free ammonia could also act as an inhibitor. The threshold concentration for inhibition is when the pH goes above 7.4 (Demirel & Scherer, 2008). In order to combat rapid pH changes buffering capacity must be built into the reactor (Tauseef *et al.*, 2013).

2.5.3.2.2 Anaerobic general

As previously mentioned, anaerobic processes occur in the absence of oxygen. These processes have several advantages. In general anaerobic processes are simple to design and easy to operate (Eleutheria *et al.*, 2016).

The operating conditions required are not extreme as they are generally run at temperatures of 35° C, atmospheric pressure and usually at a pH of roughly 7.0 (Eleutheria *et al.*, 2016). The production of methane-rich biogas means that some of the energy can be recuperated. Methane production of the facility can be as large as 12×10^6 BTU of methane per 1 000 kg COD converted to methane (Show & Lee, 2016). Another advantage of anaerobic processes is the low sludge production volume as illustrated in Fig. 4 (Andreottola *et al.*, 2009; Mosse *et al.*, 2011).

Despite the many advantages of anaerobic processes there are the inevitable disadvantages. Possibly the biggest drawback with anaerobic processes is that there is production of many VFA's which emits a foul odour (Bories *et al.*, 2005). Methanogens have a slow growth rate leading to an increase in retention time for anaerobic reactors. Added to this is that methanogens are very sensitive to changes in environmental conditions (Show & Lee, 2016). Consequently, anaerobic reactors generally require a long start-up period as the bacteria require a long acclimatisation period (Andreottola *et al.*, 2009; Amani *et al.*, 2010).

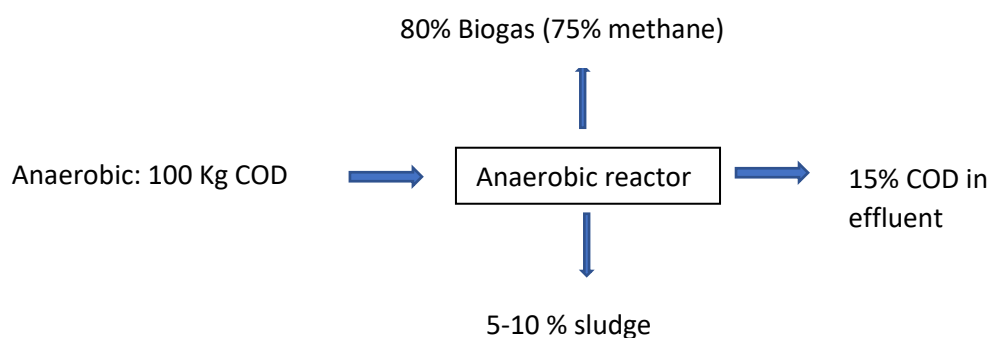


Figure 2.4 Representation of anaerobic process. Adapted from (Chetty & Pillay, 2015).

2.5.3.2.3 Applications of anaerobic processes

A number of studies have been conducted to assess the remediation of winery effluent using anaerobic processes (Ruiz *et al.*, 2002; Shao *et al.*, 2008; Lu *et al.*, 2015). An anaerobic sequencing batch reactor was used to treat brewery wastewater. When the COD was controlled between 1.5 and 5.0 kg COD. $\text{m}^{-3}.\text{d}^{-1}$ along with a hydraulic retention time (HRT) of 1 day the COD removal efficiency was more than 90 % (Shao *et al.*, 2008).

Another anaerobic sequencing batch reactor was used by Ruiz (2002) to treat winery wastewater. The reactor had a COD removal efficiency of greater than 98 % and it operated under the following conditions; Organic loading rate of 8.6 g COD. $\text{L}^{-1}.\text{d}^{-1}$, an HRT of 2.2 days and specific organic loading rate of 0.96 gCOD.gVSS $^{-1}.\text{d}^{-1}$ (Ruiz *et al.*, 2002).

The efficacy of a lab-scale UASB reactor treating starch wastewater was investigated using variable hydraulic retention times (HRT). The optimal HRT was found to be 6 h and COD removal efficiency was found to be between 81.1 – 98.7 % (Lu *et al.*, 2015).

A pilot-scale strengthened circulation anaerobic reactor was built with a working volume of 27 m³ to treat industrial textile wastewater. Influent COD had values between 1 398 – 4 143 mg.L⁻¹. The reactor had a HRT of 13.5 h and was able to reduce the COD by 62.7 % (Yang *et al.*, 2018).

Different anaerobic reactors with their advantages and disadvantages is represented in **Table 2.8**.

Table 2. 7 Comparison of aerobic and anaerobic processes.

| | Aerobic | Anaerobic |
|----------------|---|--|
| Start-up | Very short start-up | Long start-up period |
| Process | <ul style="list-style-type: none"> • High volume of sludge produced • Require many nutrients • Oxygen requirement (Energy to incorporate O₂) • Large reactor Volume Required • No malodours | <ul style="list-style-type: none"> • Low volume sludge production • Lower nutrient requirement • Zero O₂ requirement • Small reactor volumes sufficient • Biomass preserved up to years without activity deterioration • Malodour a.r.o. VFA accumulation |
| Carbon balance | <ul style="list-style-type: none"> • 40-50% CO₂ • 30-60% Sludge production | <ul style="list-style-type: none"> • 80-90% converted into biogas • 5-10% sludge production |
| Energy Balance | <ul style="list-style-type: none"> • 40% lost as heat • 60% used for new biomass • Energy used to incorporate oxygen | <ul style="list-style-type: none"> • 90% as methane • Only 5% lost as heat • 5-7% used for new biomass formation |
| Cost | <ul style="list-style-type: none"> • Low capital investment required • High operational costs | <ul style="list-style-type: none"> • Moderate capital investment required • Low operational costs |
| Development | <ul style="list-style-type: none"> • Developed and established | <ul style="list-style-type: none"> • Still developing |

Table 2. 8 Advantages and disadvantages of the various anaerobic treatments from selected publications.

| Treatment | Advantages | Disadvantages | COD Reduction | Reference |
|--------------------------|--|--|---------------|---|
| AnSBR | <ul style="list-style-type: none"> • Biogas production possible • Low sludge volume produced | <ul style="list-style-type: none"> • Batch feeding required • Moderate installation costs • Long start-up times | 90-98% | (Ruiz <i>et al.</i> , 2002; Shao <i>et al.</i> , 2008; Jiraprasertwong <i>et al.</i> , 2018) |
| UASB | <ul style="list-style-type: none"> • Low volumes of sludge produced • Good settleability. • Sludge is highly active | <ul style="list-style-type: none"> • High installation costs, • Scum accumulates on the water surface | 80-98% | (Keyser <i>et al.</i> , 2003; Moletta, 2005; Andreottola <i>et al.</i> , 2009; Lu <i>et al.</i> , 2015) |
| Covered anaerobic lagoon | <ul style="list-style-type: none"> • Biogas capture possible • Low capital investment | <ul style="list-style-type: none"> • Long start-up times | 65-95% | (Moletta, 2005; Blanco <i>et al.</i> , 2015) |

2.6 Anaerobic sequencing batch reactor

The anaerobic sequencing batch reactor (ANSBR) is a fill and draw system involving only one reactor in which all the steps of the process occur (Gurtekin, 2014). Sedimentation as well as clarification takes place in the sequencing batch reactor, but it differs from conventional activated sludge systems as everything occurs in the same tank (Gurtekin, 2014).

The ANSBR involves the repetition of four step cycle, being feed, react, settle and decant, however many studies have included a fifth stage named the idle stage (Sung & Dague, 1995; Shizas & Bagley, 2002; Sarti *et al.*, 2007; Gurtekin, 2014; Khanal *et al.*, 2017). These four steps are illustrated in **Figure 2.5**.

2.6.1 Feed

In the feeding step, wastewater is added to the biomass that remained from the previous cycle. It may either be raw wastewater or could even be primary effluent from another treatment process (Al-Rekabi *et al.*, 2007; Singh & Srivastava, 2011). Normally the volume fed into the reactor is equal to the volume decanted from the reactor (Sung & Dague, 1995). The volume of feed is determined by a number of factors, being the volume of the tank, number of, if any, parallel tanks in operation, the desired HRT, organic loading as well as the settling characteristics of the granular biomass (Sung & Dague, 1995; Al-Rekabi *et al.*, 2007).

The ANSBR may be fed using a batch process (shorter feeding time) or a fed-batch process (longer feeding time). There are two types of fill that can be implemented, depending on the objective of the process. This can be static fill or mixed fill (Gurtekin, 2014). During a static fill scenario there is no mixing taking place. Mixed fill is when the mixing mechanism is active while the influent is being fed into the reactor (Gurtekin, 2014).

2.6.2 React

The react step is widely regarded as the most important step in the process as it allows the biomass to consume the substrate and convert it to biogas (Sung & Dague, 1995; Gurtekin, 2014). The total react time can be 50 % or more of the cycle time (Al-Rekabi *et al.*, 2007). Mixing is required in this step in order to maximise the contact time and contact of the surface area of the biomass and the substrate (Sung & Dague, 1995).

2.6.3 Settle

Once the settle phase has started, mixing is shut down to allow the biomass to settle on the bottom of the reactor. Biomass settleability may differ depending on the size of the granules and the amount of biogas still trapped in the treated water (Sung & Dague, 1995). This phase may last for anything from 10 minutes to 90 minutes (Gurtekin, 2014). No clarifier is required as the clarification takes place in the tank (Al-Rekabi *et al.*, 2007).

2.6.4 Decant

Upon completion of the settle phase the supernatant is discharged as effluent through the discharge port. The discharge port is located at a predetermined level which would allow for the decantation of a specific volume of treated effluent (Al-Rekabi *et al.*, 2007). The effluent may be discharged using a pump or regulated by an automatic valve and in this way the flow rate can be maintained (Gurtekin, 2014). The time required for the decant phase may differ depending on the volume that needs to be decanted as well as the decanting rate that is required (Sung & Dague, 1995). The decant time may range from 5 % to 30 % of the total cycle time, however it should not be extended unnecessarily as it may cause sludge washout due to the rising of the biomass level (Gurtekin, 2014).

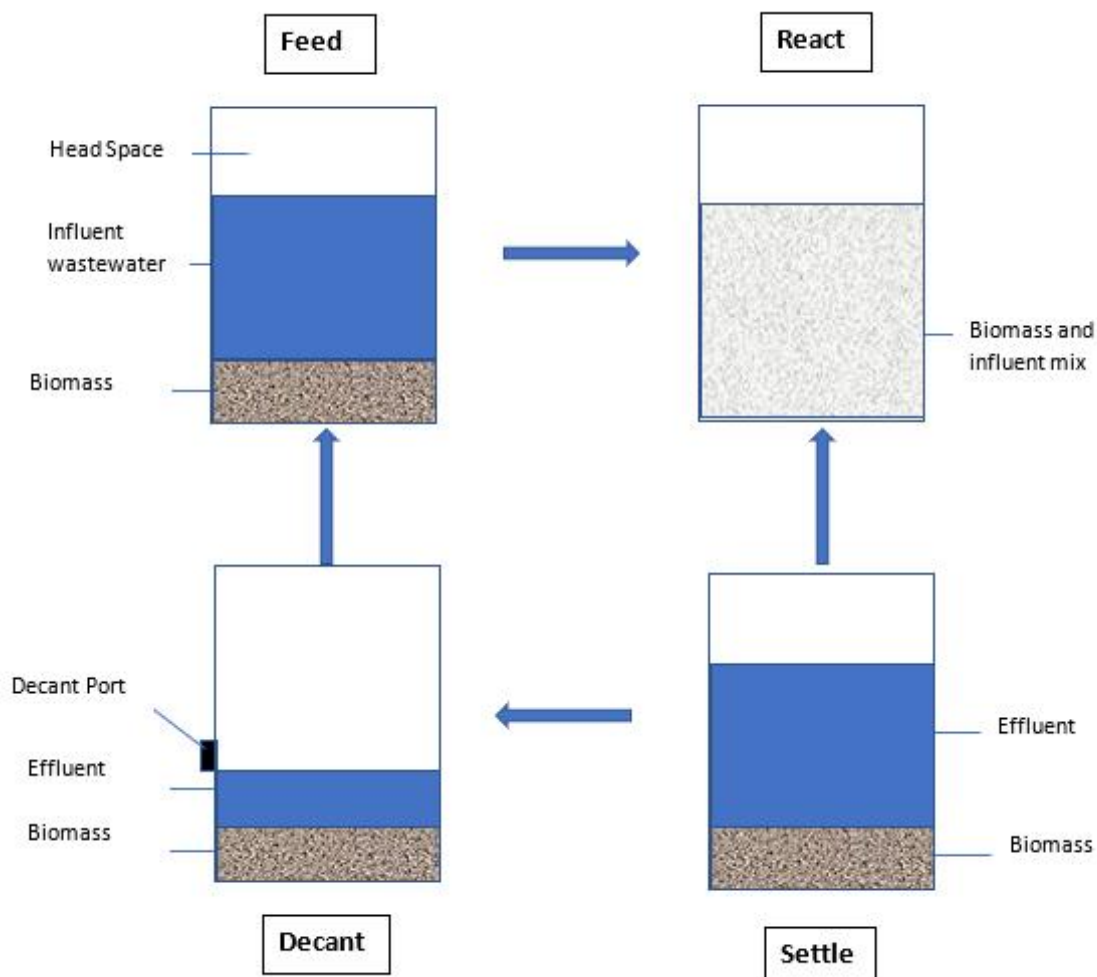


Figure 2.5 Illustration of the AnSBR process.

Advantages of AnSBR

- Flexible and can therefore treat a variable range of wastewater (Myra *et al.*, 2015). Can alter one or more of the operational control parameters such as mixing regime or feeding rate (Torrijos & Moletta, 1997)
- Static fill may enhance the formation of granule forming bacteria (Gurtekin, 2014)
- The adaptation of the sludge to varying operational conditions can lead to the system becoming robust and maintaining good performance, even when under shock from a high COD load (Gurtekin, 2014).
- Efficiently removes COD and produces methane-containing biogas (Shao *et al.*, 2008) (Myra *et al.*, 2015).
- No need for the use of an external clarifier as the clarification process happens during the process in the tank (Al-Rekabi *et al.*, 2007).
- Provides a good separation of biomass from the treated wastewater, leading to a lower loss of biomass during the decant phase (Sung & Dague, 1995; Gurtekin, 2014)
- All of the operations can occur in only one tank, decreasing the need for a big land area in order to process wastewater (Al-Rekabi *et al.*, 2007).

Disadvantages of AnSBR

- Requires a level of sophistication in the design as there are intricacies such as timing switches and specific controls (Gurtekin, 2014).
- Due to the higher level of automation required there is also a requirement for more regular maintenance in order to check and replace switches, automated valves etc. (Gurtekin, 2014).
- The reactor has a lower organic loading capacity compared to other water treatment options (Shizas & Bagley, 2002).
- Limited research on the applications of the AnSBR on winery wastewater on laboratory and pilot scale.

The differences between the anaerobic sequencing batch reactor and the upflow anaerobic sludge blanket is illustrated in **Table 2.9**.

Table 2. 9 Differences between the anaerobic sequencing batch reactor and the upflow anaerobic sludge blanket.

| UASB | AnSBR |
|---|---|
| <ul style="list-style-type: none"> • Continuous feeding of the reactor • External clarifier required • Mixing is not required • No gas displacement system required • Can only treat wastewater if low in suspended solids • Not effective settling and granular washout a possibility • No fluctuations of substrate around the granules • Application in the industry is widespread | <ul style="list-style-type: none"> • Batch fed • No external clarifier • Mixing is required (Could lead to biomass degradation if too vigorous) • Gas displacement system is required • Can treat wastewaters high in suspended solids • Granular washout less of a problem as it settles effectively during the settle phase • F:M ratio higher in the beginning of the cycle and lower towards the end of the cycle • Newer technology therefore less applications at present |

Adapted from (Sung & Dague, 1995; Angenent & Dague, 1996; Al-Rekabi *et al.*, 2007; Gurtekin, 2014).

2.7 Operational conditions that effect performance of the AnSBR

Anaerobic digestion of food waste is a complex system that must digest all the relevant carbohydrates, lipids and proteins in a single process (Zhang *et al.*, 2014). There are many operational parameters that are important to control in anaerobic digestion as the methanogens are sensitive to changes in their environment (Amani *et al.*, 2010). Operational parameters that should be controlled include temperature, pH, nutrients, mixing regime, feeding rate, OLR, hydraulic retention time (HRT), and toxicity (Amani *et al.*, 2010; Zhang *et al.*, 2014).

2.7.1 Temperature

It is possible for anaerobic reactors to operate at temperatures below 20°C, better known as the psychrophilic temperature range, however most anaerobic reactors operate in the mesophilic or thermophilic temperature ranges (Ward *et al.*, 2008). The different temperature ranges are summarised in **Table 2.10**. Thermophilic reactors have shown promise as experiments have indicated that thermophilic temperature ranges can increase the biogas production potential and consequently increase COD removal rate (Gannoun *et al.*, 2007).

Table 2. 10 Optimal temperature range of micro-organisms.

| Micro-organism class | Temperature range (°C) |
|----------------------|------------------------|
| Psychrophilic | 5-25 |
| Mesophilic | 30-35 |
| Thermophilic | 50-60 |

Reactors operating in the mesophilic temperature ranges have other advantages, namely higher process stability, lower VFA levels in the effluent, higher methane content, less inhibition of the product/substrate and possibly improvement of the degradation rates (Parawira, 2004; Ward *et al.*, 2008).

Control of the operational temperature of the reactor is essential, as a change in temperature of as little as 2°C can have detrimental effects on the efficiency of the reactor (Chae *et al.*, 2008; Ward *et al.*, 2008). Temperature fluctuations should therefore be kept to a minimum.

According to Chae *et al.* (2008) biogas yield increased from 317 to 437 mL CH₄.g VS⁻¹ when temperature of the reactor was increased from 25 to 35°C. Methane percentage was also affected by the change in temperature as only 82.6 % of the methane produced at 35°C was produced at 25°C. A similar study was performed to investigate the removal efficiency of COD and BOD at temperatures of 8, 15 and 23°C (Bodík *et al.*, 2002). The study found that for an HRT of 20 hours the COD as well as BOD removal rates were significantly higher in the 15 and 23°C reactors compared to the reactor operating at 8°C (Bodík *et al.*, 2002).

Heat is lost to the surroundings from the reactor if it is poorly insulated and should be properly insulated and mixed to maintain heat in the reactor (Buekens, 2005).

2.7.2 pH and alkalinity

Methanogens are very susceptible to changes in the pH of their environment (Amani *et al.*, 2010). Anaerobic digestion operates ideally at a pH range of 6.8-7.2, making control of pH a very important operational parameter (Gerardi, 2003; Ward *et al.*, 2008). If the pH drops to below 6.6 the growth rate of the methanogens is greatly reduced (Mosey & Fernandes, 1988). Conversely, granule disintegration can occur when the pH of the system becomes excessively alkaline (Sandberg & Ahring, 1992). Methanogens are however only one of the types of micro-organism present and each type of micro-organisms have their own specific optimum values. The optimum pH values required for hydrolysis and acidogenesis are substantially lower and fall into the pH range of 5.5-6.5 (Kim *et al.*, 2003; Ward *et al.*, 2008). Different optimal pH values of microbial populations is the reason why many people choose to use two stage anaerobic digestors to separate hydrolysis/acidification from acetogenesis and methanogenesis (Ward *et al.*, 2008). In a reactor using only one tank, the optimal pH of the process is governed by the optimal pH of the methanogens (Parawira, 2004). This is done to prevent the acid-forming bacteria becoming the dominant population and

leading to the accumulation of VFA's and subsequently, reactor failure (Parawira, 2004). In the event of increased VFA formation and subsequent pH drop, there are two strategies that can be employed to rectify the low pH. The first of these strategies is to stop the feed and allow the micro-organisms time to utilise the VFAs and reduce the concentration (Amani *et al.*, 2010). Another strategy would be to add bases and thereby raise the pH of the water and provide additional buffering capacity (Shizas & Bagley, 2002).

A study looked at different operational parameters for AnSBRs and evaluated pH as one of the important parameters (Laing, 2016). It was determined that a pH close to 7.30 is the optimal pH for a laboratory-scale AnSBR.

Alkalinity is also referred to as the buffering capacity of a system and is defined as the equilibrium of CO₂ and bicarbonate ions that provide a resistance to change in the overall pH of the system (Chernicharo, 2007). Compounds that provide buffering capacity at a pH of 7.0 include; carbonic acid (bicarbonate), hydrogen sulphide, dihydrogen phosphate and ammonia (Parawira, 2004).

Alkalinity is an important process parameter and can be used to monitor the anaerobic process, either as total alkalinity or partial alkalinity (Ward *et al.*, 2011). Total alkalinity includes the VFA buffering system compared to partial alkalinity, where the bicarbonate concentration is measured. Partial alkalinity has been proposed to be more sensitive in detecting process imbalances than total alkalinity (Jantsch & Mattiasson, 2004). Maintenance of total alkalinity is sufficient to prevent a decrease in pH of the reactor (Gerardi, 2003). Using only pH as a sole control means is not recommended as medium or well-buffered water can form a large volume of VFA's which cause a drop in pH, so monitoring of either VFA or alkalinity is essential (Lahav *et al.*, 2002).

The concentration of alkalinity, as either sodium bicarbonate (NaHCO₃) or calcium carbonate (CaCO₃), for optimal reactor performance is 1 000-3 000 mg.L⁻¹ (Amani *et al.*, 2010). A study was conducted on cheese whey to determine the ratio of alkalinity required to influent COD (Mockaitis *et al.*, 2006). The results showed that the initial concentration of alkalinity to COD should be 1:1 in the start-up phase of the reactor to maintain stability. For low COD levels (500 and 100 mg.L⁻¹) the alkalinity to COD ratio was determined to be 1:2 or 0.5mg alkalinity, as NaHCO₃, per 1mg COD. As the COD increased (2 000 and 40 000mg.L⁻¹) the ratio of alkalinity to COD was 1:4, or 25 % (Mockaitis *et al.*, 2006). This study showed that it may be useful to supplement alkalinity when wastewater is added to the reactor to maintain buffering capacity, regardless of the existing levels of alkalinity in the reactor.

2.7.3 Volatile fatty acids (VFAs)

During the monitoring of the anaerobic digestion process, VFA concentration is regarded as one of the most important parameters (Parawira, 2004). During anaerobic digestion processes, acetic acid is the predominant VFA, although propionic and butyric acids are more inhibitory to the anaerobic digestion process (Boone & Xun, 1987). The important fatty acids to monitor anaerobic digestion are butyrate and isobutyrate, as an increase in these fatty acids can indicate an overload of the reactor (Ward *et al.*, 2008). The reason behind

this is that the accumulation of VFAs results in the decrease of the pH value which leads to reactor failure (Parawira, 2004). Excessive concentrations of fatty acids along with hydrogen sulphide and ammonia are toxic and inhibit methanogenesis only when in their un-ionised forms. This is pH dependant and ammonia is un-ionised at pH values above 7 whereas fatty acids and hydrogen sulphide are toxic at pH values below 7. As winery wastewater generally has a lower pH value of around 6, it shows the importance of monitoring VFA concentration for the overall stability of the process (Vlyssides *et al.*, 2005).

2.7.4 Nutrients

Nitrogen and phosphorous, in their soluble form, are required in relatively high concentrations in an anaerobic reactor for optimum growth (Saleh & Mahmood, 2004; Amani *et al.*, 2010). Along with these nutrients, other micro-nutrients and trace elements are also required, although in significantly smaller quantities. These include barium, calcium, cobalt, copper, iron, magnesium, manganese, molybdenum, nickel, potassium, selenium, sulphur, tungsten and zinc (Rajeshwari *et al.*, 2000; Amani *et al.*, 2010). Generally, industrial wastewaters are high in these micronutrients, but the wastewater must still be analysed to determine whether some of these micronutrients should be added (Amani *et al.*, 2010). Some of these micronutrients and trace elements play important roles in the metabolism of methanogenic archaea (Khanal *et al.*, 2017). Nickel is important as it is a structural constituent of a factor called F430, which is found in methanogens. Cobalt is also important as it is a structural component of vitamin B12, which is used as a catalyst for methanogenic activity (Khanal *et al.*, 2017).

For optimal performance of the anaerobic digester, it is important to control the COD:N:P ratio. It must be in the range of 200:5:1 to 350:7:1 for low loading wastewaters and 1000:7:1 for high strength wastewaters (Rajeshwari *et al.*, 2000; Ammary, 2004; Amani *et al.*, 2010).

Carbon to nitrogen and carbon to phosphorous are two important ratios as they are used to determine the nutrient requirements of high-strength wastewaters. The desired ranges are 20:1 to 30:1 for C:N ratio and around 50:1 for C:P ratio. If the C:N ratio is lower than the optimal, then this will result in an accumulation of ammonia, resulting in inhibition of methanogenesis. Conversely, a high C:N ratio will result in lower gas production as the nitrogen will be rapidly utilised by the methanogens (Buekens, 2005).

In the study published by Ammary *et al.* (2004) they were able to reduce COD by 80 % when using a COD:N:P ratio of 900:5:1.7 in the anaerobic treatment of olive mill wastewater. A study conducted in 2010 compared COD:N:P ratios of 100:5:1 with a ratio of 100:5:0 (Tang & Liu, 2010). The effects of the differing ratios were that granulation happened more rapidly in the 100:5:1 ratio than in the 100:5:0. This study illustrates the importance for phosphorous in the granulation of the biomass during the start-up of a reactor.

2.7.5 Organic loading rate (OLR)

Organic loading rate is defined as the mass of organic matter (COD) per unit reactor volume per unit time (Khanal *et al.*, 2017). Industries such as winery, brewery and other agro-based industries produce

wastewater with very high organic content. When wastewater with a very high COD is introduced into the reactor, it could cause the reactor to fail (Zaher *et al.*, 2007). This happens as the acidogenic bacteria multiply rapidly when exposed to enough substrate. The methanogenic bacteria are not able to multiply at the same pace leading to an accumulation of acidogenic bacteria (Amani *et al.*, 2010). This would result in an increase in the formation of VFA's and therefore the subsequent decrease in pH of the reactor (Demirel & Scherer, 2008). This results in a decrease in the methanogenic population and the relative production of more VFA's until the reactor fails as a result (Zaher *et al.*, 2007; Demirel & Scherer, 2008). Well performing reactors are more at risk to sudden increases in OLR as they have a shortage of key microbial populations and are therefore less robust as a result (Amani *et al.*, 2010).

The OLR's implemented in anaerobic reactors varies greatly, depending on the substrates and their characteristics. Mockaitis *et al.* (2006) implemented organic loading rate of $0.59 \text{ kgCOD.m}^{-3}.\text{d}^{-1}$. A study conducted on brewery wastewater used organic loading rates of 1.5 to $5.0 \text{ kg COD.m}^{-3}.\text{d}^{-1}$. COD removal efficiency was able to reach 90 % for the OLR and various other operational parameters (Shao *et al.*, 2008). Winery wastewater was treated using an AnSBR and the OLR was determined to be $8.6 \text{ kg COD.m}^{-3}.\text{d}^{-1}$ (Ruiz *et al.*, 2002). COD reduction percentage for a hydraulic retention time of 2.2 days was found to be greater than 98 % at this specific OLR (Ruiz *et al.*, 2002). Olive mill wastewater and abattoir wastewaters were co-digested using an upflow anaerobic filter at mesophilic and thermophilic temperatures (Gannoun *et al.*, 2007). The OLR varied from 3 to $9 \text{ kgCOD.m}^{-3}.\text{d}^{-1}$ under mesophilic conditions and ranged from 4.1 to $12 \text{ kg.m}^{-3}.\text{d}^{-1}$ under thermophilic conditions (Gannoun *et al.*, 2007).

These studies illustrate the variation in OLR in literature, depending on the substrate being utilised, hydraulic retention time and temperature of the reactor, among other factors.

2.7.6 Mixing regime

Mixing of the contents of an AnSBR is done to ensure consistent conditions throughout the reactor. This is done by enabling the suspended biomass to be circulated throughout the reactor, thereby interacting with a greater volume of water in the reactor. Conditions are kept constant as a result of efficient heat transfer as well as the fact that mixing can cause degradation of organic matter resulting in an increase in surface area, therefore faster reaction times (Karim *et al.*, 2005). Another reason mixing is required is to release gas bubbles that may be trapped. Mixing, either intermittent or continuous, is used to prevent biomass sedimentation to the bottom of the reactor (Ward *et al.*, 2008; Ghanimeh *et al.*, 2012; Huang *et al.*, 2018).

As mentioned above, reactors, be it aerobic or anaerobic, have different mixing regimes that can be implemented. These include continuous or intermittent mixing and it also includes use of different approaches such as mechanical mixing, with aid of an impeller, recirculation of the biogas using air pumps and recirculation of the contents of the digester (Karim *et al.*, 2005; Ward *et al.*, 2008). Whilst none of these approaches offers clear advantages, it is important to consider the speed of mixing conditions as slow speed mixing conditions are associated with more stable reactor conditions (Gomez *et al.*, 2006).

The granular structure of sludge within anaerobic reactors is important for the digestibility of organic compounds in the wastewater (Ward *et al.*, 2008). Excessive agitation of the reactor could result in granule degradation and therefore a decrease in the ability to digest organic substrate (McMahon *et al.*, 2001). Homogenous distribution of granules and organic matter is accomplished using molecular diffusion in laminar flow (Stroock *et al.*, 2002). Rate of flow is increased when turbulence is induced, resulting in large gradients in velocity as well as high shear rates (Huang *et al.*, 2018). High shear rates increase the forces on the bacterial granules resulting in damage of the bacterial cells and ultimately tearing of the sludge (Huang *et al.*, 2018).

A study published in 2012 compared two reactors performing under similar conditions. One of the reactors was continuously slow stirred, whilst the other reactor was not agitated (Ghanimeh *et al.*, 2012). Initially both reactors showed similar trends during start-up when considering methane production. Continuous stirring however resulted in a more stable reactor as indicated by lower VFA levels, lower VFA:Alkalinity and decreased levels of propionate. Further the stirred reactor also resulted in an ultimate higher loading capacity as well as increase in COD removal rate.

Karim *et al.* (2005) compared the efficacy of different modes of mixing namely; unmixed, biogas recirculation, impeller mixing and slurry recirculation. These experiments were repeated at increasing COD concentrations. At the lowest concentration there was no significant differences between any of the mixing regimes. As the concentration increased the mixed reactors showed significant increases in methane production rate when compared to the unmixed reactor. The reactors mixed with the impeller and the reactor mixed by slurry recirculation showed the highest methane yield. At the highest concentration the slurry mixed recirculation could not be done as it was not possible due to large amounts of slurry, indicating a shortcoming in this mixing technique. The unmixed reactor showed low methane production yield whereas the biogas mixed reactor resulted in the highest methane yield. Mixing was shown to be important in the production of methane and therefore also COD removal when compared to unmixed reactors.

Laing (2016) investigated the optimal mixing parameters for the treatment of synthetic winery wastewater using an AnSBR. The reactor had a volume of 14.7 L and it was determined that less frequent mixing was optimal based on performance efficiency parameters such as COD reduction (%) and methane percentage of the biogas. The optimal mixing interval was found to be every 110.5 minutes. The water was recirculated in the reactor using a washing machine pump.

Stroot *et al.* (2001) investigated the effect of mixing conditions, i.e. stirred continuously and intermittently, on digester performance. Laboratory scale reactors were used in this experiment. The conclusion of this study was that reducing the amount of mixing improved the performance of the reactor. Lower levels of mixing resulted in more stable reactors when subjected to high OLR. This study also showed that a reactor that is unstable could be stabilised by altering the mixing level from continuous to intermittent. The results show the importance of mixing, but it is necessary to limit the amount of mixing to avoid

instability. These experiments were however performed at laboratory-scale and with an extremely small working volume of only 500 mL so the results should be taken with caution.

Continuously stirred reactors can be effective for removal of COD. A study was performed by Mockaitis *et al.* (2006) to investigate the effect of supplemental alkalinity and OLR. This meant that different mixing regimes were not investigated. The results still show that continuously stirred reactors with an impeller can achieve good COD reductions. The mixing was done at 50 RPM at lower concentrations up to 2 000 mg.L⁻¹ COD and 75 RPM at 4 000 mg.L⁻¹ COD. None of the reactors had a COD removal of 90 %. Despite not comparing mixing regimes directly, an indirect observation can illustrate that continuous stirring can result in good COD removal rates on the condition that the stirring rate is kept relatively low.

A magnetic stirrer was used with an AnSBR when treating brewery wastewater (Shao *et al.*, 2008). The COD content of the wastewater ranged from 1 500 – 5 000 mg.L⁻¹. The stirrer was operated at 150 RPM and this experiment resulted in a COD reduction of above 90 % (Shao *et al.*, 2008). This once again illustrates that mixing intensity should be investigated on a case by case basis, but caution should be exercised to ensure that granule disintegration is not a problem.

In a study conducted in 2003, synthetic domestic wastewater was treated in an AnSBR (Rodrigues *et al.*, 2003). The experiment compared different mixing rates in the COD reduction efficiency. The working volume of the reactor was 2.0 litres as it was a laboratory-scale experiment and treated a COD of 500 mg.L⁻¹. The agitation rates varied from no mixing to 75 RPM using an impeller. The results showed that at 50 RPM there was good solids retention and a COD reduction of approximately 88 % was achieved. At 75 RPM there was granule breakup and therefore was not viable as an option. Agitation of the reactor led to a decrease in total cycle time.

Mixing regime, with regards to intensity and duration of mixing, is a very important process control parameter. It can lead to a more efficient reactor that becomes more cost effective as it reduces the cycle time, however caution should be exercised when choosing a mixing regime, as overmixing, vigorous mixing and improper impeller design could lead to degradation of the biomass and subsequently, biomass washout.

2.7.7 Inhibition and toxicity

Industrial effluents may contain toxic substances or they may be generated by the microorganisms themselves, as a result of their metabolic activity during the anaerobic digestion process (Khanal *et al.*, 2017). Toxic substances that may be present in wastewater include ammonia, heavy metals, cyanide, phenol and halogenated compounds (Khanal *et al.*, 2017). Microorganisms are responsible for the presence of ammonia, sulphide as well as long-chain fatty acids (Khanal *et al.*, 2017). There is however a lot of variation in the inhibition or toxicity levels for most substances as reported in literature (Chen *et al.*, 2008). Acclimation, synergism, antagonism and complexing leads to the observed variation in inhibitory concentrations (Chen *et al.*, 2008)

An inhibitory substance is defined by the ability to shift the microbial population or inhibit bacterial growth (Chen *et al.*, 2008). Inhibition of the anaerobic digestion process can manifest in various ways such as a decrease in microbial population, VFA accumulation and a reduction in pH (Amani *et al.*, 2010).

Ammonia is produced in its free and ionised form by the anaerobic degradation of nitrogenous compounds (Chen *et al.*, 2008; Amani *et al.*, 2010). An increase in ammonia concentration leads to a lower rate of glucose degradation as a result of inhibition of glycolytic pathways (Mata-Alvarez *et al.*, 2000). Ammonia in its free form and at a concentration above 700 – 1 700 mg.L⁻¹ is the most toxic form as it can pass through the cell membrane, leading to an imbalance in protons as well as a potassium deficiency within the microbial cell (Nakakubo *et al.*, 2008; Amani *et al.*, 2010). Ionic ammonia on the other hand is less toxic and the system can handle concentrations of up to 5 000 mg.L⁻¹ and only experience a decrease in efficacy of methanogens by 50 % (Sung & Liu, 2003). The effect that pH has on the ionised to free ammonia concentration is very important. As the pH within the reactor increases, the ratio of free ammonia to ionised ammonia increases, thereby increasing the toxicity level (Amani *et al.*, 2010). To avoid ammonia toxicity it is important to keep the pH in the range of 6.8 - 7.2, to dilute the contents of the reactor or by increasing the organic load and thereby increase the C:N ratio (Mata-Alvarez *et al.*, 2000; Amani *et al.*, 2010).

Ammonia is not the only substance that can cause inhibition and toxicity. Sulphate is a compound that is often found in wastewaters (Chen *et al.*, 2008). The reduction of sulphate to sulphide is accomplished by the action of sulphate reducing bacteria (SRB) (Hilton & Oleszkiewicz, 1988). Sulphides can inhibit methanogenesis in one of two ways, namely primary and secondary inhibition (Chen *et al.*, 2008). Primary inhibition is characterised by suppression of methane production by the competitive inhibition of SRB, i.e. the SRB utilises compounds that are also used for methanogenesis (Chen *et al.*, 2008; Luo *et al.*, 2015). SRB have a kinetic advantage over methanogens as they have a higher maximum specific growth rate as well as a lower half saturation value (Luo *et al.*, 2015). This allows the SRB to compete more vigorously for acetate and hydrogen which is a common intermediate in methanogenesis (Wang & Banks, 2007). Secondary inhibition is characterised by bacterial groups being susceptible to sulphide (Chen *et al.*, 2008).

When an experiment kept the sulphide concentration at a value that was roughly 250 mg.L⁻¹ the COD removal percentage saw a decrease from close to 80 % to a level of 32 % (Yilmaz *et al.*, 2012). It is possible to decrease the effect of sulphide inhibition by dosing the reactor with FeCl₃ (Luo *et al.*, 2015). The COD:SO₄²⁻ ratio of a UASB treating starch wastewater was decreased to study the influence on granule formation (Lu *et al.*, 2016). A decrease in this ratio from 10 to 2 resulted in a higher proportion of granules larger than 2.8 mm from less than 10 % to 58.8 - 69.4 % of the granules. (Lu *et al.*, 2016). The granules also developed filaments that were hydrophilic and had a high affinity for biogas bubbles, facilitating biomass washout (Lu *et al.*, 2016). Dosing FeCl₃ decreases sulphate reduction and results in iron sulphide precipitation instead (Luo *et al.*, 2015).

It is however possible for methanogenic bacteria and sulphates to exist in the same system (Vossoughi *et al.*, 2003). When COD:SO₄ ratio was decreased from 16.7 to 6 by increasing the SO₄ concentration the COD removal percentage was not affected and was 86 % (Vossoughi *et al.*, 2003).

Minerals such as: sodium, potassium, calcium, sulphur, Ammonium and magnesium are important for proliferation of bacterial populations on the condition that the concentrations are kept relatively low (Zaher *et al.*, 2007; Chen *et al.*, 2008). An increase in the concentrations of these minerals could cause inhibition of the methanogenic process. (Zaher *et al.*, 2007; Chen *et al.*, 2008). These elements can be released by the breakdown of organic matter during the anaerobic process, or by addition of salts to adjust the pH of the reactor (Chen *et al.*, 2008). The inhibitory concentrations for some minerals are as follows: magnesium shows moderate inhibition at concentrations between 1 000-1 500 mg.L⁻¹ and strong inhibition occurs at concentration above 3 000 mg.L⁻¹; The concentrations for moderate and strong inhibition for potassium are 2 500 - 4 500 mg.L⁻¹ and 12 000 mg.L⁻¹ respectively; Levels of sodium to have shown moderate and strong inhibition is reported as 3 500 - 5 500 mg.L⁻¹ and 8 000mg.L⁻¹; calcium inhibition occurs at 2 500 - 4 500 mg.L⁻¹ and 8 000 mg.L⁻¹ (Zaher *et al.*, 2007).

Toxic metals are a concern in anaerobic degradation as they can be found in large quantities in sludge as well as sewage (Chen *et al.*, 2008). The concern with toxic metals in the water is that there is an accumulation to the point where they may become toxic. This is due to the fact that they are not biodegradable and the anaerobic bacteria are not able to remove them from the reactor (Chen *et al.*, 2008). The most important, or toxic, metals include copper, zinc, nickel, chromium, iron and cobalt (Zaher *et al.*, 2007).

One last factor that may contribute to inhibition of the anaerobic bacteria is low temperature (Luo *et al.*, 2015). Temperature directly affects anaerobic digestion rate and generally the reactors operate best at mesophilic and thermophilic temperatures (Gannoun *et al.*, 2007; Ward *et al.*, 2008; Luo *et al.*, 2015). As mentioned previously, reactors operating in the mesophilic and thermophilic temperature range have process advantages. One of the main reasons that low temperatures become an issue is due to the costs of keeping the reactor at the required temperature as well as extra capital expenditure (Zaher *et al.*, 2007; Luo *et al.*, 2015).

Inhibition and toxicity clearly have many causes and it is essential to keep these parameters under control to keep the reactor functioning optimally as well as to avoid the eventual failure of the reactor.

2.7.8 HRT

Hydraulic retention time (HRT) is the measure of the flow of substrate into and out of the reactor (Zaher *et al.*, 2007). It is determined by the average time taken for the organic contents of the reactor to be digested (Zaher *et al.*, 2007). The HRT should be kept at a minimum time that eliminates dead zones in the reactor, so that complete digestion can occur (Amani *et al.*, 2010). This optimal time is dependent on various factors such as feedstock, time of year and process details (Buekens, 2005). With longer residence time, the rate of

degradation decreases, therefore complete digestion will not take place and the process should be optimised taking financial implications into consideration (Buekens, 2005).

The HRT is generally up to 3 days, but different times have been experimented with in literature (Sung & Dague, 1995; Ruiz *et al.*, 2002; Shizas & Bagley, 2002). An HRT of 1 day was used with varying OLR's and achieved a COD removal percentage of 90 % (Shao *et al.*, 2008). A different study used an HRT of 2.2 days with varying OLR's and subsequently achieved a COD removal rate of more than 98 % (Ruiz *et al.*, 2002). The following formula is used to determine the HRT (Shizas & Bagley, 2002).

$$HRT = \frac{\text{Volume of reactor}}{(\text{Volume decanted per cycle})(\text{Cycles per day})}$$

2.8 Chemical quantification methods

Laboratory quantification methods are of vital importance to determine many process markers to characterise the water in terms of quality. The following tests are some of the most important that need to be conducted during anaerobic digestion. This includes tests for; total alkalinity; turbidity; pH; VFA's; polyphenols; total dissolved solids (TDS); electrical conductivity, total suspended solids (TSS) and COD (APHA, 2005). Many of these tests such as; alkalinity; turbidity; pH; total polyphenols and TDS; can be conducted using calibrated meters and simple titrations and are therefore rapid and accurate. Two very important parameters to determine for process stability in anaerobic digesters are COD and TSS. The tests for these parameters are however time consuming.

COD is an indicator that is used to determine the degree of organic pollution of water (Yang *et al.*, 2009; Pan *et al.*, 2011). Routinely, the determination of COD is performed in a laboratory and is a time consuming method that requires chemical reactions, the reaction with potassium dichromate, to quantify the levels in water (Yang *et al.*, 2009; Pan *et al.*, 2011). Total suspended solids are the solids that remain on a filter paper once it has been dried. It may affect effluent quality adversely (APHA, 2005). Both these methods take anywhere between 150 and 180 minutes.

Rapid methods using Near Infrared (NIR) spectroscopy have been used to quantify both COD and TSS in wastewater. NIR is rapid, a non-destructive, simultaneous measurement of different parameters. This allows it to give representation of the entire process instead of just a window into the process (Huang *et al.*, 2008; Perlins Sánchez, 2014).

Numerous studies have been performed which illustrate the ability of NIR to predict COD concentrations in different wastewaters (Páscoa *et al.*, 2008; Sarragaça *et al.*, 2009; Yang *et al.*, 2009; Pan *et al.*, 2011; Melendez-Pastor *et al.*, 2013; Dahlbacka *et al.*, 2014). Similarly, studies have been performed that illustrate the potential of NIR to predict TSS values (Páscoa *et al.*, 2008; Sarragaça *et al.*, 2009).

2.9 Near-infrared (NIR) spectroscopy

The discovery of Near-Infrared (NIR) spectroscopy can be ascribed to Herschel in the year 1800 (Siesler *et al.*, 2008). From its first use in industry in the mid 1900's, NIR has made immeasurable progress with increasing advances in the technology (Siesler *et al.*, 2008).

The wavelength region of 780 – 2 500 nm is the region in which NIR is located and is often referred to as the overtone region (Pasquini, 2003; Siesler *et al.*, 2008). This is so because the NIR absorption of polymers originates from the first overtones of N-H, C-H, S-H and O-H bending and stretching vibrations, making measurements in the organic and biological fields feasible (Huang *et al.*, 2008; Zhang *et al.*, 2009b). The specific wavelength range supplies molecules with enough energy to reach the lowest, excited vibrational state (Pasquini, 2003). The spectrum originates from the transferral of radiation energy to mechanical energy and can be observed because of molecular vibrations associated with the energy absorption (Pasquini, 2003; Siesler *et al.*, 2008). Radiation that interacts with the sample of interest can interact in 3 different ways namely being absorbed, reflected or transmitted (Huang *et al.*, 2008). These 3 interactions can then be further classified into 5 measurement modes being transmittance, transreflectance, diffuse reflectance, interactance and transmittance through a scattering media (Pasquini, 2003).

Conventional UV-Vis spectroscopy makes use of transmittance, where substances that are transparent are measured in glass or quartz cuvettes with varying path lengths (Pasquini, 2003). Transreflectance is similar to absorbance in that the radiation passes through the transparent sample, but then is reflected back through the sample for a 2nd time using mirrors, in essence doubling the path length before it reaches the detector (Halsey, 1985; Pasquini, 2003). Beer's Law is applicable for the use of transmittance and transreflectance as the concentration of a substance has a linear relationship to the absorbance of that specific substance, therefore if the concentration of a substance of interest is higher, then absorption will be increased for that substance (Pasquini, 2003). Diffuse reflectance is affected by the absorbance and scattering of solid granules which change the intensity of the signal (Malin *et al.*, 1999). For interactance mode the probability of the incident beam to interact with the sample is higher than the probability of it being reflected from the surface. The beam emerging from the sample contains specific information regarding the composition of the sample (Siesler *et al.*, 2008). Transmittance through a dense sample has been used to quantify the active components of certain pharmacological compounds. This is because there is a longer pathlength as a result of internal scattering of light, giving a better representation of the average constituents of the sample (Pasquini, 2003). The above is illustrated in **figure 2.6** below with a) representing transmittance, b) transreflectance, c) diffuse reflectance, d) interactance, e) transmittance through scattering media.

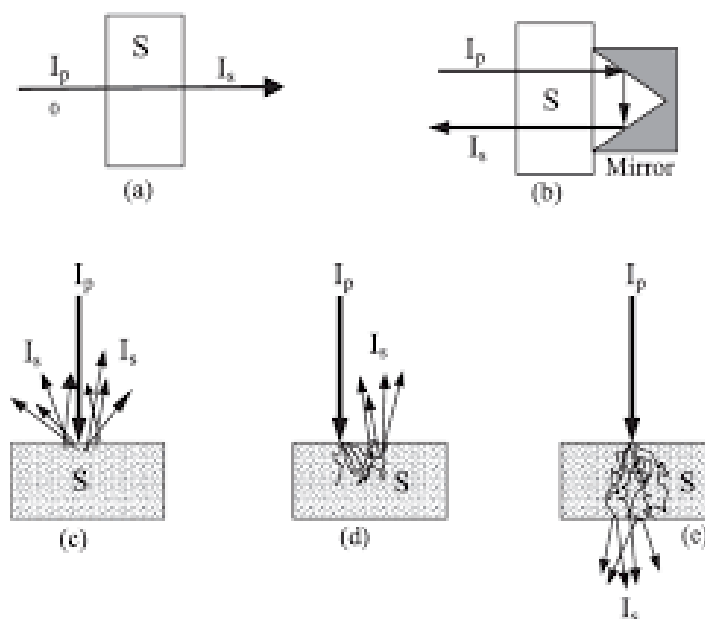


Figure 2.6 Different modes of spectral acquisition; (a) transmittance, (b) transflectance, (c) diffuse reflectance, (d) interactance, (e) transmittance through scattering media.

NIR spectroscopy is a very powerful tool that has the potential to be used for quantitative and qualitative purposes, but needs to be used in conjunction with chemometric techniques for complete analysis (Zhang *et al.*, 2009b). Chemometrics is defined as the use of mathematics and statistics to extract proper information from the spectral data (Pasquini, 2003). Spectra obtained from the near-infrared region is full of information and therefore is very advantageous. To extract the correct information from the spectra precise spectral analysis must be done or it could lead to incorrect information being extracted (Ozaki *et al.*, 2006). NIR spectra data can often suffer from baseline shifts as well as variations (Li Vigni, 2013). These disturbances can be caused by the following; Scattering of light from solids or turbid solutions; pathlength variations that can lead to poor reproducibility; difference in temperature, density and size as well as distribution of the sample; lastly spectral noise from an amplifier or detector (Ozaki *et al.*, 2006; Siesler *et al.*, 2008). There are four types of pre-treatment methods namely noise reduction; baseline correction; resolution and enhancement and centering and normalisation (Ozaki *et al.*, 2006).

Noise reduction methods are implemented to reduce the noise associated with chemical or physical interferences (Vannucci *et al.*, 2005). The noise can be high or low frequency with high frequency noise associated with the instrument's electronic circuits and detector (Bevilacqua *et al.*, 2013). Low frequency noise can be caused by drift in the instrumentation (Ozaki *et al.*, 2006). Baseline correction are used to correct baseline shifts that have occurred due to reasons listed earlier in this section. Resolution enhancement methods have been used to separate overlapping bands and amplifying bands that are obscured (Ozaki *et al.*, 2006). Mean centering is used to reposition the centre of the data to the origin of the coordinate system and normalisation is an alteration to data that results in equal magnitudes for each sample (Bevilacqua *et al.*, 2013). There are many different methods to elucidate the correct information from a data

set after pre-treatment and these techniques can be summarised in 11 different methods as defined by Ozaki *et al* (2006).

- PCA loading plots
- Derivative spectra
- Isotope exchange
- Curve fitting
- Analysis from group frequencies
- Analysis from perturbations
- Correlation between the spectra and chemical structure
- Fourier self-deconvolution
- Difference spectra
- Spectral interpretation by polarisation measurements
- Theoretical calculations of frequencies of bands.

NIR spectroscopy is clearly a very useful technology when used in conjunction with chemometrics and can extract important information. NIR has been applied to wastewater in the past to extract relevant information relating to operating parameters.

2.10 NIR for determination of COD and TSS in literature

NIR spectroscopy has been used to determine COD and TSS values for the purpose of in-line monitoring of reactors. COD was determined along with BOD using NIR spectroscopy treating domestic sewage (Yang *et al.*, 2009). Samples (120) were analysed using NIR spectroscopy and compared to standard methods for determination of COD and BOD. Each sample was scanned three times and then averaged to obtain one average spectra. Pre-treatment of the data was performed and smoothing, Savitsky-Golay 1st derivative and 2nd derivative was compared. Partial least squares regression was used to quantify COD and BOD from the spectral data. Correlation coefficients of the models were high at 0.9542 and 0.9652 for COD and BOD, respectively. A good indicator for model accuracy for quantification is the root mean square error of prediction (RMSEP) and the RMSEP for COD and BOD were 25.24 and 12.13 mg.L⁻¹ respectively. The range of measured values were 496.6 mg.L⁻¹ and 289.2 mg.L⁻¹ for COD and BOD. This translates to error values of 5.1 % for COD quantification and 4.2 % for BOD determination, which can be considered very accurate and within allowable error ranges for process control requirements (Yang *et al.*, 2009).

The range error ratio (RER) is equal to the range of the compositional values divided by the SEP and it provides thresholds to determine model performance. An RER value of more than four is applicable for screening method, a value of more than 10 indicates that the model is acceptable for quality control purposes and a value of above 15 means the model can be used to for quantification. Unfortunately, this study does not provide a SEP value and therefore RER cannot be calculated from it.

For the prediction model, 10 samples were used and compared to their predicted value obtained from the model. The error of prediction for COD and BOD was 1.48 % and 1.66 %, respectively, indicating a very accurate model capable of predicting COD and BOD to a level similar to that of the standard methods (Yang *et al.*, 2009).

An aerobic reactor was used to treat dairy residues and was monitored on-line by NIR spectroscopy using a transreflectance probe (Páscoa *et al.*, 2008). The wavelengths obtained from the probe were from 900 – 1 700 nm. A total of 48 samples were collected and each sample was scanned 32 times and an average spectrum obtained and these spectra were compared to reference values for COD, TS and TSS. Standard normal variate and Savitsky-Golay filtering (45 nm filtering window, 2nd order polynomial and 1st derivative) was applied as pre-processing for the model. The models were applied successfully to determine COD, TS and TSS. The models for COD showed a RER value of 9.8 and 12.5 using standard normal variate in combination with Savitsky-Golay filtering and for Savitsky-Golay filtering respectively. Together with the RER value the root mean square error of cross validation (RMSECV) was 67.4 and 86.6 mg.L⁻¹ COD. This indicates that the model was fairly accurate and according to RER values it is possible to use NIR to predict COD for the purpose of screening (Páscoa *et al.*, 2008). This study also looked at TS and TSS values and the RER values were 15.6 and 15.8, respectively. The RPD values were 3.48 and 3.54 for TS and TSS, respectively. In order for a model to be used for process control, it is necessary for the RER and RPD to be above 15 and 3.5 respectively (Páscoa *et al.*, 2008). Results obtained from this study showed that NIR in conjunction with the appropriate pre-processing can predict TS, TSS and COD values to a fairly accurate degree (Páscoa *et al.*, 2008).

Wavelength selection is important to determine specific characteristics of wastewater using NIR. Wavelength selection was implemented using moving window partial least square (MWPLS) (Pan *et al.*, 2011). Sugar refinery wastewater was used in this study and 81 samples in total were collected. A reference chemical method was used to determine the COD for a specific sample using the potassium permanganate oxidation method. The spectral region used was 400 – 2 500 nm. Each sample was scanned 3 times and one average spectrum was calculated. When the whole spectrum was investigated a RMSEP value of 82.4 mg.L⁻¹ was obtained which translates into an error of 25.2 % when compared to the range of 55 to 382 (327). When MWPLS was used to determine the optimal wavelength range of 820 – 850 nm the RMSEP was reduced to 25.5 mg.L⁻¹ which is equivalent to an error of 7.8 %. This study clearly indicates that when using wavelength selection strategies, the accuracy of a computer based NIR model can be increased (Pan *et al.*, 2011).

A lab-scale anaerobic digester was used to determine the COD of synthetic wastewater using a NIR spectrophotometer (Sarraguça *et al.*, 2009). The wavelength range of the specific instrument was 900 – 1 700 nm and was collected using a transreflectance probe that had an optical path length of 1.0 cm. Standard methods were used to determine the reference values for COD and TSS (Sarraguça *et al.*, 2009). The models that were used in this study were developed using PLS regression with leave one out cross validation. Different pre-processing techniques were used in various combinations to produce the most accurate

models. The techniques used were Savitsky-Golay, multiplicative scatter correction and standard normal variate. After the pre-processing was applied, the data was subjected to mean centering. The prediction of COD was shown to be inaccurate as it produced a relative error of 52.4 % in the wavelength region of 900 – 1 400 nm. This was due to the fact that water is a strong absorber in that wavelength range and may mask other C-H stretching vibrations and this in turn results in a decreased sensitivity for organic matter (Sarraguça *et al.*, 2009). The study also had a very narrow range from 17.24 – 99.53 mg.L⁻¹ for COD and it is well established that it is important to have a large range to ensure a robust model. Although COD quantification was ineffective, TSS quantification showed promise in this study. The relative error for TSS was 14.1 % when using the NIR range of 900 – 1 400 nm and a correlation coefficient of 0.91. This shows that NIR can be used to detect physical changes within a reactor. Whilst this study showed that TSS could be predicted accurately, further work needs to be done to accurately determine COD concentration using NIR.

Chemical oxygen demand, along with BOD and TSS were evaluated using visible and short wave NIR spectroscopy (Melendez-Pastor *et al.*, 2013). Urban wastewater was used as the substrate for this study and was collected at different stages of the treatment process. Variability was obtained by collecting samples over four months and at different days in the week (Melendez-Pastor *et al.*, 2013). A total of 84 samples were collected for analysis. Standard laboratory methods were used to determine COD, BOD and TSS as reference values. The wavelength range studied was 325 – 1 075 nm which includes the visible as well as short wave NIR (Melendez-Pastor *et al.*, 2013). Each sample was scanned five times and then an average spectrum for the five scans was obtained. Savitsky-Golay smoothing (3rd order polynomial, moving window 10 nm) was used as pre-processing to eliminate noise. Partial least squares regression was used as the statistical method to quantify the three parameters. Wavelength ranges of 400 – 1 000 nm, 400 – 700 nm and 700 – 1 000 nm were investigated. The RMSEP values were lowest for BOD and COD at ranges of 400 – 700 nm. The corresponding values were 10.37 and 9.19 % for BOD and COD respectively at 400 – 700 nm. At the wavelength range 700 – 1000 nm only the cross-validation results were given as the predictions were only done using the best results from the cross validation. However, the RMSECV values for COD and BOD at 700 – 1000 nm was very similar to the best models at 8.62 % compared to 8.48 % for optimal BOD and 9.37 % compared to 9.31 % for COD. The TSS parameter was determined most effectively in the 400 – 1000 nm range and returned values of 10.34 % for RMSEP. The RER values for the optimal BOD, COD and TSS parameters were 9.64, 10.88 and 9.67 respectively, indicating that the models could be used for screening and for COD could be used for quality control purposes. The drawback with this study is that the best results were achieved at low wavelength ranges and not in the NIR wavelength range. More work needs to be done using NIR in the 780 – 2500 nm wavelength range to determine its efficacy for prediction of wastewater quality parameters.

2.11 Conclusion

The South African wine industry is important for economic growth for the country. This industry however generates large volumes of wastewater every harvest season, placing strain on the available freshwater resources (Howell & Myburgh, 2018). The wastewater that is generated by the wine industry is challenging to treat due to its high strength and variable composition (Da Ros *et al.*, 2014; Bories & Sire, 2016). Re-use of generated wastewater could reduce the wine industry's reliance on freshwater for the irrigation of vineyards during the year (Meneses *et al.*, 2010)

Biological treatment methods have been shown to be very effective for the removal of organic material from winery wastewater (Mosse *et al.*, 2011). Biological treatment methods can be broadly divided into aerobic and anaerobic digestion methods (Ioannou *et al.*, 2015). Anaerobic methods have a few advantages compared to aerobic processes, with low sludge produce and production of biogas being just two of these (Andreottola *et al.*, 2009; Show & Lee, 2016). Anaerobic processes have been used to treat winery wastewater in the past with great success (Ruiz *et al.*, 2002; Moletta, 2005). Anaerobic sequencing batch reactor is a type of anaerobic treatment that can be used for the treatment of winery wastewater. Advantages of this technology include: flexibility of operational parameters; no need for an external clarifier and it has a kinetic advantage because of alternating F:M ratio during the cycle (high in the beginning and lower towards the end of the cycle) (Al-Rekabi *et al.*, 2007; Myra *et al.*, 2015).

Many physical and chemical factors may affect the performance of the AnSBR including: temperature; organic loading rate (OLR); mixing regime; feeding time; substrate to microorganisms ratio (F:M) and hydraulic retention time (HRT), pH; alkalinity; volatile fatty acids (VFAs) and toxicity in the digester. There is limited research available that utilises the AnSBR technology to treat winery wastewater, specifically at pilot-scale. Knowledge of optimal operational parameters for pH, feeding strategy and mixing intervals is equally limited and needs to be explored further.

Two performance measures for anaerobic reactors are COD and TSS. Currently the methods to determine the concentrations of these parameters is time-consuming and laborious. Currently no methods exist for the rapid determination of COD and TSS of winery wastewater. Near-infrared technology has been used to quantify COD and TSS concentration in wastewater of different origins e.g. sugar refinery wastewater or domestic sewage (Yang *et al.*, 2009; Pan *et al.*, 2012b). The feasibility of using NIR spectroscopy for the quantification and classification of COD and TSS in winery wastewater must be investigated to determine whether a rapid, non-destructive method can be proposed.

2.12 References

- Agustina, T.E., Ang, H. & Pareek, V. (2008). Treatment of winery wastewater using a photocatalytic/photolytic reactor. *Chemical Engineering Journal*, **135**, 151-156.
- Al-Rekabi, W.S., Qiang, H. & Qiang, W.W. (2007). Review on sequencing batch reactors. *Pakistan Journal of nutrition*, **6**, 11-19.
- Alexandratos, N. & Bruinsma, J. (2012). World agriculture towards 2030/2050: the 2012 revision.
- Amani, T., Nosrati, M. & Sreekrishnan, T. (2010). Anaerobic digestion from the viewpoint of microbiological, chemical, and operational aspects—a review. *Environmental Reviews*, **18**, 255-278.
- Ammary, B.Y. (2004). Nutrients requirements in biological industrial wastewater treatment. *African Journal of Biotechnology*, **3**, 236-238.
- Andreottola, G., Foladori, P. & Ziglio, G. (2009). Biological treatment of winery wastewater: an overview. *Water Science and Technology*, **60**, 1117-1125.
- Angenent, L.T. & Dague, R.R. (1996). A laboratory-scale comparison of the UASB and ASBR processes. Ann Arbor Press, Inc., Chelsea, MI (United States).
- APHA (2005). Standard methods for the examination of water and wastewater. *American Public Health Association (APHA): Washington, DC, USA*.
- Artiga, P., Ficara, E., Malpei, F., Garrido, J. & Mendez, R. (2005). Treatment of two industrial wastewaters in a submerged membrane bioreactor. *Desalination*, **179**, 161-169.
- Arvanitoyannis, I.S., Ladas, D. & Mavromatis, A. (2006). Wine waste treatment methodology. *International journal of food science & technology*, **41**, 1117-1151.
- Baulcombe, D., Crute, I., Davies, B., Dunwell, J., Gale, M., Jones, J., Pretty, J., Sutherland, W. & Toulmin, C. (2009). *Reaping the benefits: science and the sustainable intensification of global agriculture*. The Royal Society.
- Betancourt, W.Q. & Rose, J.B. (2004). Drinking water treatment processes for removal of Cryptosporidium and Giardia. *Veterinary parasitology*, **126**, 219-234.
- Bevilacqua, M., Bucci, R., Magrì, A.D., Magrì, A.L., Nescatelli, R. & Marini, F. (2013). *Chemometrics in Food Chemistry: Chapter 5. Classification and Class-Modelling*. Elsevier Inc. Chapters.
- Blanco, D., Suárez, J., González, F., Álvarez, L., Cabeza, E., Verde, J. & Jiménez, J. (2015). Efficiency of the treatment of pig production residues in covered lagoon digesters. *Pastos y Forrajes*, **38**.
- Blignaut, J. & Van Heerden, J. (2009). The impact of water scarcity on economic development initiatives. *Water Sa*, **35**, 415-420.
- Bodík, I., Herdová, B. & Drtil, M. (2002). The use of upflow anaerobic filter and AnSBR for wastewater treatment at ambient temperature. *Water Research*, **36**, 1084-1088.
- Bolzonella, D., Fatone, F., Pavan, P. & Cecchi, F. (2010). Application of a membrane bioreactor for winery wastewater treatment. *Water Science and Technology*, **62**, 2754-2759.

- Boone, D.R. & Xun, L. (1987). Effects of pH, temperature, and nutrients on propionate degradation by a methanogenic enrichment culture. *Appl. Environ. Microbiol.*, **53**, 1589-1592.
- Bories, A. & Sire, Y. (2016). Impacts of winemaking methods on wastewaters and their treatment. *South African Journal of Enology and Viticulture*, **31**, 38-44.
- Bories, A., Sire, Y. & Colin, T. (2005). Odorous compounds treatment of winery and distillery effluents during natural evaporation in ponds. *Water Science and Technology*, **51**, 129-136.
- Brito, A.G., Peixoto, J., Oliveira, J.M., Oliveira, J.A., Costa, C., Nogueira, R. & Rodrigues, A. (2007). Brewery and winery wastewater treatment: some focal points of design and operation. In: *Utilization of by-products and treatment of waste in the food industry*. Pp. 109-131. Springer.
- Brucculeri, M., Bolzonella, D., Battistoni, P. & Cecchi, F. (2005). Treatment of mixed municipal and winery wastewaters in a conventional activated sludge process: a case study. *Water Science and Technology*, **51**, 89-98.
- Bruwer, J. (2003). South African wine routes: some perspectives on the wine tourism industry's structural dimensions and wine tourism product. *Tourism management*, **24**, 423-435.
- Buekens, A. (Year). Energy recovery from residual waste by means of anaerobic digestion technologies. In: *Conference "The future of residual waste management in Europe"*. Pp. 17-18. Month and 2005
- Buyts, W.Y. (2015). Investigating the effect of wine and distillery wastewater on the efficacy of an upflow anaerobic sludge blanket (UASB) and enhancing biomass immobilisation by the addition of magnetisable foam glass particles (MP). Stellenbosch: Stellenbosch University.
- Carpenter, S.R., Stanley, E.H. & Vander Zanden, M.J. (2011). State of the world's freshwater ecosystems: physical, chemical, and biological changes. *Annual review of Environment and Resources*, **36**, 75-99.
- Chae, K., Jang, A., Yim, S. & Kim, I.S. (2008). The effects of digestion temperature and temperature shock on the biogas yields from the mesophilic anaerobic digestion of swine manure. *Bioresource technology*, **99**, 1-6.
- Chen, Y., Cheng, J.J. & Creamer, K.S. (2008). Inhibition of anaerobic digestion process: a review. *Bioresource technology*, **99**, 4044-4064.
- Chernicharo, C. (2007). *Anaerobic Reactors*. IWA.
- Chetty, S. & Pillay, K. (2015). Application of the DIY carbon footprint calculator to a wastewater treatment works. *Water Sa*, **41**, 263-272.
- Conradie, A. (2015). Influence of winemaking practices on the chemical characteristics of winery wastewater and the water usages of wineries. Stellenbosch: Stellenbosch University.
- Cooley, H., Ajami, N., Ha, M.-L., Srinivasan, V., Morrison, J., Donnelly, K. & Christian-Smith, J. (2014). Global water governance in the twenty-first century. In: *The world's water*. Pp. 1-18. Springer.
- Cusmano, L., Morrison, A. & Rabellotti, R. (2010). Catching up trajectories in the wine sector: A comparative study of Chile, Italy, and South Africa. *World Development*, **38**, 1588-1602.

- Da Ros, C., Cavinato, C., Pavan, P. & Bolzonella, D. (2014). Winery waste recycling through anaerobic co-digestion with waste activated sludge. *Waste Management*, **34**, 2028-2035.
- Dahlbacka, J., Nyström, J., Mossing, T., Geladi, P. & Lillhonga, T. (2014). On-line measurement of the chemical oxygen demand in wastewater in a pulp and paper mill using near infrared spectroscopy. *Spectral Analysis Review*, **2**, 19.
- Demirel, B. & Scherer, P. (2008). The roles of acetotrophic and hydrogenotrophic methanogens during anaerobic conversion of biomass to methane: a review. *Reviews in Environmental Science and Bio/Technology*, **7**, 173-190.
- Devesa-Rey, R., Vecino, X., Varela-Alende, J., Barral, M., Cruz, J. & Moldes, A. (2011). Valorization of winery waste vs. the costs of not recycling. *Waste Management*, **31**, 2327-2335.
- Eleutheria, N., Maria, I., Vasiliki, T., Alexandros, E., Alexandros, A. & Vasileios, D. (2016). Energy Recovery and Treatment of Winery Wastes by a Compact Anaerobic Digester. *Waste and Biomass Valorization*, **7**, 799-805.
- Ene, S.A., Teodosiu, C., Robu, B. & Volf, I. (2013). Water footprint assessment in the winemaking industry: a case study for a Romanian medium size production plant. *Journal of Cleaner Production*, **43**, 122-135.
- Eusebio, A., Petruccioli, M., Lageiro, M., Federici, F. & Duarte, J.C. (2004). Microbial characterisation of activated sludge in jet-loop bioreactors treating winery wastewaters. *Journal of Industrial Microbiology and Biotechnology*, **31**, 29-34.
- FAO (2016). South Africa. [WWW document]. http://www.fao.org/nr/water/aquastat/countries_regions/Profile_segments/ZAF-WU_eng.stm. 27/07/2017
- Fumi, M.D., Parodi, G., Parodi, E., Silva, A. & Marchetti, R. (1995). Optimisation of long-term activated-sludge treatment of winery wastewater. *Bioresource technology*, **52**, 45-51.
- Gallert, C. & Winter, J. (2008). Propionic acid accumulation and degradation during restart of a full-scale anaerobic biowaste digester. *Bioresource technology*, **99**, 170-178.
- Gannoun, H., Othman, N.B., Bouallagui, H. & Moktar, H. (2007). Mesophilic and thermophilic anaerobic co-digestion of olive mill wastewaters and abattoir wastewaters in an upflow anaerobic filter. *Industrial & Engineering Chemistry Research*, **46**, 6737-6743.
- Gao, B., Hahn, H. & Hoffmann, E. (2002). Evaluation of aluminum-silicate polymer composite as a coagulant for water treatment. *Water Research*, **36**, 3573-3581.
- García-Carpintero, E.G., Gallego, M.G., Sánchez-Palomo, E. & Viñas, M.G. (2012). Impact of alternative technique to ageing using oak chips in alcoholic or in malolactic fermentation on volatile and sensory composition of red wines. *Food chemistry*, **134**, 851-863.
- Gerardi, M.H. (2003). The microbiology of anaerobic digesters. Pp. 99-103 New Jersey: John Wiley & Sons.
- Ghanimeh, S., El Fadel, M. & Saikaly, P. (2012). Mixing effect on thermophilic anaerobic digestion of source-sorted organic fraction of municipal solid waste. *Bioresource technology*, **117**, 63-71.

- Gomez, X., Cuetos, M., Cara, J., Moran, A. & Garcia, A. (2006). Anaerobic co-digestion of primary sludge and the fruit and vegetable fraction of the municipal solid wastes: conditions for mixing and evaluation of the organic loading rate. *Renewable energy*, **31**, 2017-2024.
- Gurtekin, E. (2014). Sequencing batch reactor. *Akademik Platform, ISEM2014 Adiyaman–Turkey*.
- Halsey, S. (1985). The use of transmission and transmittance near infrared spectroscopy for the analysis of beer. *Journal of the Institute of Brewing*, **91**, 306-312.
- Hilton, B.L. & Oleszkiewicz, J.A. (1988). Sulfide-induced inhibition of anaerobic digestion. *Journal of environmental engineering*, **114**, 1377-1391.
- Hirzel, D.R., Steenwerth, K., Parikh, S.J. & Oberholster, A. (2017). Impact of winery wastewater irrigation on soil, grape and wine composition. *Agricultural Water Management*, **180**, 178-189.
- Howell, C. & Myburgh, P. (2018). Management of winery wastewater by re-using it for crop irrigation-A review. *South African Journal of Enology and Viticulture*, **39**, 116-131.
- Huang, H., Yu, H., Xu, H. & Ying, Y. (2008). Near infrared spectroscopy for on/in-line monitoring of quality in foods and beverages: A review. *Journal of Food Engineering*, **87**, 303-313.
- Huang, Y., Dehkordy, F.M., Li, Y., Emadi, S., Bagtzoglou, A. & Li, B. (2018). Enhancing anaerobic fermentation performance through eccentrically stirred mixing: Experimental and modeling methodology. *Chemical Engineering Journal*, **334**, 1383-1391.
- Ioannou, L., Puma, G.L. & Fatta-Kassinos, D. (2015). Treatment of winery wastewater by physicochemical, biological and advanced processes: A review. *Journal of hazardous materials*, **286**, 343-368.
- Jantsch, T.G. & Mattiasson, B. (2004). An automated spectrophotometric system for monitoring buffer capacity in anaerobic digestion processes. *Water Research*, **38**, 3645-3650.
- Jiraprasertwong, A., Vichaitanapat, K., Leethochawalit, M. & Chavadej, S. (2018). Three-stage anaerobic sequencing batch reactor (ASBR) for maximum methane production: Effects of COD loading rate and reactor volumetric ratio. *Energies*, **11**, 1543.
- Joshi, V., Sharma, S. & Thakur, A. (2017). Wines: White, Red, Sparkling, Fortified, and Cider. In: *Current Developments in Biotechnology and Bioengineering*. Pp. 353-406. Elsevier.
- Jury, W.A. & Vaux, H.J. (2007). The emerging global water crisis: managing scarcity and conflict between water users. *Advances in agronomy*, **95**, 1-76.
- Kalyuzhnyi, S., Veeken, A. & Hamelers, B. (2000). Two-particle model of anaerobic solid state fermentation. *Water Science and Technology*, **41**, 43-50.
- Karim, K., Hoffmann, R., Klasson, K.T. & Al-Dahhan, M. (2005). Anaerobic digestion of animal waste: Effect of mode of mixing. *Water Research*, **39**, 3597-3606.
- Keyser, M., Witthuhn, R., Ronquest, L.-C. & Britz, T. (2003). Treatment of winery effluent with upflow anaerobic sludge blanket (UASB)–granular sludges enriched with *Enterobacter sakazakii*. *Biotechnology letters*, **25**, 1893-1898.

- Khanal, S., Giri, B., Nitayavardhana, S. & Gadhamshetty, V. (2017). Anaerobic bioreactors/digesters: design and development. In: *Current Developments in Biotechnology and Bioengineering*. Pp. 261-279. Elsevier.
- Kim, M., Gomec, C.Y., Ahn, Y. & Speece, R. (2003). Hydrolysis and acidogenesis of particulate organic material in mesophilic and thermophilic anaerobic digestion. *Environmental technology*, **24**, 1183-1190.
- Kirzhner, F., Zimmels, Y. & Shraiber, Y. (2008). Combined treatment of highly contaminated winery wastewater. *Separation and Purification Technology*, **63**, 38-44.
- Kondusamy, D. & Kalamdhad, A.S. (2014). Pre-treatment and anaerobic digestion of food waste for high rate methane production—A review. *Journal of Environmental Chemical Engineering*, **2**, 1821-1830.
- Lahav, O., Morgan, B.E. & Loewenthal, R.E. (2002). Rapid, simple, and accurate method for measurement of VFA and carbonate alkalinity in anaerobic reactors. *Environmental science & technology*, **36**, 2736-2741.
- Laing, M. (2016). Investigating the performance of a novel Anaerobic Sequencing Batch Reactor (AnSBR) and optimisation of operational parameters to treat synthetic winery wastewater. Stellenbosch: Stellenbosch University.
- Li Vigni, M., Durante, C & Cocchi, M (2013). Exploratory data analysis. In: *Chemometrics in food chemistry* (edited by F. Marini). Pp. 65. Amsterdam: Newnes.
- López-Palau, S., Pinto, A., Basset, N., Dosta, J. & Mata-Álvarez, J. (2012). ORP slope and feast–famine strategy as the basis of the control of a granular sequencing batch reactor treating winery wastewater. *Biochemical engineering journal*, **68**, 190-198.
- Lu, X., Zhen, G., Estrada, A.L., Chen, M., Ni, J., Hojo, T., Kubota, K. & Li, Y.-Y. (2015). Operation performance and granule characterization of upflow anaerobic sludge blanket (UASB) reactor treating wastewater with starch as the sole carbon source. *Bioresource technology*, **180**, 264-273.
- Lu, X., Zhen, G., Ni, J., Hojo, T., Kubota, K. & Li, Y.-Y. (2016). Effect of influent COD/SO₄²⁻ ratios on biodegradation behaviors of starch wastewater in an upflow anaerobic sludge blanket (UASB) reactor. *Bioresource technology*, **214**, 175-183.
- Luo, J., Qian, G., Liu, J. & Xu, Z.P. (2015). Anaerobic methanogenesis of fresh leachate from municipal solid waste: A brief review on current progress. *Renewable and Sustainable Energy Reviews*, **49**, 21-28.
- Malin, S.F., Ruchti, T.L., Blank, T.B., Thennadil, S.N. & Monfre, S.L. (1999). Noninvasive prediction of glucose by near-infrared diffuse reflectance spectroscopy. *Clinical chemistry*, **45**, 1651-1658.
- Mata-Alvarez, J., Mace, S. & Llabres, P. (2000). Anaerobic digestion of organic solid wastes. An overview of research achievements and perspectives. *Bioresource technology*, **74**, 3-16.
- Maynard, H., Ouki, S. & Williams, S. (1999). Tertiary lagoons: a review of removal mechanisms and performance. *Water Research*, **33**, 1-13.

- McMahon, K.D., Stroot, P.G., Mackie, R.I. & Raskin, L. (2001). Anaerobic codigestion of municipal solid waste and biosolids under various mixing conditions—II: microbial population dynamics. *Water Research*, **35**, 1817-1827.
- McNabb, D.E. (2019). The population growth barrier. In: *Global Pathways to Water Sustainability*. Pp. 67-81. Springer.
- Melendez-Pastor, I., Almendro-Candel, M.B., Navarro-Pedreño, J., Gómez, I., Lillo, M.G. & Hernández, E.I. (2013). Monitoring urban wastewaters' characteristics by visible and short wave near-infrared spectroscopy. *Water*, **5**, 2026-2036.
- Meneses, M., Pasqualino, J.C. & Castells, F. (2010). Environmental assessment of urban wastewater reuse: treatment alternatives and applications. *Chemosphere*, **81**, 266-272.
- Mockaitis, G., Ratusznei, S.M., Rodrigues, J.A., Zaiat, M. & Foresti, E. (2006). Anaerobic whey treatment by a stirred sequencing batch reactor (ASBR): effects of organic loading and supplemented alkalinity. *Journal of Environmental Management*, **79**, 198-206.
- Mohana, S., Acharya, B.K. & Madamwar, D. (2009). Distillery spent wash: Treatment technologies and potential applications. *Journal of hazardous materials*, **163**, 12-25.
- Moharikar, A., Purohit, H.J. & Kumar, R. (2005). Microbial population dynamics at effluent treatment plants. *Journal of Environmental Monitoring*, **7**, 552-558.
- Moletta, R. (2005). Winery and distillery wastewater treatment by anaerobic digestion. *Water Science and Technology*, **51**, 137-144.
- Montalvo, S., Guerrero, L., Rivera, E., Borja, R., Chica, A. & Martín, A. (2010). Kinetic evaluation and performance of pilot-scale fed-batch aerated lagoons treating winery wastewaters. *Bioresource technology*, **101**, 3452-3456.
- Mosey, F. & Fernandes, X. (1988). Patterns of hydrogen in biogas from the anaerobic digestion of milk-sugars. In: *Water Pollution Research and Control Brighton*. Pp. 187-196. Elsevier.
- Mosse, K., Patti, A., Christen, E. & Cavagnaro, T. (2011). Winery wastewater quality and treatment options in Australia. *Australian Journal of Grape and Wine Research*, **17**, 111-122.
- Myra, T., David, H., Judith, T., Marina, Y., Ricky, B.J. & Reynaldo, E. (2015). Biological treatment of meat processing wastewater using anaerobic sequencing batch reactor (ASBR). *International Research Journal of Biological Sciences*, **4**, 66-75.
- Nakakubo, R., Møller, H.B., Nielsen, A.M. & Matsuda, J. (2008). Ammonia inhibition of methanogenesis and identification of process indicators during anaerobic digestion. *Environmental Engineering Science*, **25**, 1487-1496.
- OIV (2019). 2019 Statistical report on world vitiviniculture. [WWW document]. <http://www.oiv.int/public/medias/6782/oiv-2019-statistical-report-on-world-vitiviniculture.pdf>.
- Oliveira, M., Queda, C. & Duarte, E. (2009). Aerobic treatment of winery wastewater with the aim of water reuse. *Water Science and Technology*, **60**, 1217-1223.

- Ozaki, Y., McClure, W.F. & Christy, A.A. (2006). *Near-infrared spectroscopy in food science and technology*. John Wiley & Sons.
- Pan, T., Chen, W.W., Chen, Z.H. & Xie, J. (Year). Waveband selection for NIR spectroscopy analysis of wastewater COD. In: *Key Engineering Materials*. Pp. 393-396. Month and 2011
- Pan, T., Chen, Z., Chen, J. & Liu, Z. (2012). Near-infrared spectroscopy with waveband selection stability for the determination of COD in sugar refinery wastewater. *Analytical Methods*, **4**, 1046-1052.
- Parawira, W. (2004). Anaerobic treatment of agricultural residues and wastewater. *University of Lund Department of Biotechnology*.
- Páscoa, R.N., Lopes, J.A. & Lima, J.L. (2008). In situ near infrared monitoring of activated dairy sludge wastewater treatment processes. *Journal of Near Infrared Spectroscopy*, **16**, 409-419.
- Pasquini, C. (2003). Near infrared spectroscopy: fundamentals, practical aspects and analytical applications. *Journal of the Brazilian chemical society*, **14**, 198-219.
- Perlines Sánchez, M. (2014). Effluents characterization using NIR and UV-Vis spectroscopy.
- Petruccioli, M., Duarte, J. & Federici, F. (2000). High-rate aerobic treatment of winery wastewater using bioreactors with free and immobilized activated sludge. *Journal of bioscience and bioengineering*, **90**, 381-386.
- Petruccioli, M., Duarte, J.C., Eusebio, A. & Federici, F. (2002). Aerobic treatment of winery wastewater using a jet-loop activated sludge reactor. *Process Biochemistry*, **37**, 821-829.
- Quayle, W.C., Fattore, A., Zandona, R., Christen, E.W. & Arienzo, M. (2009). Evaluation of organic matter concentration in winery wastewater: a case study from Australia. *Water Science and Technology*, **60**, 2521-2528.
- Rajeshwari, K., Balakrishnan, M., Kansal, A., Lata, K. & Kishore, V. (2000). State-of-the-art of anaerobic digestion technology for industrial wastewater treatment. *Renewable and Sustainable Energy Reviews*, **4**, 135-156.
- Rengasamy, P. & Marchuk, A. (2011). Cation ratio of soil structural stability (CROSS). *Soil Research*, **49**, 280-285.
- Rodrigues, J.A.D., Ratusznei, S.M., de Camargo, E.F.M. & Zaiat, M. (2003). Influence of agitation rate on the performance of an anaerobic sequencing batch reactor containing granulated biomass treating low-strength wastewater. *Advances in Environmental Research*, **7**, 405-410.
- Ruiz, C., Torrijos, M., Sousbie, P., Martinez, J.L., Moletta, R. & Delgenes, J. (2002). Treatment of winery wastewater by an anaerobic sequencing batch reactor. *Water Science and Technology*, **45**, 219-224.
- Saleh, M.M. & Mahmood, U.F. (Year). Anaerobic digestion technology for industrial wastewater treatment. In: *Proceedings of the Eighth International Water Technology Conference, IWTC, Alexandria, Egypt*. Pp. 26-28. Month and 2004
- Sandberg, M. & Ahring, B. (1992). Anaerobic treatment of fish meal process waste-water in a UASB reactor at high pH. *Applied Microbiology and Biotechnology*, **36**, 800-804.

- Sarraguça, M.C., Paulo, A., Alves, M.M., Dias, A.M., Lopes, J.A. & Ferreira, E.C. (2009). Quantitative monitoring of an activated sludge reactor using on-line UV-visible and near-infrared spectroscopy. *Analytical and bioanalytical chemistry*, **395**, 1159-1166.
- Sarti, A., Fernandes, B.S., Zaiat, M. & Foresti, E. (2007). Anaerobic sequencing batch reactors in pilot-scale for domestic sewage treatment. *Desalination*, **216**, 174-182.
- Scholes, R. (2001). Regional Implementation Plan for Southern Africa. United Nations FAO, South Africa.
- Shao, X., Peng, D., Teng, Z. & Ju, X. (2008). Treatment of brewery wastewater using anaerobic sequencing batch reactor (ASBR). *Bioresource technology*, **99**, 3182-3186.
- Sheridan, C., Hildebrand, D. & Glasser, D. (2014). Turning wine (waste) into water: toward technological advances in the use of constructed wetlands for winery effluent treatment. *AIChE Journal*, **60**, 420-431.
- Shivajirao, P.A. (2012). Treatment of distillery wastewater using membrane technologies. *International journal of advanced Engineering Research and studies*, **1**, 1275-1283.
- Shizas, I. & Bagley, D.M. (2002). Improving anaerobic sequencing batch reactor performance by modifying operational parameters. *Water Research*, **36**, 363-367.
- Show, K. & Lee, D. (2016). Anaerobic Treatment Versus Aerobic Treatment. *Current Developments in Biotechnology and Bioengineering: Biological Treatment of Industrial Effluents*, 205.
- Siesler, H.W., Ozaki, Y., Kawata, S. & Heise, H.M. (2008). *Near-infrared spectroscopy: principles, instruments, applications*. John Wiley & Sons.
- Singh, M. & Srivastava, R. (2011). Sequencing batch reactor technology for biological wastewater treatment: a review. *Asia-Pacific Journal of Chemical Engineering*, **6**, 3-13.
- Sivakumar, B. (2011). Water crisis: from conflict to cooperation—an overview. *Hydrological Sciences Journal*, **56**, 531-552.
- Soleas, G.J., Diamandis, E.P. & Goldberg, D.M. (1997). Wine as a biological fluid: history, production, and role in disease prevention. *Journal of clinical laboratory analysis*, **11**, 287-313.
- Solera, R., Romero, L. & Sales, D. (2002). The evolution of biomass in a two-phase anaerobic treatment process during start-up. *Chemical and biochemical engineering quarterly*, **16**, 25-30.
- Stroock, A.D., Dertinger, S.K., Ajdari, A., Mezić, I., Stone, H.A. & Whitesides, G.M. (2002). Chaotic mixer for microchannels. *Science*, **295**, 647-651.
- Stroot, P.G., McMahon, K.D., Mackie, R.I. & Raskin, L. (2001). Anaerobic codigestion of municipal solid waste and biosolids under various mixing conditions—I. Digester performance. *Water Research*, **35**, 1804-1816.
- Sung, S. & Dague, R.R. (1995). Laboratory studies on the anaerobic sequencing batch reactor. *Water Environment Research*, **67**, 294-301.
- Sung, S. & Liu, T. (2003). Ammonia inhibition on thermophilic anaerobic digestion. *Chemosphere*, **53**, 43-52.

- Tang, H. & Liu, G.-z. (Year). Cross Effects of Organic Loading Rates and Substrate COD/N/P Ratios on Aerobic Granulation. In: *Bioinformatics and Biomedical Engineering (iCBBE), 2010 4th International Conference on*. Pp. 1-4. Month and 2010
- Tauseef, S., Abbasi, T. & Abbasi, S. (2013). Energy recovery from wastewaters with high-rate anaerobic digesters. *Renewable and Sustainable Energy Reviews*, **19**, 704-741.
- Torrijos, M. & Moletta, R. (1997). Winery wastewater depollution by sequencing batch reactor. *Water Science and Technology*, **35**, 249-257.
- UN (2006). Human Development Report 2006. Beyond Scarcity: Power, poverty and the global water crisis. . In: Human Development Report (edited by B. Ross-Larson, M.d. Coquereaumont & C. Trott). Pp. 131-169. New York: United Nations Development Programme.
- UNESCO (2017). The United Nations World Water Development Report 2017 : Water and Jobs. Pp. 1-12. Italy: United Nations.
- Van Schoor, L. (2005). Guidelines for the management of wastewater and solid waste at existing wineries. *Winetech, PO Box*, **528**.
- Vannucci, M., Sha, N. & Brown, P.J. (2005). NIR and mass spectra classification: Bayesian methods for wavelet-based feature selection. *Chemometrics and Intelligent laboratory systems*, **77**, 139-148.
- Visvanathan, C. & Asano, T. (2009). The potential for industrial wastewater reuse. *Wastewater Recycl. Reuse Reclam*, **1**, 299-313.
- Vlyssides, A., Barampouti, E. & Mai, S. (2005). Wastewater characteristics from Greek wineries and distilleries. *Water Science and Technology*, **51**, 53-60.
- Vossoughi, M., Shakeri, M. & Alemzadeh, I. (2003). Performance of anaerobic baffled reactor treating synthetic wastewater influenced by decreasing COD/SO₄ ratios. *Chemical Engineering and Processing: Process Intensification*, **42**, 811-816.
- Wang, Z. & Banks, C. (2007). Treatment of a high-strength sulphate-rich alkaline leachate using an anaerobic filter. *Waste Management*, **27**, 359-366.
- Ward, A.J., Hobbs, P.J., Holliman, P.J. & Jones, D.L. (2008). Optimisation of the anaerobic digestion of agricultural resources. *Bioresource technology*, **99**, 7928-7940.
- Ward, A.J., Hobbs, P.J., Holliman, P.J. & Jones, D.L. (2011). Evaluation of near infrared spectroscopy and software sensor methods for determination of total alkalinity in anaerobic digesters. *Bioresource technology*, **102**, 4083-4090.
- Welz, P., Holtman, G., Haldenwang, R. & Le Roes-Hill, M. (2016). Characterisation of winery wastewater from continuous flow settling basins and waste stabilisation ponds over the course of 1 year: implications for biological wastewater treatment and land application. *Water Science and Technology*, **74**, 2036-2050.
- Woodard, F. (2001). *Industrial waste treatment handbook*. Butterworth-Heinemann.

- Yang, B., Xu, H., Yang, S., Bi, S., Li, F., Shen, C., Ma, C., Tian, Q., Liu, J. & Song, X. (2018). Treatment of industrial dyeing wastewater with a pilot-scale strengthened circulation anaerobic reactor. *Bioresource technology*, **264**, 154-162.
- Yang, Q., Liu, Z. & Yang, J. (2009). Simultaneous determination of chemical oxygen demand (COD) and biological oxygen demand (BOD5) in wastewater by near-infrared spectrometry. *Journal of Water Resource and Protection*, **4**, 286-289.
- Yilmaz, T., Erdirencelebi, D. & Berktaş, A. (2012). Effect of COD/SO ratio on anaerobic treatment of landfill leachate during the start-up period. *Environmental technology*, **33**, 313-320.
- Zaher, U., Cheong, D.-Y., Wu, B. & Chen, S. (2007). Producing energy and fertilizer from organic municipal solid waste. *Department of Biological Systems Engineering, Washington State University*.
- Zhang, C., Su, H., Baeyens, J. & Tan, T. (2014). Reviewing the anaerobic digestion of food waste for biogas production. *Renewable and Sustainable Energy Reviews*, **38**, 383-392.
- Zhang, M., Sheng, G. & Yu, H. (2009). Near-infrared spectroscopy-based quantification of substrate and aqueous products in wastewater anaerobic fermentation processes. *Chinese Science Bulletin*, **54**, 1918-1922.
- Zularisam, A., Ismail, A. & Salim, R. (2006). Behaviours of natural organic matter in membrane filtration for surface water treatment—a review. *Desalination*, **194**, 211-231.

Chapter 3

Determination of Chemical Oxygen Demand (COD) and Total Suspended Solids (TSS) Using Near-Infrared (NIR) Spectroscopy

Abstract

The use of near-infrared (NIR) spectroscopy was evaluated for the quantification and classification of chemical oxygen demand (COD) and total suspended solids (TSS) concentration in winery wastewater. Spectra were acquired using a benchtop Büchi NIR-Flex N500 FT-NIR spectrophotometer with a wavelength range of 1 000 – 2 500 nm as well as a portable Viavi handheld spectrophotometer with a wavelength range of 900 – 1 700 nm. Exploratory data analysis (PCA) was performed to identify possible wavelengths of importance. Different pre-processing methods were performed to identify the best pre-processing method along with principal component regression (PCR) or partial least squares regression (PLS-R) for quantification. Different discriminant analysis techniques were performed to identify the most effective technique for classification of COD and TSS. The concentration of COD could be predicted with a RMSEP value of 893 mg.L⁻¹, an error of 9.9 % compared to the range of the reference values, using PCR along with orthogonal signal correction (OSC). This was achieved using the wavelength range 2 060 – 2 340 nm on the benchtop instrument. The PCR model could be used as a screening method to rapidly determine the COD concentration of winery wastewater. The concentration of TSS could be predicted with a RMSEP of 136.94 mg.L⁻¹, an error of 5.72 %, using the benchtop instrument. The prediction model for TSS achieved a prediction performance that was almost comparable to the reference method, meaning it is suitable for screening purposes. Classification accuracies of 90.4 % (COD) & 100 % (TSS), 80.1 % (COD) & 95 % (TSS) could be achieved with the benchtop and handheld instruments respectively. The handheld device could not quantify COD or TSS to a satisfactory degree for the purpose of screening. The above classification accuracies for the handheld instrument indicates that classification of winery wastewater, into low or high strength categories, may be possible for in-line monitoring of winery wastewater and screening via category instead of quantification.

3.1 Introduction

Water is the most important natural resource on Earth and is of vital importance for humans, plants, animals, ecosystems and environments (Sivakumar, 2011). The most abundant use of water is found in the agricultural sector, with this sector using roughly 70 % of all fresh water globally (UNESCO, 2017). Industrial use of fresh water is much less at approximately 19 % of fresh water globally, however the wastewater produced from industry is very high strength and therefore has the potential to pollute large quantities of water (Moharikar *et al.*, 2005; UNESCO, 2017). Wineries generate copious amounts of high strength wastewater in terms of chemical oxygen demand (COD) (Da Ros *et al.*, 2014).

One method of reducing COD in winery wastewater is through the use of an anaerobic sequencing batch reactor (AnSBR) (Mosse *et al.*, 2011). The premise of an AnSBR is that anaerobic bacteria form granules, consisting of methanogens, acidogens and acetogens, which use organic compounds in the wastewater as substrate (Show & Lee, 2016). This technology has been shown to work numerous times treating winery wastewater with COD reduction percentages of up to 98 % (Ruiz *et al.*, 2002; Shao *et al.*, 2008). The one problem that persists is one of reactor overload. This is when the COD level coming into the reactor is too high and causes reactor failure, as microorganisms perish. It is therefore important to establish the COD of incoming wastewater before feeding the AnSBR. Routinely, the determination of COD is performed in a laboratory and is a time consuming method that requires chemical reactions, the reaction with potassium dichromate, to quantify the levels in water (Yang *et al.*, 2009; Pan *et al.*, 2011). This reaction involves a digestion step of 120 minutes at 148°C. Thereafter a cooling step of at least 30 minutes is required to cool the sample before inserting it into a spectrophotometer and calculating COD values (APHA, 2005).

Near-infrared (NIR) spectroscopy has been used in several studies to determine COD concentration in water. Chemical oxygen demand (COD) as well as biochemical oxygen demand (BOD) was determined simultaneously in domestic sewage using NIR spectroscopy (Yang *et al.*, 2009). The method had a correlation coefficient of 0.9542 and 0.9652 for COD and BOD, respectively. A good indicator for model accuracy for quantification is the root mean square error of prediction (RMSEP) and the RMSEP for COD and BOD were 25.24 and 12.13 mg.L⁻¹, respectively. The range of measured values were 496.6 mg.L⁻¹ and 289.2 mg.L⁻¹ for COD and BOD. This translates to error values of 5.1 % for COD quantification and 4.2 % for BOD determination, which can be considered very accurate and within allowable error ranges for process control requirements (Yang *et al.*, 2009).

Wastewater was assessed for COD determination using NIR spectroscopy and the RMSEP value was found to be 25.5 mg.L⁻¹ (Pan *et al.*, 2011). This correlates to a 7.7 % error when taking the range of 330 mg.L⁻¹ into consideration. The study proved that COD determination can be achieved fairly accurately using NIR at the wavelength range of 820 – 850 nm and using moving window partial least squares (MWPLS) as a chemometric evaluation.

Total soluble solids have been previously quantified using NIR. Partial least squares regression (PLS-R) has been used to predict the concentration of TSS in an activated sludge reactor. The error for prediction was 14.1 % and the correlation coefficient (R^2) was 0.91 (Sarraguça *et al.*, 2009).

Wastewater has been assessed for the quantification of TSS using UV-Vis spectroscopy. The root mean square error of calibration (RMSECV) was 16.6 % for the cross-validated results (Rieger *et al.*, 2006)

Near-infrared spectroscopy can be used to quantify COD in various wastewaters, however it has not been quantified for winery wastewater in literature. Added to this is that most of the literature is based on COD quantification of low strength wastewaters, with no studies investigating wastewaters with COD approaching 10 000 mg.L⁻¹. No work has yet been done to predict TSS concentration of winery wastewater using NIR spectroscopy.

The aim of this study was to investigate the performance of NIR spectroscopy to determine COD and TSS concentrations in winery wastewater, as well as classify the water based on COD and TSS strength, using a benchtop FT-NIR spectrophotometer and a handheld spectrophotometer. An error percentage of less than 10 % compared to the range of the independent validation set will be deemed suitable to fulfil the aim of this study.

3.2 Materials and methods

3.2.1 Samples

Winery Wastewater was collected from four different farms in the Stellenbosch wine region from the end of March to the beginning of May 2018. The samples were collected in 2L Schott bottles from various locations on each farm. Water was collected from the stream that flows to the wastewater collection dam on Farm A. The wastewater from Farm B was collected from the gullies in the cellar. Farm C had a water filtration system and water was collected during the different phases of the treatment as well as from gullies in the cellar. Farm D had a collection dam on its premises and water was subsequently collected from the dam, however after 3 replicates, it was decided that water would not be sourced from that farm anymore, as winery wastewater could not be sourced without contamination. Wastewater was collected for 23 days and 80 samples were collected in total. The samples were transported to the lab where they were sieved using a 600-micron sieve to eliminate particulate matter. This was performed to ensure that scattering during NIR scanning can be minimised. The samples were then kept at ambient temperature (23°C) for analysis which commenced immediately upon arrival at the laboratory.

3.2.2 Analytical methods

Several parameters of the wastewater were determined using Standard Methods (APHA, 2005), namely: pH (senTix 41 probe); alkalinity and total suspended solids (TSS).

Alternative methods were used to determine the following parameters:

1. COD (mg.L^{-1})
 - I. Measured using Spectroquant® COD cell test kits (Merck, Darmstadt, Germany) with the ranges
100 – 1 500 mg.L^{-1} , 500 – 10 000 mg.L^{-1} and 0 – 90 000 mg.L^{-1} .

3.2.3 NIR instrumentation

Two instruments were used in this experiment to acquire near-infrared spectra. A benchtop FT-NIR spectrophotometer was used along with a handheld portable spectrophotometer.

The benchtop instrument used was the Büchi NIRFlex N-500 FT-NIR spectrophotometer (Büchi, Flawil, Switzerland) with the liquids attachment. A quartz cuvette with a declared optical pathlength of 0.1

mm and a volume of 26 μL and detachable windows was used for this analysis. The illumination source of the instrument consisted of two tungsten halogen lamps. This instrument is equipped with an extended range Indium Gallium Arsenide (InGaAs) detector. The spectral range of the instrument with the liquid attachment is 1 000 – 2 500 nm and the resolution used was 16 cm^{-1} . Internal temperature of the instrument was kept constant at 35°C . The scans were performed in transmittance mode.

The handheld instrument used was the MicroNIR Onsite spectrophotometer (Viavi Solutions Inc., Milpitas, USA). This instrument is equipped with two integrated vacuum tungsten lamps along with an InGaAs photodiode array detector. Spectra were acquired in the spectral range of 908 – 1 676 nm with a resolution $< 12.5\text{ nm}$. The samples were scanned in a white Teflon well with a volume of 900 μL .

3.2.4 Spectral acquisition

Wastewater that had been previously filtered was kept at ambient temperature (23°C) during spectral acquisition.

3.2.4.1 Benchtop instrument

In order to acquire a single spectrum, the benchtop instrument scans the sample 16 times and displays one average spectrum. Each 2 L Schott bottle representing a single farm was considered a single sample (**Figure 3.1**). From this sample a subsample was pipetted and placed into the cuvette for spectral acquisition. This was defined as one subsample. Each subsample was scanned five times in the benchtop instrument so that 5 spectra were acquired for each subsample. In total 10 subsamples were scanned for every farm's 2 L sample, which resulted in 50 spectra acquired per farm per day. After each subsample was scanned, the cuvettes were cleaned using distilled water and dried using a glass cloth. Thereafter 30 μL of sample was placed into the cuvette for subsequent scanning.

3.2.4.2 Handheld instrument

The handheld instrument displays one average spectrum per scan consisting of 100 spectra. Each subsample was scanned 32 times resulting in acquisition of 320 spectra per sample. This was done as scanning time of the handheld instrument was significantly faster than the benchtop instrument. After each subsample was scanned, the cuvettes were cleaned with distilled water and dried with a cloth. Thereafter 900 μL of sample was placed into cuvette for subsequent scanning.

3.2.5 Spectral analysis

Analysis of the spectral data were analysed using The Unscrambler X10.5 (Camo Software AS., Oslo, Norway) software. Spectral analysis for the benchtop and handheld instruments were conducted independently of each other. For the benchtop instrument the 5 spectra obtained for each subsample were averaged to one average spectrum for each subsample. Each sample was therefore represented by 10 spectra prior to pre-

processing step. For the handheld instrument the 32 spectra obtained for every subsample were averaged to one spectrum, meaning that each sample was also represented by 10 average spectra. The mean spectra were computed and plotted onto a graph to investigate potential wavelengths of importance.

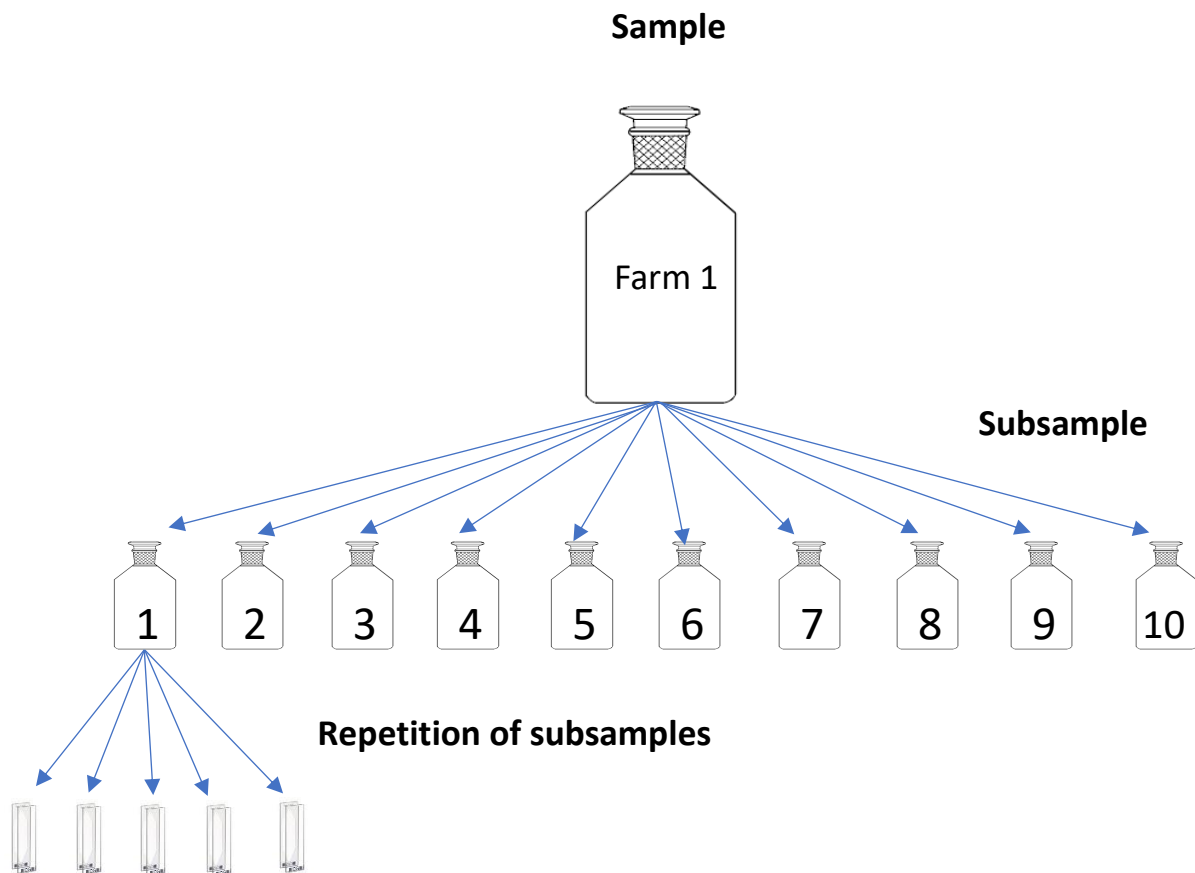


Figure 3.1 Diagram illustrating spectral acquisition of samples for the benchtop instrument. One sample was divided into 10 subsamples with each subsample being scanned 5 times. In total 50 spectra obtained per farm per day.

3.2.6 Pre-processing

Pre-processing was performed on the data to minimise the contribution that the physical effects have on the NIR spectra and prepare the data for consequent analysis (Pizarro *et al.*, 2004). No smoothing was performed on the spectroscopic data prior to pre-processing. Several pre-processing techniques, standard normal variate (SNV) (Barnes *et al.*, 1989), detrending, Savitzky-Golay first and second derivatives (Savitzky & Golay, 1964) and orthogonal signal correction (OSC) (Wold *et al.*, 1998), were investigated to determine which techniques would yield the best results.

3.2.7 Exploratory data analysis (EDA)

Principal component analysis (PCA) was performed on the mean spectra. The analysis was performed using seven principal components (PCs) to ensure consistency in the analysis. Principal component analysis can be

used to detect outliers in the sample set. This is done by using the PCA scores plots along with the influence plot (Payne, 2019). No statistical outliers were detected using the PCA scores plots in combination with the influence plot. In addition to outlier identification, scores plots, loading line plots and correlation loadings were investigated to identify wavelengths of interest.

3.2.8 Multivariate data analysis

3.2.8.1 Model development

Two quantification techniques were investigated to determine accuracy of the prediction for COD and TSS concentrations in winery wastewater. The techniques in question were partial least squares regression (PLS-R) (Lorber *et al.*, 1987) and principal component regression (PCR) (Hotelling, 1957). Linear discriminant analysis (LDA) and quadratic discriminant analysis (QDA) was performed to classify COD into 3 distinct categories; in, warning and out. The same classification techniques were performed to classify TSS into two distinct categories; low and high. Once pre-treatment and outlier removal were completed, the data was divided into calibration and validation sets. Approximately 70 % of the data was used for the calibration set and 30 % used as an independent validation set. Partial least squares regression, PCR, LDA and QDA models were developed for each parameter independently and their performance evaluated. For each analysis the average spectrum of each farm was calculated from the validation data and those 21 (COD) and 20 (TSS) average spectra were used for the validation to retain realism of a real-world environment.

3.2.8.2 Partial least squares regression (PLSR)

Partial least squares regression is a technique which combines multiple regression and PCA (Abdi, 2003). It is a projection method that is used to predict a property, \hat{Z} , based on the relationship between the predictors X (absorbance) and the response Y (COD/TSS) (Trygg & Wold, 1998). To achieve the best predictive power, this technique extracts orthogonal factors (latent variables) derived from the predictors (Abdi, 2003). The PLS-R models were used to predict COD and TSS concentrations. Full cross validation was performed on the data set. The calibration matrix (70 %) was used to train the algorithm to predict the Y response based on the X predictors. These calibration models were applied to the independent validation set (30 %) and the output was analysed based on coefficient of determination (R^2), RMSEP values and SEP/SEL.

3.2.8.3 Principal component regression (PCR)

Principal component regression is a technique that combines principal component analysis with least squares regression (Keithley *et al.*, 2009). It is important to transform a set of variates into their principal components if the independent variables are highly colinear, or if there are many potential reasons for the variation. Biological samples are highly variable so by transforming the data to its principal components, the sample space can be simplified (Massy, 1965). Full cross validation was performed on the data set. The data was

divided into calibration and independent validation sets as with PLS-R. Output was analysed based on R^2 , RMSEP values and SEP/SEL.

3.2.8.3 Discriminant analysis (DA)

Principal component (PC) scores were used to construct DA models. To determine the number of PCs to use the explained variance plot was analysed and PCs were selected that explains the most variance in the least amount of PCs. The number of PCs was decided once the difference in explained variance showed an increase of <5 % compared to the previous PC. Linear discriminant analysis calculates an optimal linear projection which minimises the intra-class variance and simultaneously maximises the variance between classes (Fisher, 1936). Quadratic discriminant analysis works by calculating a non-linear boundary, using a quadratic function, between classes. The model that had the best classification rate was selected for use and calibration models were built. Samples were classified based on the distance to the centre of each class. The model was subsequently applied to the independent validation set and an output was generated and analysed.

3.2.9 Performance measures

To assess the performance of the models with the respective pre-processing techniques the following calculations were performed. The classification accuracy (equation 3.1) illustrates the efficacy of the overall model. False positive error (equation 3.2) occurred when an incorrect class was classified as a correct class. A false negative error (equation 3.3) occurred when a correct class was incorrectly classified as an incorrect class. Various other performance measures were calculated (equations 3.4 – 3.8) to determine the optimal model.

$$\text{Classification accuracy (\%)} = \frac{TP+TN}{TP+TN+FP+FN} \times 100 \quad \text{Equation 3.1}$$

$$\text{False positive error (\%)} = \frac{FP}{TP+TN+FP+FN} \times 100 \quad \text{Equation 3.2}$$

$$\text{False negative error (\%)} = \frac{FN}{TP+TN+FP+FN} \times 100 \quad \text{Equation 3.3}$$

$$\text{Sensitivity or recall (\%)} = \frac{TP}{TP+FN} \times 100 \quad \text{Equation 3.4}$$

$$\text{Specificity (\%)} = \frac{TN}{TN+FP} \times 100 \quad \text{Equation 3.5}$$

$$\text{Precision (\%)} = \frac{TP}{TP+FP} \times 100 \quad \text{Equation 3.6}$$

$$\text{F1 Score (\%)} = \frac{2 \times \text{precision} \times \text{recall}}{\text{precision} + \text{recall}} \times 100 \quad \text{Equation 3.7}$$

$$\text{Misclassification rate} = \frac{FP+FN}{TP+TN+FP+FN} \times 100 \quad \dots \text{equation 3.8}$$

Where:

TP = True positive (Positive correctly classified as positive i.e low TSS classified as low TSS)

TN = True negative (Negative correctly classified as negative i.e high TSS classified as high TSS)

FP = False positive (Negative incorrectly classified as positive i.e high TSS classified as low TSS)

FN = False negative (Positive incorrectly classified as negative i.e low TSS classified as high TSS)

3.3 Results and discussion

3.3.1 COD quantification and classification (benchtop)

3.3.1.1 Spectral analysis

The average spectra were computed between the wavelengths of 1 000 - 2 500 nm and it was subsequently plotted to determine and compare the chemical properties of the wastewater. The data were manually classified into 3 categories for ease of comparison and to investigate trends related to COD (**Figure 3.2**).

Categories were identified as follows;

- In: COD values between 0 and 4 999 mg.L⁻¹
- Warning: COD values between 5 000 and 6 999 mg.L⁻¹
- Out: COD values above 7 000mg.L⁻¹

For the three categories the absorption trend was similar, however there was a difference in intensity and overlap between categories. Differences in intensity can possibly be attributed to physical effects such as light scattering in the unprocessed spectra. Three absorption bands were seen to be prominent at 1 448, 1 929 and 2 210 nm.

The absorption band at 1 448 nm is related to the O-H stretch first overtone of water (Cozzolino *et al.*, 2007). The absorption band at 1 929 nm is related to O-H stretch and deformation vibrations of water (Cozzolino *et al.*, 2007). Glucose, fructose and ethanol, which are large contributors to COD in winery wastewater, can be attributed to the wavebands between 2 200 nm and 2 300nm (Dambergs *et al.*, 2002; Cozzolino *et al.*, 2006; Cozzolino *et al.*, 2007).

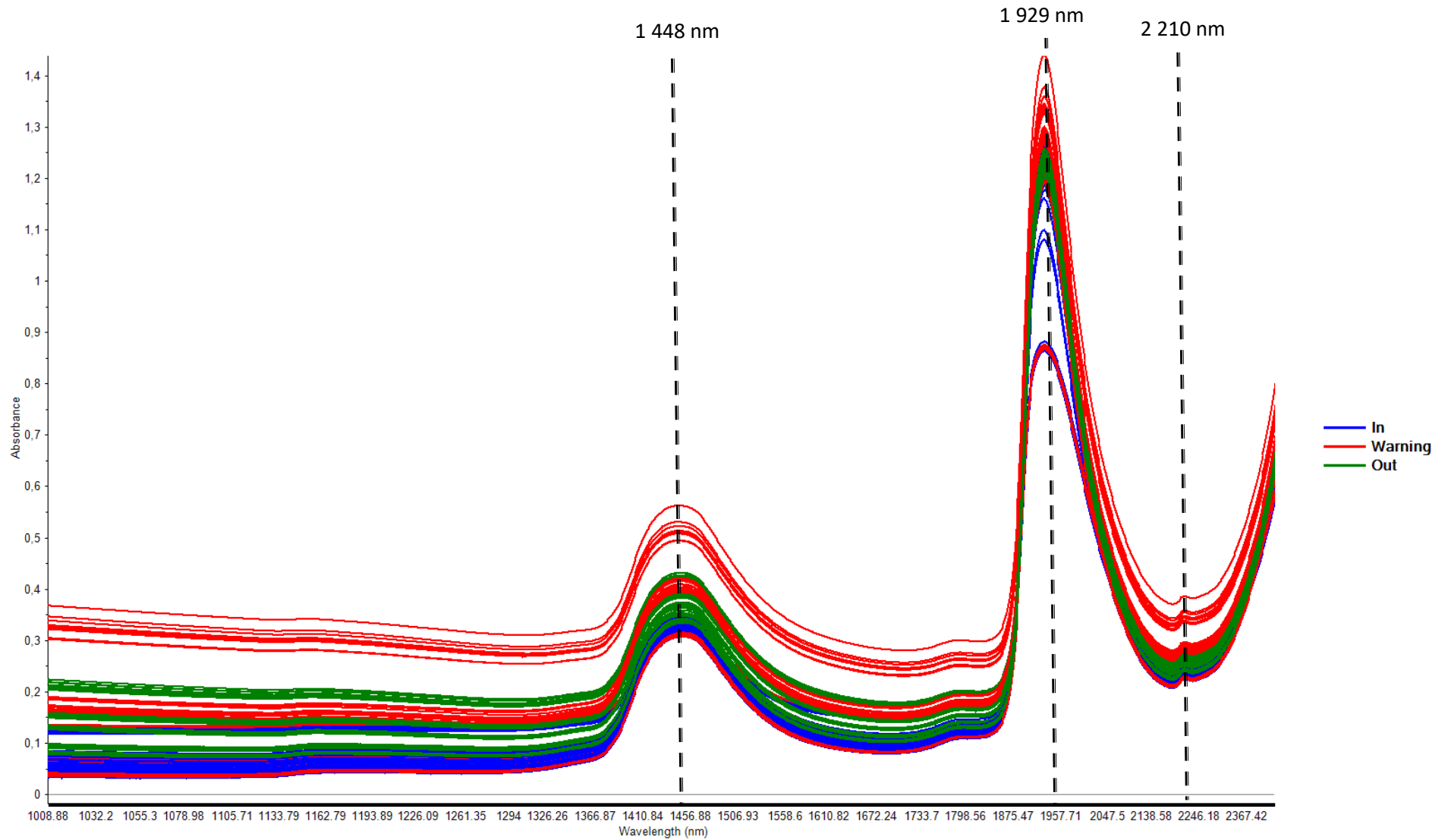


Figure 3. 2 Unprocessed spectra of COD divided into three categories; In (Blue), Warning (Red) and Out (Green).

3.3.1.2 Exploratory data analysis

3.3.1.2.1 Principal component analysis

Separation between the classes; in, warning and out was observed in the PCA scores plot of the OSC corrected data (**Figure 3.3**). Significant overlap between classes was also observed. It is expected that there be class overlap as the classes are based on a sliding scale of increasing concentration. This means that a COD of 4 999 mg.L⁻¹ and a COD of 5 001 mg.L⁻¹ will have different classes, yet are only 2 mg.L⁻¹ different in concentration. Increasing COD is correlated with a shift from left to right in PC1. PC1 accounted for 100 % of the variation in the data. The variation can therefore be explained by PC1 and the loadings plot was investigated to determine the source of the separation. Factors that could explain the separation could be differences in concentration of glucose, fructose and ethanol (Damberg *et al.*, 2002; Cozzolino *et al.*, 2006; Cozzolino *et al.*, 2007).

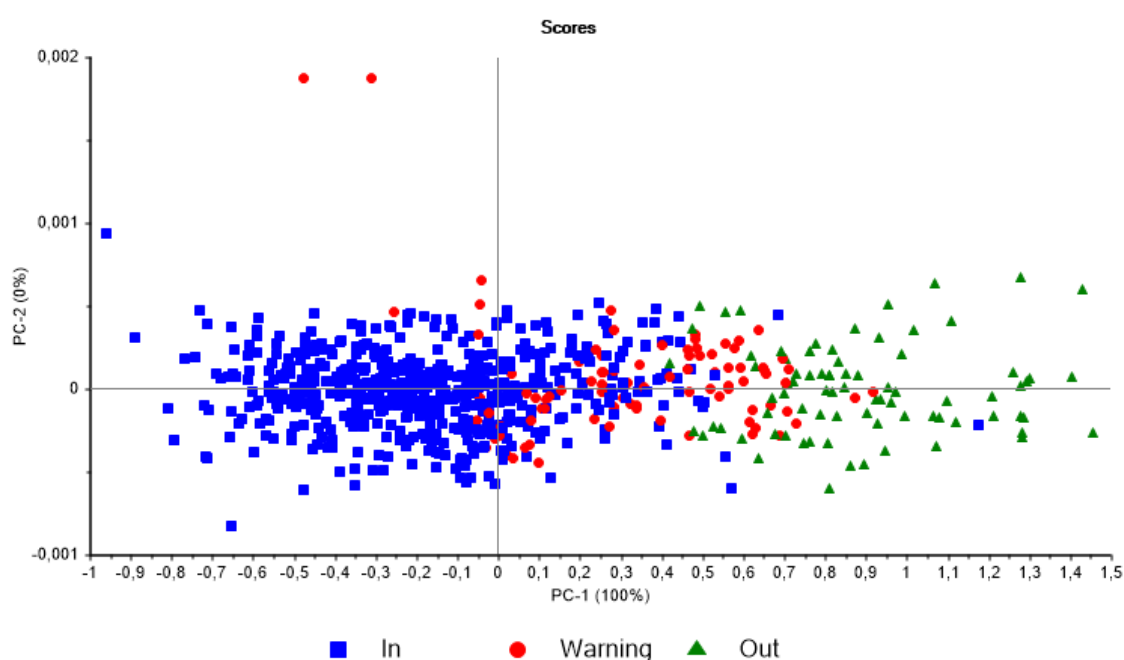


Figure 3.3 PCA (OSC corrected) analysis of spectral data for three COD categories; In (Blue), Warning (Red) and Out (Green). Separation 100 % explained in PC 1.

Differences in the interactions between water and other ions can also be a possible cause for the separation. To investigate the differences between the classes, the score plot along with the loadings line plot is used. Score scatter plots allow for the inspection of the samples for similarity and can offer a visualisation of where the samples are located within the PC space (Li Vigni, 2013). This allows for easy detection of groups or trends within the PC space. The loading vectors represent the variable contribution (wavelength) to the PCs and the correlation of the variables can then be investigated in the loading line plots (Li Vigni, 2013). The loadings can therefore be interpreted as the weights of each wavelength used in the analysis. This allows for the identification of important wavelengths that contribute to the separation of classes. The loadings line plot (**Figure 3.4**) in conjunction with the correlations loadings was used to determine wavelengths that contribute to the separation. From **Figure 3.4** three bands were identified that

could explain the separation. These wavebands were at 1 380 – 1 500 nm, 1 930 nm and 2 250 – 2 290 nm. The wavebands at 1 380 – 1 500 and 1 930 nm can be attributed to O-H stretch vibrations of water (Cozzolino *et al.*, 2006). The band at 2 250 – 2 290 nm can be attributed mainly to glucose, fructose and ethanol. The absorption band at 2 270 nm specifically is assigned to the CH-stretch from the methyl group of ethanol (Damberg *et al.*, 2002; Cozzolino *et al.*, 2006). In addition to the loadings line plot, the correlations loadings plot (**Figure 3.5**) can also be used to identify wavelengths that are important to identify the possible reason for separation.

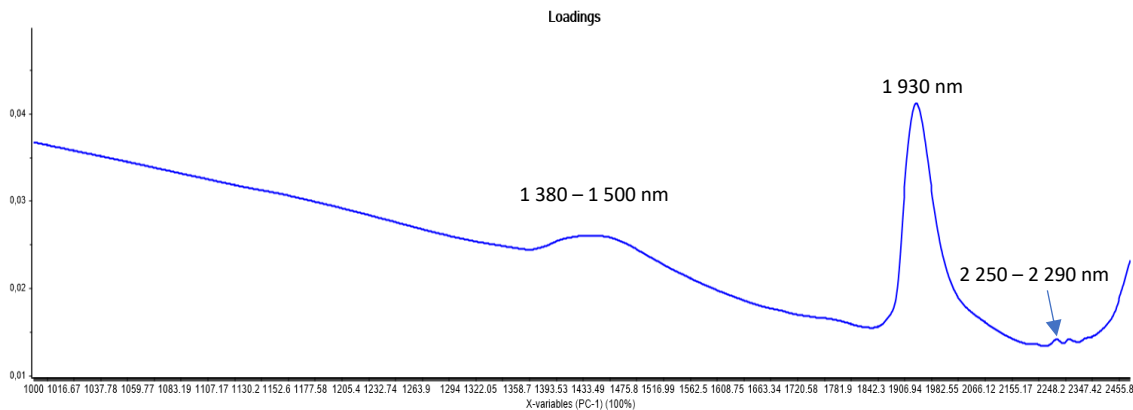


Figure 3. 4 PCA loadings line plot for PC1 (100 % explained) with interpretable bands at 1 380 -1 500 nm, 1 930 nm and 2 250 - 2 290 nm.

The correlation loadings plot indicates the significant wavelengths that are the reasons for the separation. The red dotted lines are the upper and lower bounds and values that lie within these bounds are modelled by the PCA. The upper line indicates 100 % of the explained variance and the lower line indicates 50 % of the explained variance. Values lying between the two lower bounds are not considered for the analysis. Both the positive and the negative values are used to determine wavelengths of importance. **Figure 3.5** indicates that for spectral data with OSC pre-processing all the wavelengths were important to derive separation. This could be because the winery wastewater has a lot of variables that can be explained at all the wavelengths. For example, pH can be explained at wavelengths of 1 332 – 1 640 nm and 2 173 – 2 355 nm in wine (Ye *et al.*, 2014). As wine and grape juice are the predominant contributors to winery wastewater it can be assumed that pH for winery wastewater will also be explained at these wavelengths. Total acidity can also be a contributing factor in the separation as it can be explained at wavelengths similar to pH at 1 640 – 1 730 nm (Ye *et al.*, 2014). Because OSC does not mean centre the data or correct for scattering it is also possible that the turbidity and total suspended solids can cause scattering effects, specifically at 1 000 – 1 400 nm as seen in **Figure 3.2**.

To investigate if that was a possibility multiplicative scatter correction (MSC) was performed alongside OSC and a PCA was calculated. The corresponding correlations loading plot is shown in **Figure 3.6**. It is evident from **Figure 3.6** that scattering is not responsible for the separation as the scattering was

corrected using MSC. The data was centred around zero and therefore the correlation loadings still showed that all wavelengths were important to separate the classes. The plot varies from negative to positive, but all wavelengths are between the dotted red line in either positive 1 or negative 1. Other factors must therefore be responsible for the separation other than turbidity and TSS. OSC may not be the most effective pre-processing method for wavelength selection as the method removes variation from the X data that are not related to the responses. Wavelength selection will be discussed in the following section.

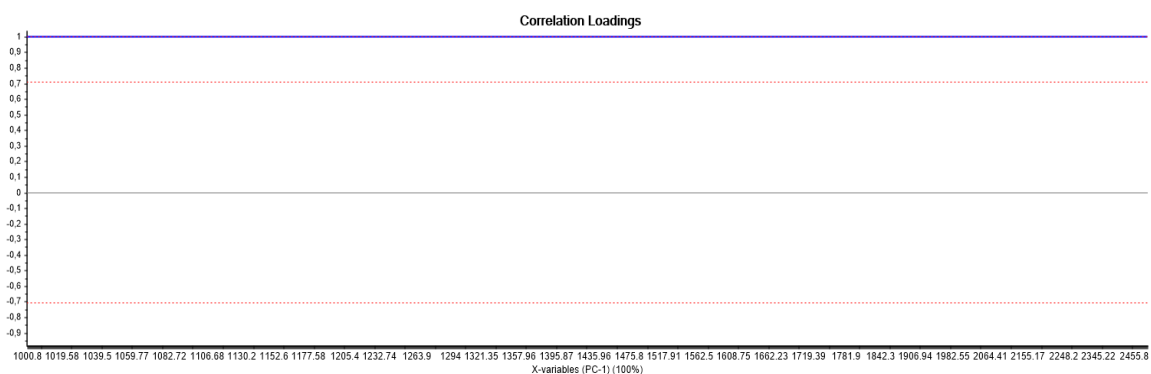


Figure 3. 5 Correlation loadings plot for PC1 on OSC corrected data showing all wavelengths (1 000 – 2 500 nm) important for separation.

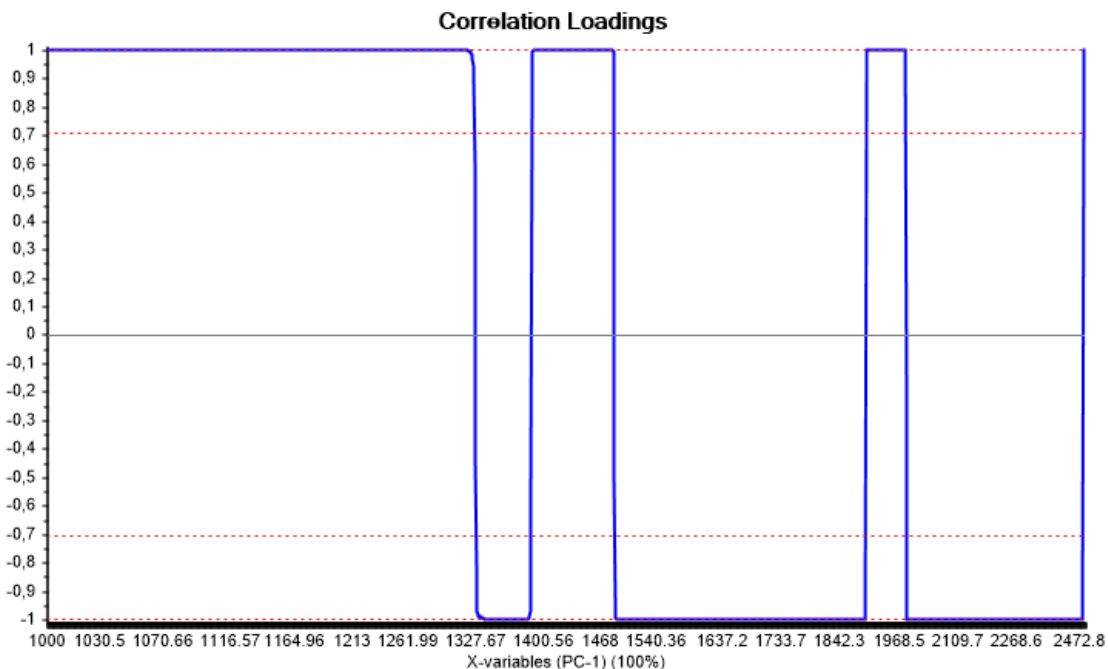


Figure 3. 6 Correlation loadings plot for PC1 on MSC and OSC corrected data illustrating important wavelengths.

3.3.1.2.2 Wavelength selection

Processing speed of The Unscrambler X.5 software is slow when using all wavelengths so it becomes important to select specific wavelengths that can be used to speed up the analysis. The selected wavelengths need to perform to a similar standard, compared to the full spectrum of the instrument, for classification and quantification. As mentioned earlier, OSC is not the optimal pre-processing technique to use for wavelength selection. Savitzky-Golay second derivative (SGD2) (3rd polynomial, 19 smoothing points) in combination with MSC was used to identify important wavelengths (**Figure 3.7**). From **Figure 3.7** it is evident that there is some separation in terms of the 3 COD classes. This separation is not as definitive as the pre-processing with OSC but can still be useful in terms of wavelength selection. Most of the variance in the data is explained by PC1 (94 %) and 5 % is explained by PC2.

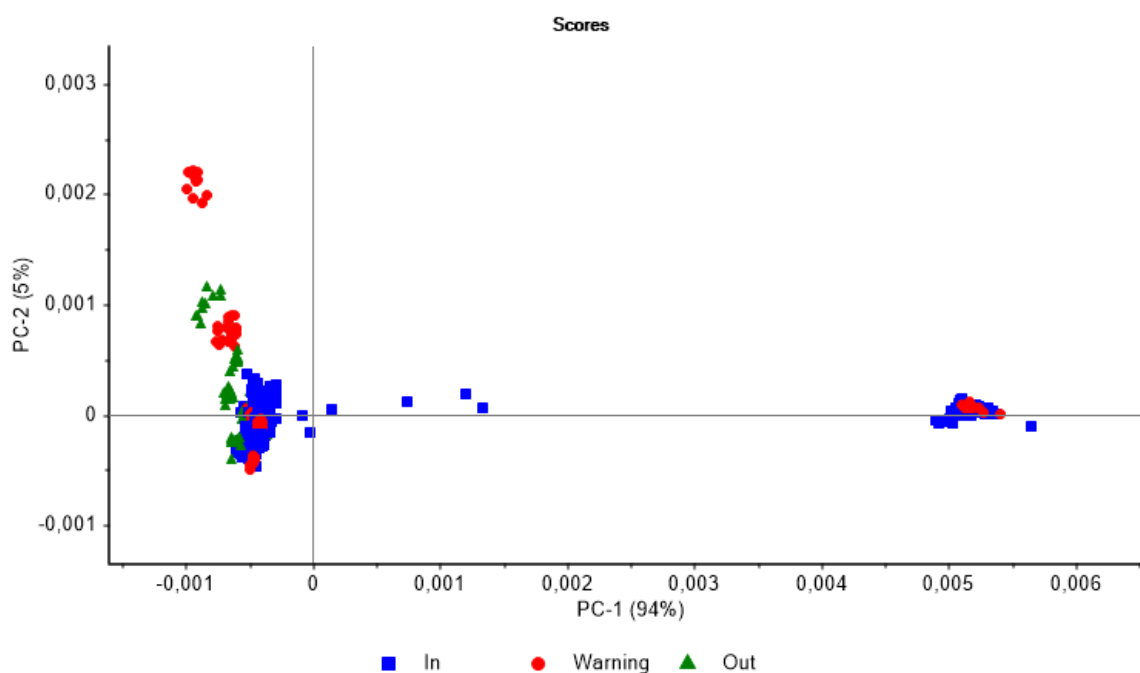


Figure 3.7 PCA (MSC and Savitzky-Golay second derivative) scores plot (PC1 (94 %) vs PC2 (5 %)) for COD categories; In (Blue), Warning (Red) and Out (Green).

When investigating the correlation loadings plot (**Figure 3.8**) there are several wavelengths that have an influence on the separation. The range 1 389 – 1 544 nm is one such example of a prominent waveband. Another prominent contributor to the separation is 1 800 – 2 000 nm. Both of these aforementioned ranges have been shown to describe interactions of ions, metals and other components with water (Tsenkova *et al.*, 2018). Winery wastewater does not just consist of wine, there is also considerable amounts of cleaning products such as NaOH or Cl⁻ (Vlyssides *et al.*, 2005). These may cause perturbations in the water and influence the resulting spectra (Tsenkova *et al.*, 2018). This field of study is known as aquaphotomics and these principles were not applied in this research. For this reason, when performing wavelength selection, the ranges 1 389 – 1 544 and 1 800 – 2 000 nm were not used. Important wavelengths at 2 060 – 2 170 nm and 2 260 – 2 340 nm explain some of the variation observed in PC 1 (**Figure 3.8**). It has been established that

ethanol may be the primary molecule being detected in the wastewater at 2 270 and 2 300 nm (Cozzolino *et al.*, 2007). The wavelength range 2 200 – 2 300 nm also represents sugars, as seen when a previous study tracked fermentation of wine over time with NIR and attributed changes in that region to conversion of sugars to ethanol (Cozzolino *et al.*, 2007). Another possible reason for a prominent peak can be attributed to tannins in the wine absorbing at 2 140 nm (Soukupova *et al.*, 2002). These findings by previous authors are consistent with the main contributors to COD in winery wastewater. Organic compounds contributing the most to COD are organic acids, esters, sugars, polyphenolic compounds and ethanol (Mosse *et al.*, 2011; Bories & Sire, 2016).

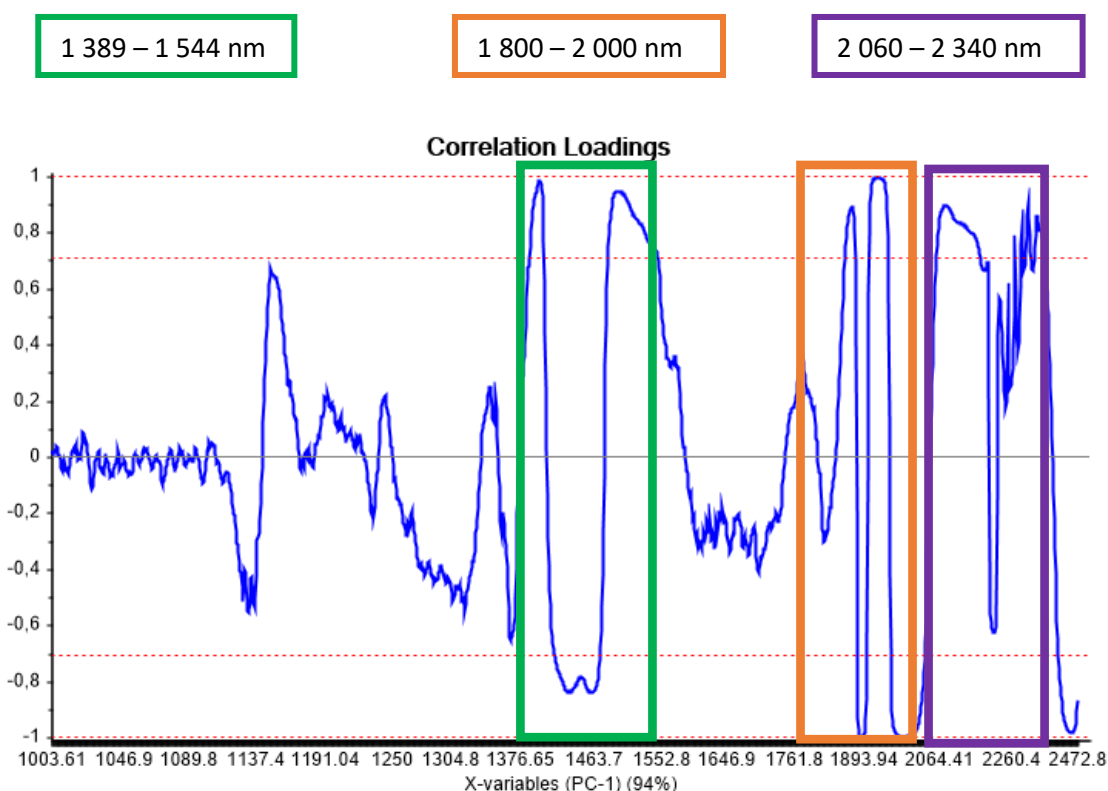


Figure 3. 8 Correlation loadings plot (PC 1) of data pre-processed with MSC and SGD2 showing prominent wavebands at 1 389 – 1 544 nm (Green), 1 800 -2 000 nm (Orange) and 2 060 – 2 340 nm (Purple).

The goal of wavelength selection is to decrease the wavelengths so that processing of the data can proceed more swiftly whilst ensuring that accuracy of the prediction is not compromised. The data without wavelength selection was selected and processed with PLS-R to investigate the prediction accuracy of the model using MSC and SGD2 (**Figure 3.9**). The RMSECV obtained when performing PLS-R was 915.93 mg.L⁻¹. The range of the COD represented was 102.5 – 10 570 mg.L⁻¹. The error of the prediction was therefore 8.75 % from the actual values on average. Wavelengths 2 060 – 2 340 nm were selected and processed with PLS-R to investigate the accuracy of the prediction using the same pre-processing but using limited wavelengths (**Figure 3.10**). The RMSECV obtained from this analysis was 925.12 mg.L⁻¹. The range was once

again $102.5 - 10\,570 \text{ mg}\cdot\text{L}^{-1}$, therefore the error of prediction was 8.84 %. By having RMSECV values so close together it confirmed that the wavelength range $2\,060 - 2\,340 \text{ nm}$ may be accurate for predicting COD.

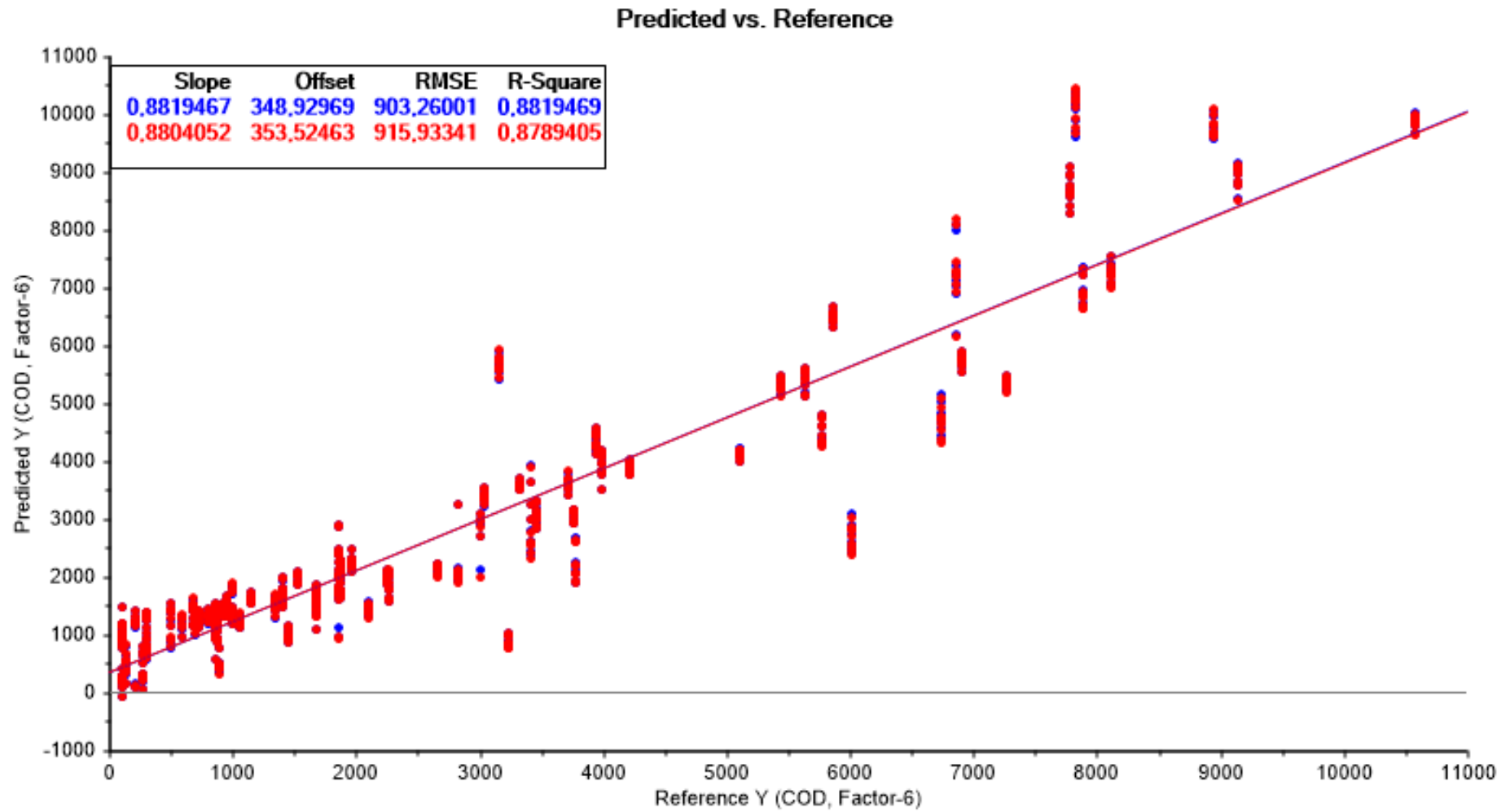


Figure 3. 9 PLS-R of the data (MSC + SGD2) showing the predicted vs reference values for COD using all wavelengths.

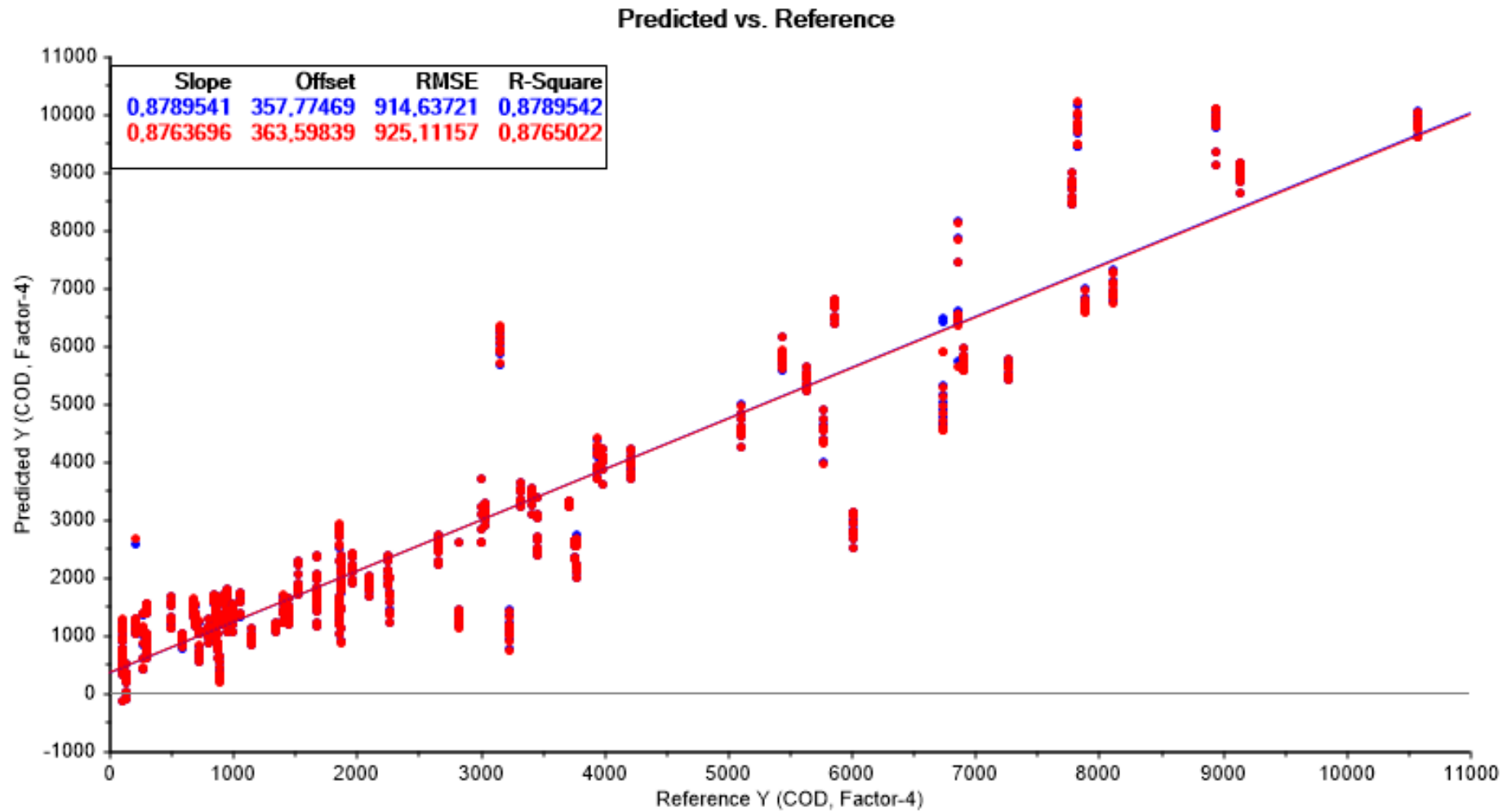


Figure 3. 10 PLS-R of the data (MSC + SGD2) showing the predicted vs reference values for COD using the wavelengths 2 060 – 2 340 nm.

3.3.1.3 Multivariate data analysis: Model development (benchtop)

3.3.1.3.1 Principal component regression (PCR)

Four pre-processing techniques were investigated using principal component regression (**Table 3.1**). The SNV and detrend model did not predict the COD concentration to a satisfactory degree. The root mean square error of calibration (RMSEC) was 1 837.10 mg.L⁻¹ with a COD range of 102.5 – 10 570 mg.L⁻¹ (10 467 mg.L⁻¹). This translates to an error percentage of 17.55 %. Root mean square error of cross validation (RMSECV) was comparable to the RMSEC albeit slightly worse as it uses samples within the calibration set and tries to predict the concentration of the COD. The correlation coefficient (R²) values for calibration and cross validation were 0.439 and 0.410 respectively. The prediction of the independent validation set performed slightly worse than the calibration set. An RMSEP value of 1 901.39 mg.L⁻¹ was achieved, yet the correlation coefficient was 0.632. It is clear that SNV and detrend as pre-processing is not optimal for the prediction of COD. A possible explanation for this is because SNV centres and scales the information and corrects for scattering effects, similar to MSC (Barnes *et al.*, 1989). Whilst this is a useful transformation, SNV and detrending cannot amplify small differences in the spectra. Savitzky-Golay second derivative transformation can be used to amplify spectral information. This may be necessary as water absorption bands are predominant and could possibly dominate other spectral information in those wavebands. PCR has also been less successful than PLS-R for the prediction of COD in literature. A 2014 study determined COD of paper mill wastewater and found PCR to be inferior to PLS-R for the prediction of COD (Dahlbacka *et al.*, 2014). To date very little work has been done on PCR for quantification of COD as most literature made use of PLS regression. When looking at the scores plot for SNV and detrending in the PCR model it becomes clear that there is not a great deal of separation between the 3 classes (**Figure 3.11**). There is considerable overlap of classes in the centre of the plot, leading to poor prediction performance.

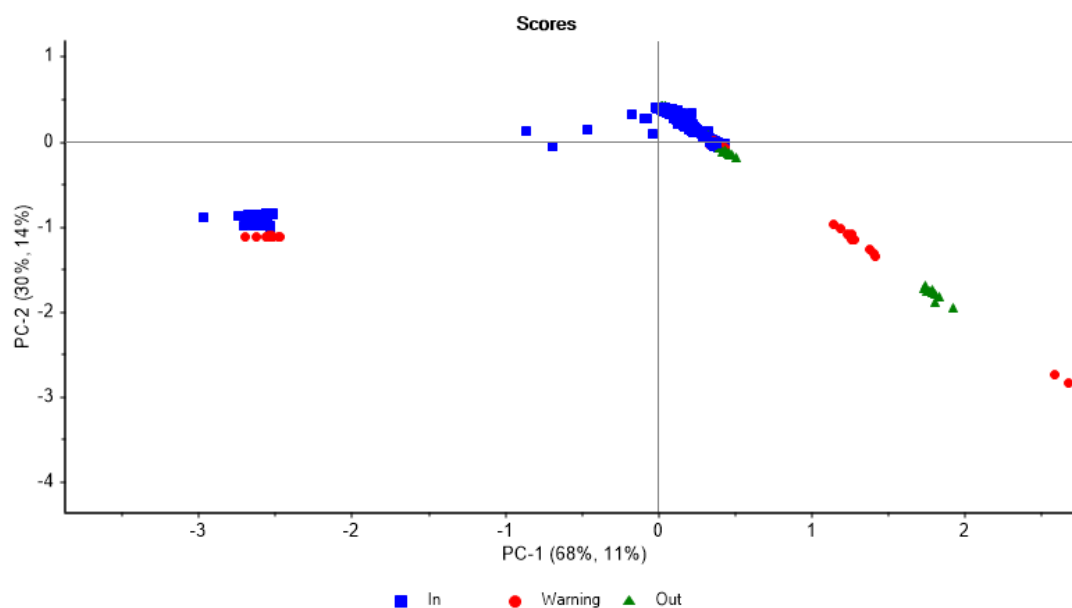


Figure 3. 11 PCA scores plot of SNV and detrended data using PCR. Overlap of classes in the centre of the scores plot leads to poor prediction of COD concentration.

Table 3. 1 Principal component regression calibration, cross validation and prediction results of COD concentration for four different pre-processing combinations.

| Model | | RMSE (mg.L ⁻¹) | R ² | SEP / SEL |
|--------------------|------------------|----------------------------|----------------|-----------|
| SNV + Detrend | Calibration | 1837.10 | 0.439 | |
| | Cross-validation | 1887.42 | 0.410 | |
| | Prediction | 1901.39 | 0.632 | 3.98 |
| SNV + Detr. + SGD2 | Calibration | 809.65 | 0.891 | |
| | Cross-validation | 822.36 | 0.888 | |
| | Prediction | 1215.15 | 0.830 | 2.74 |
| MSC + SGD2 | Calibration | 998.79 | 0.834 | |
| | Cross-validation | 1009.50 | 0.831 | |
| | Prediction | 1512.25 | 0.735 | 3.42 |
| OSC | Calibration | 875.100 | 0.873 | |
| | Cross-validation | 883.118 | 0.871 | |
| | Prediction | 1006.13 | 0.883 | 2.25 |

For the SNV, detrend and Savitzky-Golay 2nd derivative, the predictive power was considerably better compared to SNV and detrending on its own. Correlation coefficient values for calibration, cross validation and prediction were all above 0.80 (**Table 3.1**). Root mean square error values were also much lower with values of RMSECV and RMSEP values being 822.36 and 1215.15 mg.L⁻¹ respectively. The reason for improved predictive power is that derivatives eliminate peak overlap or increase resolution as well as eliminate a constant baseline drift between samples (Huang *et al.*, 2010). During conversion of the signal from analog to digital, rounding errors can occur which form shoulders upon transformation with second derivative specifically (Kitamura & Hozumi, 1987). Savitzky-Golay filter smooths the data and eliminates the shoulders (noise) from the spectral data (Kitamura & Hozumi, 1987). Another performance measure to consider is SEP (Standard error of prediction) / SEL (Standard error of laboratory). Acceptance of a model can be based on the SEP/SEL ratio. An acceptable model has a ratio of < 2 (Corredor *et al.*, 2015). The SEP/SEL ratio for all the pre-processing techniques with PCR are above 2. The SEP/SEL for the SNV, detrend and derivative model was 2.74 as the SEP was 1243.38 and the SEL was 453 mg.L⁻¹.

The model with the best performance was OSC in conjunction with PCR. Values for RMSECV and RMSEP are the most accurate of all the models evaluated for PCR. An RMSEP value of 1006.13 mg.L⁻¹ translates to an error percentage of 11.14 % of the range. The model is a good fit as the R² is 0.883. Values greater than 0.75 are generally accepted as good predictors of fit for regression models. Previous studies have used OSC for classification of wine vinegar and alcohol vinegar with 100 % success (Sáiz-Abajo *et al.*, 2005). Whilst this was not a quantification experiment it does highlight that OSC can be used on wine products with great success. Another study showed that OSC can be used to correct for light scattering in very turbid solutions that contain grape musts (Preys *et al.*, 2008). The authors could predict ethanol content to within 3.6°.

Turbidity of winery wastewater collected in this study ranged from 25 – 880 NTU. This large range with moderate turbidity values could explain why prediction accuracy was improved when using OSC. When

comparing the scores plot for OSC there is greater separation between the classes compared to other models (**Figure 3.12**). Reference data collected from laboratory analyses are very accurate in predicting COD. It is important for OSC that the reference data be accurate as the algorithm removes only X data that is not related to the reference data. The algorithm aims to minimise the covariance between spectra and reference data to remove all information that is not related to the reference data (Wold *et al.*, 1998). Orthogonal signal correction works well with spectral data as there are many variables (wavelengths) that try to explain a limited number of observations (COD, TSS etc).

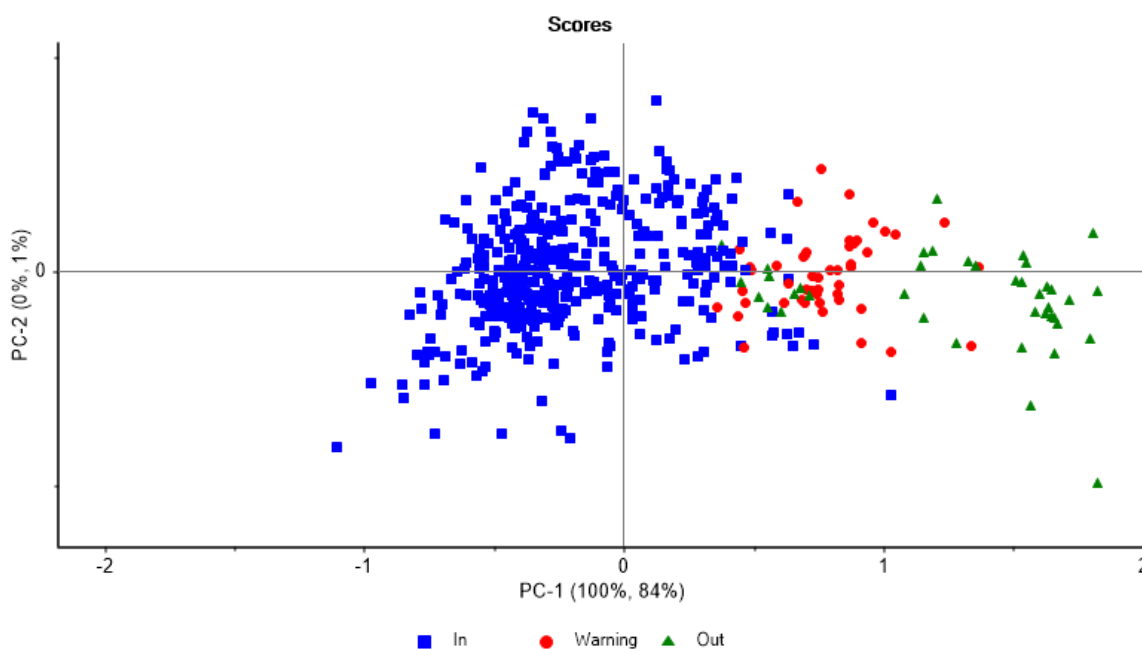


Figure 3.12 Scores plots of OSC corrected data in PCR showing distinct separation explained by PC 1 for the 3 COD classes.

3.3.1.3.2 Wavelength selection performance

The most accurate model was used to evaluate the performance of waveband selection. The waveband selected was 2 060 – 2 340 nm as discussed earlier in the chapter. The OSC model with waveband selection performed better than the model without waveband selection. The RMSECV and RMSEP were 760.64 and 893.81 mg.L⁻¹ respectively (**Table 3.2**). Error of prediction was therefore 9.9 % and is comparable to previous studies, although previous studies focused on PLS-R rather than PCR. Values of 0.912 for R² show an excellent model fit. This model has a SEP/SEL that is <2 and can therefore be concluded that this model is effective at predicting COD concentration for screening purposes. This model achieved the requirements of predicting COD with a 10 % error or less. Refer to **section 3.3.1.3.1** for a detailed explanation as to why OSC was the most accurate model.

Table 3. 2 Principal component regression results for COD concentration prediction using OSC for wavelengths 2 060 – 2 340 nm.

| Model | | RMSE (mg.L ⁻¹) | R ² | SEP/SEL |
|--------------------------|------------------|----------------------------|----------------|---------|
| OSC (Waveband selection) | Calibration | 751.96 | 0.906 | |
| | Cross-validation | 760.64 | 0.904 | |
| | Prediction | 893.81 | 0.912 | 1.94 |

3.3.1.3.3 Partial least squares regression (PLS-R)

Partial least squares regression in combination with SNV and detrend proved to be more successful than the same pre-processing using PCR. Values for RMSECV, RMSEP and R² all improved markedly. The RMSECV was 1 040.92 mg.L⁻¹ (**Table 3.3**) and the range of the samples was 102.5 – 10 570 mg.L⁻¹. Error rate of RMSECV was therefore 9.9 %. Prediction of COD was a lot worse than the cross validation, which is to be expected, but still shows an improvement of 295 mg.L⁻¹ compared to the data processed with PCR. Current literature does not use SNV and detrend for prediction of COD but rather uses second derivative in general. By looking at SEP/SEL this model is not sufficient for predicting COD even for screening purposes.

Table 3. 3 Partial least squares regression results for calibration, cross validation and prediction of COD for four different pre-processing combinations.

| Model | | RMSE (mg.L ⁻¹) | R ² | SEP/SEL |
|--------------------|------------------|----------------------------|----------------|---------|
| SNV + Detrend | Calibration | 1009.19 | 0.831 | |
| | Cross-validation | 1040.92 | 0.821 | |
| | Prediction | 1606.90 | 0.733 | 3.60 |
| SNV + Detr. + SGD2 | Calibration | 775.62 | 0.900 | |
| | Cross-validation | 791.26 | 0.896 | |
| | Prediction | 1182.45 | 0.841 | 2.67 |
| MSC + SGD2 | Calibration | 794.55 | 0.895 | |
| | Cross-validation | 823.51 | 0.888 | |
| | Prediction | 1224.80 | 0.827 | 2.76 |
| OSC | Calibration | 724.48 | 0.913 | |
| | Cross-validation | 742.01 | 0.909 | |
| | Prediction | 937.93 | 0.905 | 2.02 |

When PLS-R was combined with SNV, detrend and Savitzky-Golay 2nd derivative the prediction improved when compared to data pre-processed with only SNV and detrend. This is to be expected as second derivative can increase the resolution and expose peaks that could not previously be seen due to peak overlap (Kitamura & Hozumi, 1987; de Aragão & Messaddeq, 2008). A previous study was conducted to predict COD values in domestic sewage (Yang *et al.*, 2009). The average error of prediction was not reported as RMSEP for validation samples. However for calibration, SEP values of 25-30 mg.L⁻¹, depending on pre-processing, were reported in the calibration range of 28.6 – 528 mg.L⁻¹ (499.6 mg.L⁻¹). The SEP for calibration using PLS-R and second derivative was 30.18 and translates to an error of 6.04 % (Yang *et al.*, 2009). Another

study determined COD of water containing sucrose and water containing bovine serum albumin (BSA) using PLS-R and second derivative as pre-processing (Innocent *et al.*, 2007). The prediction results for the sucrose containing water was 172 mg.L⁻¹ and a COD range of 7.5 - 1 397 mg.L⁻¹ resulting in a relative error of 12 % which is similar to the results obtained from PLS-R in this study. When water containing BSA was analysed, the RMSECV of 138 mg.L⁻¹ leading to a relative error of 13.1 %. The study used cross validation for the validation and not an independent validation set, so these results must be compared to cross validated data in this study. Cross validated error was calculated to be 7.56 % which exceeds the results published in literature. A potential reason for this is due to correction of scattering effects from SNV pre-processing which could improve the prediction accuracy.

A study using second derivative combined with auto-scaling and mean-centering was used to predict COD concentration of paper mill wastewater. The authors achieved a RMSEP value of 149 mg.L⁻¹ which corresponds to an error of approximately 10 % (Dahlbacka *et al.*, 2014). The values obtained in this study are comparable to those found in literature, but the concentrations of COD far exceed the concentrations used in literature. Therefore, bigger RMSEP values are to be expected, yet the relative error to the range is comparable as the error achieved was 13 % using SNV, detrend and SGD2. The SEP/SEL ratio (**Table 3.3**) achieved was 2.67 which means that although the prediction improved, it is still above a ratio of 2 which is the limit for a good model.

The model that used MSC and SGD2 was very comparable to the model using SNV, detrending and SGD2. This was expected, as MSC and SNV are very similar as both correct for scattering. Although SNV and MSC are fundamentally different as SNV transforms individual spectra whereas MSC uses the mean spectrum to correct for scattering. Differences are therefore expected in the results, but the results should be comparable. From **Table 3.3**, RMSEP of MSC and SGD2 is 42.35mg.L⁻¹ higher, which corresponds to 0.47 % difference. This illustrates the similarity in the two pre-processing techniques.

Orthogonal signal correction used as pre-processing for PLS-R method performed the best out of all the regression models. When comparing OSC in combination with PLS-R the RMSECV was 742.01 mg.L⁻¹ (**Table 3.3**). This result is lower than the 883 mg.L⁻¹ (**Table 3.1**) achieved from PCR and OSC using all wavelengths. The RMSEP of OSC and PLS-R was 937.93 mg.L⁻¹ which is a 10.38 % error to the range which is comparable to studies previously mentioned. Previous work has not specifically been done on COD and OSC as pre-treatment, however PLS-R along with OSC has been used to predict ethanol content in the effluent of an anaerobic hydrogen bioreactor (Zhang *et al.*, 2009a). Using OSC as pre-processing and PLS-R the ethanol content could be predicted with an RMSEP value of 59.1 mg.L⁻¹. The range of the predicted measurements was 489.9 mg.L⁻¹, resulting in an error of 12.06 % (Zhang *et al.*, 2009a). This is comparable to previous literature as well as to this study. It was expected that OSC and PLS-R would work well as a combination as both techniques take the response variables into account when calculating the latent variables (Niazi *et al.*, 2007). When comparing results from **Table 3.1** and **Table 3.3**, PLS-R outperforms PCR by a small margin. These methods are very similar, with PCR only taking the wavelengths into account in the prediction, whereas

PLS-R includes the responses in the calculation of latent variables (Hemmateenejad *et al.*, 2007). Both methods give very similar results in literature, with PLS sometimes outperforming PCR, but not to a large extent (Wentzell & Montoto, 2003).

3.3.1.3.4 Wavelength selection performance

The model with the lowest RMSEP was used to evaluate the performance of waveband selection. The OSC model with waveband selection performed better than OSC and PLS-R without waveband selection. The RMSEP value was 898.67 mg.L⁻¹ which resulted in an error of 9.95 % and is consistent with findings in literature for prediction of COD using PLS-R (Yang *et al.*, 2009; Pan *et al.*, 2011; Pan *et al.*, 2012b). Correlation coefficient of the model was above 0.9 indicating a very good fit for the data. The SEP/SEL was 1.93, indicating suitability of the model to be used as a screening method to determine COD of winery wastewater. Principal component regression using OSC and waveband selection performed slightly better (4.86 mg.L⁻¹)(**Table 3.2**) than OSC and PLS-R when using waveband selection (**Table 3.4**). This difference is very small and both models could be said to have the same predictive capability. The improvement in the model when waveband selection is employed may be because some regions in the spectra contain other analytes, interferences and interactions which may degrade model accuracy (Hemmateenejad *et al.*, 2007). When waveband selection was performed for the comparison of performance of PCR and PLS-R in literature, there was not a significant difference in the predictive power of both techniques (Hemmateenejad *et al.*, 2007), confirming the results of this study.

Table 3. 4 Partial least squares regression results for COD concentration prediction using OSC for wavelengths 2 060 – 2 340 nm.

| Model | | RMSE (mg.L ⁻¹) | R ² | SEP/SEL |
|--------------------------|------------------|----------------------------|----------------|---------|
| OSC (Waveband selection) | Calibration | 749.45 | 0.907 | |
| | Cross-validation | 760.42 | 0.904 | |
| | Prediction | 898.67 | 0.913 | 1.93 |

3.3.1.3.5 Discriminant analysis (DA)

All of the calibration models had a classification accuracy above 85.0 % (**Table 3.5**). However, this does not always mean that the models are good as they may be overfit. This is the case when using SNV, Detrending and Savitzky-Golay 2nd derivative which had a validation classification accuracy of 57.14 %. Linear discriminant analysis with OSC provided a classification accuracy of 90.4 % for validation and had a calibration classification accuracy of 93.35 %. The data is therefore not overfit as the classification and the validation accuracies are similar. The accuracy of the model suggests that LDA and OSC can be used to distinguish between the 3 classes of COD accurately. Quadratic discriminant analysis along with OSC as pre-processing could also be used as it yields good prediction capability.

Table 3. 5 DA model results to assess the performance of the different pre-processing along with optimal method (LDA, QDA or Mahalanobis) for COD discrimination.

| Number of PCs | Method | Model | Classification | Accuracy (%) | |
|---------------|-------------|---------------|----------------|--------------|-------|
| 5 | Linear | SNV, DET SGD2 | Calibration | 91.25 | |
| | | | Validation | 80.90 | |
| | | OSC | Calibration | 93.35 | |
| | | | Validation | 90.40 | |
| | | Quadratic | SNV, DET SGD2 | Calibration | 88.21 |
| | | | | Validation | 57.14 |
| | OSC | | Calibration | 97.53 | |
| | | | Validation | 85.70 | |
| | Mahalanobis | SNV, DET SGD2 | Calibration | 96.20 | |
| | | | Validation | 66.67 | |
| | | OSC | Calibration | 97.53 | |
| | | | Validation | 80.95 | |

The best model from **Table 3.5** was further investigated to determine its performance parameters. Classification of each class was high with the model being capable of differentiating between each class with an accuracy above 90 % for each (**Table 3.6**). The warning class had the worst accuracy of 90.48 % which could be because it was a transition category between In and Out categories. There could therefore easily be misclassification. As an example, in **Figure 3.12** it is evident that there is overlap between the categories on the PCA. The precision of prediction for classes warning and out are 75 % (**Table 3.6**). This shows that the model struggles to correctly predict warning class and out class correctly. This model therefore struggles to differentiate between warning and out. It does however predict the in class with 100 % precision. It is therefore still a useful model, specifically as a screening method, as it can predict the in class without error. The sensitivity of the warning class is low at 75.00%. Sensitivity describes the possibility that a positive response would be correctly classified as positive. Therefore, that the warning class is correctly classified as warning. Literature has not classified COD, preferring to focus on quantification studies. It can be concluded that NIR can be used to classify COD which could be useful for screening purposes in bioreactors. If quantification is not important to the operator and only whether the water is of too high strength, then classification of COD is beneficial. LDA in combination with OSC can be used to classify COD in winery wastewater to an acceptable level for screening purposes.

Table 3. 6 Performance measures used to assess the LDA model (5 PCs) with OSC as pre-processing for the classification of COD into three classes.

| Class | Classification accuracy | False positive error (%) | False negative error (%) | Sensitivity (%) | Specificity (%) | Precision (%) | F1 Score (%) |
|---------|-------------------------|--------------------------|--------------------------|-----------------|-----------------|---------------|--------------|
| In | 95.00 | 0.00 | 5.00 | 92.86 | 100.00 | 100.00 | 96.30 |
| Warning | 90.48 | 4.76 | 4.76 | 75.00 | 94.12 | 75.00 | 75.00 |
| Out | 95.00 | 5.00 | 0.00 | 100.00 | 94.12 | 75.00 | 85.71 |

3.3.2 COD quantification and classification (handheld)

3.3.2.1 Spectral analysis

The average spectra for the portable NIR instrument was computed between the wavelengths of 908 – 1 651 nm. The spectra were plotted to compare chemical properties of the winery wastewater. Data were again classified into 3 categories; in, warning and out.

Three absorption bands were found to be prevalent from the raw spectra. These bands were located at 970, 1 160 and 1 400 nm. The absorption band at 970 nm may be attributed to moisture (Li *et al.*, 2007). The band at 1 160 nm may be attributed to the C=O stretching fourth overtone as well as some aromatic groups (Debebe *et al.*, 2017; Rosa *et al.*, 2017). Carbonyl groups are often found in wine and can be either aldehydes or ketones and they are mostly compounds associated with odours in wine e.g. acetaldehyde (Lago & Welke, 2019). Absorption band between 1 400 and 1 650 nm may be attributed to the first overtone of O-H stretching of methanol and ethanol or possibly water (Cozzolino *et al.*, 2006; Debebe *et al.*, 2017; Tsenkova *et al.*, 2018). From **Figure 3.13** there is a lot of overlap between the 3 classes but there are samples with increased intensity from 908 – 1 400 nm. These could be spectral outliers, as TSS should not lead to an increase in absorption at those wavelengths as previously discussed.

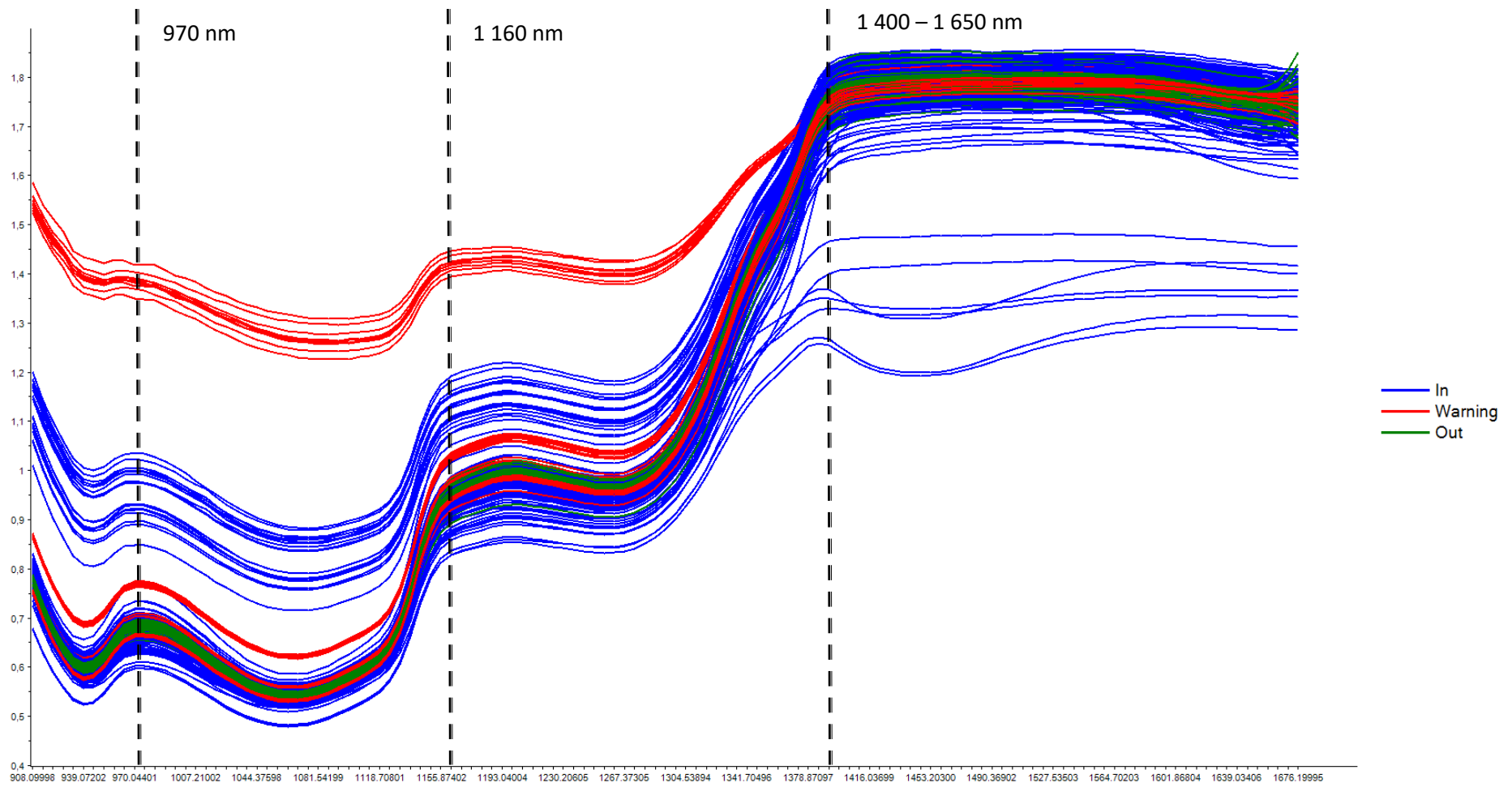


Figure 3. 13 Unprocessed spectra in wavelength range 908 – 1 651 nm in three categories; In (Blue), Warning (Red) and Out (Green).

3.3.2.2 Exploratory data analysis

3.3.2.2.1 Principal component analysis

No separation of classes was observed when investigating the raw spectra. There is considerable overlap between all three classes and no clear separation of classes can be observed (**Figure 3.14**). The class labelled warning that separated to the right in PC1 is the same farm for which the absorbance in **Figure 3.13** was increased. Pre-processing had to be performed to try and separate classes based on COD concentration.

Upon pre-processing with OSC there was more clear separation between classes with PC1 explaining 100 % of the variation (**Figure 3.15**). There was still overlap between classes, but this was mostly between the in and warning classes, which is to be expected as the warning class is a transition class between in and out classes. Because COD concentration is on a spectrum, complete separation is unlikely. The variation between the classes can be completely explained by PC1 and the loadings line plot can be investigated to determine the cause of the separation.

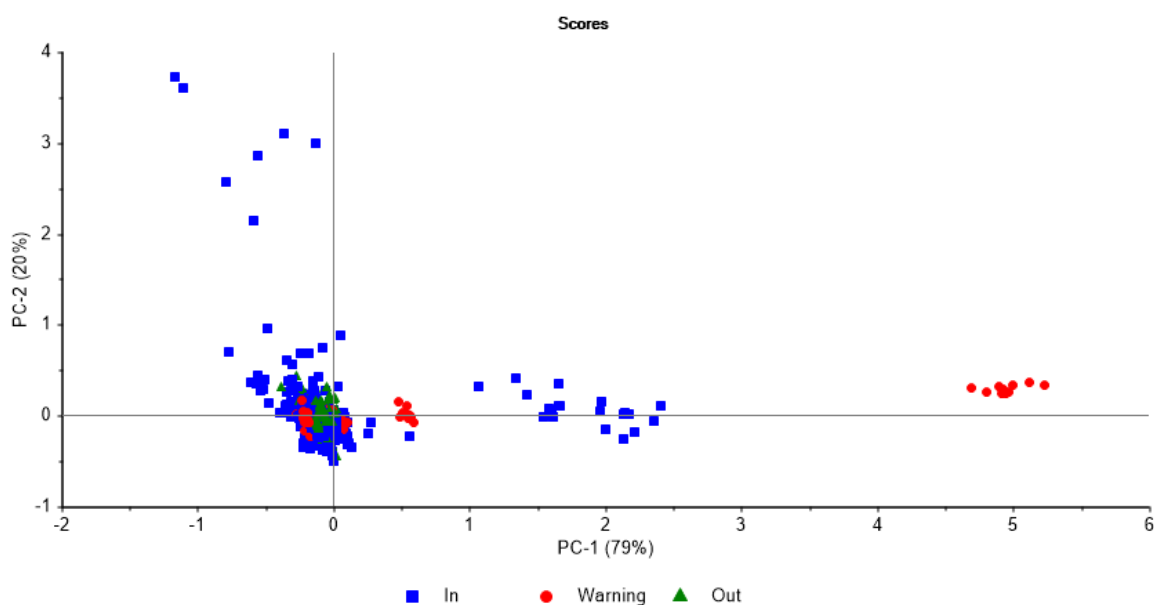


Figure 3. 14 PCA of raw spectra (PC1 vs PC2) for the three categories of COD concentration; In (Blue), Warning (Red) and Out (Green).

From the loadings line plot (**Figure 3.16**) three wavebands have some importance. These are 1 120, 1 162 and 1 378 nm. The band at 1 120 nm may be related to fatty acid content in the wastewater (Moscetti *et al.*, 2015). Absorption bands around 1 400 nm can be attributed to C-H and O-H bonds associated with TSS (Cozzolino *et al.*, 2006). At 1 400 nm absorption bands may also be attributed to O-H bonds of water (Cozzolino *et al.*, 2006). To investigate this further the correlations loadings plot was investigated (**Figure 3.17**).

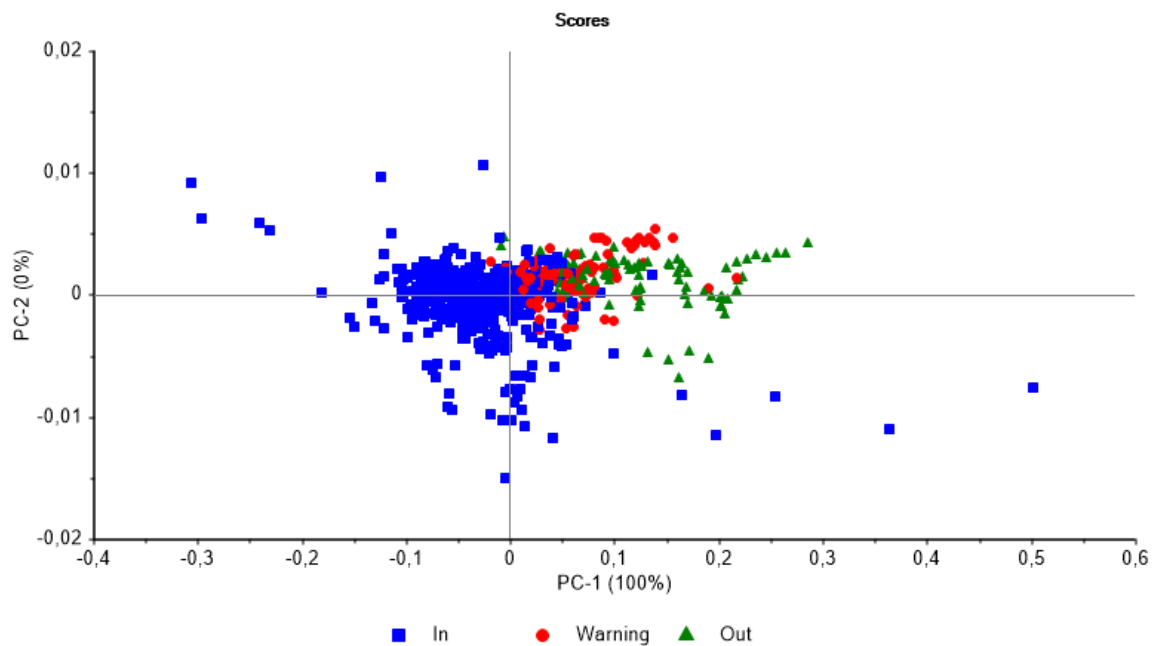


Figure 3. 15 PCA of OSC processed spectra (PC 1 vs PC 2) for the three COD categories; In (Blue), Warning (red) and Out (Green).

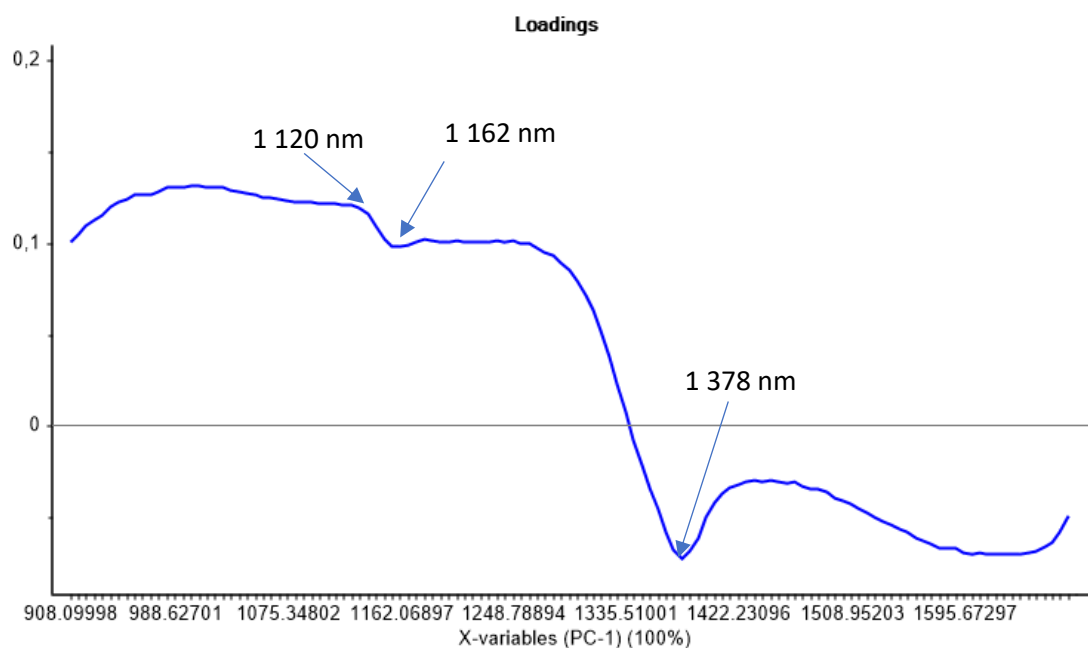


Figure 3. 16 Loadings line plot indicating 3 wavelengths that may explain separation of COD classes at 1 120, 1 162 and 1 378 nm.

The correlations loadings plot indicates that all the wavelengths may have been important for the classification of COD (**Figure 3.17**). The plot shows that all the wavelengths lie between the outer and lower bounds (Delineated by red dotted lines) meaning that all the wavelengths may be important. This may be so as a result of the portable device having a smaller wavelength range compared to the benchtop instrument.

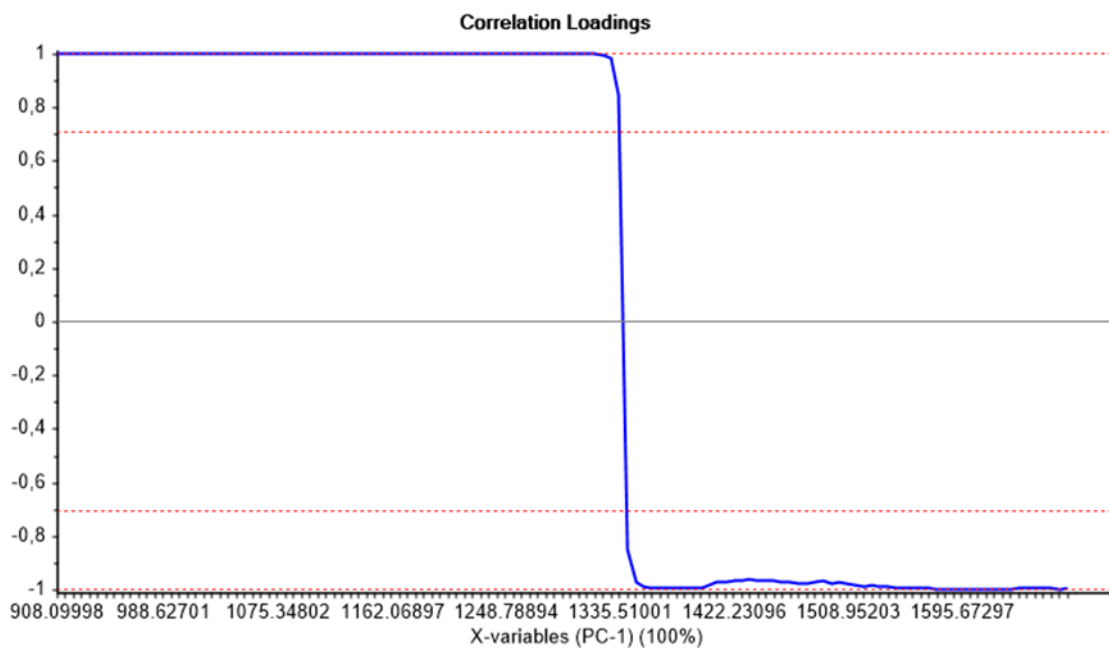


Figure 3. 17 Correlation loadings for PC1 to determine important wavelengths in the range 908 – 1 651 nm. All wavelengths were deemed important to explain the separation.

However, when investigating the important wavelengths with the benchtop instrument all the wavelengths were also deemed to be important for the separation. A more likely explanation may be because 100 % of the variation is explained by PC1. If PC1 explained less of the variation, there may have been wavelengths that are deemed unimportant to explain the separation. Another reason is that OSC as a pre-processing technique might be responsible, as it removes X data that are not related to the Y response.

Wavelength selection was not performed on the spectral data as there are few wavelengths available when compared to the benchtop instrument. The portable instrument contains 125 wavelengths across the range 908 – 1 651 nm whereas the benchtop instrument contained 156 wavelengths once wavelength selection was completed. Wavelength selection will therefore have no benefit to the speed of processing.

3.3.2.3 Multivariate data analysis: Model development (handheld)

3.3.2.3.1 Principal component regression

For the portable device only two pre-processing techniques were investigated upon identification of the two most accurate pre-processing techniques using the benchtop instrument. These techniques were SNV, detrending and Savitzky-Golay 2nd derivative and OSC (**Table 3.7**).

Table 3.7 illustrates that SNV, detrending and Savitzky-Golay 2nd derivative was not suitable for prediction of COD concentration. The RMSEC was 2 211.16 mg.L⁻¹ an error of 21.13 %. Calibration data had an R² of 0.44 which is very low and does not correlate well with the COD data. Prediction of the independent validation set decreased further and the RMSEP was 2 296.98 mg.L⁻¹ which translates to an error of 25.43 % as the range was 9 032 mg.L⁻¹. The value of R² improved to 0.615 which indicates some positive correlation, yet it falls below the 0.75 needed to indicate a good model fit. The SEP/SEL was 5.19 meaning that the model

was not suited for prediction of COD data at all. Winery wastewater is very complex and there may be too few variables when using the portable device to explain the complexity of the wastewater. The 4 nm increments between wavelengths means that there is a lot of information lost when compared to the benchtop instrument (1 nm increments). Principal component regression relies on the principal components to be the predictors for the response; however PCs do not always correlate with the responses (Westad *et al.*, 2013). The main goal of PCA is to extract information that describes the variation in the X variables best. In scenarios where there is a lot of information not related to Y or if there is a high level of noise the PCs may be very poorly related to the responses and therefore result in a poor prediction (Westad *et al.*, 2013). This could be the reason for SNV, detrending and Savitzky-Golay 2nd derivative not working well with PCR for prediction of COD in winery wastewater.

Table 3. 7 Principal component regression results for calibration, cross-validation and prediction of COD concentration for two different pre-processing combinations.

| Model | | RMSE (mg.L ⁻¹) | R ² | SEP/SEL |
|-------------------------|------------------|----------------------------|----------------|---------|
| SNV + Detrend + SGD2 | Calibration | 2211.16 | 0.44 | |
| | Cross-validation | 2268.67 | 0.207 | |
| | Prediction | 2296.98 | 0.615 | 5.19 |
| OSC | Calibration | 1554.31 | 0.626 | |
| | Cross-validation | 1572.21 | 0.619 | |
| | Prediction | 1531.39 | 0.80 | 3.40 |

A previous study was undertaken to determine polyphenols in wine using PCR and PLS-R and NIR (Martelo-Vidal & Vázquez, 2014). The authors found that PCR did not work as well as PLS-R for the quantification. There were instances when using SNV and detrending along with SGD2 was reliable for prediction, but with PLS-R instead of PCR. Using PCR no such combinations were performed, however MSC smoothing and SGD2 were performed, but to no great accuracies (Martelo-Vidal & Vázquez, 2014).

As PCR makes use of PCA for its predictions, it is useful to investigate the PCA scores plot to explain poor predictive power. **Figure 3.18** shows the PCA scores plot for the data pre-treated with SNV, detrending and SGD2. There is poor separation between the classes, with extreme overlap. Even with increasing concentration of COD there are no clear clusters forming.

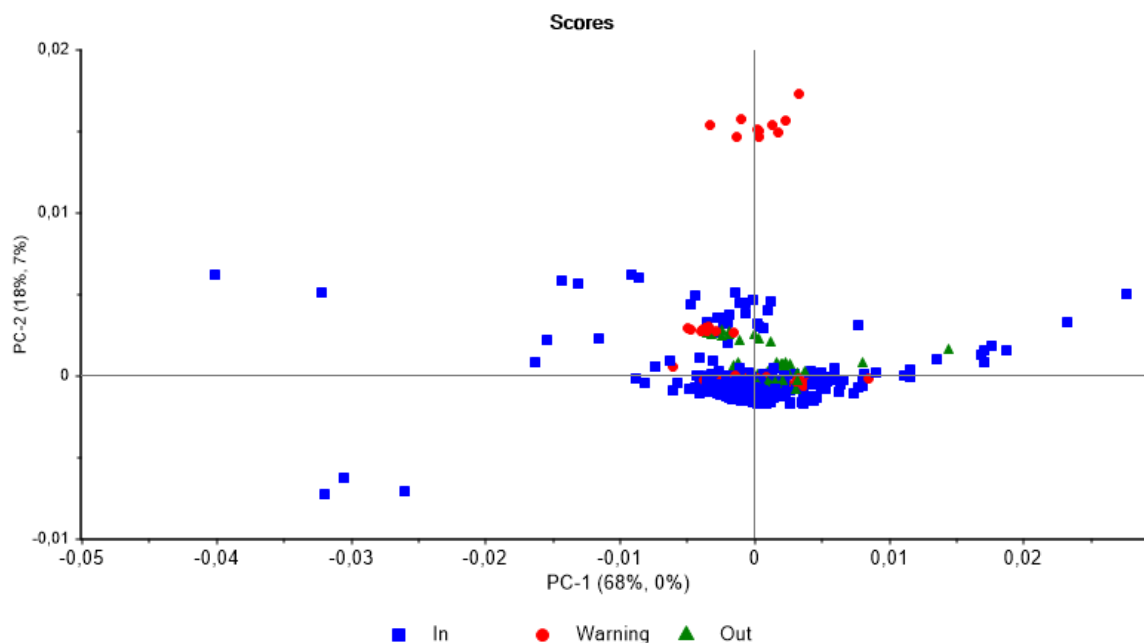


Figure 3. 18 PCA scores plot for COD concentration on spectra pre-processed with SNV, detrending and SGD2.

For the data processed with OSC and PCR the prediction improves considerably. The RMSEC was $1\ 554.31\ \text{mg.L}^{-1}$ which results in an error of calibration to the range ($102.5 - 10\ 570\ \text{mg.L}^{-1}$) of 14.85 %. There is an absolute improvement of 6.28 % for the prediction of COD compared to the first model. Correlation of the data of 0.626 indicate that the fit is not ideal but is far superior to the previous model. The predictive power of the OSC and PCR model is improved with the RMSEP being $1\ 531.39\ \text{mg.L}^{-1}$. An error of 16.96 % was achieved for the prediction. The portable instrument does not perform to the same standard as the benchtop instrument, as its range is smaller, and it has lower resolution. When looking at SEP/SEL the model is not suitable for prediction as the value of 3.40 is greater than the prescribed limit of 2 (Corredor *et al.*, 2015). This pre-processing technique performs better for the prediction of COD as OSC removes X data that is not correlated to the response. As PCR does not remove unrelated X data, this may explain the improvement of the predictive power of the OSC and PCR model. None of these models are powerful enough to be considered useful for prediction of COD in winery wastewater.

3.3.2.3.2 Partial least squares regression

Partial least squares regression was performed on the data with 2 different pre-processing approaches (Table 3.8). From Table 3.8 it is evident that SNV, detrending and SGD2 in combination with PLS-R was not ideal for predicting COD concentration. The value for RMSEC was $1\ 835.78\ \text{mg.L}^{-1}$ meaning that the error to the range is 17.53 %. This is considerably lower than the RMSEC of the PCR model with the same pre-processing. The correlation coefficient of 0.479 is low and does not show a good fit for the model. The RMSEP value for this combination is $1\ 843.06$ with an R^2 value of 0.718. There is a correlation, but it is not strong as it is under 0.75. Error of the prediction is 20.41 %. When comparing the same pre-processing and regression

technique to the benchtop instrument, the benchtop outperforms the portable instrument by 7.41 % in absolute terms. These data suggest that this specific model is not a good predictor for COD in winery wastewater. A previous study used PLS-R to determine COD in wastewater using wavelengths of 820 -850 nm. The prediction error was 7.79 % compared to the range of the independent validation set. It is therefore possible to use limited wavelengths although this portable instrument cannot scan at those wavelengths (Pan *et al.*, 2011). Very little analysis has been performed on grape juice, must or wine for these wavelengths so comparing the results to literature is not possible for similar substrates.

When OSC was used in combination with PLS-R the RMSECV was considerably better than using SNV, detrending and SGD2. The RMSECV was 1009.19 mg.L⁻¹ resulting in an error of 9.64 %. Correlation coefficient value was 0.843 which indicates that the model is a good fit (Colton & Bower, 2002). This may not always be the case, but it can be a good indicator for the detail explained by the model. A study was performed to evaluate the monitoring of COD in a sequential batch reactor for dairy sludge (Páscoa *et al.*, 2008). The instrument used had a wavelength range of 900 – 1 700 nm and could predict COD concentration to 86.6 mg.L⁻¹, however the range was 52.8 – 905.8 86.6 mg.L⁻¹. Error of prediction for the cross-validated data was therefore 11.6 %. The model was not subjected to an independent validation set so this study used the RMSECV. This compares favourably for the OSC pre-processed data that had an RMSECV of 9.64 %. This study improved upon the prediction with a similar wavelength range. Root mean square error of prediction for the model was 1 047.97 mg.L⁻¹ meaning the error was 11.60 %. This is greater than the 10 % goal set forth in the aim of this study but shows that OSC along with PLS-R has potential to predict COD concentration in winery wastewater for screening purposes. It is possible that this combination worked better because of the fundamental differences between PLS-R and PCR with PLS-R incorporating the responses into the model (Hemmateenejad *et al.*, 2007).

Table 3. 8 Partial least squares regression results for calibration, cross-validation and prediction for two different pre-processing approaches

| Model | | RMSE (mg.L ⁻¹) | R ² | SEP/SEL |
|-------------------------|------------------|----------------------------|----------------|---------|
| SNV + Detrend + SGD2 | Calibration | 1835.78 | 0.479 | |
| | Cross-validation | 1934.99 | 0.423 | |
| | Prediction | 1843.06 | 0.718 | 4.15 |
| OSC | Calibration | 1009.19 | 0.843 | |
| | Cross-validation | 1162.76 | 0.792 | |
| | Prediction | 1047.97 | 0.879 | 2.36 |

3.3.2.3.3 Discriminant analysis

Linear discriminant analysis yielded positive results for the classification of COD for both pre-processing techniques with SNV, detrending and SGD2 yielding a calibration accuracy of 76.29 % and validation accuracy of 76.19 %. Both the calibration and validation had similar classification performance, which would suggest that this model is not overfit, and the correct number of components was chosen to model the data. The

accuracy is not very high, but the data suggest that this pre-processing technique may have potential to predict COD using LDA.

Quadratic discriminant analysis in combination with SNV, detrending and SGD2 achieved bad classification accuracies. Calibration accuracy was 31.99 % and classification accuracy was 19.05 %. These data suggest that QDA is not suitable for prediction of COD using this specific pre-processing. A possible explanation for this may be that QDA requires the variance-covariance to be similar for the two different classes, which is not the case for these samples (Siqueira *et al.*, 2017). Classes are very similar as they are classified based on a spectrum of COD and not two distinct wastewaters, e.g. winery wastewater versus dairy wastewater.

Mahalanobis discriminant analysis achieved good prediction results with a calibration accuracy of 86.40 % and a validation accuracy of 76.19 %. Because the calibration and the validation accuracy is 10 % different, this model may be slightly overfit, which may reduce predictive capability of the model. The PCA plot for this pre-processing combination (**Figure 3.17**) shows a lot of overlap between classes and this may be a reason why the mahalanobis discriminant analysis technique performed worse than LDA. The best classification results were achieved using OSC as pre-processing technique. Linear discriminant analysis and OSC had a calibration accuracy of 86.95 % and a validation accuracy of 80.95 %. This would suggest that LDA along with OSC as pre-processing is a useful model for the prediction of COD classes. When QDA was used along with OSC the calibration was improved (89.15 %), but the validation accuracy remained at 80.95 %. This would suggest that the LDA and OSC model is most likely the more robust model, as the difference in classification and validation accuracies are smaller.

Performance of the portable NIR spectrophotometer was decreased compared to the benchtop instrument, which was expected as the resolution of the benchtop instrument is superior and the range of the instrument is larger, resulting in more information being able to be acquired to model the data. The benchtop instrument could scan samples above 2 000 nm where glucose fructose and ethanol absorb. These parameters are some of the main contributors to COD in winery wastewater and this can explain the difference in prediction results (Mosse *et al.*, 2011).

The performance measures for LDA and QDA using OSC as pre-processing is shown in **Table 3.10** to determine the best model for prediction of COD. The best model was LDA using OSC as this model has slightly better precision and sensitivity. Most of the other performance measures are very similar and the choice of LDA is a combination of slightly superior precision, sensitivity and less difference between classification and validation accuracies. If the goal is to predict the “In” class the most accurately, then the LDA model may be the best choice, as it predicts the “In” class correctly 100 % of the time. Higher overall precision and F1 scores indicate that the optimal model is linear discriminant analysis.

Performance of the portable spectrophotometer indicates that this instrument could differentiate between 3 different classes of COD with an 81 % accuracy. Whilst this accuracy may not be sufficient for implementation at this moment, there is potential for a portable instrument to be used for classifying COD.

One shortcoming of this instrument is a reduced wavelength range and it may be necessary for an investigation into the performance of a portable instrument with a wavelength range of 2 000 – 2 500 nm.

Table 3. 9 DA model results to assess the performance of the different pre-processing along with optimal method (LDA, QDA or Mahalanobis) for COD discrimination.

| Number of PCs | Method | Model | Classification | Accuracy (%) |
|---------------|-------------|---------------|----------------|--------------|
| 5 | Linear | SNV, DET SGD2 | Calibration | 76.29 |
| | | | Validation | 76.19 |
| | | OSC | Calibration | 86.95 |
| | | | Validation | 80.95 |
| | Quadratic | SNV, DET SGD2 | Calibration | 31.99 |
| | | | Validation | 19.05 |
| | | OSC | Calibration | 89.15 |
| | | | Validation | 80.95 |
| | Mahalanobis | SNV, DET SGD2 | Calibration | 86.40 |
| | | | Validation | 76.19 |
| | | OSC | Calibration | 87.50 |
| | | | Validation | 71.43 |

Table 3. 10 Performance measures used to assess the LDA and QDA models using OSC as pre-processing for the classification of COD into three classes.

| Number of PCs | Class | Classification accuracy | False positive error (%) | False negative error (%) | Sensitivity (%) | Specificity (%) | Precision (%) | F1 Score (%) |
|---------------|---------|-------------------------|--------------------------|--------------------------|-----------------|-----------------|---------------|--------------|
| 5 (LDA) | In | 94.44 | 5.56 | 0.00 | 100.00 | 83.33 | 92.31 | 96.00 |
| | Warning | 80.85 | 4.76 | 14.29 | 50.00 | 93.33 | 75.00 | 60.00 |
| | Out | 85.00 | 10.00 | 5.00 | 66.67 | 88.24 | 50.00 | 57.14 |
| 5 (QDA) | In | 94.44 | 0.00 | 5.56 | 92.86 | 100.00 | 100.00 | 96.30 |
| | Warning | 80.85 | 9.52 | 9.52 | 50.00 | 88.24 | 50.00 | 50.00 |
| | Out | 85.00 | 10.00 | 5.00 | 66.67 | 88.24 | 50.00 | 57.14 |

3.3.3 TSS quantification and classification (benchtop)

3.3.3.1 Spectral analysis

The average spectra were computed between the wavelength range of 1 000 – 2 500 nm and was plotted to investigate the chemical properties of the wastewater. The data were classified into two categories of total suspended solids (TSS). Categories were identified as the following;

- Low: TSS values between 0 and 999 mg.L⁻¹
- High: TSS values higher than 1 000 mg.L⁻¹

The raw spectra of the samples look similar, however there is a clear difference in intensity of the low and high categories with the low (Blue) categories generally having lower absorbance values than the high (Red) category (**Figure 3.19**). These differences in intensity may be because of light scattering due to increased TSS of each sample. The absorption bands were previously discussed in **section 3.3.1.1** and the bands may primarily be attributed to water (1 448 nm and 1 929 nm) and glucose, fructose and ethanol (2 200 – 2 300) (Damberg *et al.*, 2002; Cozzolino *et al.*, 2006; Cozzolino *et al.*, 2007).

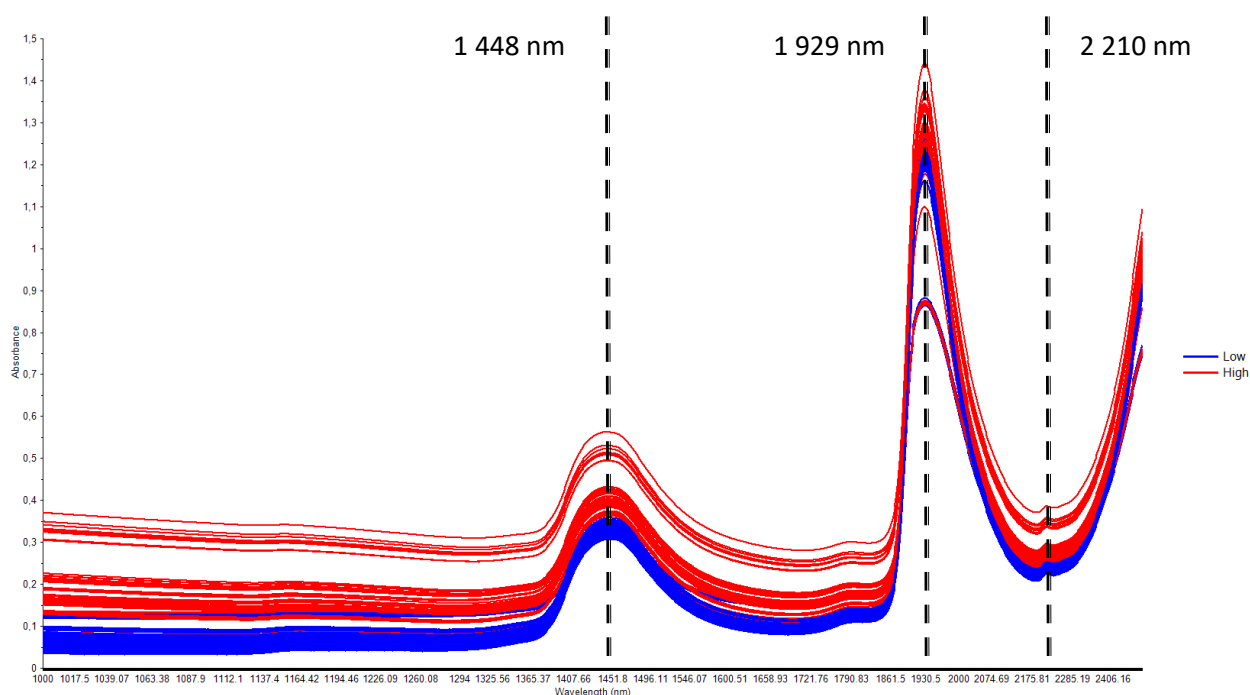


Figure 3. 19 Raw spectra for TSS data divided into two categories; Low (Blue) and High (Red) using the benchtop spectrophotometer.

3.3.3.2 Exploratory data analysis

3.3.3.2.1 Principal component analysis

From the PCA there is separation between the two TSS classes (**Figure 3.20**). There is overlap between the classes and this was expected as the classes are not two very distinct classes. The two classes are just a continuation on a spectrum of COD and therefore overlap should be expected, especially at concentrations

that are close to the boundary of each class. An increase in TSS is correlated with a shift from left to right in PC1. This accounted for 100 % of the data in PC1. The loadings line plot for OSC pre-treatment of TSS data shows the same peaks as **Figure 3.3**. The possible compounds absorbing at those wavelengths was discussed in **section 3.3.1.2.1**. The loadings line plot of MSC and Savitzky-Golay 2nd derivative for TSS is shown in **Figure 3.21**.

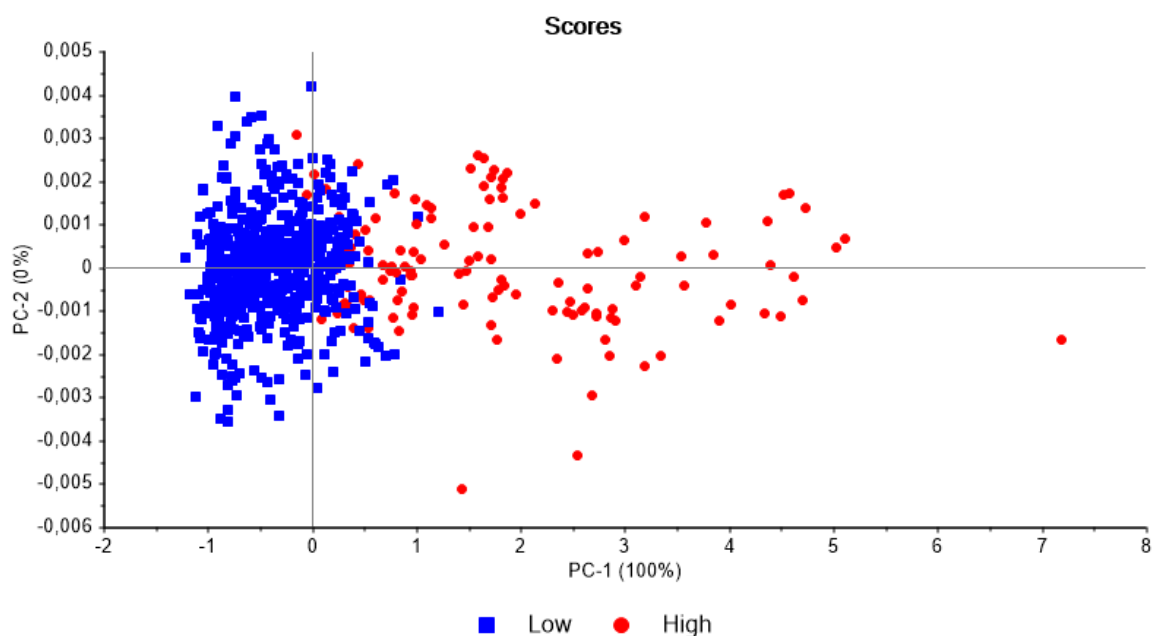


Figure 3. 20 PCA (OSC corrected) analysis of spectral data for two TSS categories; Low (Blue) and High (Red). Separation 100 % explained in PC1.

Principal component 1 explains 95 % of the X-variance, but 0 % of the Y-variance, whereas PC2 explains very little X-variance (4 %) but explains 61 % of the Y-variance. By exploring the wavelengths identified by the loadings and correlation loadings it is possible to identify possible causes for the separation of classes. There are four wavebands of importance identified from **Figure 3.21**. These are at 1 388 – 1 410, 1 881, 1 904 and 2 200 – 2 400 nm. As previously stated in **section 3.3.1.2** the bands at 1 388 – 1 410, 1 881 and 1 904 nm are all associated with the absorbance of water in the NIR region (Damberg *et al.*, 2002; Cozzolino *et al.*, 2006). Other studies have however found that the wavelengths at 1 350 – 1 400 and 1 880 – 1 920 nm may correspond with fatty acid absorbers (Velasco *et al.*, 1997). A wavelength at 1 410 nm corresponds to the 1st overtone of an alcohol, most likely ethanol. Wavelengths between 2 200 – 2 400 nm most likely correspond to ethanol and sugars (Workman Jr, 2000).

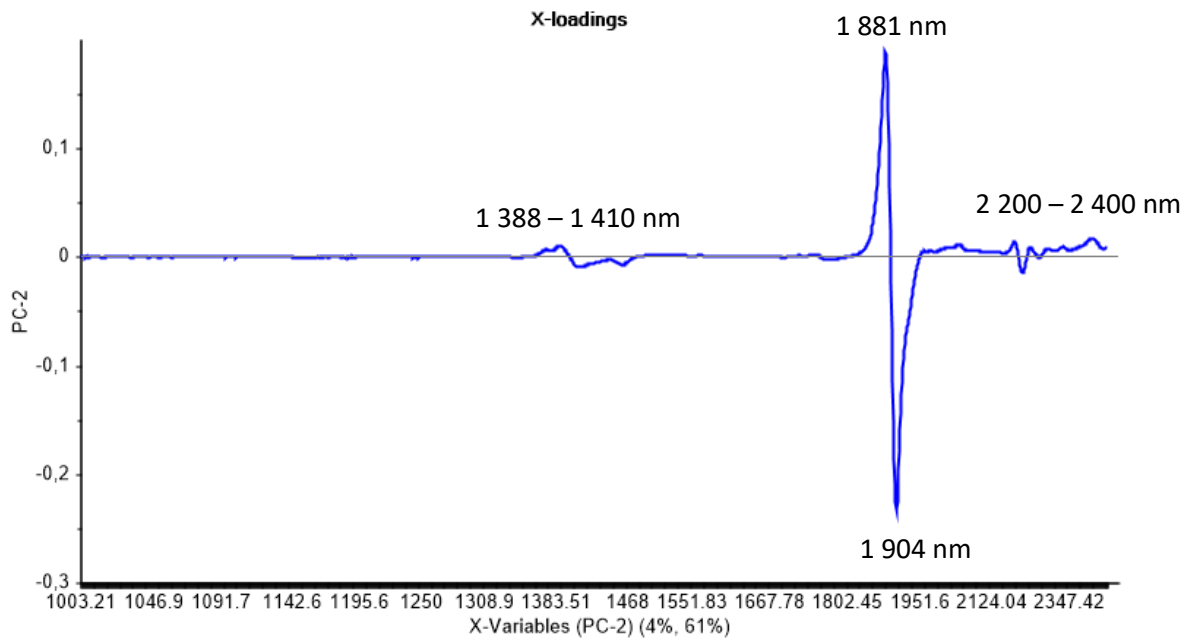


Figure 3. 21 Loadings line plot for PC2 (61 % Y-Variance explained) with four wavebands of importance at 1 388 - 1 410, 1 881, 1 904 and 2 200 – 2 400 nm.

3.3.3.2.2 Wavelength selection

Wavelength selection is an important consideration in NIR spectroscopy as it may decrease processing speed of the analysis. As mentioned previously, the selected wavelengths must be able to be used in a prediction model and yield similar results to the full spectrum of the instrument. Multiplicative scatter correction in combination with SGD2 was used to identify wavelengths of importance. The loadings line plot (**Figure 3.21**) along with the correlation's loadings plot (**Figure 3.22**) was used to determine which wavelengths may be useful for predicting TSS. From **Figure 3.22** it is apparent that there are eight wavelengths that fall within the bounds of the red dotted lines. These are; 1 378, 1 407, 1 780, 1 839, 1 882, 1 904, 2 045 and 2 394 nm. Bands that have not previously been mentioned include 1 780, 1 839, 2 045 and 2 394 nm. The band at 1 780 nm may be caused by the C-H stretch of aromatic compounds. These compounds are found in wastewater and may contribute to TSS of the wastewater (Ramos *et al.*, 2016). The waveband at 1 839 nm may be attributed to the C-H stretch of a methyl group, likely bonded to aromatic compounds in the wastewater (Workman Jr, 2000). A N-H or C-N band may be observed at 2 045 – 2 050 nm and this may be attributed to nitrogen found in winery wastewater, albeit at low concentrations (Moletta, 2005). The nitrogen may be as a result of cleaning practices of the farms if these farms were to use a nitrogen-based cleaning product. The waveband at 2 394 nm corresponds to C-H combination tones in wine and this may influence the TSS (Cozzolino *et al.*, 2005).

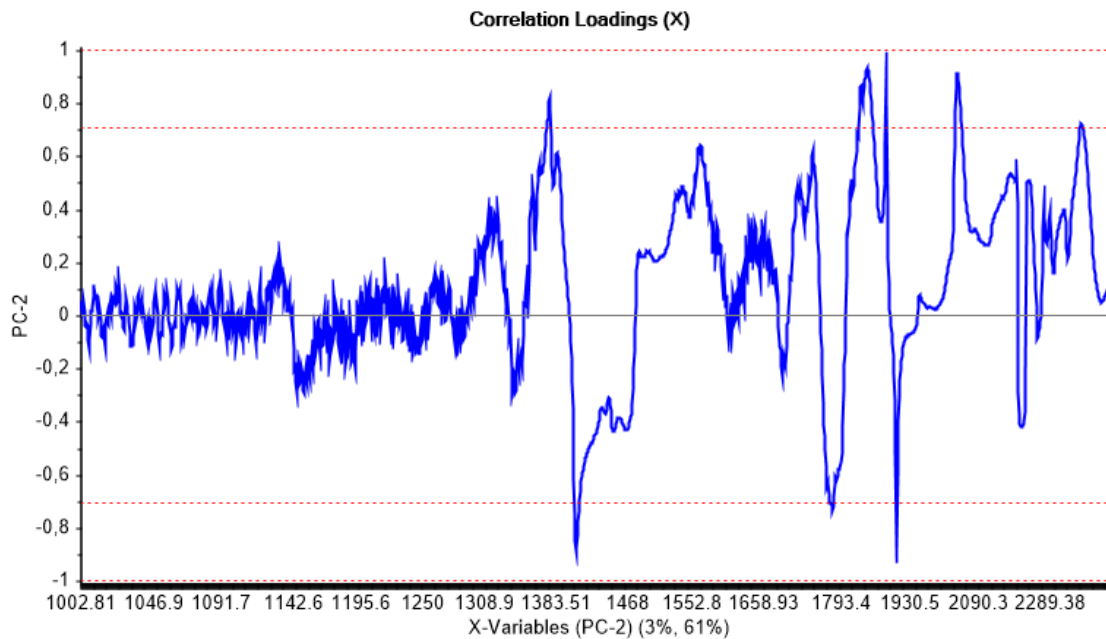


Figure 3.22 Correlation loadings on MSC and SGD2 pre-processed data showing prominent wavebands at 1 378, 1 407, 1 780, 1 839, 1 882, 1 904, 2 045 and 2 394 nm.

Upon inspection of above figures the waveband selected was 1 900 – 2 500 nm as the absorption bands at 1 300 – 1 400 nm is predominantly associated with water. The organic molecules associated with wavelengths above 1 900 nm are most likely to be associated with TSS, as they contain sugars, ethanol, aromatic compounds and potentially inorganic nitrogen.

The data was subjected to PLS-R using OSC as pre-treatment to determine the RMSECV using all wavelengths (**Figure 3.23**). The RMSECV obtained for this data set was 202.93 mg.L⁻¹ and the range of the TSS represented was 14.00 – 2 863.00 mg.L⁻¹. The error associated with this prediction was therefore 7.12 %. Wavelengths in the range 1 900 – 2 500 nm were identified and processed with OSC and PLS-R to investigate the accuracy of the prediction using limited wavelengths (**Figure 3.24**). The RMSECV obtained for this data set was 216.20 mg.L⁻¹ for the same range resulting in an error of 7.59 %. This result indicates that wavelength selection was comparable to the full spectrum and that there is clear potential to predict TSS of winery wastewater for screening purposes using a benchtop FT-NIR instrument with the wavelength range 1 900 – 2 500 nm.

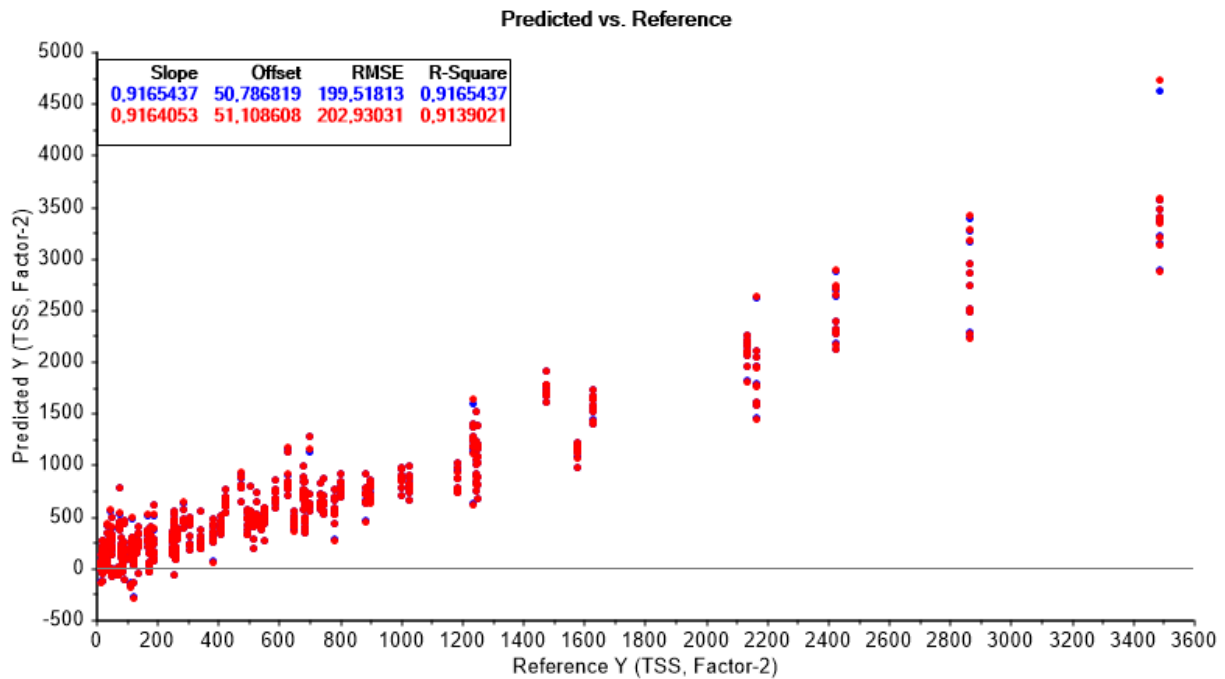


Figure 3. 23 Partial least squares regression on OSC corrected data for prediction of TSS using all wavelengths. RMSECV (Red) of 202.93 mg.L⁻¹.

Figure 3. 24 Partial least squares regression on OSC corrected data for prediction of TSS using all wavelengths. RMSECV (Red) of 202.93 mg.L⁻¹.

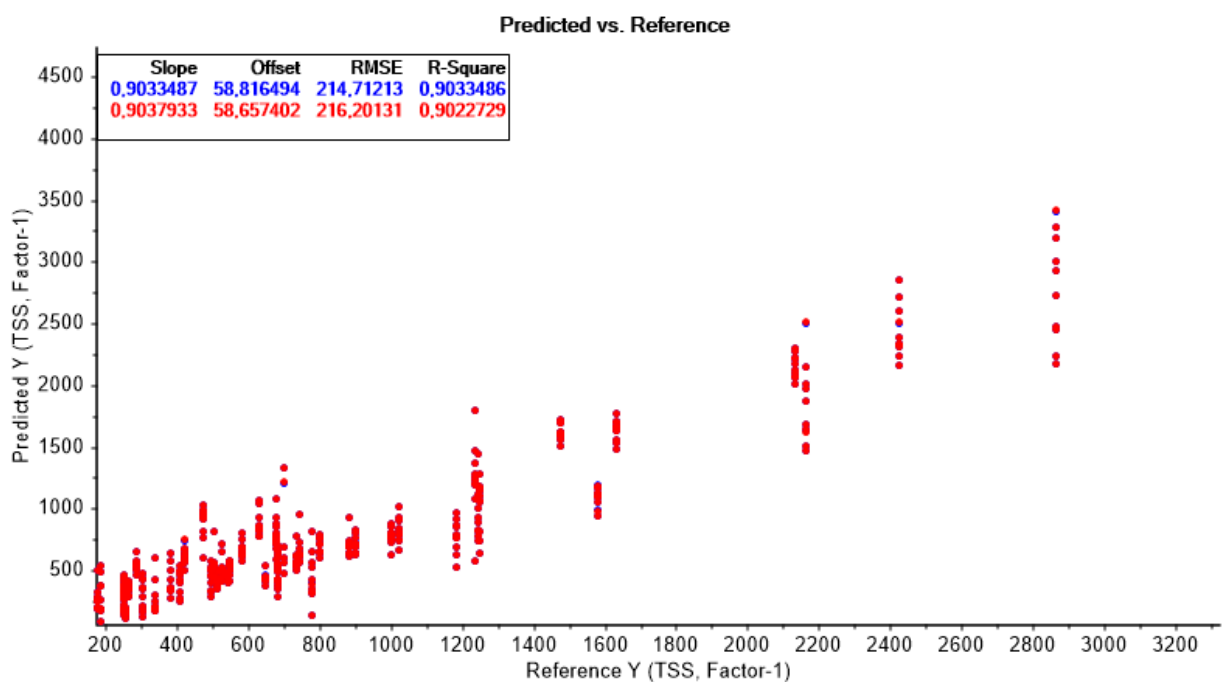


Figure 3. 25 Partial least squares regression on OSC corrected data for prediction of TSS using reduced wavelengths (1 900 – 2 500 nm). RMSECV (Red) of 216.20 mg.L⁻¹.

3.3.3.3 Multivariate data analysis: Model development (benchtop)

3.3.3.3.1 Principal component regression

Four pre-processing combinations were trialled along with principal component regression to determine TSS concentration in winery wastewater (**Table 3.11**). The performance of SNV and detrend was very good for the prediction of an unknown sample. The RMSECV for this model was 411.18 mg.L⁻¹ which corresponds to 11.82 % compared to the range of samples (14 – 3 490 mg.L⁻¹). Prediction of the independent validation set resulted in a RMSEP value of 224.67 mg.L⁻¹ compared to the range of 33 – 2 425 mg.L⁻¹. An error of 9.39 % was therefore achieved for the independent validation check. Previous work has been performed to monitor an activated sludge reactor in real time and the authors were able to predict TSS content with a 14 % relative error (Sarraguça *et al.*, 2009). The NIR instrument used only had a wavelength range of 900 – 1 400 nm which is considerably smaller than that of a benchtop FT-NIR instrument. Only 14 samples were used in that study for calibration, which is far too few for calibration. These factors indicate a possible reason for an increased predictive performance of this thesis as 53 samples were used, and 526 spectra were scanned in developing the calibration model.

It is important to check the SEP/SEL. The SEL for the laboratory analyses was calculated to be 112 mg.L⁻¹. This means that the standard error of the laboratory is 112 mg.L⁻¹ for the specific analyst. The ratio is 1.77 which is in the required range of 1.50 – 2.0 for the method to be accepted as an appropriate screening method (Corredor *et al.*, 2015). These pre-processing techniques may work well because there is a constant baseline vertical shift (offset). Standard normal variate functions by centering and scaling the data, eliminating the offset that is not useful for the model (Li Vigni, 2013). Detrending works in a similar way, by eliminating background noise when the analysis is done correctly (Li Vigni, 2013). It is possible that TSS correlates better with the X – data than COD does, as this method was ineffective for predicting COD.

Table 3. 11 Principal component regression results for calibration, cross-validation and prediction for four different pre-processing approaches to predict TSS in winery wastewater.

| Model | | RMSE (mg.L ⁻¹) | R ² | SEP / SEL |
|--------------------|------------------|----------------------------|----------------|-----------|
| SNV + Detrend | Calibration | 407.84 | 0.690 | |
| | Cross-validation | 411.18 | 0.686 | |
| | Prediction | 224.67 | 0.884 | 1.77 |
| SNV + Detr. + SGD2 | Calibration | 411.06 | 0.685 | |
| | Cross-validation | 415.60 | 0.679 | |
| | Prediction | 254.92 | 0.845 | 2.04 |
| MSC + SGD2 | Calibration | 430.38 | 0.654 | |
| | Cross-validation | 434.49 | 0.649 | |
| | Prediction | 229.98 | 0.855 | 2.08 |
| OSC | Calibration | 214.67 | 0.903 | |
| | Cross-validation | 216.16 | 0.902 | |
| | Prediction | 124.84 | 0.961 | 1.04 |

The model for SNV, detrend and Savitzky-Golay 2nd derivative showed similar predictive power for calibration and cross validation, compared to SNV and detrend. Prediction of the independent validation set was slightly worse with RMSEP being 254.92 mg.L⁻¹. The prediction may not seem significantly large, but it drives the SEP/SEL above 2.0 meaning this model is not suitable for prediction of TSS. Pre-processing with MSC and Savitzky-Golay 2nd derivative produced the worst RMSECV and SEP / SEL values. Lower predictive power may be due to the large differences between samples other than TSS, as MSC corrects for background noise using the mean or median values instead of correcting each spectrum's individual background noise (Li Vigni, 2013). The R² values for the calibration and cross-validation set for all the pre-processing techniques, except for OSC, were above 0.6, but below 0.7. This reinforces the RMSEP and SEP/SEL ratios obtained and indicates that these models do not explain all the variation in the model and may therefore not be the most effective at predicting TSS in winery wastewater (Colton & Bower, 2002).

The most effective pre-treatment for the prediction of TSS was OSC. Compared to the other three pre-processing approaches, this approach yielded the most accurate results. This is illustrated by greatly reduced RMSE values, a R² value above 0.9 for calibration, cross-validation and prediction and a SEP/SEL ratio of 1.04. When R² values exceed 0.9 the model can be said to explain more than 90 % of the variance in the sample data (Colton & Bower, 2002). Model selection should not focus primarily on R² as it may be a misleading statistic if other values such as RMSEP are ignored. In this case RMSEP is 124.84 mg.L⁻¹ corresponding to a 5.22 % error of prediction compared to the range. Very few studies have used NIR to predict TSS in wastewater (Mesquita *et al.*, 2017). A study from 2008 published results using NIR to predict TSS and the authors could predict TSS to within a 10 % error of the measured range (Páscoa *et al.*, 2008). Another statistic that the authors used to describe the data was the range error ratio (RER). This statistic uses the range and divides it by the error. The value obtained by the authors was 15.8. The RER of OSC and PCR was 2392 / 124.84, which equated to 19.16. A study monitoring urban wastewaters characterisation predicted TSS using NIR (Melendez-Pastor *et al.*, 2013). Cross-validation predicted TSS with an 8.8 % error and had an RMSEP error of 10.34 % (Melendez-Pastor *et al.*, 2013). The results (**Table 3.11**) improved upon this and had an error of 5.22 %.

Further studies have been performed to predict TSS using UV-Vis spectroscopy. One of these studies could predict TSS with only a 36.67 % error, although the concentration of TSS was very low in the samples (<15 mg.L⁻¹) (Rieger *et al.*, 2004). Artificial neural networks in combination with UV-Vis was used to predict TSS in sewage wastewater (Jeong *et al.*, 2007). The average error of prediction for TSS was 21.6 % compared to the range.

The reason that the prediction of OSC and PCR was superior is first and foremost due to a more powerful instrument with greater wavelength range, compared to other studies mentioned. Another reason may be that OSC is a very powerful pre-processing when the reference method for measurements is very accurate. There are also many wavelengths that can explain a limited number of observations in the wastewater.

3.3.3.3.2 Partial least squares regression

Partial least squares regression worked very well for three of the four pre-processing approaches. The worst predictive power was achieved using SNV and detrending (**Table 3.12**). This was evidenced by the RMSEP value of 308.24 which is an error of 12.89 %. The SEP/SEL was marginally above 2.0 and can therefore not be considered a viable option. The predictive power was consistently more accurate using PLS-R compared to PCR because of lower SEP/SEL values and lower RMSE values. This can be explained by PCR using the principal components to predict the Y responses, but the principal components may not always correlate with the responses because of variability in the sample, background noise or too many uninformative variables (Li Vigni, 2013).

The model using SNV, detrending and SGD2 showed improved performance for all RMSE values compared to those obtained by PCR. Root mean square error of cross-validation was 375.69 and PMSER value was 211.8 mg.L⁻¹. The corresponding errors are 10.81 % and 8.85 %. Correlation coefficient for the independent validation set is 0.888 which implies that a lot of the variability was explained by the model. A value of 1.88 was achieved for SEP/SEL and this indicates that this model may be used for screening purposes to predict TSS. The large difference in RMSECV and RMSEP does not mean that the model is underfit. The range of the calibration included more extreme values as calibration data must include data on the end of the range so as not to artificially increase the range of prediction and make it appear as if the prediction is better than reality. The errors for cross-validation and prediction are more important in this case as it takes the effect of the range into consideration and these errors are similar.

From **Table 3.12** it is evident that MSC and SGD2 have similar predictive values compared to SNV, detrend and Savitzky-Golay 2nd derivative. This is because MSC essentially performs the same function as SNV and detrending. This is contrary to the PCR models, mainly because PLS-R makes use of latent variables to perform the prediction which are more accurate than the principal components used for PCR (Abdi, 2003).

The model using OSC and PLS-R was the most accurate to predict TSS in winery wastewater. The RMSECV was 217.69 and the RMSEP was 144.16 mg.L⁻¹. The corresponding errors of prediction are 4.59 % and 6.03 % respectively. Correlation coefficient for the prediction of 0.955 indicates a very good fit for the model. A value of 1.17 for SEP / SEL indicates a very powerful predictive power for this model as it performs to nearly the same accuracy as the laboratory technique.

Partial least squares regression was used to predict TSS in an activated sludge reactor and had prediction errors of roughly 14.1 % and an R² value of 0.91. The study however only made use of 142 wavelengths to predict TSS (Sarraguça *et al.*, 2009). Three different wastewater treatment plants were analysed for TSS prediction us UV-VIS spectrophotometry. The error for calibration was 16.6 % for the local calibration (Rieger *et al.*, 2006). The previous studies performed are less accurate than the current study, mainly because less powerful instrumentation was used and the wavelength ranges did not reach high enough wavelengths, as TSS is correlated to wavelengths above 1 000 nm.

The results of PLS-R and OSC were slightly worse than PCR and OSC. This is most likely a function of OSC pre-processing eliminating X-data not relevant to the Y-response, mitigating the limitations of PCR for prediction (Li Vigni, 2013). Orthogonal signal correction and PLS-R or PCR can therefore be used as an effective screening method to determine TSS of winery wastewater.

Table 3. 12 Partial least squares regression results for calibration, cross-validation and prediction for four different pre-processing approaches to predict TSS in winery wastewater.

| Model | | RMSE (mg.L ⁻¹) | R ² | SEP/SEL |
|--------------------|------------------|----------------------------|----------------|---------|
| SNV + Detrend | Calibration | 354.02 | 0.766 | |
| | Cross-validation | 366.21 | 0.751 | |
| | Prediction | 308.24 | 0.851 | 2.03 |
| SNV + Detr. + SGD2 | Calibration | 359.85 | 0.758 | |
| | Cross-validation | 375.69 | 0.738 | |
| | Prediction | 211.80 | 0.888 | 1.88 |
| MSC + SGD2 | Calibration | 378.61 | 0.732 | |
| | Cross-validation | 393.73 | 0.711 | |
| | Prediction | 208.95 | 0.895 | 1.78 |
| OSC | Calibration | 212.21 | 0.816 | |
| | Cross-validation | 217.69 | 0.912 | |
| | Prediction | 144.16 | 0.955 | 1.17 |

3.3.3.3.3 Wavelength selection performance PCR and PLS-R

To investigate the effect of wavelength selection on predictive ability of TSS, the OSC models for PCR and PLS-R were used. Wavelengths were identified in **section 3.3.3.2.2** by looking at the loadings line plot and the correlation loadings plot. The identified wavelengths were 1 900 – 2 500 nm. The OSC model and PCR performed identically to the PLS-R and OSC model. The RMSECV, RMSEP, R² and SEP/SEL values were identical for both regression methods. The RMSECV for the methods were 235.31 mg.L⁻¹ resulting in an error of 9.50%. The RMSEP is 136.94 translating to an error of 5.72 %. Correlation coefficient of 0.961 for the prediction indicates that the variability in the data is very well explained. This coupled with a SEP/SEL of 1.07 indicates that these wavelengths predict TSS very accurately using OSC and either PLS-R or PCR. These methods are very similar and similar results are to be expected (Hemmateenejad *et al.*, 2007). Total suspended solids seem to correlate better with the spectral data than COD and therefore when OSC is applied to the data, the important information is extracted for the prediction. Wavelength selection performed almost as well as the full spectrum for PCR and OSC. It can be concluded that the wavelengths from 1 900 – 2 500 nm can be used to predict TSS in winery wastewater for screening purposes for this specific FT-NIR benchtop spectrophotometer.

Table 3. 13 Partial least squares regression and principal component regression results for calibration, cross-validation and prediction for OSC pre-processed data to predict TSS in winery wastewater using wavelengths 1 900 – 2 500 nm.

| Model | | RMSE (mg.L ⁻¹) | R ² | SEP/SEL |
|-------------|------------------|----------------------------|----------------|---------|
| PCR (OSC) | Calibration | 232.70 | 0.899 | |
| | Cross-validation | 235.31 | 0.897 | |
| | Prediction | 136.94 | 0.961 | 1.07 |
| PLS-R (OSC) | Calibration | 232.70 | 0.899 | |
| | Cross-validation | 235.31 | 0.897 | |
| | Prediction | 136.94 | 0.961 | 1.07 |

3.3.3.3.4 Discriminant analysis

Classification was performed using the 2 best performing pre-treatments for quantification namely; MSC + SGD2 and OSC. All the models showed good performance for classifying TSS into its two categories; Low and High (**Table 3.14**). The worst performing model had an overall classification accuracy of 75.00 % for the independent validation set. This model was the QDA with OSC as pre-processing technique. For the MSC and Savitzky-Golay 2nd derivative pre-processing and LDA the calibration accuracy was 86.50 % and the validation accuracy was 80 % (**Table 3.14**). Multiplicative scatter correction and Savitzky – Golay 2nd derivative was used with QDA and mahalanobis discriminant analysis and had identical validation accuracies of 90 %. The calibration accuracy of the mahalanobis discriminant analysis was low at 70.34 %. Using MSC and Savitzky-Golay 2nd derivative, LDA and QDA are the most useful discriminant techniques for classification of TSS in winery wastewater.

Orthogonal signal correction and mahalanobis discriminant analysis had a calibration accuracy of 88.97 % and a validation accuracy of 90 % (**Table 3.14**). This is a very good classification accuracy and can be useful to predict TSS in winery wastewater. The best combination for classification was OSC in combination with LDA. This combination yielded a calibration accuracy of 94.68% and a classification accuracy of 100 %. A possible explanation for this could be because of the fundamental difference between LDA and other DA methods. In LDA the aim is to maximise the ratio of the between group variance and the within-group variance. The aim of this is to have each sample within each group as close together as possible, leading to less scattering and therefore the groups/classes are at maximum distances away from each other (Stanimirova *et al.*, 2013). Linear discriminant analysis is reliant on the variances and covariances of the data to be homogenous to classify with a linear decision boundary (Bevilacqua *et al.*, 2013). Based on the above explanation, it needs to be assumed that the variances of the data are homogenous when using OSC as the pre-processing technique removes variance/covariance of the X-data that is not related to the Y-responses.

Previous work has been done using LDA along with SNV and derivatives to classify wines based on their fermentation period (Di Egidio *et al.*, 2010). The wine was separated into 4 classes for specific time points. Using NIR with LDA the average classification of the 4 classes was 87.1 % for the prediction. For the final stage the classification was 100 % accurate. This study did not use TSS as the reason for the separation,

but rather the change in glucose, fructose and alcohol content as the fermentation process proceeded. It is not customary to classify TSS into categories as generally it is more prudent that the concentration be known and not to which class it belongs. However there is a benefit to classifying into low and high classes if the goal is to perform basic screening as effluent is pumped out of the cellar or to prevent reactor overload if the wastewater were to be treated (Di Egidio *et al.*, 2010).

Table 3. 14 DA model results to assess the performance of the different pre-processing along with optimal method (LDA, QDA or Mahalanobis) for TSS discrimination.

| Number of PCs | Method | Model | | Classification Accuracy (%) |
|---------------|-------------|------------|-------------|-----------------------------|
| 5 | Linear | MSC + SGD2 | Calibration | 86.50 |
| | | | Validation | 80.00 |
| | | OSC | Calibration | 94.68 |
| | | | Validation | 100.00 |
| | Quadratic | MSC + SGD2 | Calibration | 82.70 |
| | | | Validation | 90.00 |
| | | OSC | Calibration | 95.63 |
| | | | Validation | 75.00 |
| | Mahalanobis | MSC + SGD2 | Calibration | 70.34 |
| | | | Validation | 90.00 |
| | | OSC | Calibration | 88.97 |
| | | | Validation | 90.00 |

The best model from **Table 3.14** was investigated for the determination of the performance parameters (**Table 3.15**). Because the overall classification of this model was 100 % all the performance measures scored 100 % except for false positive and false negative error as no samples were incorrectly classified. For the validation set 20 farms were used but each was reduced to one spectrum per farm instead of 10 spectra per farm. To investigate whether the one average spectrum may be artificially inflating the accuracy of the model, all 200 spectra were used for the validation set as a sanity check. The results from this classification was 99 % as there were two incorrectly classified spectra. So, one spectrum from a farm of 10 spectra was incorrectly classified each time, therefore the average spectra are more likely to resemble the 9 correctly classified spectra, instead of the one incorrectly classified spectrum. This indicates that the data was not artificially inflating the accuracy of the model. It would still be good practice to collect more samples and to incorporate them into the model to get a more robust model. These results show that NIR

spectroscopy can be used to differentiate between low and high TSS of winery wastewater without the need for time consuming laboratory analyses.

Table 3. 15 Performance measures used to assess the LDA model (5 PCs) for the classification of TSS into two classes.

| Class | Classification accuracy | False positive error (%) | False negative error (%) | Sensitivity (%) | Specificity (%) | Precision (%) | F1 Score (%) |
|-------|-------------------------|--------------------------|--------------------------|-----------------|-----------------|---------------|--------------|
| Low | 100 | 0 | 0 | 100 | 100 | 100 | 100 |
| High | 100 | 0 | 0 | 100 | 100 | 100 | 100 |

3.3.4 TSS quantification and classification (handheld)

3.3.4.1 Spectral analysis

The average spectra were computed between the wavelengths of 908 – 1 651 nm. The spectra were plotted to compare chemical properties and possible points of difference related to TSS in winery wastewater. Data were classified into the following two categories:

- Low: TSS values ranging from 0 – 999 mg.L⁻¹
- High: TSS values > 1 000 mg.L⁻¹

The same three absorbance bands were again found to be prominent as in **section 3.3.2.1** and these were 970, 1 160 and 1 400 – 1 600 nm. Refer to **section 3.3.2.1** for detailed analysis of these bands. In summary they correlate with moisture (970 nm & 1 400 – 1 650 nm), C=O stretch overtone and aromatic groups and carbonyl groups from aldehydes and ketones (1 160 nm) and methanol and ethanol (1 400 – 1 650 nm) (Cozzolino *et al.*, 2006; Li *et al.*, 2007; Debebe *et al.*, 2017; Rosa *et al.*, 2017; Tsenkova *et al.*, 2018).

The average spectra for the portable NIR instrument was computed between the wavelengths of 908 – 1 651 nm. The spectra were plotted to compare chemical properties of the winery wastewater. Data were again classified into 2 categories, low and high.

From **Figure 3.25** TSS groups into low and high in the raw spectra especially at wavelengths below 1 300 nm. There is overlap between the two classes but low TSS can generally be associated with lower absorbance values. This is because high TSS values will have more particulate matter and therefore more scattering of the light will take place. The light will not reach the detector and it will seem as if there was an increased absorbance from a compound when the light never reached the detector. This is fixed by using an appropriate pre-processing technique.

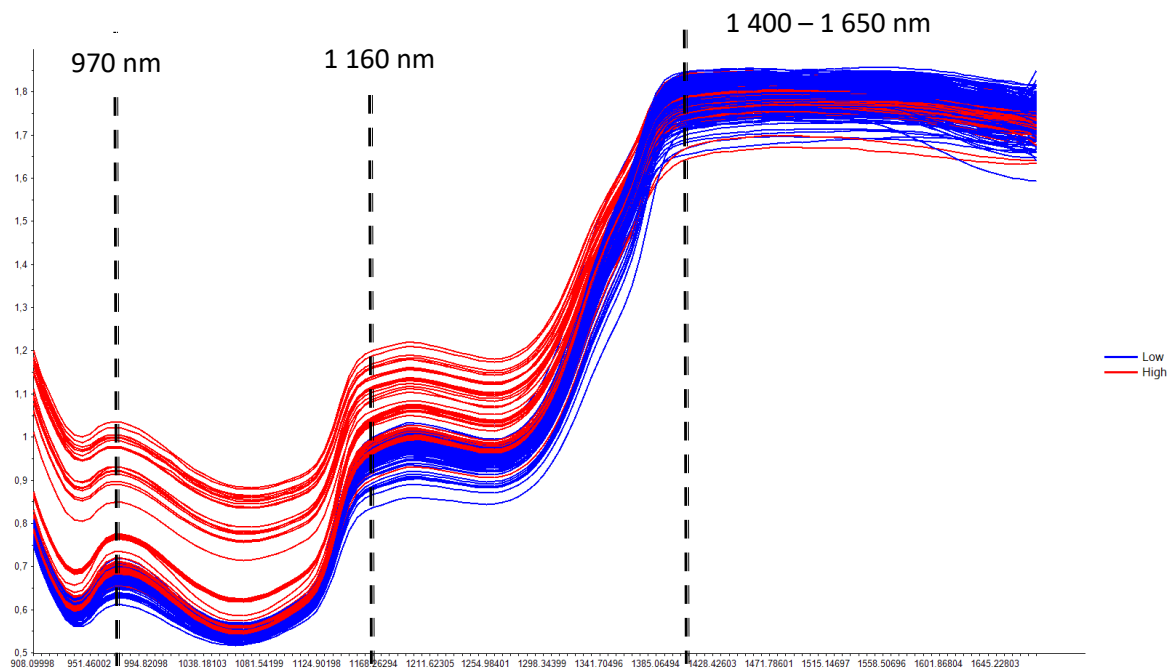


Figure 3. 26 Raw spectra of winery wastewater for the wavelength range 908 – 1 651 nm showing the two categories of TSS: Low (Blue) and High (Red).

3.3.4.2 Exploratory data analysis

3.3.4.2.1 Principal component analysis

It is clear that there is class overlap between the two classes when scrutinising the PCA of the unprocessed spectra (**Figure 3.26**). Most of the variation can be explained by PC1 which accounts for 80 % of the variation. There is some variation explained by PC2 (16 %) and PC3 (3 %). Orthogonal signal correction was performed on the data as that pre-processing technique was the most effective for all the predictions thus far.

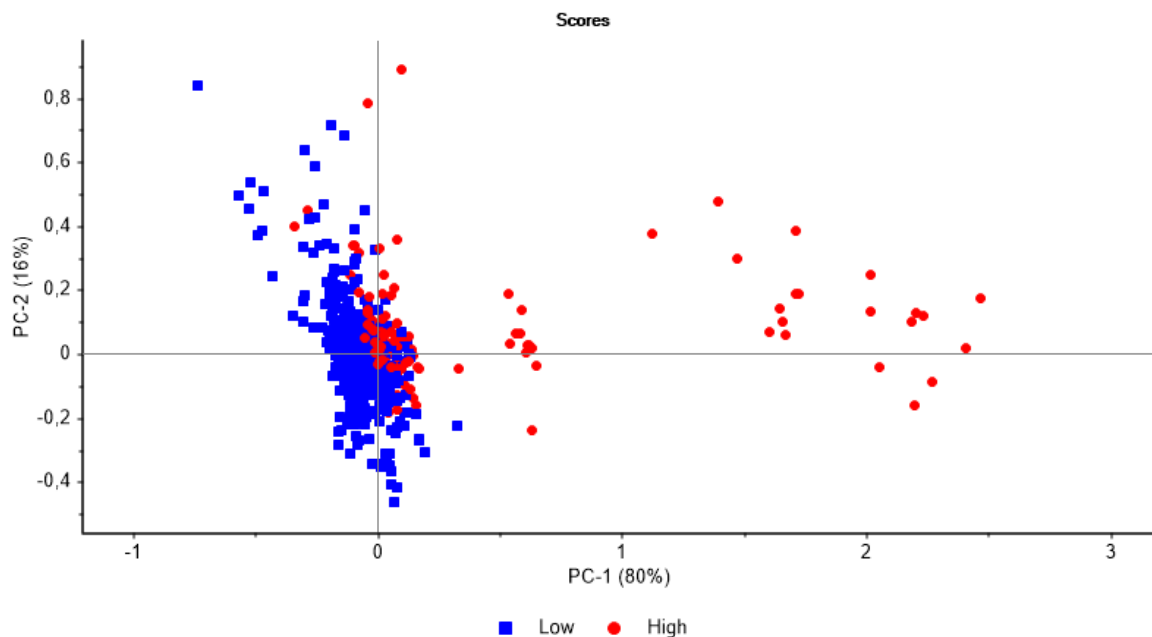


Figure 3. 27 PCA scores plot (PC1 vs PC2) for unprocessed data indicating some separation between the two classes; Low (Blue) and High (Red).

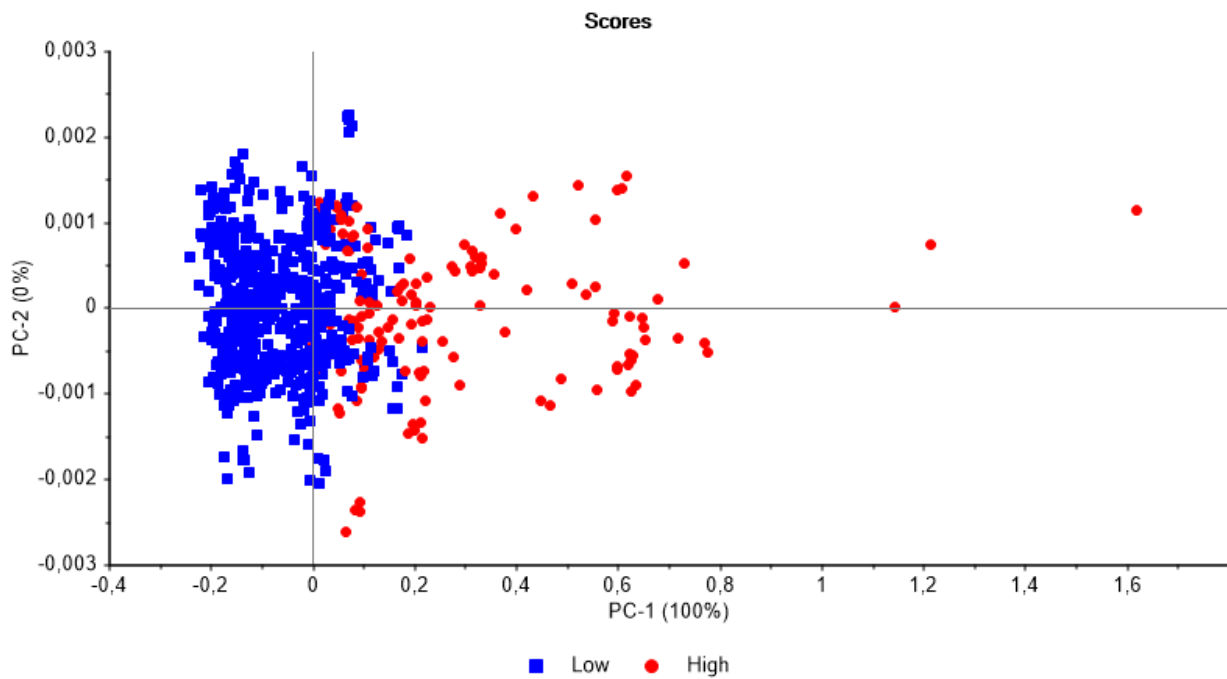


Figure 3. 28 PCA scores plot (PC1 vs PC2) for data processed with OSC for the two categories of TSS; Low (Blue) and High (Red).

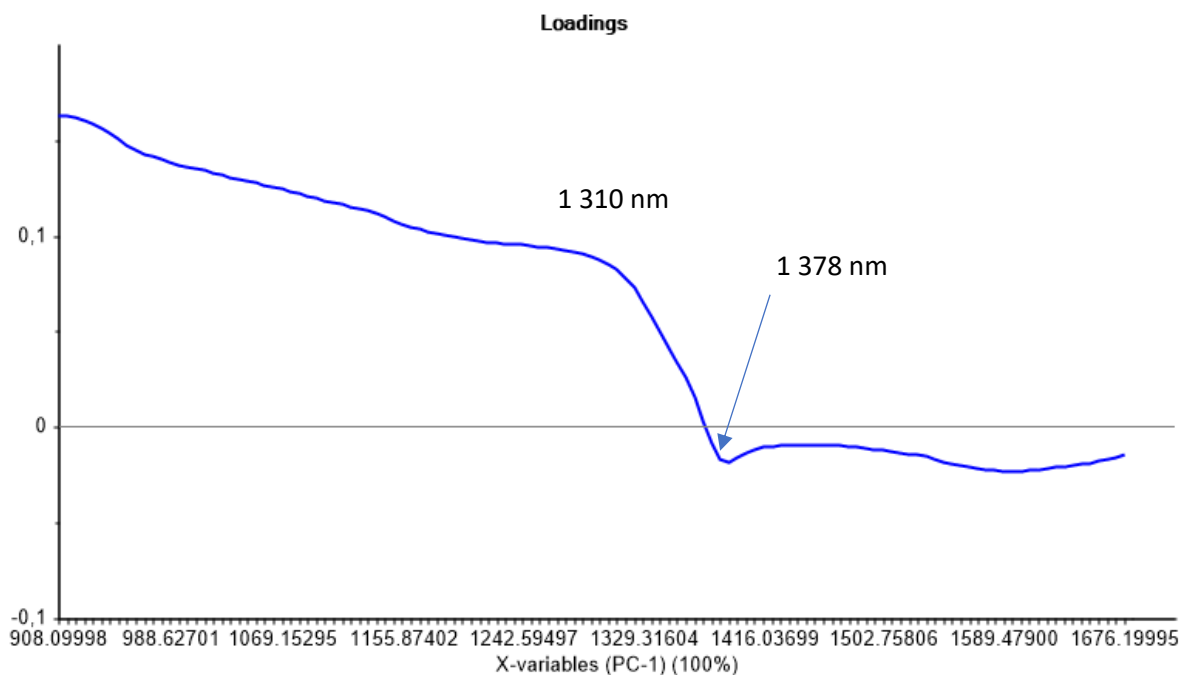


Figure 3. 29 Loadings line plot of OSC data with perturbations at 1 310 nm and 1 378 nm.

Upon pre-processing with OSC there was more distinct separation between classes with PC1 explaining 100 % of the variation (**Figure 3.27**). A higher TSS concentration is associated with a shift from left to right in PC1. Because the two classes are based off a spectrum and are not two totally distinct groups, e.g. olive oil and sunflower oil, overlap between classes can be expected. The loadings line plot was investigated for PC1 to determine important wavelengths. From the loadings line plot (**Figure 3.28**) two wavebands of

importance can be seen. These are the bands before at 1 310 nm and those before it and 1 378 nm and the wavebands after it. Compared to **Figure 3.16** there are not deflections at 1 120 and 1 162 nm. Please refer to **section 3.3.2.2.1** for an explanation of important wavelengths and the loadings line plot.

Wavelength selection was not performed for the portable device as there are already a very limited number of wavelengths and therefore limited data. Processing speed will not be significantly decreased by performing wavelength selection, while prediction performance may suffer.

3.3.4.3 Multivariate data analysis: Model development (handheld)

3.3.4.3.1 Principal component regression

The two best performing pre-processing methods from the prediction of TSS with the benchtop instrument were used to predict TSS concentration. These techniques were MSC and SGD2 (9 smoothing points 3rd polynomial) and OSC (**Table 3.16**).

For the data treated with MSC and SGD2 the RMSECV was 402.15 mg.L⁻¹. The range of the TSS concentration for the calibration set was (14 – 3490 mg.L⁻¹). The relative error of cross validation is therefore 11.57 %. The correlation coefficient of the cross-validated data was 0.644, indicating a model that explains some variation, but not to a satisfactory degree for implementation as a screening method. This poor R² coupled with a big RMSEP (405.04 mg.L⁻¹) value means that this combination may not be suitable for determining TSS. This was confirmed by the SEP/SEL of 3.34 which means the average error is more than three times more than the average error of the laboratory. An improved R² of 0.74 indicates that the variance in the predicted data can be explained by the model, but it is possible that this is not related to TSS and rather one of the many other parameters in wine such as pH. The reduced wavelengths and reduced wavelength range of the portable device means that lots of spectral information is lost, compared to the benchtop FT-NIR instrument. This explains the decrease in performance of the portable instrument. For an explanation as to why PCR might not predict the TSS well with reduced spectral information please refer to **section 3.3.2.3.1**.

The data processed with OSC and PCR improved the predictive power of the portable instrument. The RMSECV was 272.96 mg.L⁻¹ which translates to an error of 7.85 %. This is a very good cross-validation prediction however to determine if the model is robust enough the RMSEP needs to be considered simultaneously. When looking at the RMSEP of 311.49 mg.L⁻¹ it translates to an error of 13.02 % for the range (33 – 2425 mg.L⁻¹). The R² for all of the calibration, cross-validation and prediction is above 0.83. This indicates a model which explains a large amount of variation, but which still considers unrelated information in the prediction (Colton & Bower, 2002). The SEP/SEL is 2.85 which is too high to be considered a viable option for screening purposes (Corredor *et al.*, 2015). This pre-processing worked better due to the nature of OSC that removes irrelevant data (Wold *et al.*, 1998) Whilst this method may not be suitable for screening purposes, it is a big improvement on the prediction of COD with the portable instrument. None of these models should be considered for the prediction of TSS in winery wastewater.

Table 3. 16 Principal component regression results for calibration, cross-validation and prediction of TSS concentration for two different pre-processing combinations.

| Model | | RMSE (mg.L ⁻¹) | R ² | SEP/SEL |
|------------|------------------|----------------------------|----------------|---------|
| MSC + SGD2 | Calibration | 393.31 | 0.658 | |
| | Cross-validation | 402.15 | 0.644 | |
| | Prediction | 405.04 | 0.74 | 3.34 |
| OSC | Calibration | 268.67 | 0.840 | |
| | Cross-validation | 272.96 | 0.836 | |
| | Prediction | 311.49 | 0.857 | 2.85 |

3.3.4.3.2 Partial least squares regression

As with PCR, two different pre-processing approaches were investigated for their predictive performance of TSS in winery wastewater (**Table 3.17**). Partial least squares regression in combination with MSC and SGD2 has RMSECV and RMSEP values of 331.93 and 351.89 mg.L⁻¹ respectively. The relative error for the prediction is 14.71 %. This value is higher than the 10.34 % obtained in a previous study (Melendez-Pastor *et al.*, 2013). This pre-processing method is not suitable for screening of TSS in winery wastewater.

When PLS-R was used in combination with OSC as pre-processing technique, the predictive power increased. The RMSECV and the RMSEP were both lower than those corresponding values using MSC and SGD2 (**Table 3.17**). The RMSECV corresponds to an error of cross validation of 6.39 %. However, it is possible that the model is overfitted as the prediction of an external validation set is considerably worse, with an error of 13.02 %. The R² value for the prediction of OSC is 0.857 which shows a good fit for the data. However, when looking at SEP/SEL it becomes clear that the model is not powerful enough to be used as a screening method. Interestingly, the prediction data for PCR and for PLS-R with OSC is identical. The same phenomenon was observed in **section 3.3.3.3** when wavelength selection was performed on the benchtop instrument. It is difficult to postulate a reason other than PCR overcoming its limitation of not incorporating the Y-responses into the calculation. This is done by OSC, which might decrease the small gap in performance for PCR in general (Hemmateenejad *et al.*, 2007).

When investigating the predicted response, one sample was very badly predicted. When this sample was removed to see what the effect would be the error of prediction dropped to 7.2 %. This sample is not a statistical outlier so this cannot be used as it would be cherry-picking data. However, it does warrant investigation as to why it may have been poorly predicted. When looking at the wet chemistry data it can be seen that this sample has a very high pH of 11.82, high turbidity value of 690.5 NTU and an alkalinity of 2 200 mg.L⁻¹ CaCO₃. One of these factors may have influenced the instrument. This sample is not a true statistical outlier so it cannot be discarded, but with more sample acquisition this problem may be overcome, and better prediction results may be possible.

A study was performed that used a spectrophotometer with the range of 900 – 1 400 nm. This study reported similar as error of 14 % for the prediction of COD (Sarraguça *et al.*, 2009). A further study could predict TSS using UV-Vis spectroscopy with an error of 16.6 % (Rieger *et al.*, 2006). Both results are comparable to the results obtained in this thesis. There are certainly limitations for using NIR portable instruments, or instruments of limited wavelengths. It is necessary to investigate whether TSS could be predicted with a portable device that has a range from 1 900 – 2 500 nm.

Table 3.17 Partial least squares regression results for calibration, cross-validation and prediction for MSC and SGD2 OSC pre-processed data to predict TSS in winery wastewater.

| Model | | RMSE (mg.L ⁻¹) | R ² | SEP/SEL |
|------------|------------------|----------------------------|----------------|---------|
| MSC + SGD2 | Calibration | 305.73 | 0.793 | |
| | Cross-validation | 331.93 | 0.757 | |
| | Prediction | 351.89 | 0.799 | 3.04 |
| OSC | Calibration | 196.39 | 0.915 | |
| | Cross-validation | 221.96 | 0.892 | |
| | Prediction | 311.49 | 0.857 | 2.85 |

3.3.4.3.3 Discriminant analysis

Classification was performed on two pre-processing techniques (**Table 3.19**). Performance of the mahalanobis discriminant analysis performed the worst, with classification accuracies of 70 and 55 % for the independent validation sets of MSC and SGD2 and OSC respectively. The rest of the models all had a prediction of the independent validation set of 95 %. The differences between the models are all from the calibration. The models using OSC as pre-treatment were the most accurate for the calibration set with accuracies of 91.15 % and 90.96 % for LDA and QDA respectively. Multiplicative scatter correction and Savitzky-Golay 2nd performed slightly worse, although still achieved results close to 90 %. The LDA models performed marginally better than the QDA models and were far superior to the Mahalanobis models. Differences between LDA and QDA were discussed in **section 3.3.3.3.4** The performance measures of the two LDA models is shown in **Table 3.18**.

Both models were very similar in their performance measures with only a few small differences. The model using OSC in combination with LDA was found to be the best model as it had a greater overall sensitivity for the two classes and a greater average specificity for the two classes. The precision of the MSC and SGD2 was higher than for the OSC pre-treated data. The OSC data was had slightly better F1 scores and overall the LDA model with OSC will give the best prediction results for TSS in winery wastewater.

Classification of geographical origin of Chinese rice wines was performed using NIR (Yu *et al.*, 2007). Classification was possible with 100 % accuracies when using certain 1 300 – 1 650 nm and dropped to 96.6 % when using 1 650 – 1 850 nm or 1 850 -2 200 nm. Riesling wine characterisation by country of origin

has been performed using NIR and PLS-DA (Liu *et al.*, 2008). The wines could be correctly classified into the country of origin with 97.5 % accuracies for Australian Riesling, 80 % for New Zealand Riesling and 70.5 % for European Riesling (Liu *et al.*, 2008). Whilst these studies did not look at TSS they showed the potential for characterisation of liquids using NIR. As winery wastewater often contains large volumes of wine, it can be used to compare results against. The classification results in literature are comparable to the results obtained in this study and a portable NIR spectrophotometer shows potential in the classification of wastewater with regards to TSS strength.

Table 3. 18 Performance measures used to assess LDA models for the classification of TSS into two classes.

| Number of PCs | Class | Classification accuracy | False positive error (%) | False negative error (%) | Sensitivity (%) | Specificity (%) | Precision (%) | F1 Score (%) |
|---------------------|-------|-------------------------|--------------------------|--------------------------|-----------------|-----------------|---------------|--------------|
| 5 (LDA MSC SGD2) | Low | 95.00 | 5.00 | 0.00 | 100 | 66.67 | 94.44 | 97.14 |
| | High | 95.00 | 0.00 | 5.00 | 66.67 | 100.00 | 100.00 | 80.00 |
| 5 (LDA OSC) | Low | 95.00 | 0.00 | 5.00 | 94.12 | 100.00 | 100.00 | 96.97 |
| | High | 95.00 | 5.00 | 0.00 | 100.00 | 94.12 | 75.00 | 85.71 |

Table 3. 19 DA model results to assess the performance of the different pre-processing along with optimal method (LDA, QDA or Mahalanobis) for TSS discrimination.

| Number of PCs | Method | Model | Classification Accuracy (%) | | |
|---------------|-------------|------------|-----------------------------|-------------|-------|
| 5 | Linear | MSC + SGD2 | Calibration | 89.27 | |
| | | | Validation | 95.00 | |
| | | OSC | Calibration | 91.15 | |
| | | | Validation | 95.00 | |
| | | Quadratic | MSC + SGD2 | Calibration | 88.70 |
| | | | | Validation | 95.00 |
| | OSC | | Calibration | 90.96 | |
| | | | Validation | 95.00 | |
| | Mahalanobis | MSC + SGD2 | Calibration | 64.41 | |
| | | | Validation | 70.00 | |
| | | OSC | Calibration | 77.40 | |
| | | | Validation | 55.00 | |

3.4 Conclusion

NIR spectroscopy, using a benchtop instrument, combined with multivariate data analysis could predict COD and TSS concentrations in winery wastewater with enough accuracy for a screening method. This could be done irrespective of other interferences in the water such as pH or turbidity and could be accomplished irrespective of the farm origin of the wastewater. The models which predicted COD concentration most accurately was either PLS-R or PCR using OSC as pre-processing and making use of the wavelengths 2 060 – 2 340 nm. The RMSEP was 898 mg.L⁻¹ which equates to an error of 9.9 % compared to the reference range of the independent validation set. This result falls below the 10 % error threshold that was targeted in the aim. A low error percentage combined with a SEP/SEL of 1.93 confirms that NIR spectroscopy can predict COD concentration to a suitable degree for screening purposes.

Principal component regression along with OSC yielded the best predictive results for TSS with an RMSEP of 124.84 mg.L⁻¹ and an SEP/SEL of 1.04. This translates to an error rate of only 5.22 % which is well below the target set forth for the aim of this study. An SEP/SEL of 1.04 indicates that the TSS model using the benchtop instrument was very similar to the standard method used to determine the reference values. This result far exceeded the goal set forth in the aim for the study. The wavelengths 1 900 – 2 500 nm could be used to accurately predict TSS concentration with an RMSEP of 136.94 mg.L⁻¹ for PCR or PLS-R and OSC as pre-processing. A smaller wavelength range did not severely impact the prediction performance and the subsequent error of the model was 5.72 %. It can be definitively stated that a benchtop FT-NIR can predict TSS concentration with an accuracy suitable for screening purposes.

Classification of COD with the benchtop instrument was very accurate with an overall classification accuracy of 90.4 % using LDA and OSC. This means that 90.4 % of the samples were correctly classified as either “In” (COD of 0 – 4 999 mg.L⁻¹), “Warning” (COD of 5 000 – 6 999 mg.L⁻¹) or “Out” (COD above 7 000mg.L⁻¹). The reason for a lower classification than TSS could be due to there being three categories for COD, where TSS was only divided into two categories. The LDA model using OSC as pre-processing yielded the best results and could effectively differentiate between low and high TSS concentrations with a classification accuracy of 100 %.

The portable handheld NIR instrument did not predict either COD or TSS concentration to a satisfactory degree for the purpose of screening. This was illustrated by the SEP/SEL values which were above 2.0 for all the models. For a model to be considered a potential screening method, the SEP/SEL must be in the range of 1.5 – 2.0. The reduced predictive power of the handheld instrument may be due to the smaller spectral range of the instrument of 900 – 1 700 nm. Optimal performance of the benchtop instrument was accomplished at wavelengths above 1 900 nm. The handheld instrument showed promise and had error rates that are comparable to those found in literature. The effectiveness of portable spectrophotometers need to be investigated using higher wavelengths if on-line monitoring of reactors is to be accomplished. If the technology can develop to include wavelength ranges up to 2 500 nm it is possible that the handheld instrument could perform with similar accuracies compared to the benchtop instrument.

Classification of COD and TSS was considered accurate when using the portable instrument. Classification accuracies of 81 % and 95 % for COD and TSS respectively were achieved using the portable instrument. Classification of COD will improve if only “In” and “Out” classes are created for the classification. A classification accuracy of 95 % for TSS indicates that the portable instrument can effectively classify winery wastewater based on the TSS concentration. This could allow wineries to classify the wastewater based on the current legislation defined limits to determine whether the wastewater would need to be treated before irrigation.

OSC was the best pre-processing technique for all these applications as the laboratory reference values were accurate, allowing the technique to eliminate information from the spectra that do not predict the responses. This allows for a method that reduces noise and increases the accuracy of prediction. More research will need to be done to investigate the potential of portable NIR spectrophotometers for the quantification of COD and TSS in winery wastewater.

3.5 References

- Abdi, H. (2003). Partial least square regression (PLS regression). *Encyclopedia for research methods for the social sciences*, **6**, 792-795.
- APHA (2005). Standard methods for the examination of water and wastewater. *American Public Health Association (APHA): Washington, DC, USA*.
- Barnes, R., Dhanoa, M.S. & Lister, S.J. (1989). Standard normal variate transformation and de-trending of near-infrared diffuse reflectance spectra. *Applied spectroscopy*, **43**, 772-777.
- Bevilacqua, M., Bucci, R., Magrì, A.D., Magrì, A.L., Nescatelli, R. & Marini, F. (2013). *Chemometrics in Food Chemistry: Chapter 5. Classification and Class-Modelling*. Elsevier Inc. Chapters.
- Bories, A. & Sire, Y. (2016). Impacts of winemaking methods on wastewaters and their treatment. *South African Journal of Enology and Viticulture*, **31**, 38-44.
- Colton, J.A. & Bower, K.M. (2002). Some misconceptions about R2. *International Society of Six Sigma Professionals, EXTRAOrdinary Sense*, **3**, 20-22.
- Corredor, C.C., Lozano, R., Bu, X., McCann, R., Dougherty, J., Stevens, T., Both, D. & Shah, P. (2015). Analytical method quality by design for an on-line near-infrared method to monitor blend potency and uniformity. *Journal of Pharmaceutical Innovation*, **10**, 47-55.
- Cozzolino, D., Liu, L., Cynkar, W., Damberg, R., Janik, L., Colby, C. & Gishen, M. (2007). Effect of temperature variation on the visible and near infrared spectra of wine and the consequences on the partial least square calibrations developed to measure chemical composition. *Analytica chimica acta*, **588**, 224-230.
- Cozzolino, D., Parker, M., Damberg, R.G., Herderich, M. & Gishen, M. (2006). Chemometrics and visible-near infrared spectroscopic monitoring of red wine fermentation in a pilot scale. *Biotechnology and bioengineering*, **95**, 1101-1107.

- Cozzolino, D., Smyth, H.E., Lattey, K.A., Cynkar, W., Janik, L., Damberg, R.G., Francis, I.L. & Gishen, M. (2005). Relationship between sensory analysis and near infrared spectroscopy in Australian Riesling and Chardonnay wines. *Analytica chimica acta*, **539**, 341-348.
- Da Ros, C., Cavinato, C., Pavan, P. & Bolzonella, D. (2014). Winery waste recycling through anaerobic co-digestion with waste activated sludge. *Waste Management*, **34**, 2028-2035.
- Dahlbacka, J., Nyström, J., Mossing, T., Geladi, P. & Lillhonga, T. (2014). On-line measurement of the chemical oxygen demand in wastewater in a pulp and paper mill using near infrared spectroscopy. *Spectral Analysis Review*, **2**, 19.
- Damberg, R.G., Kambouris, A., Francis, I.L. & Gishen, M. (2002). Rapid analysis of methanol in grape-derived distillation products using near-infrared transmission spectroscopy. *Journal of Agricultural and Food Chemistry*, **50**, 3079-3084.
- de Aragão, B.J. & Messaddeq, Y. (2008). Peak separation by derivative spectroscopy applied to FTIR analysis of hydrolized silica. *Journal of the Brazilian chemical society*, **19**, 1582-1594.
- Debebe, A., Temesgen, S., Abshiro, M. & Chandravanshi, B.S. (2017). Partial least squares– near infrared spectrometric determination of ethanol in distilled alcoholic beverages. *Bulletin of the Chemical Society of Ethiopia*, **31**, 201-209.
- Di Egidio, V., Sinelli, N., Giovanelli, G., Moles, A. & Casiraghi, E. (2010). NIR and MIR spectroscopy as rapid methods to monitor red wine fermentation. *European Food Research and Technology*, **230**, 947-955.
- Fisher, R.A. (1936). The use of multiple measurements in taxonomic problems. *Annals of eugenics*, **7**, 179-188.
- Hemmateenejad, B., Akhond, M. & Samari, F. (2007). A comparative study between PCR and PLS in simultaneous spectrophotometric determination of diphenylamine, aniline, and phenol: effect of wavelength selection. *Spectrochimica Acta Part A: Molecular and Biomolecular Spectroscopy*, **67**, 958-965.
- Hotelling, H. (1957). The relations of the newer multivariate statistical methods to factor analysis. *British Journal of Statistical Psychology*, **10**, 69-79.
- Huang, J., Romero-Torres, S. & Moshgbar, M. (2010). RAMAN: practical considerations in data pre-treatment for NIR and Raman spectroscopy. *American Pharmaceutical Review*, **13**, 116.
- Innocent, M.R., Morita, K. & Miyazato, Y. (2007). Rapid Estimation of Chemical Oxygen Demand of some Organic Solutions by using NIR and Chemometrics. *Journal of the Japanese Society of Agricultural Technology Management*, **14**, 107-114.
- Jeong, H.-S., Lee, S.-H. & Shin, H.-S. (2007). Feasibility of on-line measurement of sewage components using the UV absorbance and the neural network. *Environmental monitoring and assessment*, **133**, 15-24.
- Keithley, R.B., Wightman, R.M. & Heien, M.L. (2009). Multivariate concentration determination using principal component regression with residual analysis. *TrAC Trends in Analytical Chemistry*, **28**, 1127-1136.

- Kitamura, K. & Hozumi, K. (1987). Effect of savitzky—golay smoothing on second-derivative spectra. *Analytica chimica acta*, **201**, 301-304.
- Lago, L.O. & Welke, J.E. (2019). Carbonyl compounds in wine: factors related to presence and toxic effects. *Ciência Rural*, **49**.
- Li Vigni, M., Durante, C & Cocchi, M (2013). Exploratory data analysis. In: *Chemometrics in food chemistry* (edited by F. Marini). Pp. 65. Amsterdam: Newnes.
- Li, X., He, Y., Wu, C. & Sun, D.-W. (2007). Nondestructive measurement and fingerprint analysis of soluble solid content of tea soft drink based on Vis/NIR spectroscopy. *Journal of Food Engineering*, **82**, 316-323.
- Liu, L., Cozzolino, D., Cynkar, W., Damberg, R., Janik, L., O’neill, B., Colby, C. & Gishen, M. (2008). Preliminary study on the application of visible—near infrared spectroscopy and chemometrics to classify Riesling wines from different countries. *Food chemistry*, **106**, 781-786.
- Lorber, A., Wangen, L.E. & Kowalski, B.R. (1987). A theoretical foundation for the PLS algorithm. *Journal of Chemometrics*, **1**, 19-31.
- Martelo-Vidal, M. & Vázquez, M. (2014). Determination of polyphenolic compounds of red wines by UV–VIS–NIR spectroscopy and chemometrics tools. *Food chemistry*, **158**, 28-34.
- Massy, W.F. (1965). Principal components regression in exploratory statistical research. *Journal of the American Statistical Association*, **60**, 234-256.
- Melendez-Pastor, I., Almendro-Candel, M.B., Navarro-Pedreño, J., Gómez, I., Lillo, M.G. & Hernández, E.I. (2013). Monitoring urban wastewaters’ characteristics by visible and short wave near-infrared spectroscopy. *Water*, **5**, 2026-2036.
- Mesquita, D.P., Quintelas, C., Amaral, A.L. & Ferreira, E.C. (2017). Monitoring biological wastewater treatment processes: recent advances in spectroscopy applications. *Reviews in Environmental Science and Bio/Technology*, **16**, 395-424.
- Moharikar, A., Purohit, H.J. & Kumar, R. (2005). Microbial population dynamics at effluent treatment plants. *Journal of Environmental Monitoring*, **7**, 552-558.
- Moletta, R. (2005). Winery and distillery wastewater treatment by anaerobic digestion. *Water Science and Technology*, **51**, 137-144.
- Moscetti, R., Radicetti, E., Monarca, D., Cecchini, M. & Massantini, R. (2015). Near infrared spectroscopy is suitable for the classification of hazelnuts according to Protected Designation of Origin. *Journal of the Science of Food and Agriculture*, **95**, 2619-2625.
- Mosse, K., Patti, A., Christen, E. & Cavagnaro, T. (2011). Winery wastewater quality and treatment options in Australia. *Australian Journal of Grape and Wine Research*, **17**, 111-122.
- Niazi, A., Azizi, A. & Leardi, R. (2007). A comparative study between PLS and OSC-PLS in the simultaneous determination of lead and mercury in water samples: effect of wavelength selection. *Can. J. Anal. Sci. Spectrosc*, **52**, 365-374.

- Pan, T., Chen, W.W., Chen, Z.H. & Xie, J. (Year). Waveband selection for NIR spectroscopy analysis of wastewater COD. In: *Key Engineering Materials*. Pp. 393-396. Month and 2011
- Pan, T., Chen, Z., Chen, J. & Liu, Z. (2012). Near-infrared spectroscopy with waveband selection stability for the determination of COD in sugar refinery wastewater. *Analytical Methods*, **4**, 1046-1052.
- Páscoa, R.N., Lopes, J.A. & Lima, J.L. (2008). In situ near infrared monitoring of activated dairy sludge wastewater treatment processes. *Journal of Near Infrared Spectroscopy*, **16**, 409-419.
- Payne, K. (2019). Rapid differentiation of South African game meat using portable near-infrared (NIR) spectroscopy. Stellenbosch: Stellenbosch University.
- Pizarro, C., Esteban-Díez, I., Nistal, A.-J. & González-Sáiz, J.-M.a. (2004). Influence of data pre-processing on the quantitative determination of the ash content and lipids in roasted coffee by near infrared spectroscopy. *Analytica chimica acta*, **509**, 217-227.
- Preys, S., Roger, J. & Boulet, J. (2008). Robust calibration using orthogonal projection and experimental design. Application to the correction of the light scattering effect on turbid NIR spectra. *Chemometrics and Intelligent laboratory systems*, **91**, 28-33.
- Ramos, C., Suárez-Ojeda, M.E. & Carrera, J. (2016). Long-term performance and stability of a continuous granular airlift reactor treating a high-strength wastewater containing a mixture of aromatic compounds. *Journal of hazardous materials*, **303**, 154-161.
- Rieger, L., Langergraber, G. & Siegrist, H. (2006). Uncertainties of spectral in situ measurements in wastewater using different calibration approaches. *Water Science and Technology*, **53**, 187-197.
- Rieger, L., Langergraber, G., Thomann, M., Fleischmann, N. & Siegrist, H. (2004). Spectral in-situ analysis of NO₂, NO₃, COD, DOC and TSS in the effluent of a WWTP. *Water Science and Technology*, **50**, 143-152.
- Rosa, L.N., de Figueiredo, L.C., Bonafé, E.G., Coqueiro, A., Visentainer, J.V., Março, P.H., Rutledge, D.N. & Valderrama, P. (2017). Multi-block data analysis using ComDim for the evaluation of complex samples: Characterization of edible oils. *Analytica chimica acta*, **961**, 42-48.
- Ruiz, C., Torrijos, M., Sousbie, P., Martinez, J.L., Moletta, R. & Delgenes, J. (2002). Treatment of winery wastewater by an anaerobic sequencing batch reactor. *Water Science and Technology*, **45**, 219-224.
- Sáiz-Abajo, M.-J., González-Sáiz, J.-M. & Pizarro, C. (2005). Orthogonal signal correction applied to the classification of wine and molasses vinegar samples by near-infrared spectroscopy. Feasibility study for the detection and quantification of adulterated vinegar samples. *Analytical and bioanalytical chemistry*, **382**, 412-420.
- Sarragaça, M.C., Paulo, A., Alves, M.M., Dias, A.M., Lopes, J.A. & Ferreira, E.C. (2009). Quantitative monitoring of an activated sludge reactor using on-line UV-visible and near-infrared spectroscopy. *Analytical and bioanalytical chemistry*, **395**, 1159-1166.
- Savitzky, A. & Golay, M.J. (1964). Smoothing and differentiation of data by simplified least squares procedures. *Analytical chemistry*, **36**, 1627-1639.

- Shao, X., Peng, D., Teng, Z. & Ju, X. (2008). Treatment of brewery wastewater using anaerobic sequencing batch reactor (ASBR). *Bioresource technology*, **99**, 3182-3186.
- Show, K. & Lee, D. (2016). Anaerobic Treatment Versus Aerobic Treatment. *Current Developments in Biotechnology and Bioengineering: Biological Treatment of Industrial Effluents*, 205.
- Siqueira, L.F., Júnior, R.F.A., de Araújo, A.A., Morais, C.L. & Lima, K.M. (2017). LDA vs. QDA for FT-MIR prostate cancer tissue classification. *Chemometrics and Intelligent Laboratory Systems*, **162**, 123-129.
- Sivakumar, B. (2011). Water crisis: from conflict to cooperation—an overview. *Hydrological Sciences Journal*, **56**, 531-552.
- Soukupova, J., Rock, B. & Albrechtova, J. (2002). Spectral characteristics of lignin and soluble phenolics in the near infrared—a comparative study. *International Journal of Remote Sensing*, **23**, 3039-3055.
- Stanimirova, I., Daszykowski, M. & Walczak, B. (2013). Robust Methods in Analysis of Multivariate Food Chemistry Data. In: *Data Handling in Science and Technology*. Pp. 315-340. Elsevier.
- Trygg, J. & Wold, S. (1998). PLS regression on wavelet compressed NIR spectra. *Chemometrics and Intelligent Laboratory Systems*, **42**, 209-220.
- Tsenkova, R., Muncan, J., Kovacs, Z. & Pollner, B. (2018). Essentials of aquaphotomics and its chemometrics approaches. *Frontiers in chemistry*, **6**, 363.
- UNESCO (2017). The United Nations World Water Development Report 2017 : Water and Jobs. Pp. 1-12. Italy: United Nations.
- Velasco, L., Fernández-Martínez, J. & De Haro, A. (1997). Determination of the fatty acid composition of the oil in intact-seed mustard by near-infrared reflectance spectroscopy. *Journal of the American Oil Chemists' Society*, **74**, 1595-1602.
- Vlyssides, A., Barampouti, E. & Mai, S. (2005). Wastewater characteristics from Greek wineries and distilleries. *Water Science and Technology*, **51**, 53-60.
- Wentzell, P.D. & Montoto, L.V. (2003). Comparison of principal components regression and partial least squares regression through generic simulations of complex mixtures. *Chemometrics and Intelligent Laboratory Systems*, **65**, 257-279.
- Westad, F., Bevilacqua, M. & Marini, F. (2013). *Chemometrics in Food Chemistry: Chapter 4. Regression*. Elsevier Inc. Chapters.
- Wold, S., Antti, H., Lindgren, F. & Öhman, J. (1998). Orthogonal signal correction of near-infrared spectra. *Chemometrics and Intelligent Laboratory Systems*, **44**, 175-185.
- Workman Jr, J. (2000). *The Handbook of Organic Compounds, Three-Volume Set: NIR, IR, R, and UV-Vis Spectra Featuring Polymers and Surfactants*. Elsevier.
- Yang, Q., Liu, Z. & Yang, J. (2009). Simultaneous determination of chemical oxygen demand (COD) and biological oxygen demand (BOD5) in wastewater by near-infrared spectrometry. *Journal of Water Resource and Protection*, **4**, 286-289.

- Ye, M., Yue, T., Yuan, Y. & Li, Z. (2014). Application of FT-NIR spectroscopy to apple wine for rapid simultaneous determination of soluble solids content, pH, total acidity, and total ester content. *Food and bioprocess technology*, **7**, 3055-3062.
- Yu, H., Zhou, Y., Fu, X., Xie, L. & Ying, Y. (2007). Discrimination between Chinese rice wines of different geographical origins by NIRS and AAS. *European Food Research and Technology*, **225**, 313-320.
- Zhang, M.-L., Sheng, G.-P., Mu, Y., Li, W.-H., Yu, H.-Q., Harada, H. & Li, Y.-Y. (2009). Rapid and accurate determination of VFAs and ethanol in the effluent of an anaerobic H₂-producing bioreactor using near-infrared spectroscopy. *Water Research*, **43**, 1823-1830.
- .

Chapter 4

Investigating the Performance and Optimisation of pH, Feeding Time and Mixing Intervals of an Anaerobic Sequencing Batch Reactor (AnSBR) for the Treatment of Winery Wastewater

Abstract

A pilot-scale anaerobic sequencing batch reactor (AnSBR) with an effective volume of 165 L was operated for 16 consecutive cycles using winery wastewater as the substrate. The length of each cycle was 24 h and the hydraulic retention time (HRT) was approximately 1.85 days. Initially the reactor was seeded with 22 kg anaerobic granules. This resulted in an organic loading rate of $0.38 \text{ kgCOD.kgVSS}^{-1}.\text{d}^{-1}$. The anaerobic granules were acclimatised to the wastewater for two months with wastewater of increasing strength until the microorganisms could reduce wastewater of $7\,000 \text{ mg.L}^{-1}$ COD by 70 %. A central composite experiment design (CCD) was performed to determine optimal operational parameters. The pH, feed time and mixing intervals were the selected operational parameters for optimisation. Mean COD reduction of 68.32 % was achieved. The optimal values were determined as: pH 7.30; feed time 180.91 minutes and a mixing interval of 84.17 minutes. This demonstrates the feasibility of the AnSBR technology to successfully treat winery wastewater with a COD range of $3\,200 - 9\,700 \text{ mg.L}^{-1}$.

4.1 Introduction

The wine industry is a very important source of revenue for South African farmers, particularly in the Western Cape. The Western Cape has 445 of the 468 private cellars in the country (SAWIS, 2018). Currently South Africa is the 9th leading producer of wine in the world (OIV, 2019). Production on this scale has ramifications when it comes to water usage as for every litre of wine produced 2 – 14 L of wastewater can be generated (Oliveira *et al.*, 2009). However recent data suggest this is decreasing to roughly 1 kg wastewater per 1 litre of wine produced (Barbera & Gurnari, 2018). In South Africa it is estimated that roughly 2m^3 of water is used per tonne of grapes crushed in the wine making process (Howell & Myburgh, 2018). Generation of winery wastewater is estimated to be approximately 50 % of the total water usage (Howell & Myburgh, 2018). South African wineries crushed an estimated 1.24 million tonnes of grapes in 2018 meaning that approximately 1.24 billion litres of winery wastewater was produced in the harvest season (Howell & Myburgh, 2018; SAWIS, 2018). Winery wastewater is a high strength wastewater of seasonal nature and has variable characteristics making it complicated to treat. Organic compounds which contribute to the high COD are mainly sugars, organic acids, esters, polyphenolic compounds and alcohol giving the wastewater not only high COD but generally an acidic pH (Mosse *et al.*, 2011).

Anaerobic digestion (AD) is an established treatment for winery wastewater, however not a lot of research has been performed on anaerobic sequencing batch reactors (AnSBR) for the treatment of winery wastewater (Ruiz *et al.*, 2002; Keyser *et al.*, 2003; Moletta, 2005). There is a shortage of knowledge regarding the optimal operating conditions for treating winery wastewater with an AnSBR. Research regarding optimal feeding time, mixing regime and pH of the technology is not established, specifically for treatment of substrate with varying strength.

Previous work done on winery wastewater using AnSBR technology produced COD reduction percentage of 98 % (Influent COD: 19.7 g.l⁻¹) (Ruiz *et al.*, 2002). This experiment was however performed in a lab-scale AnSBR with a working volume of 5 L (Ruiz *et al.*, 2002).

A study was performed on a larger AnSBR with a volume of 45 L to treat brewery wastewater and achieved a COD reduction of greater than 90 % (OLR: 3.0kg COD.m⁻³.d⁻¹) (Shao *et al.*, 2008). That study was performed on a different substrate, on a scale smaller than the study described in this thesis.

A more recent study was conducted using an AnSBR for the removal of polyphenols in winery wastewater (Ortiz-Cabrera *et al.*, 2018). This study was performed on a lab-scale reactor with a working volume of 2.25 L. Polyphenol reduction percentage achieved in this study was 95 % and COD reduction percentages of 95 -98 % were achieved.

The aim of this study was to evaluate whether the AnSBR technology could successfully treat winery wastewater of varying quality from day-to-day and what the optimal operational parameters for the reactor would be. The AnSBR has an effective volume of 165 L which is significantly larger than previous AnSBRs used. The aim was achieved by using a CCD experiment to determine optimal parameters for pH, feed time and mixing intervals and simultaneously the feasibility of the technology for wider implementation.

4.2 Materials and methods

4.2.1 Experimental phases

The study was conducted in two phases. Phase 1 involved setting the anaerobic sequencing batch reactor (AnSBR) up on the farm and acclimatisation of the anaerobic granules to increasing concentrations of chemical oxygen demand (COD). Phase 2 of the experiment was performed to evaluate the efficacy of the AnSBR at a pilot-scale treating winery wastewater of varying composition and concentrations.

4.2.2 AnSBR design

A pilot-scale anaerobic sequencing batch reactor (AnSBR) was designed and purpose-built for the requirements of this study. The reactor was designed and built at Stellenbosch University (Department of Process Engineering workshop). The vessel was constructed out of stainless steel and was comprised of two parts. A round cylinder and a conical base. The conical base was built by Fabrinox (Paarl). The conical base had an internal diameter of 400 mm and cylindrical wall heights of 130 mm (**Figure 4.1**). The conical floor of the cylinder was set at an angle of 25°. A 25 mm socket with internal threading was attached to the bottom

of the cone to allow for attachment of a ball valve. Three additional sockets, all with internal threading, were incorporated into the base. One socket housed a 1.5 kW geyser element and the socket above it was the inlet for the wastewater. The additional socket was for another possible inlet for the wastewater. The cone had a 6 mm flange with bolt holes to allow for connection with top of vessel. An intermediate plate of 6 mm polyvinyl chloride was manufactured, and eight filter nozzles were inserted to facilitate even distribution of water through the nozzles (**Figure 4.2**).

The round stainless-steel cylinder screwed into the conical base via the 6 mm flange. The top cylinder had a length of 1 150 mm and an internal diameter of 400 mm. Seven internally threaded sockets (25 mm) were incorporated into the cylinder, each with its own purpose (**Figure 4.3**). The total volume of the reactor was 160 L with around 10 % headspace, leaving a working volume of roughly 144 L. A floating lid was used in the design and a 10 L gas bag (SupelTM-Inert Gas Sampling Bags with ThermogreenTM LB-2 Septa) was connected to an outlet pipe from the top of the lid. The floating lid was made of linear low-density polyethylene (LLDPE) and used polystyrene to allow the lid to float.

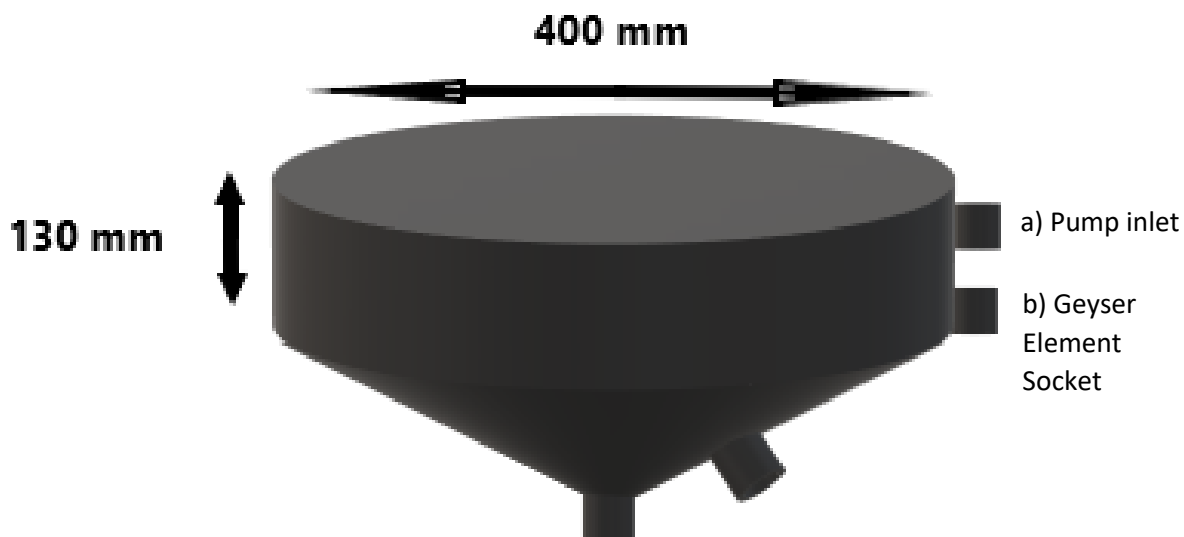


Figure 4.1 Conical base of the AnSBR made from stainless steel. The cone has a diameter of 400 mm and a volume of roughly 16 L.

The reactor was set up on a wine farm on the R304 road outside Stellenbosch (GPS Coordinates: -33.834493, 18.797875). In order to get the water to the reactor a submersible pump (Speroni 0.8 kW 140 L.min⁻¹) was dropped into the sump, where the winery wastewater collects on the farm. The submersible pump was placed inside a basket with very small openings to act as a filter to avoid pump blockage by grape skins. A black 25 mm HDPE pipe was connected to the submersible pump and laid along the ground to a collection tank approximately 40 m away. The collection tank was a 210 L LLDPE water drum and the inlet was covered with a swimming pool filter basket to catch any smaller particulate matter that may block the pumps or the filter nozzles. This 210 L drum was connected with a pipe and ball valve to a 90

L tank with a heating element. Heating of the water to 35°C took place in this tank. This tank was connected to the reactor via a pump (Calpeda 0.45 kW, 4 800 L.h⁻¹). The substrate would be fed to the reactor using this water pump. The water entered the reactor from the top socket on the side of the base (**Figure 4.3**) and the pressure pumped the water through the filter nozzle bed for even distribution of the water. A water pump (Speroni CAM 80) was used as the recirculation pump. Feeding and mixing times were controlled using a Delta PLC. The water would flow from the top of the reactor into a 50 L overflow tank. This overflow tank was used as a reservoir for liquid recirculation. The recirculation pump would pump the water from the overflow tank back into the reactor at intervals determined by the experimental design.

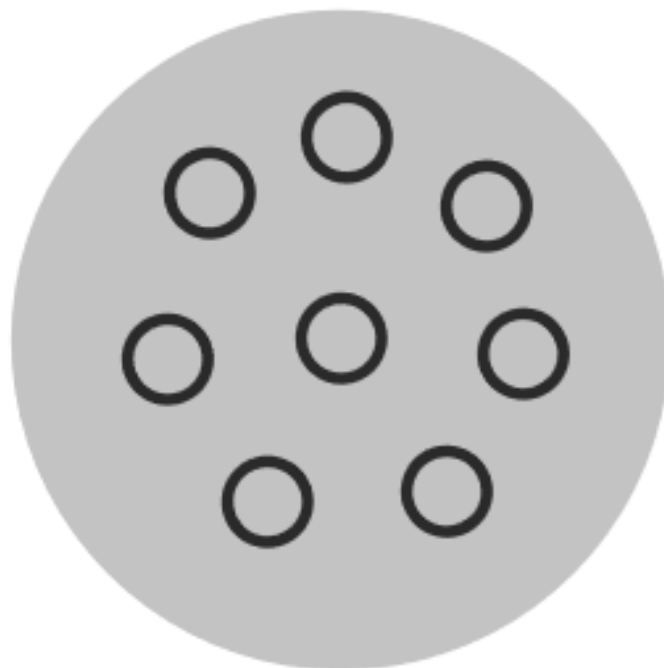


Figure 4.2 Diagram of the layout of the filter nozzles and the PVC plate.

Feeding and mixing strategies were controlled using the Delta PLC and the mixing pump was set to mix for 10 seconds at a time. A pH probe (Hanna HI6100405) was fitted onto the reactor and the pH was controlled using a mini pH controller (Hanna BL931700-1). The pH mini controller was connected to a peristaltic dosing pump (Watson Marlow 302S), when the pH dropped below the operating pH, the mini controller would switch on the dosing pump and 2M KOH would be dosed into the reactor until the pH returned to operating levels. The temperature was controlled using a PT 100 connected to temperature controllers which would switch on the geyser element in the reactor or 90 L tank if the temperature dropped below 35°C. Decanting occurred from the decanting port of the reactor. The water would pass through the copper heating coils in the 90 L tank to assist in the heating of incoming wastewater from the next batch. After each cycle, approximately 90 L of wastewater was decanted, leaving 50 L to assist with maintenance of alkalinity of the reactor.

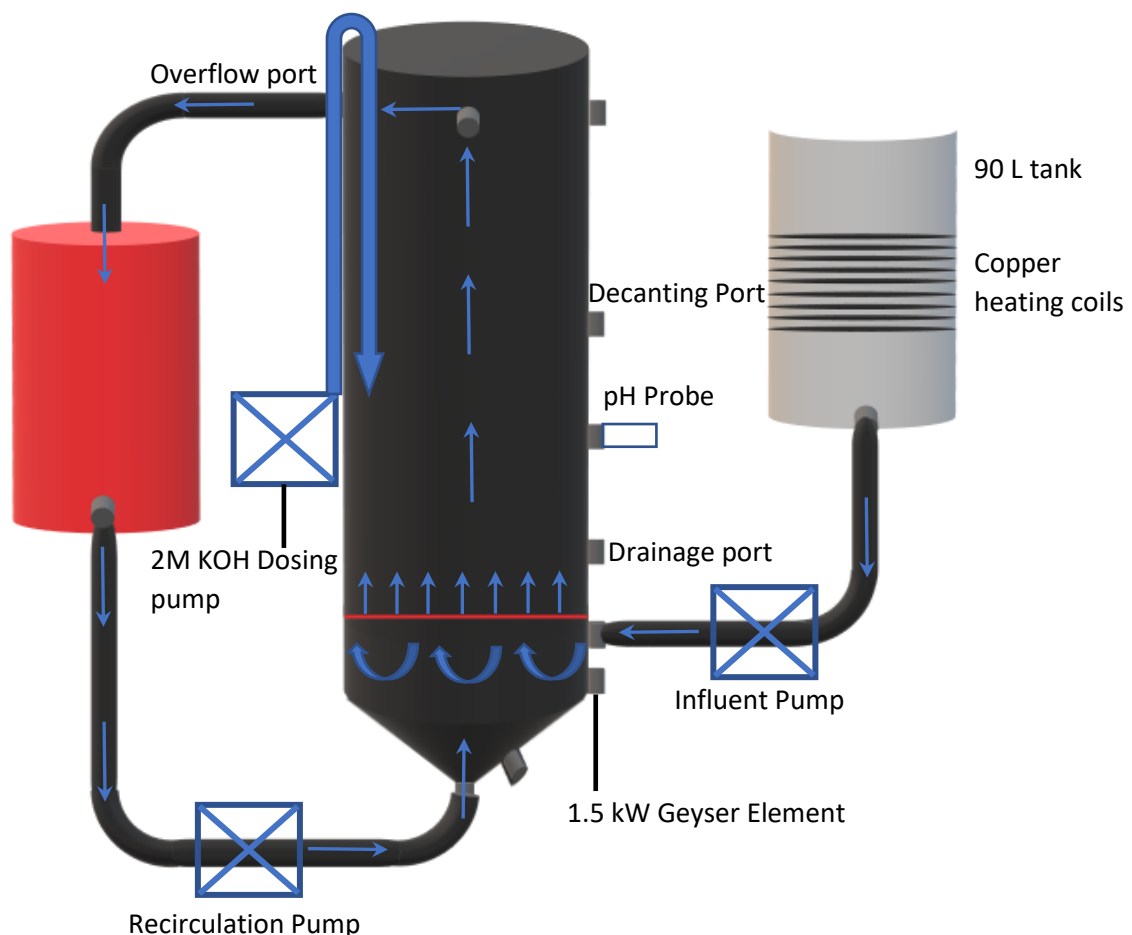


Figure 4.3 Diagram of the AnSBR. Water flowed from 90 L tank into reactor, into the overflow tank and recirculated in the reactor.

4.2.3 Reactor start-up and operation

Approximately 140 L of water was pumped into the reactor and an additional 20 – 25L of water was always kept in the overflow tank during the first phase. Automation was trialled for the first 3 – 4 weeks using clean water and no anaerobic granules. The design of the reactor was adjusted to correct for blockages of pumps and filter nozzles until the design was settled upon as stated in **section 4.2.2**. Once it was established that the reactor was reliable it was seeded with 22 kg of anaerobic granules which were obtained from a full-scale UASB which was treating distillery wastewater. The granules were obtained from the James Sedgwick Distillery in Wellington, South Africa. The water was dosed with CaCO_3 to increase the alkalinity to roughly $2\,000\text{ mg}\cdot\text{L}^{-1}$. A trace element solution was also added to the reactor and every 3 weeks 140 mL of the solution was added to the reactor (**Table 4.1**). The reactor operated in four steps during each cycle. The first step is the feed step, which feeds 90 L of substrate to the reactor. The next step is the react step. The anaerobic bacteria reacted with the wastewater whilst being routinely mixed every 60 minutes for 10 seconds at a time. The next step is the settling step where all mixing was suspended and allowed the biomass to settle to the filter bed. Finally, 90 L of wastewater was decanted, leaving 50 L in the reactor and 20 – 25 L in the overflow tank to act as an alkalinity buffer. The initial load of the wastewater was $1\,000\text{ mg}\cdot\text{L}^{-1}$ COD. Wastewater from the farm was used and diluted until a concentration of $1\,000\text{ mg}\cdot\text{L}^{-1}$ COD was obtained. This was done via a

calculation and verified using a diluted sample based on the calculation. Once the reactor was able to reduce the COD by 70 % for two consecutive days, the concentration of the substrate was increased by 500 mg.L⁻¹. This was repeated until the reactor was able to handle COD concentrations of 8 000 mg.L⁻¹. This process lasted approximately 2 months until the granules were acclimatised.

Table 4. 1 Concentrations of trace elements in the trace element solution fed to the AnSBR.

| Trace Element | Concentration mg.L ⁻¹ |
|---|----------------------------------|
| Ca (as CaCl ₂) | 36 |
| Mg (as MgCl ₂ •6H ₂ O) | 24 |
| Mn (as MnSO ₄ •5H ₂ O) | 0.241 |
| Zn (as ZnCl ₂) | 0.202 |
| Se (as H ₂ SeO) | 0.091 |
| Co (as CoCl ₂) | 0.091 |
| Al (as AlCl ₃) | 0.081 |
| Mo (MoO ₃) | 0.066 |
| B (as H ₃ BO ₃) | 0.0124 |
| Ni (as NiCl ₂) | 0.006 |
| Si (as SiO ₂) | 0.004 |
| W (as Na ₂ WO ₄ •2H ₂ O) | 0.002 |

4.2.4 Operational time of the AnSBR

As mentioned in **section 4.2.3** the AnSBR operated in four steps. A fifth step can be included to describe the time that elapsed between the decant step and the next feed cycle. This step will be defined as the idle step. From the feed step until the decant step, the reactor operated for a total of 24 hours per cycle. This meant that the hydraulic retention time (HRT) was 1.83 days. The HRT was calculated from **equation 4.1**. The volume of the reactor was calculated as 140 L plus 25 L of the overflow tank for a total of 165 L. As previously stated, 90 L of water was decanted per day and the reactor ran for one cycle per day.

$$HRT = \frac{\text{volume of reactor}}{(\text{volume decanted per day}) \times (\text{Cycles per day})} \quad \text{Equation 4.1}$$

The feeding time was reliant on the experimental design and differed for each run (**Table 4.2**). During the reactor start-up phase, the feeding time was set to 120 minutes. The feeding interval was controlled by determining how fast the pump could transfer water between the tank and the reactor. This time was 70 seconds. The pump was subsequently programmed to switch on for 8 seconds at a time. The feeding interval was therefore every 13 minutes. The pump was hardwired to a level-float switch so that the pump would

switch off and could not restart until the tank was filled again, to avoid the pump running dry. Mixing of the water was also determined by the experimental design, but during start-up it was set to mix every 60 minutes for 10 seconds. No mixing occurred outside of the react phase. Settle time of 45 minutes was applied for the start-up as well as during the experiment to allow for the settling of the granular biomass. Decanting was accomplished by means of gravitational forces and took 20 – 30 minutes to drain per cycle.

4.2.5 Experimental design

In order to perform an optimisation study, a CCD experiment can be performed (Box & Wilson, 1951). The goal of the central composite design is to use as few experimental runs as possible to maximise or minimise a specific response. Factors that may influence the response are temperature, pH or time of reaction, to name a few (Box & Wilson, 1951). The data obtained from the central composite design was used and a regression function was fit to determine a prediction model which is known as the response surface methodology (RSM). Response surface methodology was applied to optimise the factors to obtain a predictive model that can accurately represent the changes in the response variables, based on the differences of the input variables; pH, feed time and mixing time (Asadollahzadeh *et al.*, 2014). The predictive model used was a regression coefficient function and is shown in **equation 4.2**.

$$Y = b_0 + b_1X_1 + b_2X_2 + b_3X_3 + b_4X_1^2 + b_5X_2^2 + b_6X_3^2 + b_7X_1 \cdot X_2 + b_8X_1 \cdot X_3 + b_9X_2 \cdot X_3$$

Equation 4.2

For **equation 4.2**:

Y = prediction response

b_0 = Model constant

b_1 ; b_2 ; b_3 = Linear coefficients

b_4 ; b_5 ; b_6 = Quadratic coefficients

b_7 ; b_8 ; b_9 = Interaction coefficients

X_1 = pH

X_2 = Feed strategy

X_3 = Mixing intervals

The design of this experiment consisted of three different parameters, each having 5 different levels. These levels are calculated based on a central composite design. These levels are:

+ α = Absolute maximum (Assigned)

+1 = Maximum value (Calculated)

0 = centre point (Calculated)

-1 = Minimum values (Calculated)

- α = Absolute minimum (Assigned)

For this central composite design, the absolute minimum and maximum values were assigned by the operator. In this case the absolute maximum and minimum values were assigned to the CCD based on the limits of the reactor to handle the specific variables. The limits of the reactor were determined by investigating literature. This was done to ensure that the parameters stay within the previously identified working conditions for the AnSBR. The values for the central composite design is summarised in **Table 4.2**. The following parameters were analysed and monitored to evaluate the efficacy of the AnSBR for the treatment of winery wastewater;

- COD Reduction percentage
- COD Ultimate
- Polyphenol reduction percentage
- TSS content of the Effluent
- Methane percentage
- Volatile fatty acid (VFA): Alkalinity

Table 4. 2 Values for the central composite design for each parameter; pH, Feed time and mixing interval.

| | | pH (X_1) | Feed Time (min) (X_2) | Mixing Interval (min) (X_3) |
|------------|------------------|--------------|---------------------------|---------------------------------|
| + α | Absolute maximum | 7.30 | 240.00 | 100.00 |
| +1 | Maximum | 7.18 | 193.38 | 81.76 |
| 0 | Centre Point | 7.00 | 125.00 | 55.00 |
| -1 | Minimum | 6.82 | 56.62 | 28.24 |
| - α | Absolute minimum | 6.70 | 10.00 | 10.00 |

The definition for COD ultimate in this study was the final COD concentration achieved after every cycle. The reason for representing COD ultimate was that the COD influent varied from day to day and only using reduction percentage may be misleading regarding the efficacy of a particular experimental run. The final or ultimate COD is therefore used as the AnSBR may have a lower limit for the removal of COD in 24 hours.

In total 16 experimental runs were performed and analysed for each response. To determine whether a parameter had a significant effect on the response, the p-value was evaluated with a 95 % confidence interval. When the function had a p-value <0.05 it indicates that the specific function had a significant effect on the specific response. The experimental design values for each of the 16 runs is shown in **Table 4.3**.

Table 4. 3 Calculated values for pH, feed time and mixing intervals used for each run in the central composite design.

| Experimental run | pH | Feed Time (Min) | Mixing Intervals (Min) |
|------------------|------|-----------------|------------------------|
| 1 | 7.18 | 193.38 | 81.76 |
| 2 | 7.00 | 125.00 | 100.00 |
| 3 | 6.70 | 125.00 | 55.00 |
| 4 | 7.00 | 10.00 | 55.00 |
| 5 | 7.00 | 240.00 | 55.00 |
| 6 | 6.82 | 193.38 | 81.76 |
| 7 | 6.82 | 56.62 | 81.76 |
| 8 | 7.00 | 125.00 | 55.00 |
| 9 | 7.30 | 125.00 | 55.00 |
| 10 | 6.82 | 56.62 | 28.24 |
| 11 | 7.18 | 56.62 | 81.76 |
| 12 | 7.18 | 56.62 | 28.24 |
| 13 | 7.00 | 125.00 | 10.00 |
| 14 | 7.00 | 125.00 | 55.00 |
| 15 | 6.82 | 193.38 | 28.24 |
| 16 | 7.18 | 193.38 | 28.24 |

4.2.6 Analytical methods

There were a number of variables monitored when evaluating the efficacy of an AnSBR for the treatment of winery wastewater. Standard Methods (APHA, 2005) were used to determine the following parameters of the winery wastewater:

1. pH (Hanna HI6100405 probe) was measured at the end of every cycle before decanting occurred.
2. Alkalinity (measured in mg CaCO₃.L⁻¹)
3. Total suspended solids (mg.L⁻¹)
4. Volatile suspended solids (mg.L⁻¹)
5. Volatile fatty acids

Alternative methods were used to determine the following parameters:

2. COD (mg.L⁻¹)
 - I. Influent measured using Spectroquant® COD cell test kits (Merck, Darmstadt, Germany) with the ranges 500 – 10 000 mg.L⁻¹ and 0 – 90 000 mg.L⁻¹.
 - II. Effluent measured using Spectroquant® COD cell test kits (Merck, Darmstadt, Germany) with the ranges 100 – 1 500 mg.L⁻¹ and 500 – 10 000 mg.L⁻¹

3. Total Polyphenols (mg.L^{-1}).

- I. Folin-Ciocalteu method (Singleton & Rossi, 1965).

4. Methane

- I. Biogas was produced during the treatment of the winery wastewater in the AnSBR. The biogas was captured in a 10 L gas bag (SupelTM-Inert gas sampling bag with LB-2 Septa). The concentration of methane (CH_4) and carbon dioxide (CO_2) was quantified using a Varian 3300 gas chromatograph. Helium was used as the carrier gas due to its inert property. The flow rate of Helium was 30 mL.min^{-1} and the oven temperature was 55°C . The gas chromatograph had a thermal conductivity detector. A 0.2 mL sample was injected into a Haysep Q (Supelco, Bellefonte, PA) 80 /100 mesh pack column packed at the Department of Food Science, Stellenbosch. Biogas volume could not be measured due to inadequate pressure in the AnSBR.

4.2.7 Data analysis

Analysis of the experimental data was performed on Design expert 12 (Stat-Ease, Inc, Minneapolis, USA). Response surface methodology contour plots were generated by analysing the regression coefficients. Optimal conditions were chosen based on the solution with the highest desirability for a specific response. The overall optimal conditions were chosen based on the solution with the overall highest desirability for the responses. Pareto charts were generated to investigate the significance of the linear, quadratic and interaction effects of each operational parameters using Minitab 19 (Minitab, LLC, State College, Pennsylvania, USA).

4.3 Results and discussion

4.3.1 Phase 1

During Phase 1 the AnSBR was seeded with 22 kg of anaerobic granules. The goal of this part of the study was to start-up the AnSBR and to stabilise to reaction so that the experimental runs could follow. The anaerobic reactor was fed with winery wastewater with COD concentrations ranging from approximately $1\,000 - 8\,000 \text{ mg.L}^{-1}$ with increases of 500 mg.L^{-1} at a time. Organic loading rate (OLR) was determined by dividing the COD by the HRT and the OLR was therefore in the range $0.54 - 4.32 \text{ kgCOD.m}^{-3}.\text{d}^{-1}$.

For the first nine cycles the COD of the substrate fed to the reactor was on average $1\,106 \text{ mg.L}^{-1}$. For those nine cycles the COD of the effluent ranged from $320 - 891 \text{ mg.L}^{-1}$. The higher concentrations of COD in the effluent were observed in the first few cycles as the granules were not properly acclimatised to the new substrate, even in very low concentrations. Acclimatisation of microbial populations in anaerobic granules for a new substrate has been shown in literature to be a time-consuming, but necessary process. Microorganisms that had been acclimated for 39 days resulted in an inferior performance of a lab-scale submerged anaerobic membrane bioreactor (SAMBR) compared to an acclimatisation time of 100 days

(Akram & Stuckey, 2008). The COD reduction for these nine cycles varied between 28.9 % in the first cycle to 80.9 % in the ninth cycle. The pH of the reactor was kept at 7.10 throughout the acclimatisation period. It is generally accepted that most functional microorganisms, including methanogens, perform well when the pH is between 6.8 and 7.2 (Gerardi, 2003). To maintain stability and reduce the effect of VFA accumulation, alkalinity was increased slowly until a concentration of roughly 2 000 mg.L⁻¹ was obtained. This was in the middle of the optimal range of 1 000 – 3 000 mg.L⁻¹ (Amani *et al.*, 2010). The COD was increased by 500 mg.L⁻¹ once a 70 % reduction of COD was obtained for two consecutive days. This continued until the functional microbial consortium was acclimatised to COD values of *ca.* 8 000 mg.L⁻¹.

The COD range of the influent was 1 016 – 8 214 mg.L⁻¹. Reduction of COD varied considerably during this period with reduction percentages ranging from 29 – 92 %. Alkalinity during this phase ranged between 926 – 2 642 mg.L⁻¹. Lower COD reduction percentages could be explained by the increasing concentration of influent COD of the winery wastewater. The efficiency of the reactor after increasing COD concentration initially decreased. One of the reasons for low COD reduction percentages was when overdosing of KOH occurred. Overdosing by the pH controller occurred occasionally because the controller only switches the dosing pump off once the set point is reached. When this was not combined with recirculation of the water it led to an increase in pH in excess of 8.0. This led to low COD removal percentages as some granule disintegration may have occurred and pH values above 8.0 are restrictive and potentially toxic to methanogens (Sandberg & Ahring, 1992; Gerardi, 2003). The pH was corrected immediately by lowering the pH of the substrate for the next cycle to roughly 5.0 so that the wastewater would gradually become more acidic. A possible reason for overdose of the reactor was depletion of alkalinity due to accumulation of short chain fatty acids (Ward *et al.*, 2008). This led to a decrease in buffering capacity of the reactor and therefore rapid changes in pH even when KOH was dosed. The addition of KOH does not increase the alkalinity of the solution to a large degree. Addition of calcium carbonate (CaCO₃) and potassium hydrogen carbonate (KHCO₃) increased alkalinity in the system. The two chemicals were mixed with the substrate to increase the alkalinity slowly in the reactor. A rapid increase of alkalinity could cause precipitation of CaCO₃, so care was taken to limit the use of it (Gerardi, 2003).

4.3.2 Phase 2

In Phase 2 the CCD was followed to evaluate the efficacy of the anaerobic digestion and to optimise operational parameters. The parameters to investigate for optimisation were pH, feeding time and mixing intervals. The CCD was followed as shown in **Table 4.3**.

4.3.2.1 COD reduction percentage

The data obtained from the CCD was used to fit the regression model described in **equation 4.2**. The regression coefficients obtained would suggest whether a specific parameter (pH, feed time and mixing interval) had a specific effect on one of the responses. It uses three parts of the function namely the linear,

quadratic and interaction effects. A simple way of illustrating this is through the use of Pareto charts. A standardised effect is calculated and shown as a bar chart. Each of the effects are represented and if a specific effect is significant the standardised effect for that parameter would be greater than 2.447 which indicates $p < 0.05$ and is shown using a red dotted line on the Pareto chart.

For COD reduction percentage the Pareto chart is shown in **Figure 4.4**. It is clear when looking at the Pareto chart that there was no significant effect influencing the COD reduction percentage. The biggest effect was the quadratic effect of mixing shown as CC. This was however not significant. If the quadratic effect were significant it would indicate that the optimal values for mixing were not at the extremes, but rather within the limits.

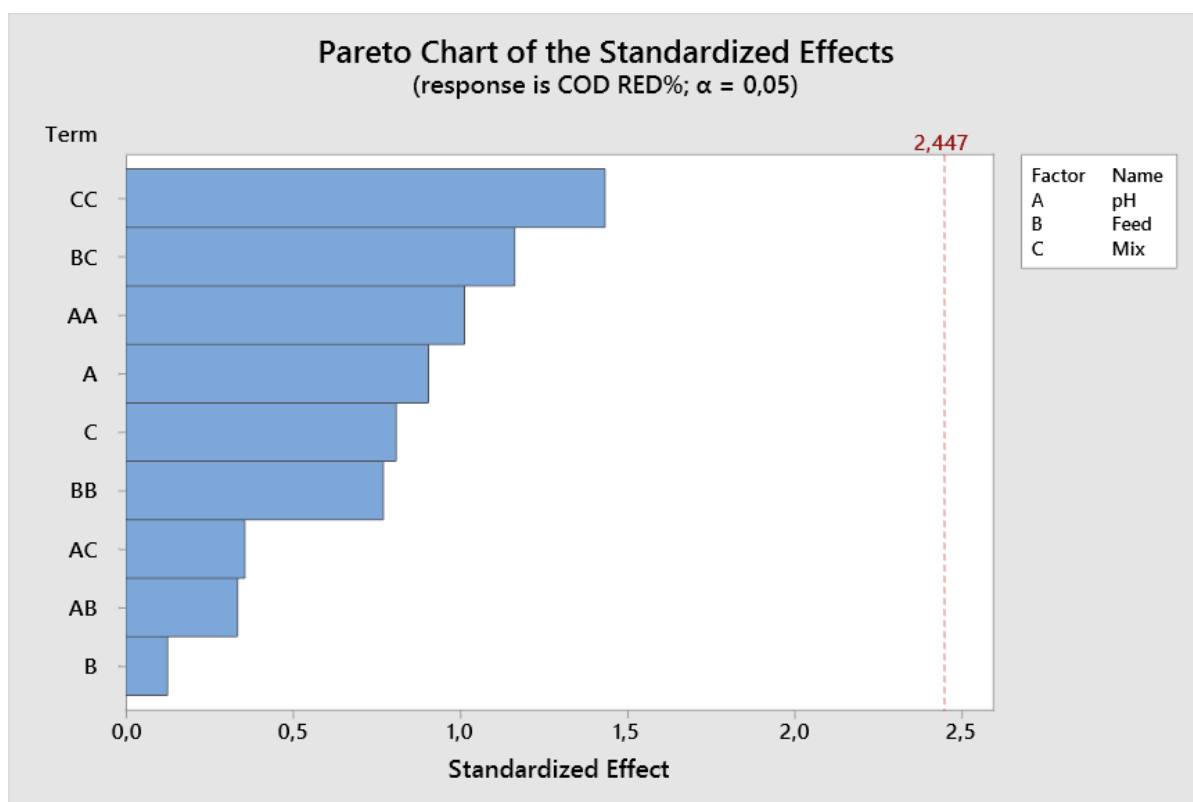


Figure 4.4 Pareto chart of COD reduction percentage.

Feeding time has a very small effect on COD reduction percentage with almost no standardised effect according to **Figure 4.4**. This may be because the AnSBR was able to dose KOH at any time during the feeding step, therefore if low pH wastewater was added to the reactor the pH could easily and rapidly be adjusted keeping the pH in the optimal range.

The mean COD reduction percentage was 68.32 % for all the parameters. COD influent of the wastewater ranged between 3 200 – 9 700 mg.L⁻¹. The range of COD reduction percentages was 41.5 – 85.4 %. The four lowest COD reduction percentages were observed during runs 10, 11, 15 and 16. This may be due to granular degradation of the methanogens as the wastewater gets pumped for mixing purposes. To maintain efficacy the biomass must remain in the system either through aggregating on inert

carriers or through self-immobilisation in the form of granules (McHugh *et al.*, 2003). Granular degradation would mean that the biomass is lost on every decant phase as there would be less settleability of the biomass. This would manifest in higher VSS values. The highest VSS values coincide with the later experimental runs. This would substantiate the theory that the anaerobic granules are being broken up and thereby decreasing efficacy of the substrate removal. The four lowest COD reduction percentages are correlated to a high ratio of VFA:Alkalinity. This is an important stability indicator as VFA:Alkalinity ratio above 0.3 – 0.4 indicate a process that is not stable and will have a decreased performance and a higher risk of acidification (Fannin, 1987). The COD removal efficiency of 41.5 – 85.4 % is lower than what is reported in most literature.

A study investigating the removal of COD for a mixture of municipal and synthetic wastewater found a COD removal percentage between 56 and 88 % (Bodík *et al.*, 2002). This was however done on a laboratory-scale AnSBR with an effective volume of 2 L.

Work on brewery wastewater has found that COD removal efficiency can be in excess of 90 % (Shao *et al.*, 2008). This work was performed on a 45 L pilot-scale plant. A possible reason for this is that the seed sludge was taken from a brewery and the substrate that the authors were testing was also brewery wastewater. Less importance would therefore need to be placed on the acclimatisation of the seed sludge.

A further study using a UASB had lower COD removal rates than those obtained in this study. The COD removal rate had a mean COD removal rate of 57 % (Parawira *et al.*, 2005). That study was, however, done on a full-scale upflow anaerobic sludge blanket with a volume of 500 m³ and a hydraulic retention time of 24 h.

A study by Ruiz *et al.* (2002) achieved a COD removal rate greater than 98 % in a 5 L lab scale AnSBR treating winery wastewater. The authors do not stipulate the seeding volume of sludge so it is possible that the wastewater had a longer contact time with anaerobic granules.

The average COD reduction of 68.32 % achieved in this study, indicates that the AnSBR technology can be used to treat winery wastewater and it has the potential to achieve high reduction percentages when used with the correct parameters.

4.3.2.2 Optimisation of control parameters (COD reduction %)

Optimisation of control parameters were obtained using the central composite design and calculating the regression coefficients. Response surface methodology (RSM) contour plots are then produced showing the optimal parameters for each response. **Figure 4.5** illustrates the COD reduction percentage for pH and feed in minutes. From this plot it is evident that a pH between 6.86 and 7.3 in conjunction with a feeding time between 108 and 240 minutes results in a COD reduction of 80 %. The red portion of the plot represents the higher reduction percentage. It must be clearly stated that none of the parameters had a significant effect on the COD reduction percentage from **Figure 4.4**. These contour plots do however show trends that occurred throughout the experiments and observations can still be made. A high reduction in COD could be obtained by increasing pH above 7.1 and increasing feeding time above 166 minutes **Figure 4.5**. Low COD

removal percentages are correlated with feeding times shorter than 98 minutes. It is possible that short feeding times of a potentially high-strength wastewater can result in VFA build-up in the reactor. It is known that a high organic loading rate can cause the acidogenic bacteria to multiply at a quicker rate than methanogens leading to a drop in pH and a subsequent drop in efficiency of the reactor (Amani *et al.*, 2010). The optimal pH of an AnSBR is between 7.0 and 7.2 and the pH indicating the highest COD reduction was in that range, however the upper limit observed was a pH of 7.3, which is slightly above the optimal levels (Gerardi, 2003).

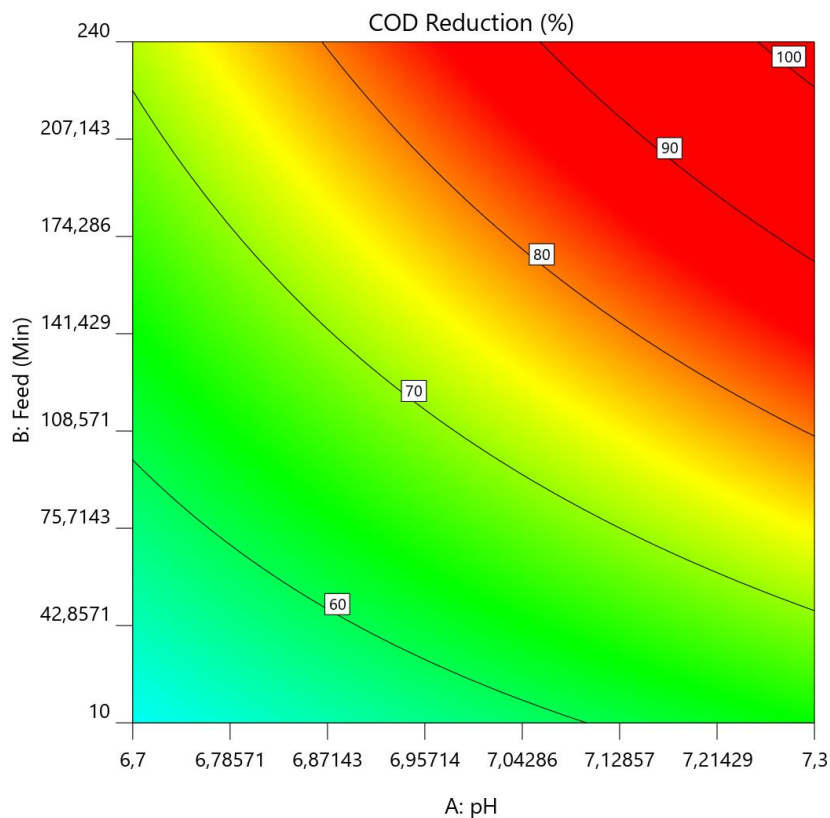


Figure 4.5 Contour plot showing COD reduction percentages for the interaction of pH and feed time.

The reduction of COD follows a very similar pattern for the interaction between pH and mixing interval (**Figure 4.6**). A pH between 6.9 and 7.3 predicted a COD reduction above 80 %. A 90 % reduction may be possible by increasing the pH to between 7.1 and 7.3. Mixing intervals between 69 and 100 minutes was correlated to a higher COD reduction percentage. The effect of pH has been previously explained in the context of COD reduction. Frequent and intense mixing has the ability to shear the anaerobic granules leading to a decrease in the ability to digest organic substrate (Sung & Dague, 1995; McMahon *et al.*, 2001; Huang *et al.*, 2018).

Longer periods between mixing may result in a reactor that is more stable and may improve the performance of the reactor (Stroot *et al.*, 2001). Longer mixing intervals have been shown to decrease breakdown of organic matter, whilst maintaining the efficacy of the reactor when compared to more frequent mixing (Gomez *et al.*, 2006). One condition of less frequent mixing is that the temperature should

still remain at 35°C and mixing should be done regularly enough to release methane gas bubbles from the anaerobic bacteria.

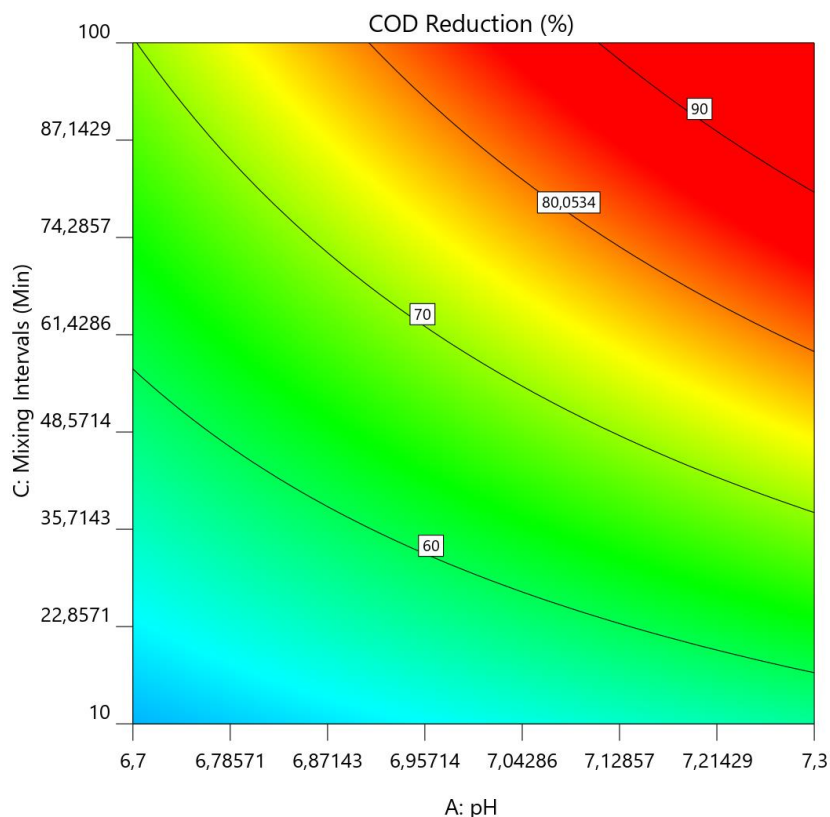


Figure 4. 6 Contour plot showing COD reduction percentages for the interaction of pH and mixing frequency.

High COD reductions were obtained due to less frequent mixing and a feed time above 100 minutes (**Figure 4.7**). Increased feeding times may result in less VFA formation and subsequently, a more stable pH. Less frequent mixing may have resulted in less breakdown of granules meaning a higher ability of the microorganisms to digest the substrate. Mixing frequency of the reactor was still frequent enough to permit even distribution of heat throughout the system, to maintain the operating temperature.

The optimal parameters for COD reduction is summarised in **Table 4.4**. These parameters were chosen based on their desirability score specifically for COD reduction percentage. The solution with the highest prediction value for COD removal was chosen. Optimal values to maximise COD reduction are a high pH, longer feeding times and a less frequent mixing regime.

Previous work conducted at the Department of Food Science in Stellenbosch on a lab-scale AnSBR treating synthetic winery wastewater found the following results for the optimisation of COD reduction (Laing, 2016). The optimal pH was reported to be 7.34, which is very similar compared to this study. The optimal feed time was longer, being 240 minutes and the mixing frequency was every 110.5 minutes. These results are similar to the results achieved in this study. There was however a 2nd experiment performed for

which the optimal values were; pH of 6.73, feed time of 6 minutes and a mixing frequency of 29.70 minutes. The big discrepancy in the two experiments was because the reactor was seeded with unacclimatised granules before the 2nd experiment, due to significant biomass washout, which altered the results obtained (Laing, 2016). The design of the lab-scale reactor differed significantly from this pilot scale reactor, which may explain some of the small discrepancies between the results obtained in this study and the results obtained previously in experiment 1. The composition of wastewater also differed considerably compared to experiment 1.

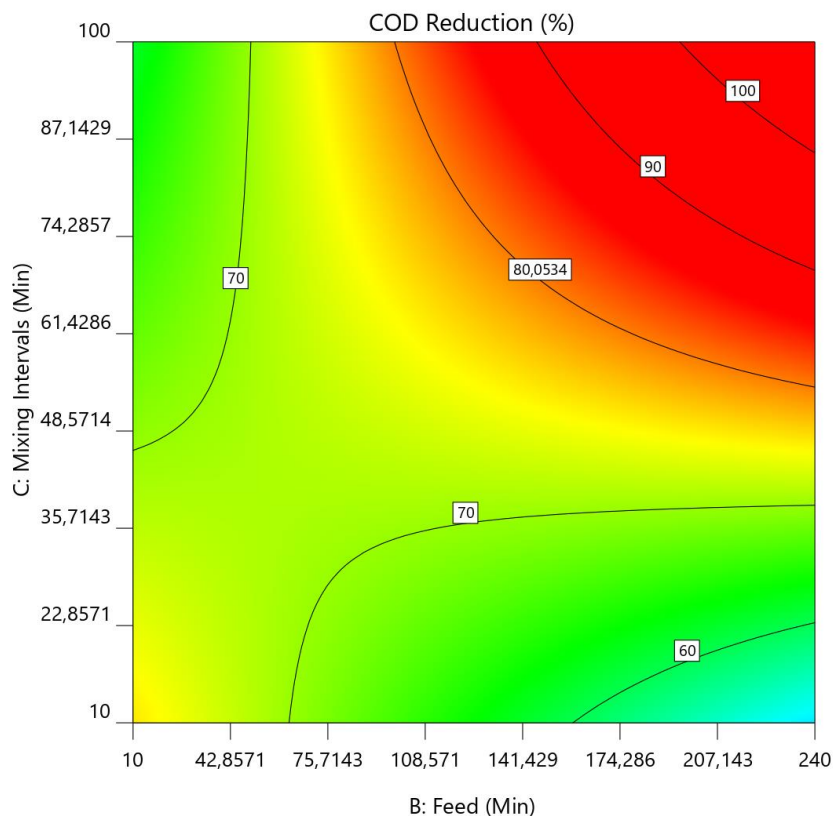


Figure 4.7 Contour plot showing COD reduction percentage for the parameters of feed time and mixing intervals.

Table 4.4 Optimal operating parameters with regards to COD reduction percentage.

| Parameter | Optimum values |
|------------------------|----------------|
| pH | 7.29 |
| Feed time (min) | 189 .68 |
| Mixing intervals (min) | 88.84 |

4.3.2.3 Ultimate COD reduction

The COD of the wastewater in this study was not kept constant, but was fed with varying strengths of wastewater with varying COD concentrations. It could be misleading to represent the data only by means of a reduction percentage as the reactor may have a limit that it can achieve in a 24 hr cycle and HRT of 1.85

days. This limit was 904 mg.L^{-1} as observed by the lowest COD achieved in this experiment. If the influent COD was $2\,000 \text{ mg.L}^{-1}$ and the ultimate COD achieved was $1\,000 \text{ mg.L}^{-1}$ it would mean that only a 50 % reduction took place. On the other hand, if a initial COD of $3\,000 \text{ mg.L}^{-1}$ was fed to the reactor and the final concentration was also $1\,000 \text{ mg.L}^{-1}$ then this would result in a 66 % reduction. For this reason ultimate COD achieved is also reported in this study.

The data obtained was used to fit the regression model described in **equation 4.2**. For COD ultimate reduction, the Pareto chart is shown in **Figure 4.8**. The Pareto chart shows that ultimate COD and COD reduction percentage are truly two independent responses as they have different t-scores for the factors. Although the influence of the factors differ from COD reduction percentage, none of the factors had a significant influence. This is illustrated by the bars not reaching the red line to the right of the Pareto chart. The most significant factor was the interaction of pH and feed time, followed by the linear effect of the mixing time.

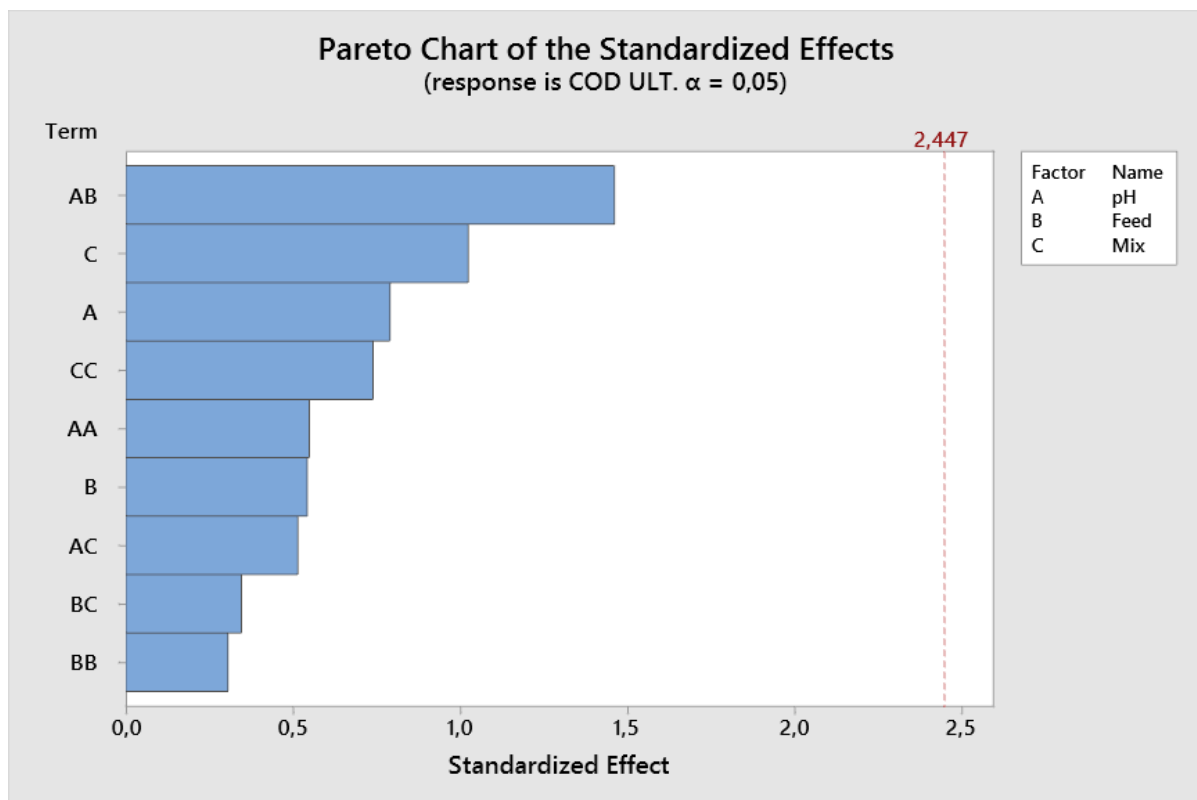


Figure 4.8 Pareto chart for the ultimate COD reduction value.

Ultimate COD concentrations ranged from $904 - 3\,340 \text{ mg.L}^{-1}$, with a mean value of $1\,766 \text{ mg.L}^{-1}$. A study was performed to evaluate the AnSBR for the treatment of landfill leachate (Timur & Öztürk, 1999). Ultimate COD values achieved in that study ranged from $684 - 5\,738 \text{ mg.L}^{-1}$. The concentration of influent leachate was however significantly higher with initial concentrations reaching COD levels of $15\,940 \text{ mg.L}^{-1}$ (Timur & Öztürk, 1999). This can explain the discrepancy in range between the two experiments, but indicate that the ultimate COD achieved in this study is comparable to literature. Another study investigated the efficacy of an AnSBR to treat slaughterhouse wastewater (Masse & Masse, 2000). Effluent COD

concentrations were reduced to 703 mg.L⁻¹ from an initial concentration of 11 500 mg.L⁻¹. These studies show that there is a clear limit of performance that can be attained for an individual reactor and that substantiates the theory that it is not correct to judge a cycle purely based on reduction percentage, but to take the performance limits of the reactor into account.

The five worst COD ultimate concentrations were obtained when at least one of the parameters were low pH (around 6.8), frequent mixing or rapid feed. From **Figure 4.8** it was shown that there was a small effect on the COD ultimate concentration by the interaction of pH and feed time, even though it was not significant. It is possible that these parameters may have had a small effect on the performance of the reactor. These results will be described in section 4.3.2.4.

4.3.2.4 Optimisation of control parameters (ultimate COD)

The optimal conditions to reduce the ultimate COD concentration is shown in **Figure 4.9**. The goal of the optimisation was to minimise the response i.e. have the lowest COD concentration for the effluent. Lower concentrations are marked by the blue areas with the green, yellow and red representing an increasing concentration of COD. It is clear that there are two areas on in the figure that correspond to low ultimate COD values, that is the top right and bottom left corner of **Figure 4.9**. This would mean that it would be possible to achieve low concentrations of COD at pH of 6.7 and at pH levels between 7.1 and 7.3. The two distinct regions are pH 6.7 – 6.8 in combination with low feed times of 10 – 43 minutes. Conditions like these would suggest that it is possible to achieve ultimate COD concentrations in the region of 1 000 – 1 500 mg.L⁻¹. From **Figure 4.9** it can be shown that the better combination of conditions would be a higher pH and a higher feed time as there is a bigger surface area represented on the graph. A bigger surface area would suggest that there is room for error during the process as the optimal conditions cover a bigger range. A feed time of 124 – 240 minutes in combination with a pH 7.1 – 7.3 would achieve the best reduction in COD. It is easier to control pH in a reactor at pH levels above 7.0 as there is a lower likelihood of accumulation of VFA's in the reactor (Amani *et al.*, 2010). This would lead to more stable pH control and ultimately a more stable process.

The efficacy of the reactor at low pH values and low feed times indicates that it could be possible to operate a reactor in these conditions, however the margins are very fine. Generally longer feeding times and higher pH values are preferred in anaerobic digestion, but it is possible to achieve good reduction of COD because the pH control was active throughout the process. The pH could therefore be adjusted continually. This would mean that the pH would not drop below the operating conditions for a significant amount of time, and would not cause reactor failure.

The interaction of mixing interval and pH is shown in **Figure 4.10**. The large blue zone on the right of the contour plot shows that higher pH values in the range of 7.06 – 7.30 are optimal for the reduction of COD. Mixing intervals were not as important as low ultimate COD values can be attained across most of the range of mixing intervals. The performance drops slightly when mixing intervals are between 10 and 20

minutes in combination with lower pH values. Mixing frequencies below 20 minutes may be too frequent and cause shearing of granules and a subsequent reduction in performance (Huang *et al.*, 2018).

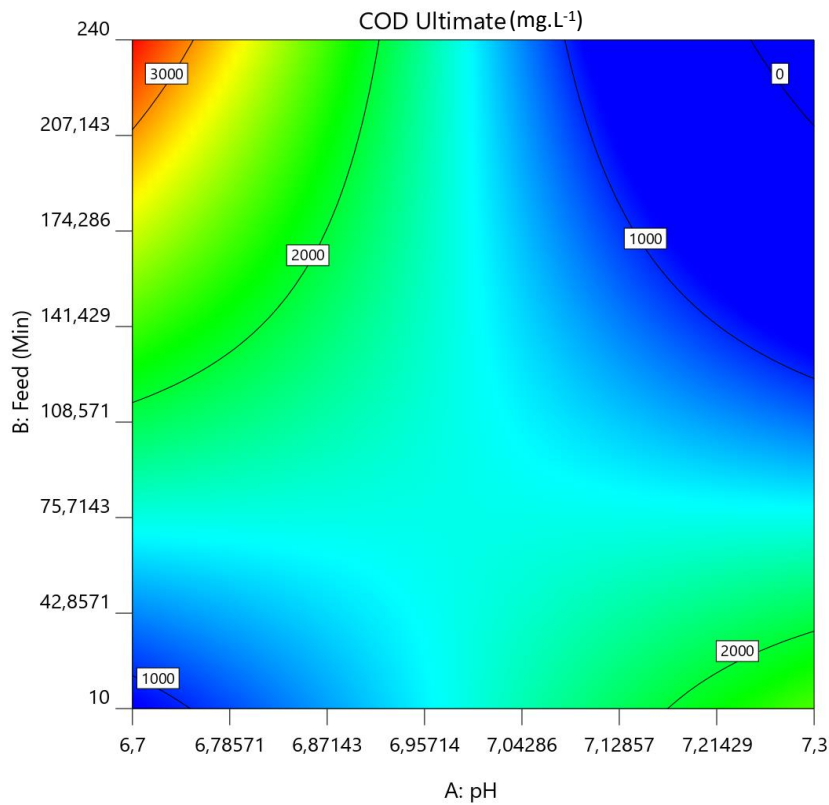


Figure 4.9 Contour plot showing COD ultimate for the parameter's pH and feed time.

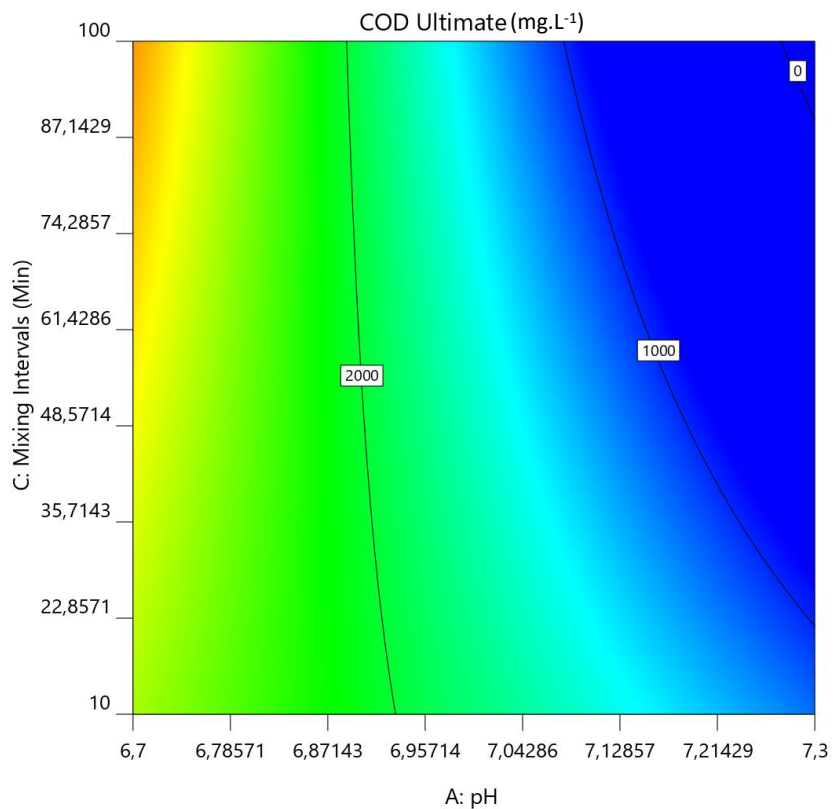


Figure 4.10 Contour plot showing the optimal parameters for pH and mixing regime to reduce ultimate COD.

pH Values below 7.0 are correlated to lower ultimate COD values even when mixing intervals are less frequent. This finding is in contrast to literature that states that infrequent mixing corresponds to better settleability of the granules and increased performance of the reactor (Sung & Dague, 1995). Contrasting evidence was published in 2012 that showed that continuous mixing may lead to higher COD removals and facilitate higher organic loading rates (Ghanimeh *et al.*, 2012). Mixing intervals are an important design consideration, but there is no standard mixing regime for all reactors. A good starting point may be to have less frequent mixing, but it is possible that reactor performance can increase when implementing a more frequent mixing regime.

Performance of the reactor is severely impacted when the mixing frequency is very low in combination with a short feed time. This is evident from the red area in **Figure 4.11**. It must be remembered that the interaction of feed time and mixing regime was the 2nd least impactful when investigating the Pareto chart. A very frequent mixing regime may result in granule disintegration and a low feed time could lead to overload of the reactor and potential acidification of the wastewater (Shizas & Bagley, 2002). Glucose is a substrate that may rapidly acidify wastewater due to its rapid breakdown by anaerobic bacteria (Shizas & Bagley, 2002). To combat this longer feeding times may be used, which ultimately lead to improved reactor performance (Kennedy *et al.*, 1991; Suthaker *et al.*, 1991; Shizas & Bagley, 2002).

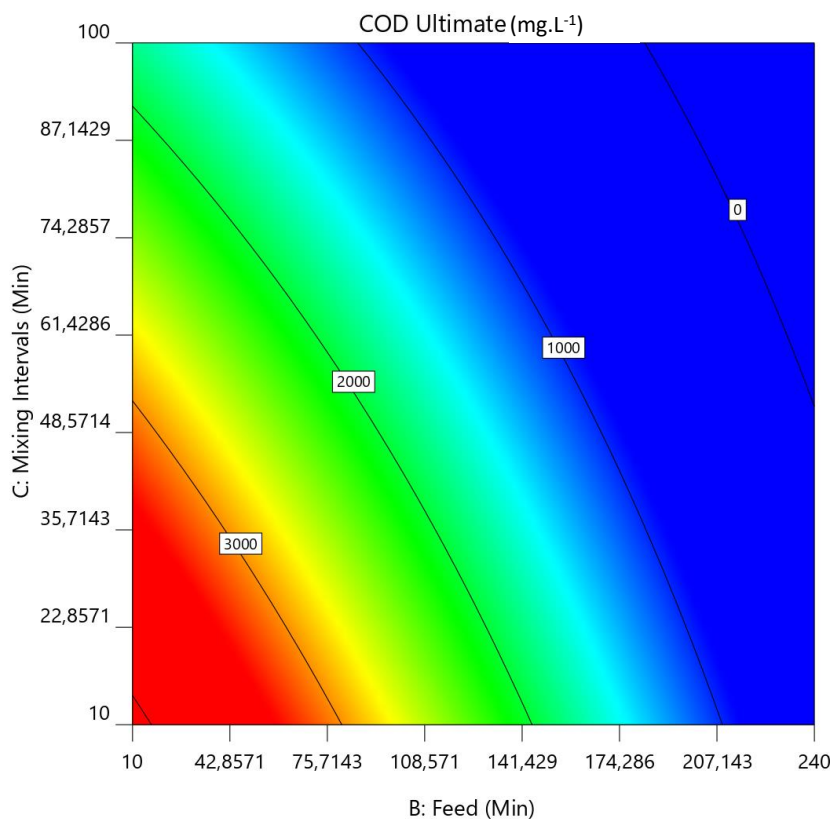


Figure 4.11 Contour plot showing the effect of feed time and mixing interval to reduce ultimate COD.

Longer feeding times between 100 and 175 minutes in combination with mixing frequencies above 55 minutes resulted in the best COD reduction. Control of pH would be most accurate with a lower OLR. Lower mixing frequencies were still sufficient to maintain temperature in the reactor and performance was not affected by the increased mixing intervals.

The optimal conditions for ultimate COD reduction is summarised in **Table 4.5**. These values were determined by the solution that had the highest desirability score for COD reduction. These results were similar to the optimum conditions needed for overall COD reduction percentage, even though there were small differences between the two methods of determining efficacy of COD removal.

Table 4.5 Optimal operating parameters with regards to ultimate COD reduction.

| Parameter | Optimum values |
|------------------------|----------------|
| pH | 7.30 |
| Feed time (min) | 197.81 |
| Mixing intervals (min) | 79.98 |

4.3.2.5 TSS content

Analysis of the regression coefficients indicate that none of the factors affected the response significantly. Investigation of Pareto chart shows that none of the factors met the threshold, delineated by the red dotted line.

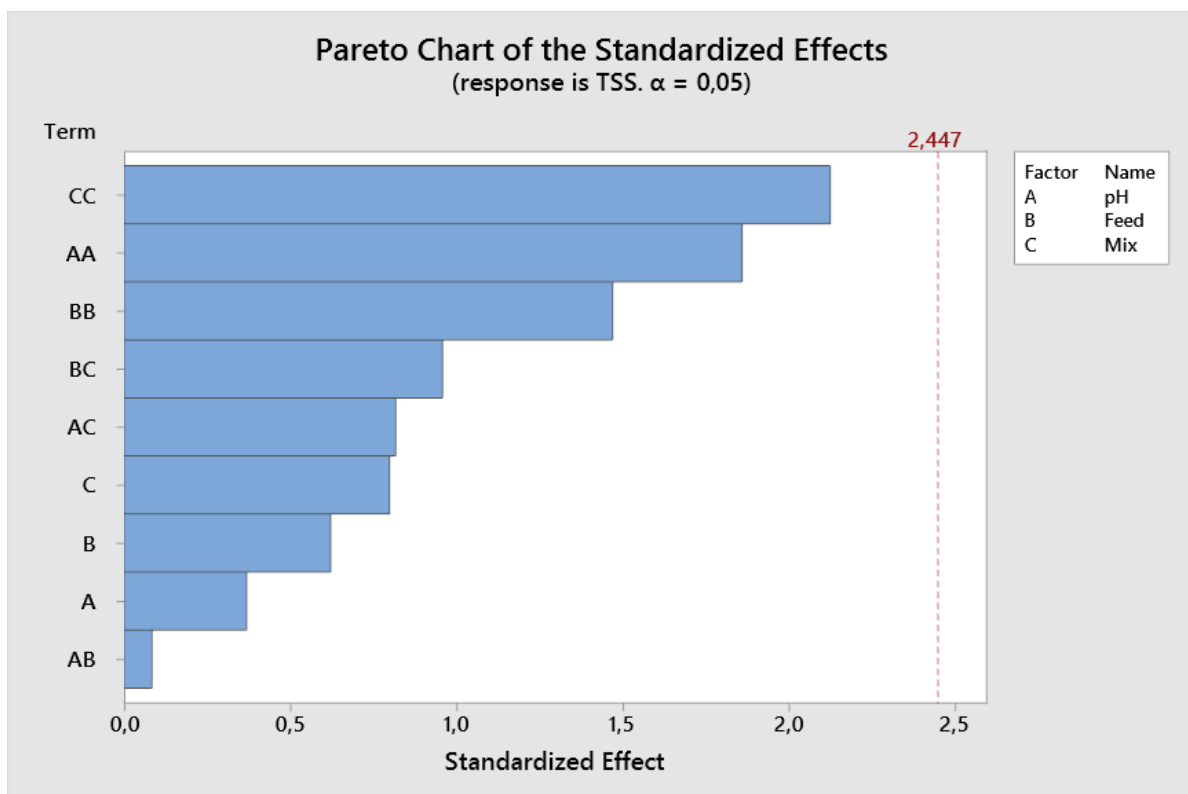


Figure 4.12 Pareto chart for the effluent TSS content of the winery wastewater.

The quadratic effects show the biggest interactions, which may allude to the optimal conditions not being in the extreme ends of the operational conditions. Of the three factors, mixing may be the most important aspect with regards to TSS content, although this relationship is not statistically significant.

The TSS content of the effluent ranged from 185 – 650 mg.L⁻¹. The mean TSS content of the effluent was 342.44 mg.L⁻¹. This would indicate that there was not a lot of biomass washout during the experiment. A possible reason is that granule disintegration did not take place. A possible reason for limited granule disintegration is a result of a short mixing time of 10 seconds every X minutes. One other possible reason is that the overflow was at the top of the reactor so very few granules would be suspended at that height, therefore very few granules would have passed through the pump during mixing.

4.3.2.6 Optimisation of control parameters for TSS content

A high TSS content of the effluent is indicated at the red zone of the contour plot (**Figure 4.13**). This correlates to a high pH and long feed times. As pH decreases along with feed time the TSS of the effluent decreases. This is in contrast to what would be expected as it would be expected that short feeding times could lead to lower TSS removal as it may impair reactor performance. Values of TSS below 100 are not realistic expectations for the effluent so values between 100 and 200 mg.L⁻¹ will be referred to as the optimal in the contour plots. For the pH range of 6.87 – 7.3 low levels of TSS in the effluent can be accomplished. However with increased feed times, a subsequent decrease in pH will result in better TSS removal rates. Optimal feed times range between 59 and 142 minutes. The one drawback to this graph is that the interaction shown in the Pareto chart for pH and feed time is extremely small and potentially plays no significant role (**Figure 4.12**). It can also be seen on the Pareto chart that pH is the factor with the least influence on the effluent TSS concentration (**Figure 4.12**). The optimum pH value may very well be somewhere within the range and not in the extremes as the quadratic effect for pH is high (**Figure 4.12**).

The interaction between mixing intervals and pH is not significant, but it is larger than the effect of pH and feed time. More information may be obtained from the subsequent contour plot (**Figure 4.14**). Higher TSS content of the effluent is correlated to a high pH and high mixing interval as well as a low pH and frequent mixing. For efficient removal of TSS it is necessary to keep the pH above 7.0 if the mixing frequency is between 10 and 41 minutes. A pH below 7.0 in combination with less frequent mixing (52 – 100 minutes) results in the most efficient removal of TSS. Low TSS at a lower pH range can potentially be because a slightly acidic condition inside the reactor would help maintain granular structure explained by the proton translocation – dehydration theory (Liu *et al.*, 2002). This theory is simply explained as the dehydration of microbial surfaces which could allow methanogens and acidogens to adhere to each other causing more stable granules (Liu *et al.*, 2002). This would help resist granule disintegration when mixing intervals are below 50 minutes.

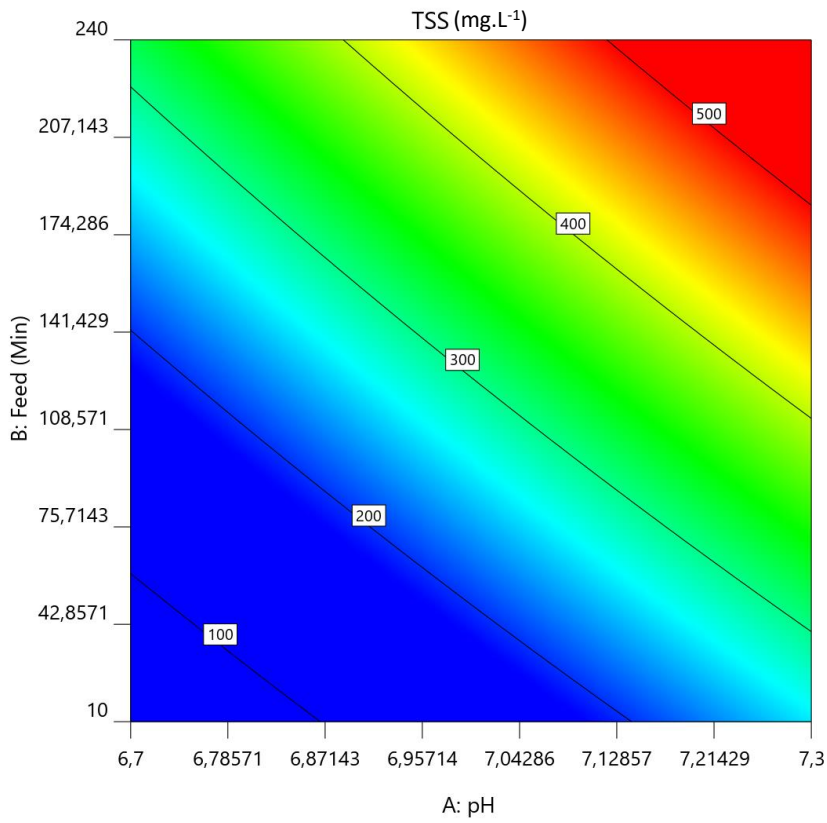


Figure 4.13 Contour plot showing optimal parameters for pH and mixing time to reduce TSS in the effluent.

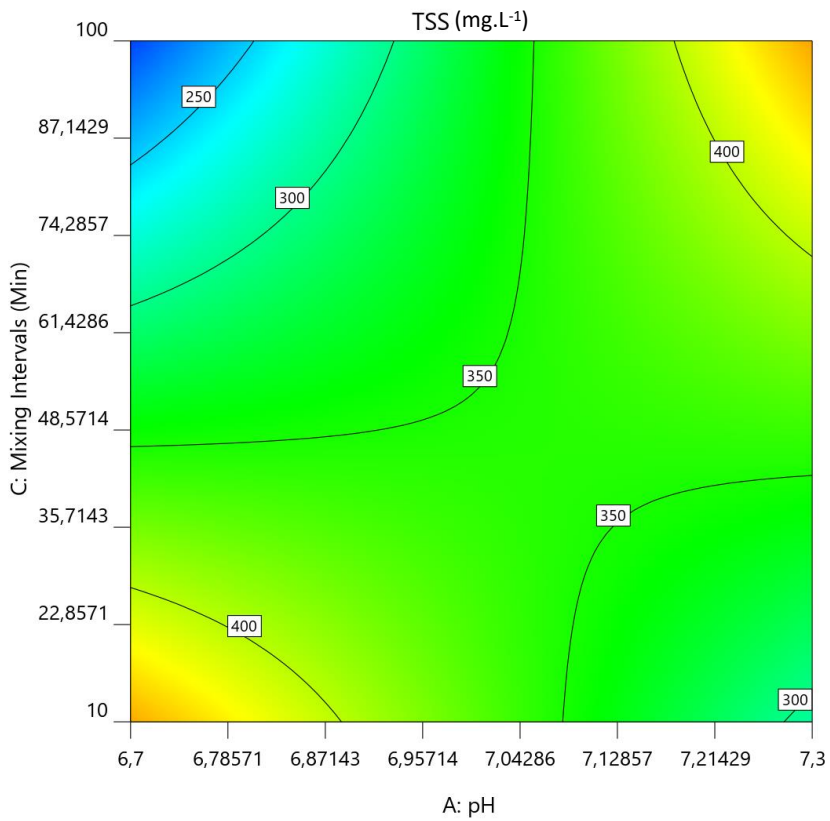


Figure 4.14 Contour plot showing optimal parameters for pH and mixing intervals related to TSS content of the effluent.

From **Figure 4.15** it is clear that a long feed time and infrequent mixing may cause increased TSS in the effluent. Lower TSS values could however be achieved with any other combination of mixing and feeding regimes. The most effective combination would be a longer mixing frequency (> 61 minutes) and a short feed time (10–99 minutes). Due to the large discrepancy in the optimal conditions for TSS it may be advisable to focus on more important parameters for the optimisation of the reactor conditions, however longer mixing intervals seem to be favoured above all other parameters.

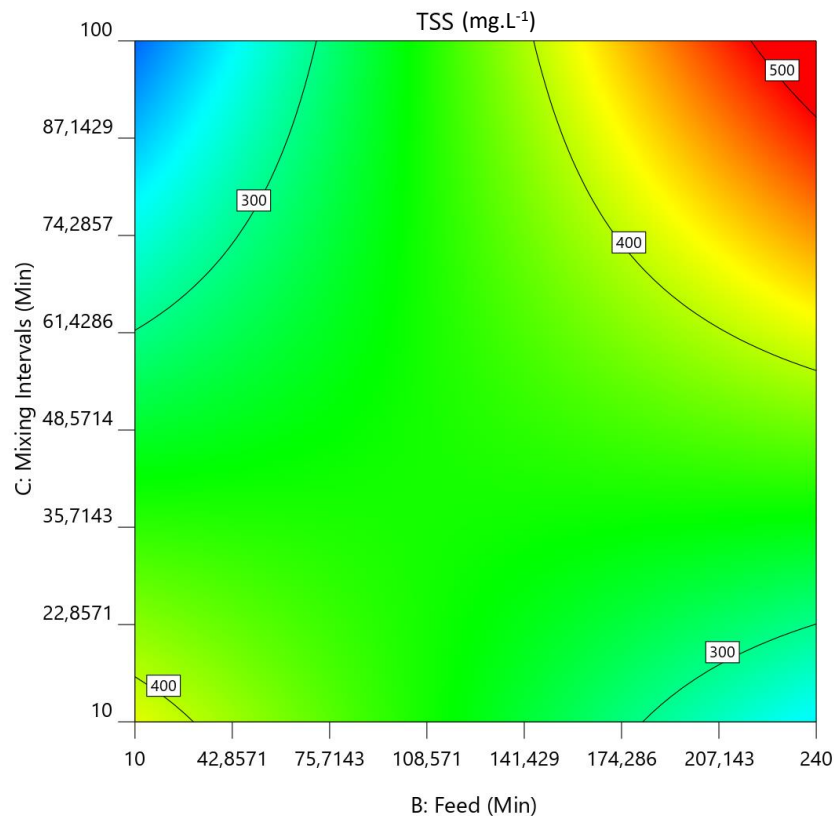


Figure 4. 15 Contour plot showing optimal parameters for feed time and mixing intervals related to TSS content of the effluent.

Table 4. 6 Optimal operating parameters with regards to TSS of the effluent.

| Parameter | Optimum values |
|------------------------|----------------|
| pH | 7.19 |
| Feed time (min) | 147.50 |
| Mixing intervals (min) | 99.76 |

Optimal values for TSS were decided on based on the desirability of the solutions. The values are summarised in **Table 4.6**. A pH of 7.19 with a medium feed time and infrequent mixing showed the best results in terms of TSS of the effluent.

4.3.2.7 Polyphenol reduction percentage

Data that was obtained from the central composite design was used to fit regression coefficients. None of the factors produced significant effects on the reduction of polyphenol content (**Figure 4.16**). The biggest effect was from the interaction of pH and mixing interval followed by the interaction of mixing interval and feed time. The linear factors with the biggest influence were pH and mixing interval.

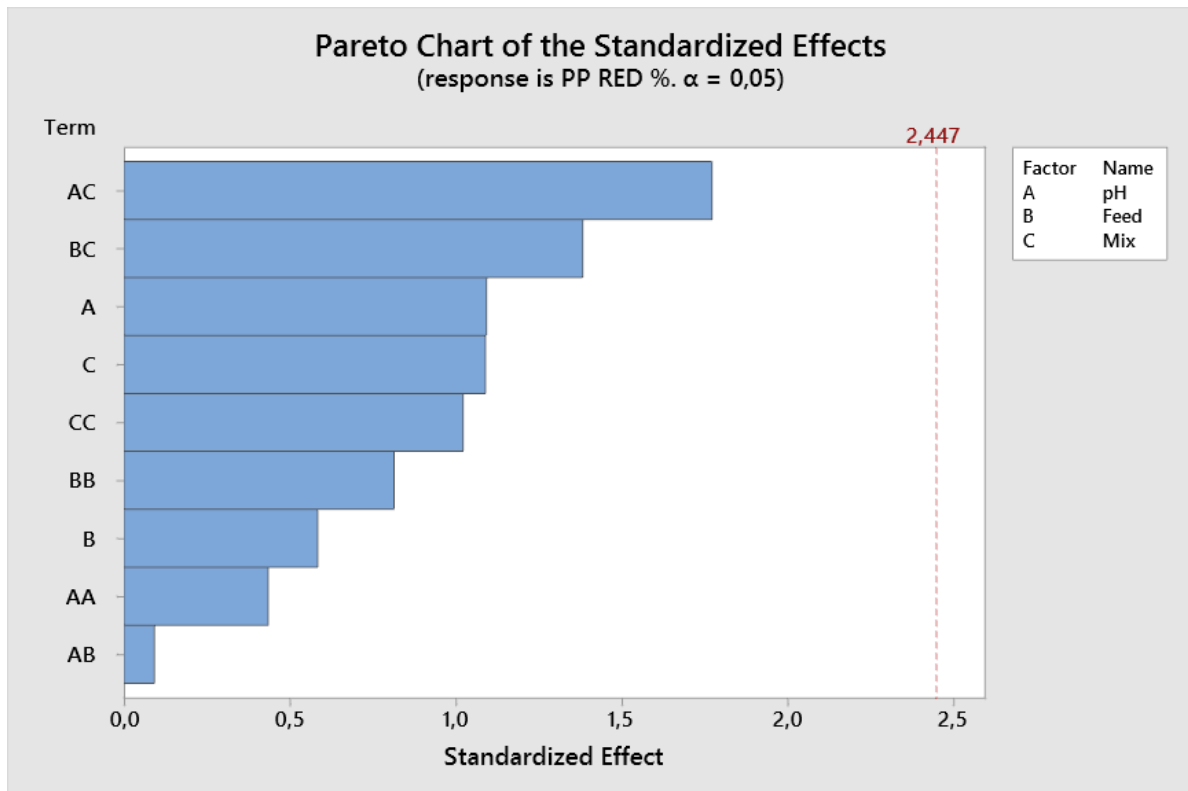


Figure 4. 16 Contour plot showing optimal parameters for feed time and mixing intervals related to TSS content of the effluent.

Polyphenols have been associated with phytotoxic and antibacterial effects which could affect the performance of anaerobic digestors (Goodwin *et al.*, 2001; Donoso-Bravo *et al.*, 2009; Ortiz-Cabrera *et al.*, 2018). It is therefore important to monitor the reduction of polyphenols in an AnSBR to ensure that the performance of the reactor is not decreased.

The polyphenol reduction was in the range of 13.11 – 77.69 % with a mean reduction of 53.35%. Previous work conducted on anaerobic reactors had obtained an average polyphenol reduction percentage of 63 % (Melamane *et al.*, 2007). This indicates that the performance of the AnSBR in this study was inferior, yet still produced reductions within an acceptable range. It is however paramount that polyphenol concentration be monitored within the reactor to ensure that build-up of polyphenols do not occur. A build-up of polyphenols may also slow down the digestion process and result in reduced removal performance of other compounds such as COD (Melamane *et al.*, 2007).

4.3.2.8 Optimisation of control parameters for polyphenol reduction percentage

The contour plot for pH and feed time shows a clear area in the top right corner where polyphenol reduction is the highest. This correlates with a pH between 7.2 and 7.3 and a feed between 174 and 240 minutes (**Figure 4.17**). It is clear from this plot that longer feeding times are required to ensure higher rates of polyphenol removal. Slower feeding times could mean that the initial load on the anaerobic bacteria is lower and that polyphenol degradation can occur earlier. No initial overload could therefore occur. The effect of pH is more prominent than that of the feed time as there is still a large tolerance for feed time between 60 and 80 % removal (**Figure 4.17**). Previously, an anaerobic digester was operated at a pH of 7.05 and a polyphenol reduction of 63 % was achieved (Melamane *et al.*, 2007). That is lower than the pH from this study, but does indicate that polyphenol reduction may occur at the higher end of the pH range for anaerobic digestion. In another study an effluent pH of 7.5 was recorded when analysing the Anaerobic Digestion Model No 1 (ADM1) for olive mill wastes (Fezzani & Cheikh, 2009). Polyphenol reductions occurred, however no percentages were stated, only effluent soluble phenol was reported. This study shows that pH values above 7.3 may well be effective at reducing polyphenol content .

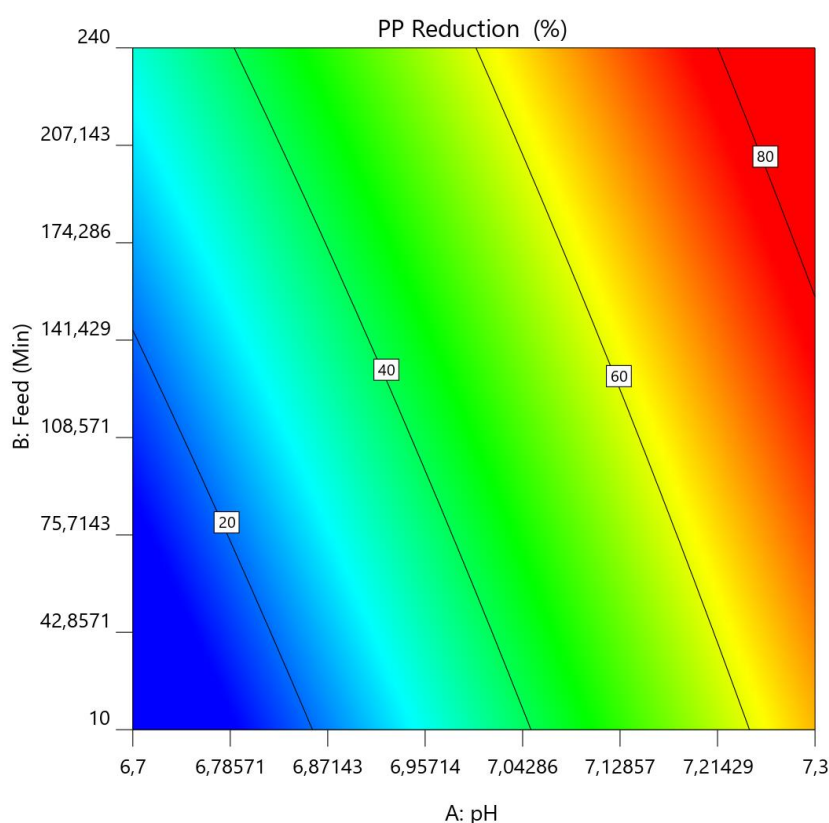


Figure 4. 17 Contour plot showing the optimal parameters of pH and feed time for the removal of polyphenol reduction percentage.

The contour plot showing the interaction for pH and mixing intervals indicates that polyphenol reduction is increased at high pH levels and infrequent mixing (Red area of contour plot)(**Figure 4.18**). This corroborates the observation from **Figure 4.17** that indicates that a pH value between 7.2 and 7.3 may be

optimal for the reduction of polyphenols in winery wastewater. As previously mentioned, anaerobic digestors perform optimally at pH values between 7.0 and 7.2 (Gerardi, 2003). Less frequent mixing is also associated with an increase in polyphenol removal. Very frequent mixing (every 22 minutes or less) is associated with poor removal of polyphenols as illustrated in the blue area of **Figure 4.18**. The reason for this may be granular disintegration, although when investigating TSS it was found that very little granular disintegration was evident in the effluent. It has been suggested that rapid mixing may disrupt the structure of flocks in reactors which could lead to the disturbance of the syntrophic relationships between organisms (Whitmore *et al.*, 1987; Dolfing, 1992).

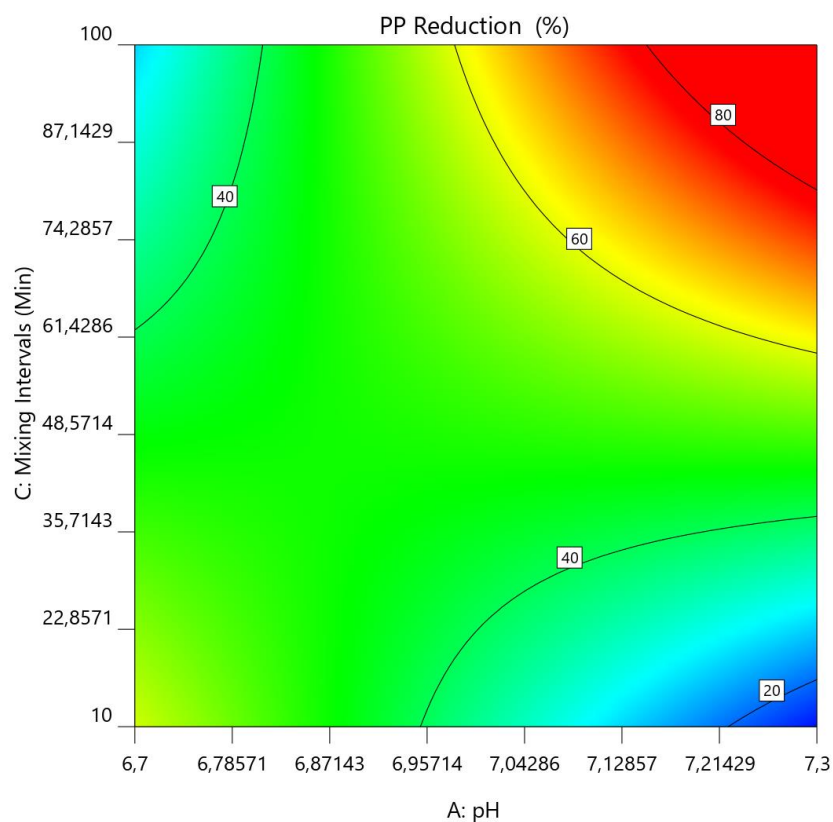


Figure 4. 18 Contour plot showing optimal conditions for pH and mixing interval for removal of polyphenols from winery wastewater.

The interaction between mixing interval and feed time is shown in **Figure 4.19**. More frequent mixing and long feeding times are associated with poor polyphenol removal efficiency (Blue zone **Figure 4.19**). More efficient removal percentages are obtained when feed time is between 174 and 240 minutes and mixing interval is between 90 and 100 minutes. As mentioned previously, longer feed times may ensure that the anaerobic organisms are not overloaded and less frequent mixing may preserve syntrophic relationships between microorganisms. Longer feeding times, less frequent mixing and higher pH values are associated with a higher removal rate of polyphenolic compounds in winery wastewater. The optimal conditions are summarised in **Table 4.7**.

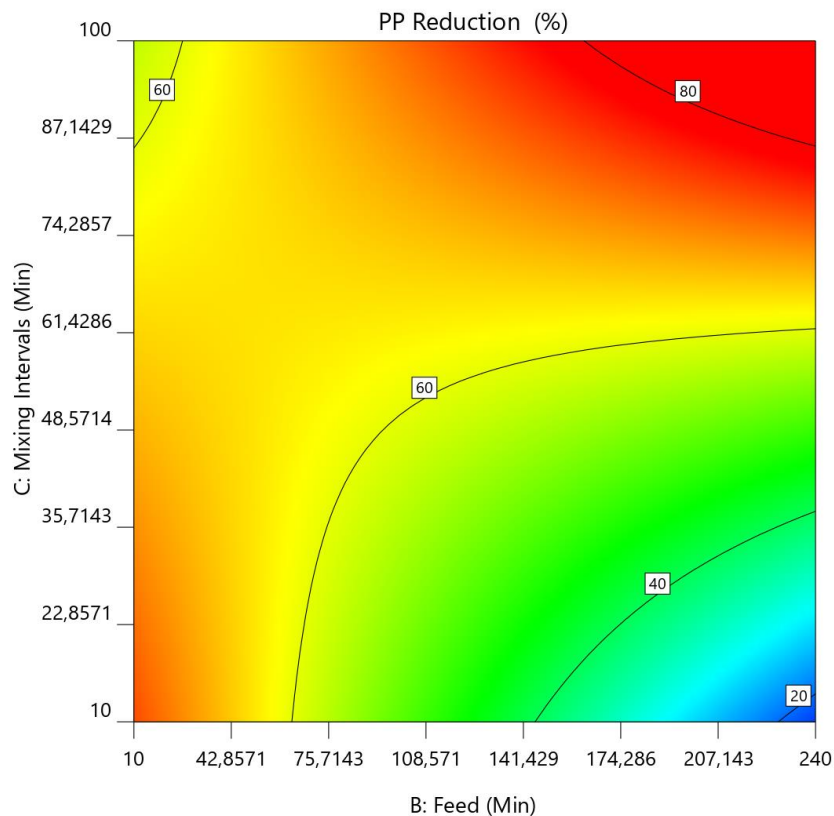


Figure 4. 19 Contour plot showing optimal conditions for feed time and mixing interval for the removal of polyphenols from winery wastewater.

Table 4.7 Optimal operating parameters with regards to polyphenol removal percentage.

| Parameter | Optimum values |
|------------------------|----------------|
| pH | 7.24 |
| Feed time (min) | 232.22 |
| Mixing intervals (min) | 88.71 |

Optimal operational parameters obtained in this study for the reduction in polyphenols is similar to the optimal parameters obtained by Laing (2016). The optimal parameters for experiment 1 in that study were pH of 7.34, feeding time of 240 minutes and a mixing interval of 110.5 minutes. Similarity of these results indicate that these may well be optimal parameters for the removal of polyphenols, even in the absence of significant statistical effects (**Figure 4.16**).

4.3.2.9 VFA: Alkalinity

Data from the CCD was used to fit the regression coefficients. None of the factors involved had a statistically significant effect on the VFA:Alkalinity ratio (**Figure 4.20**). The factor that had the largest influence was the mixing interval followed by the interaction between the feeding time and mixing interval. The effect of pH

on VFA:Alkalinity was small, mainly because pH was kept within standard operating ranges for anaerobic digestion.

The range of VFA:Alkalinity obtained was 0.0414 – 0.593 in this study. A mean ratio of 0.23 was obtained for the experimental runs indicating that the reactor was stable for the majority of the experiment. Four runs were identified when VFA:Alkalinity was greater than 0.3. These runs also coincided with the four worst COD reduction percentages, high ultimate COD values and below average methane percentage. For optimal reactor performance VFA:Alkalinity must be kept below 0.3 – 0.4 (Fannin, 1987; Brown & Li, 2013). This ratio is a common stress indicator in anaerobic digestion and can be used to monitor the stability of the reactor (Anderson & Yang, 1992).

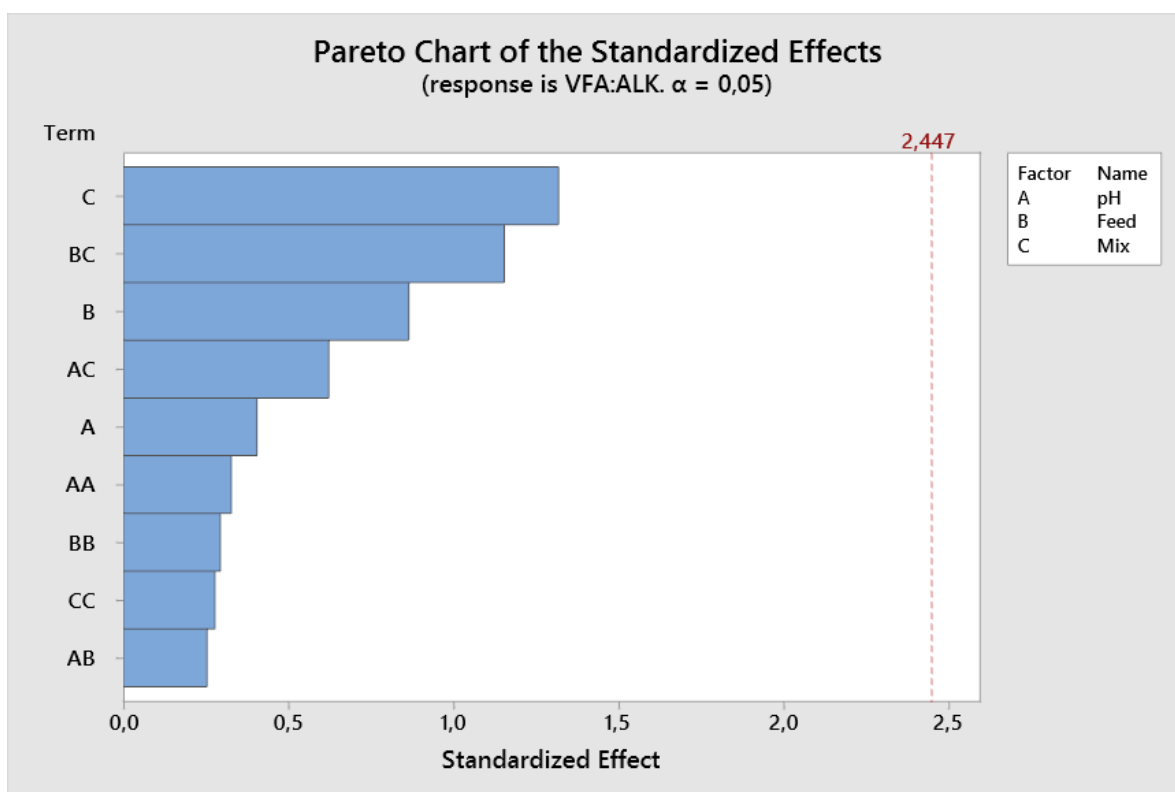


Figure 4.20 Pareto chart for the factors influencing VFA:Alkalinity.

From **Figure 4.21** it is clear that VFA:Alkalinity is low across almost the whole pH range and is more reliant upon the feed time than the pH of the reactor. For a short feeding time however, it is essential that the operating pH of the reactor is high at 7.2 – 7.3. Reactor failure along with a low methane yield can be caused by imbalances of hydrolytic, fermentative and acetogenic bacteria as well as methanogenic archaea (Brown & Li, 2013). These imbalances may be caused by an accumulation of VFA. A rapid feed may lead to an accumulation of VFA and a subsequent drop in pH, causing decreased performance or potentially even reactor failure (Brown & Li, 2013). Low pH accompanied by rapid feed can lead to a dangerously high VFA:Alkalinity. A feed time above 140 minutes leads to relatively stable VFA:Alkalinity as it decreases the chance of VFA accumulation in the reactor.

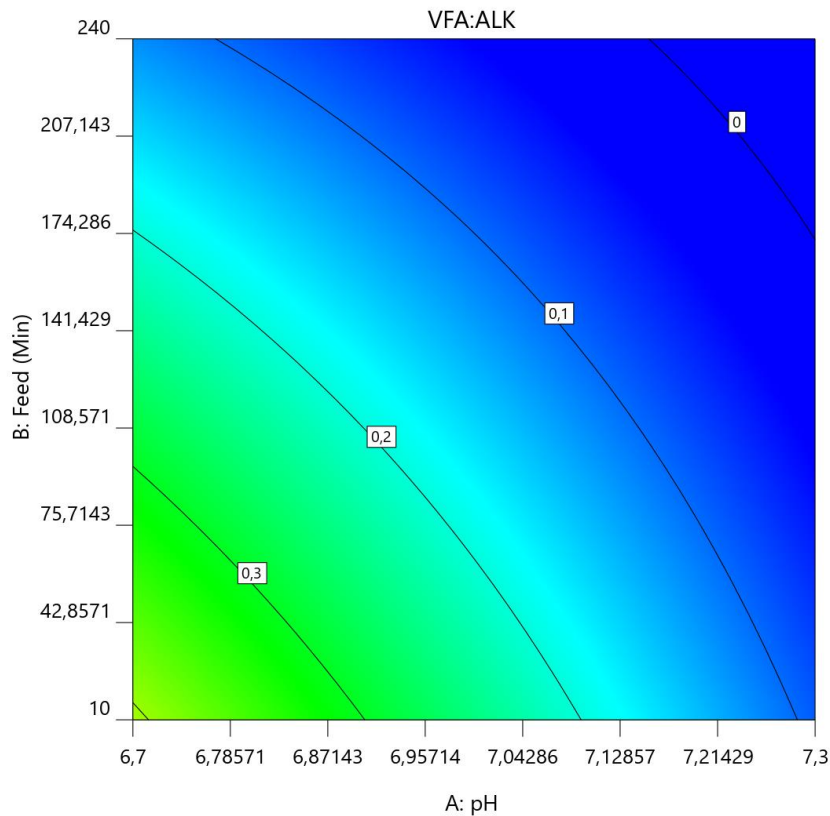


Figure 4.21 Contour plot showing optimal conditions for pH and feed time for VFA:Alkalinity.

Mixing intervals below 35 minutes are correlated with increased VFA:Alkalinity across the pH range for anaerobic digestion. In order to decrease the VFA:Alkalinity, mixing should take place less frequently (once every 74 minutes) in conjunction with an operating pH between 7.0 and 7.3 as indicated in the blue region of **Figure 4.22**. More frequent mixing may liberate more CO₂ from the microorganisms, which could lead to acidification of the water. The role of pH may not have been large because of the automatic dosing that occurred if the pH dropped below set point.

There is one large area that is associated with low VFA:Alkalinity in **Figure 4.23**. This is represented by the blue area of the contour plot. The combination of low feed time and frequent mixing as well as longer feeding times with less frequent mixing lead to lower VFA:Alkalinity.

With longer feeding times, more frequent mixing needs to be employed to ensure VFA:Alkalinity is maintained. Long feeding times with very frequent mixing is represented by the red region of **Figure 4.23**. In order to have a stable anaerobic process the range of parameters depicted in this area need to be avoided. It is unexpected that a rapid feed time did not lead to high VFA:Alkalinity. This may be in part due to the automatic 2M KOH dosing which could increase the pH in response to accumulation of VFA thereby stabilising the reactor. The optimal region would be the region in the top right represented by the dark blue shading. Longer feed times with less frequent mixing could result in the most stable conditions. The blue region in at the bottom left of **Figure 4.23** has very strict boundaries, and if these boundaries are exceeded VFA:Alkalinity increases rapidly.

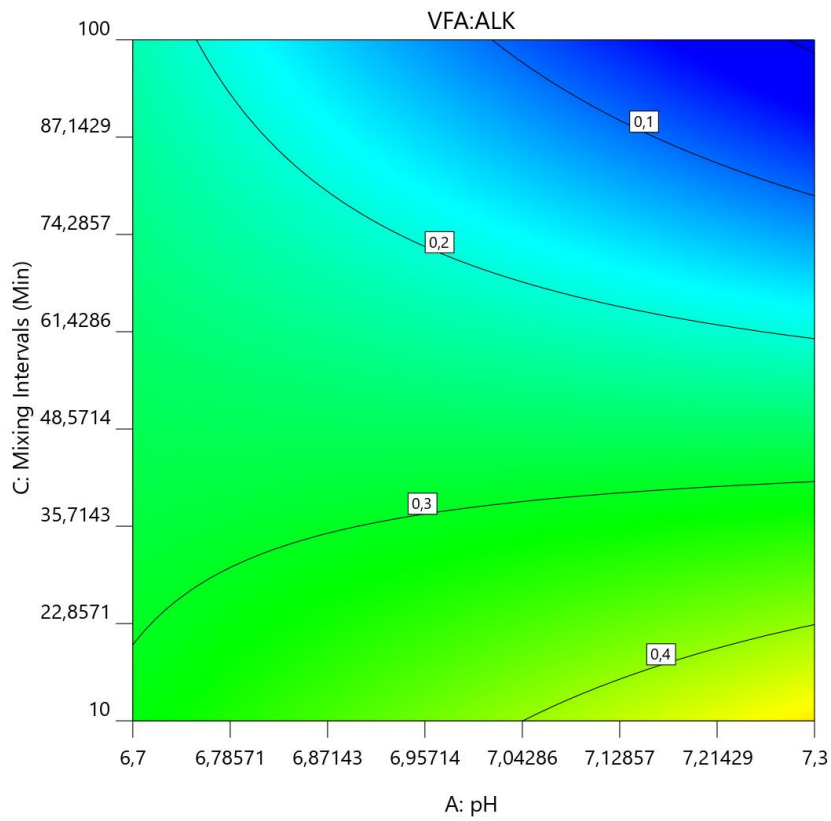


Figure 4. 22 Contour plot showing optimal conditions for pH and mixing interval for VFA:Alkalinity.

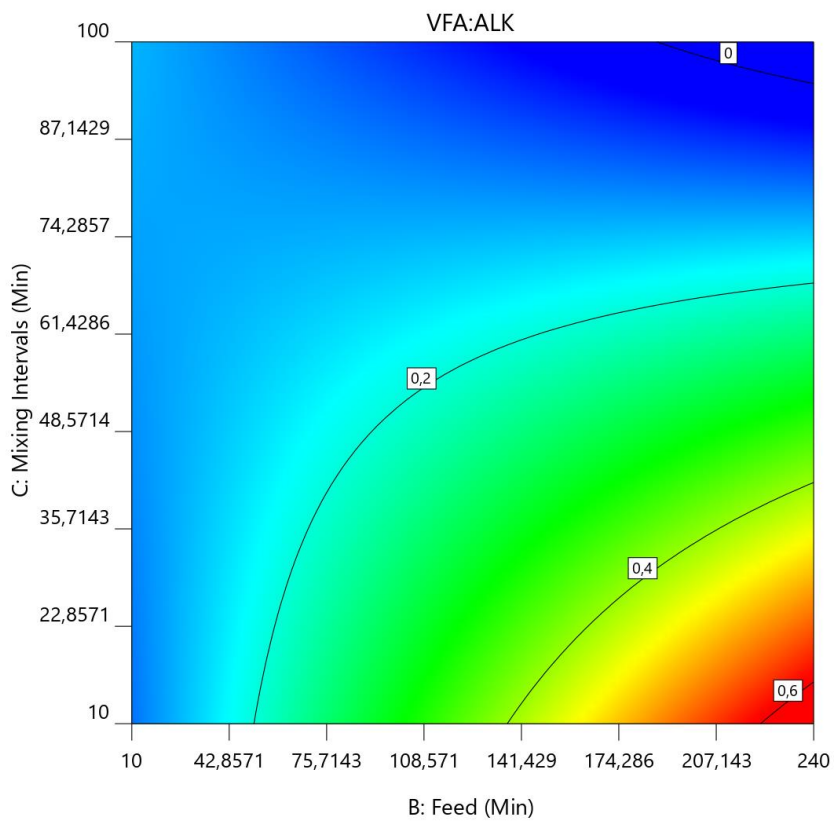


Figure 4. 23 Contour plot showing optimal conditions for feed time and mixing interval for VFA:Alkalinity..

Table 4.8 Optimal operating parameters with regards to VFA:Alkalinity.

| Parameter | Optimum values |
|------------------------|----------------|
| pH | 7.21 |
| Feed time (min) | 155.49 |
| Mixing intervals (min) | 96.49 |

Using the desirability of the solutions the optimal parameters were found to be a higher pH, intermediate feed time and longer mixing intervals (**Table 4.8**). These parameters are very similar to those observed by Laing (2016). The optimal parameters obtained in that study were;

- pH : 7.34
- Feed time : 123 minutes
- Mixing intervals : 100.40 minutes

4.3.2.10 Methane percentage

Data from the CCD was used to fit the regression coefficients. The pH had a significant statistical effect on the methane percentage achieved during the experiment (**Figure 4.24**). The quadratic effect for mixing and feed had the next largest effects, indicating that the optimal values may not lie at the extremes of the ranges, although these effects were not statistically significant (**Figure 4.24**).

Methane has the potential to be used as a clean renewable source of energy producing few atmospheric pollutants and the gas can be used at different levels of purity (Chynoweth *et al.*, 2001). During anaerobic digestion 60-70 % of the gas produced is methane and 30-40 % is carbon dioxide (Chynoweth *et al.*, 2001; Li *et al.*, 2011). Methanogens convert acetate, carbon dioxide and hydrogen to methane (Li *et al.*, 2011). Methane-forming archaea are sensitive to changes in the environment and function optimally at a pH range of 6.8-7.2 (Gerardi, 2003; Rajagopal *et al.*, 2013). The range of the methane percentage in this study was 54.89 – 72.18 %. The mean methane percentage achieved was 61.81 %. This value is slightly lower than the optimal methane percentage in biogas, but still falls within the acceptable range for methane percentage.

The pH had a significant effect on the methane percentage achieved. A high methane percentage represented by red and orange in **Figure 4.25** indicates that methane percentage is increased when pH ranges between 7.16 and 7.3. The increase in methane percentage is affected very little by feed time as pH is the significant factor for determining methane percentage of the biogas. At pH values closer to 7.2 there is however an increase in methane percentage when the feed time increases beyond 140 minutes. A slower feeding time may result in a more stable reactor, with less accumulation of VFA and therefore an increased ability to maintain the pH above 7.2. According to the Pareto chart (**Figure 4.24**) feed time is a more important factor than mixing frequency, although it is not statistically significant. Methanogens are susceptible to changes in the environment (Amani *et al.*, 2010). The ideal pH range in which anaerobic

digestion operates is 6.8-7.2, if the pH drops below 6.6 the growth rate of the methanogens is severely impacted (Mosey & Fernandes, 1988; Ward *et al.*, 2008). This could explain why the methane percentage obtained was a direct function of pH.

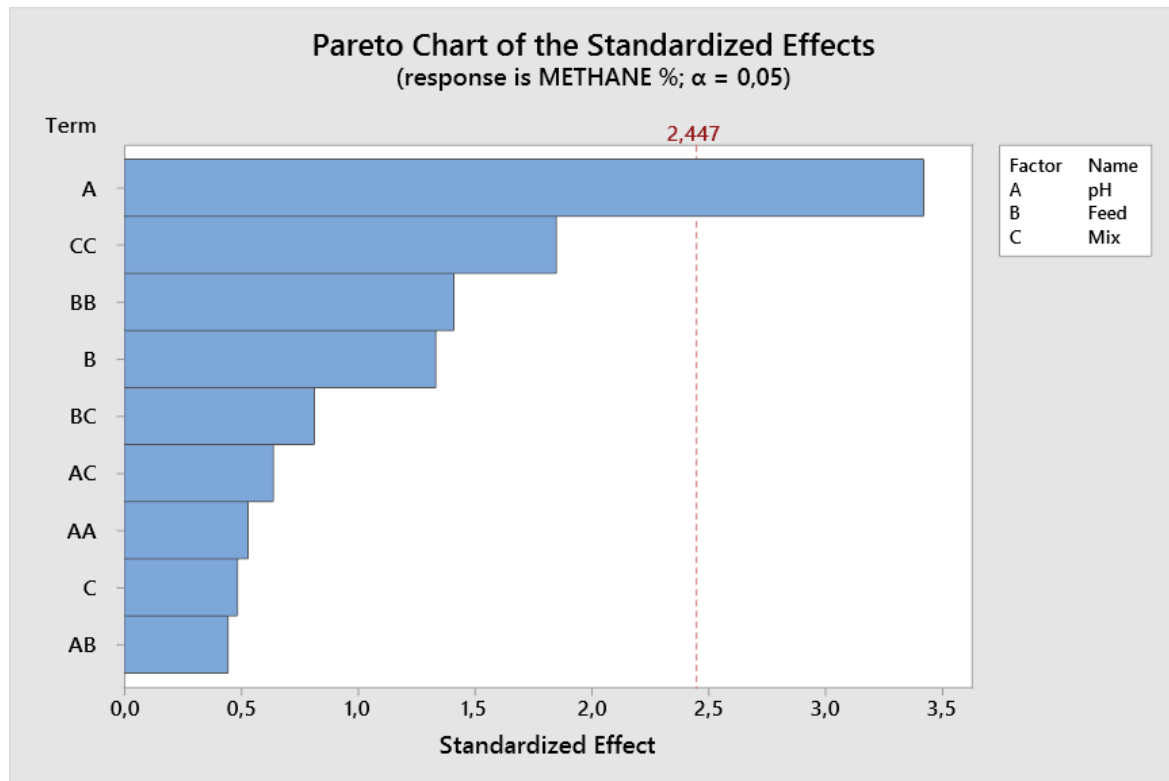


Figure 4. 24 Pareto chart for the factors influencing methane percentage.

There is a clear optimal region for methane production on the right of **Figure 4.26** indicated by the red region. Methane percentage is not affected by mixing interval at all. pH is the only factor responsible for ideal methane content of the biogas. Mixing may not have a big effect as it was established previously that there was limited granule disintegration. There are also contrasting reports in literature with regards to the ideal mixing frequency. At pH values between 7.0 and 7.2 the anaerobic digester works optimally and may favour the growth of methanogens (Gerardi, 2003). The temperature maintained in the reactor was 35°C which is the preferred temperature for the mesophilic methanogens (Gerardi, 2003). Frequent mixing may have facilitated even and constant heat distribution as the water was only heated by a geyser element from the base of the reactor. The stainless steel frame of the reactor, combined with the reactor being placed in a shipping container may have helped to avoid temperature fluctuations.

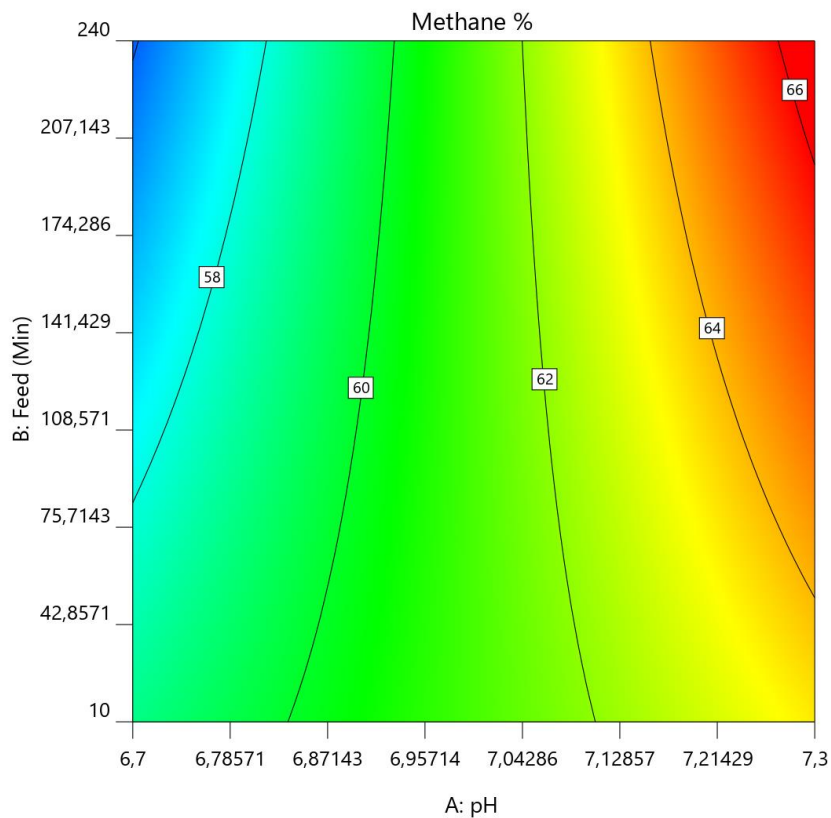


Figure 4. 25 Contour plot showing optimal conditions for pH and feed time for methane percentage.

The interaction between feeding time and mixing interval is shown in **Figure 4.27**. This is not a significant interaction but it does illustrate that longer feeding times at any mixing intervals can achieve methane percentages of 65 %. It is possible to achieve higher percentages of methane using shorter feeding time and more frequent mixing, however the goal of this optimisation was to achieve as close to 65 % as possible, as this is what is commonly reported in literature. Longer feeding times would be expected to yield better methane percentages as less substrate is introduced into the reactor at the start of the cycle. Less frequent mixing is generally preferred, as in the long run there may be significant disintegration of anaerobic granules which could result in decreased performance.

The optimal values to achieve a methane percentage of 65 % were selected based on the desirability score and the values are shown in **Table 4.9**. To achieve a methane yield of 65 % a higher pH is favoured along with long feeding time and infrequent mixing.

These results compare favourably with previous work performed at the Department of Food Science in Stellenbosch (Laing, 2016). The optimal conditions reported in that study were as follows;

- pH: 7.30
- Feed time: 240 minutes
- Mixing interval: 110 minutes

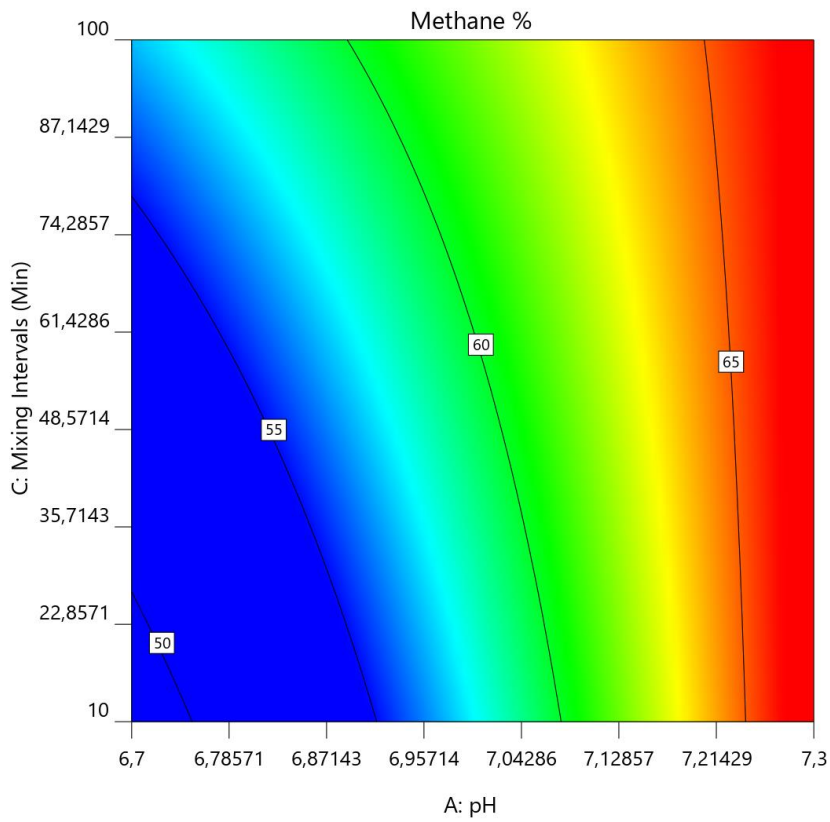


Figure 4. 26 Contour plot showing optimal conditions for pH and mixing interval for methane percentage.

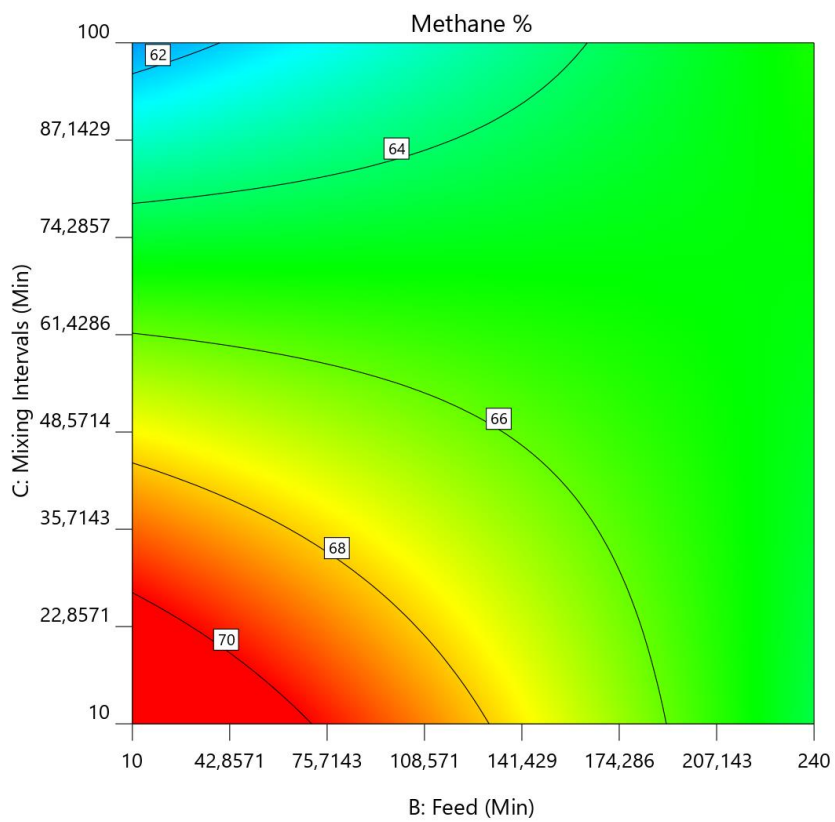


Figure 4. 27 Contour plot showing optimal conditions for feed time and mixing interval for methane percentage

Table 4.9 Optimal operating parameters with regards to methane percentage.

| Parameter | Optimum values |
|------------------------|----------------|
| pH | 7.22 |
| Feed time (min) | 240.00 |
| Mixing intervals (min) | 88.86 |

4.3.2.10 Overall optimal conditions

The optimal operating conditions achieved during the experiment is summarised for all the performance parameters in **Table 4.10**. The optimal values that need to be used to optimise all the performance parameters were calculated using overall desirability of all the parameters and is shown in **Table 4.11**. The optimum value for pH was found to 7.30 and this can be confirmed by investigating the individual optimal parameters. Optimal values for pH were consistently above 7.20 except for TSS with an optimal pH of 7.19. The feed time of 180.91 minutes obtained from **Table 11** is just below the mean feed time of 194 minutes obtained for the individual optimal values. The mixing interval was found to be slightly lower than what was achieved for the performance measures individually, however it is still an infrequent mixing regime that favours all of the performance measures. Therefore for the treatment of winery wastewater with varying degrees of strength the optimal conditions are a pH of 7.30, a feed time of 180.91 minutes and a mixing interval of 84.17 minutes.

Table 4. 10 Overall optimal values achieved for all the performance parameters evaluated during the experiment.

| | pH | Feed Time (Min) | Mixing Interval (Min) |
|---|------|-----------------|-----------------------|
| COD Reduction (%) | 7.29 | 189.68 | 88.84 |
| COD Ultimate (mg.L⁻¹) | 7.30 | 197.81 | 79.98 |
| TSS (mg.L⁻¹) | 7.19 | 147.50 | 99.76 |
| Polyphenol reduction (%) | 7.24 | 232.22 | 88.71 |
| VFA:Alkalinity | 7.21 | 155.49 | 96.49 |
| Methane (%) | 7.22 | 240.00 | 88.86 |

Table 4. 11 Optimal values achieved for the three parameters to yield the best results for all performance measure.

| Parameter | Optimum values |
|------------------------|----------------|
| pH | 7.30 |
| Feed time (min) | 180.91 |
| Mixing intervals (min) | 84.17 |

4.4 Conclusion

Winery wastewater is a high strength product that often requires treatment before the water can be reused for irrigation, or discharged into the water supply. One potential avenue is to use anaerobic digestion as a treatment option, either as the only treatment option, or for use after a primary treatment such as screening and settling to further reduce COD. An anaerobic sequencing batch reactor may fulfill the requirements for treatment of high strength wastewater as one of the byproducts is methane generation which could be reused for clean energy. Other advantages include low operational costs and very little sludge production.

This study proved that the use of a novel AnSBR to treat winery wastewater of varying strength and composition is feasible for the COD range of 3 200 – 9 700 mg.L⁻¹. A mean COD reduction percentage of 68.32 % was achieved in this study with a maximum COD reduction percentage of 85.4 %. The pH could be effectively controlled within the range of 6.7 – 7.3 and alkalinity was maintained in the system above 1 600 mgCaCO₃.L⁻¹. Reactor stability was maintained except for the last two runs with VFA:Alkalinity ratio during those two runs being 0.39 and 0.59. A VFA:Alkalinity of 0.3 and above is associated with an unstable reactor, possibly due to a high organic load and a subsequent accumulation of VFA in the reactor. It is possible that the HRT was not long enough to facilitate the complete degradation of the substrate. The occasional instability of the reactor does highlight potential problems with this technology. The design of the reactor must be very particular and the operator needs to be well trained with regards to potential problems and the cause thereof. Much of the instability could potentially be solved by upscaling the reactor to handle bigger volumes as it would potentially have better buffering capability.

Operational parameters for the AnSBR were optimised by performing a CCD experiment and generating RSM contour plots. Three operational parameters (pH, feed time and mixing intervals) were optimised for six different responses (COD reduction (%), COD ultimate reduction, TSS, VFA:Alkalinity, Polyphenol reduction (%) and methane (%)). The optimal pH obtained, by choosing the solution with the overall highest desirability, was 7.30. An optimal feed time of 180.91 minutes was obtained and the optimal mixing interval was determined to be 84.17 minutes. These values were comparable to a previous study performed on a lab-scale 14.7 L AnSBR. Those overall parameters were a pH of 7.3, feed time of 240 minutes and mixing intervals of 110 minutes.

This study corroborated the findings of the previous study and showed that the optimal parameters remain comparable in spite of varying strength of the substrate and the increase in size of the reactor. The AnSBR technology can potentially be used in the South African wine industry to treat winery wastewater of varying strengths up to a COD concentration of 9 700 mg.L⁻¹. Two independent studies have now confirmed the range of the optimal operational parameters at laboratory- and pilot-scale. The biggest hindrance for implementation at the moment is the design of the reactor. An optimal design is yet to have been achieved, with both reactors having design flaws that would decrease the performance significantly at a larger scale. It is therefore important that future studies focus more on the design and commissioning of the reactor to allow it to make use of the specific optimal operational parameters achieved in the two studies.

4.5 References

- Akram, A. & Stuckey, D. (2008). Biomass acclimatisation and adaptation during start-up of a submerged anaerobic membrane bioreactor (SAMBR). *Environmental technology*, **29**, 1053-1065.
- Amani, T., Nosrati, M. & Sreekrishnan, T. (2010). Anaerobic digestion from the viewpoint of microbiological, chemical, and operational aspects—a review. *Environmental Reviews*, **18**, 255-278.
- Anderson, G. & Yang, G. (1992). Determination of bicarbonate and total volatile acid concentration in anaerobic digesters using a simple titration. *Water Environment Research*, **64**, 53-59.
- APHA (2005). Standard methods for the examination of water and wastewater. *American Public Health Association (APHA): Washington, DC, USA*.
- Asadollahzadeh, M., Tavakoli, H., Torab-Mostaedi, M., Hosseini, G. & Hemmati, A. (2014). Response surface methodology based on central composite design as a chemometric tool for optimization of dispersive-solidification liquid–liquid microextraction for speciation of inorganic arsenic in environmental water samples. *Talanta*, **123**, 25-31.
- Barbera, M. & Gurnari, G. (2018). Water Reuse in the Food Industry: Quality of Original Wastewater Before Treatments. In: *Wastewater Treatment and Reuse in the Food Industry*. Pp. 1-16. Springer.
- Bodík, I., Herdová, B. & Drtil, M. (2002). The use of upflow anaerobic filter and AnSBR for wastewater treatment at ambient temperature. *Water Research*, **36**, 1084-1088.
- Box, G.E. & Wilson, K.B. (1951). On the experimental attainment of optimum conditions. *Journal of the Royal Statistical Society: Series B (Methodological)*, **13**, 1-38.
- Brown, D. & Li, Y. (2013). Solid state anaerobic co-digestion of yard waste and food waste for biogas production. *Bioresource technology*, **127**, 275-280.
- Chynoweth, D.P., Owens, J.M. & Legrand, R. (2001). Renewable methane from anaerobic digestion of biomass. *Renewable energy*, **22**, 1-8.
- Dolfing, J. (1992). The energetic consequences of hydrogen gradients in methanogenic ecosystems. *FEMS Microbiology Letters*, **101**, 183-187.
- Donoso-Bravo, A., Rosenkranz, F., Valdivia, V., Torrijos, M., Ruiz-Filippi, G. & Chamy, R. (2009). Anaerobic sequencing batch reactor as an alternative for the biological treatment of wine distillery effluents. *Water Science and Technology*, **60**, 1155-1160.
- Fannin, K. (1987). Start-up, operation, stability, and control. *Start-up, operation, stability, and control.*, 171-196.
- Fezzani, B. & Cheikh, R.B. (2009). Extension of the anaerobic digestion model No. 1 (ADM1) to include phenolic compounds biodegradation processes for the simulation of anaerobic co-digestion of olive mill wastes at thermophilic temperature. *Journal of hazardous materials*, **162**, 1563-1570.
- Gerardi, M.H. (2003). The microbiology of anaerobic digesters. Pp. 99-103 New Jersey: John Wiley & Sons.
- Ghanimeh, S., El Fadel, M. & Saikaly, P. (2012). Mixing effect on thermophilic anaerobic digestion of source-sorted organic fraction of municipal solid waste. *Bioresource technology*, **117**, 63-71.

- Gomez, X., Cuetos, M., Cara, J., Moran, A. & Garcia, A. (2006). Anaerobic co-digestion of primary sludge and the fruit and vegetable fraction of the municipal solid wastes: conditions for mixing and evaluation of the organic loading rate. *Renewable energy*, **31**, 2017-2024.
- Goodwin, J., Finlayson, J. & Low, E. (2001). A further study of the anaerobic biotreatment of malt whisky distillery pot ale using an UASB system. *Bioresource technology*, **78**, 155-160.
- Howell, C. & Myburgh, P. (2018). Management of winery wastewater by re-using it for crop irrigation-A review. *South African Journal of Enology and Viticulture*, **39**, 116-131.
- Huang, Y., Dehkordy, F.M., Li, Y., Emadi, S., Bagtzoglou, A. & Li, B. (2018). Enhancing anaerobic fermentation performance through eccentrically stirred mixing: Experimental and modeling methodology. *Chemical Engineering Journal*, **334**, 1383-1391.
- Kennedy, K., Sanchez, W., Hamoda, M. & Droste, R. (1991). Performance of anaerobic sludge blanket sequencing batch reactors. *Research Journal of the Water Pollution Control Federation*, 75-83.
- Keyser, M., Witthuhn, R., Ronquest, L.-C. & Britz, T. (2003). Treatment of winery effluent with upflow anaerobic sludge blanket (UASB)–granular sludges enriched with *Enterobacter sakazakii*. *Biotechnology letters*, **25**, 1893-1898.
- Laing, M. (2016). Investigating the performance of a novel Anaerobic Sequencing Batch Reactor (AnSBR) and optimisation of operational parameters to treat synthetic winery wastewater. Stellenbosch: Stellenbosch University.
- Li, Y., Park, S.Y. & Zhu, J. (2011). Solid-state anaerobic digestion for methane production from organic waste. *Renewable and Sustainable Energy Reviews*, **15**, 821-826.
- Liu, Y., Xu, H.-L., Show, K.-Y. & Tay, J.-H. (2002). Anaerobic granulation technology for wastewater treatment. *World Journal of Microbiology and Biotechnology*, **18**, 99-113.
- Masse, O. & Masse, L. (2000). Treatment of slaughterhouse wastewaters in anaerobic sequencing batch reactors. *Canadian Agricultural Engineering*, **42**, 131.
- McHugh, S., O'reilly, C., Mahony, T., Colleran, E. & O'flaherty, V. (2003). Anaerobic granular sludge bioreactor technology. *Reviews in Environmental Science and Biotechnology*, **2**, 225-245.
- McMahon, K.D., Stroot, P.G., Mackie, R.I. & Raskin, L. (2001). Anaerobic codigestion of municipal solid waste and biosolids under various mixing conditions—II: microbial population dynamics. *Water Research*, **35**, 1817-1827.
- Melamane, X., Tandlich, R. & Burgess, J. (2007). Treatment of wine distillery wastewater by high rate anaerobic digestion. *Water Science and Technology*, **56**, 9-16.
- Moletta, R. (2005). Winery and distillery wastewater treatment by anaerobic digestion. *Water Science and Technology*, **51**, 137-144.
- Mosey, F. & Fernandes, X. (1988). Patterns of hydrogen in biogas from the anaerobic digestion of milk-sugars. In: *Water Pollution Research and Control Brighton*. Pp. 187-196. Elsevier.

- Mosse, K., Patti, A., Christen, E. & Cavagnaro, T. (2011). Winery wastewater quality and treatment options in Australia. *Australian Journal of Grape and Wine Research*, **17**, 111-122.
- OIV (2019). 2019 Statistical report on world vitiviniculture. [WWW document]. <http://www.oiv.int/public/medias/6782/oiv-2019-statistical-report-on-world-vitiviniculture.pdf>.
- Oliveira, M., Queda, C. & Duarte, E. (2009). Aerobic treatment of winery wastewater with the aim of water reuse. *Water Science and Technology*, **60**, 1217-1223.
- Ortiz-Cabrera, M.A., Nayak, A. & Flotats Ripoll, X. (Year). Polyphenols removal in winery wastewater using an AnSBR. In: *Book of abstracts of the XIII Latin American Workshop and Symposium on Anaerobic Digestion*. Pp. 543-545. Month and 2018
- Parawira, W., Kudita, I., Nyandoroh, M. & Zvauya, R. (2005). A study of industrial anaerobic treatment of opaque beer brewery wastewater in a tropical climate using a full-scale UASB reactor seeded with activated sludge. *Process Biochemistry*, **40**, 593-599.
- Rajagopal, R., Massé, D.I. & Singh, G. (2013). A critical review on inhibition of anaerobic digestion process by excess ammonia. *Bioresource technology*, **143**, 632-641.
- Ruiz, C., Torrijos, M., Sousbie, P., Martinez, J.L., Moletta, R. & Delgenes, J. (2002). Treatment of winery wastewater by an anaerobic sequencing batch reactor. *Water Science and Technology*, **45**, 219-224.
- Sandberg, M. & Ahring, B. (1992). Anaerobic treatment of fish meal process waste-water in a UASB reactor at high pH. *Applied Microbiology and Biotechnology*, **36**, 800-804.
- SAWIS (2018). SA wine industry 2018 statistics NR 43. [WWW document]. http://www.sawis.co.za/info/download/Book_2018_statistics_year_english_final.pdf.
- Shao, X., Peng, D., Teng, Z. & Ju, X. (2008). Treatment of brewery wastewater using anaerobic sequencing batch reactor (ASBR). *Bioresource technology*, **99**, 3182-3186.
- Shizas, I. & Bagley, D.M. (2002). Improving anaerobic sequencing batch reactor performance by modifying operational parameters. *Water Research*, **36**, 363-367.
- Singleton, V.L. & Rossi, J.A. (1965). Colorimetry of total phenolics with phosphomolybdic-phosphotungstic acid reagents. *American Journal of Enology and Viticulture*, **16**, 144-158.
- Stroot, P.G., McMahon, K.D., Mackie, R.I. & Raskin, L. (2001). Anaerobic codigestion of municipal solid waste and biosolids under various mixing conditions—I. Digester performance. *Water Research*, **35**, 1804-1816.
- Sung, S. & Dague, R.R. (1995). Laboratory studies on the anaerobic sequencing batch reactor. *Water Environment Research*, **67**, 294-301.
- Suthaker, S., Polprasert, C. & Droste, R. (1991). Sequencing batch anaerobic reactors for treatment of a high-strength organic wastewater. *Water Science and Technology*, **23**, 1249-1257.
- Timur, H. & Öztürk, I. (1999). Anaerobic sequencing batch reactor treatment of landfill leachate. *Water Research*, **33**, 3225-3230.

- Ward, A.J., Hobbs, P.J., Holliman, P.J. & Jones, D.L. (2008). Optimisation of the anaerobic digestion of agricultural resources. *Bioresource technology*, **99**, 7928-7940.
- Whitmore, T., Lloyd, D., Jones, G. & Williams, T. (1987). Hydrogen-dependent control of the continuous anaerobic digestion process. *Applied Microbiology and Biotechnology*, **26**, 383-388.

Chapter 5

General Discussion and Conclusion

Water is one of the most important natural resources on Earth and needs to be carefully managed to meet the demand in the future, as human population is growing rapidly (Sivakumar, 2011; Cooley *et al.*, 2014; McNabb, 2019). Currently, agriculture and industry is responsible for roughly 73 % of the abstracted freshwater in South Africa (FAO, 2016). Wastewater generated by industry is high strength and has the potential to pollute large volumes of freshwater (Moharikar *et al.*, 2005). It is therefore imperative that industries treat the generated wastewater and re-use the treated wastewater to limit the volumes of freshwater needed for their production processes (Moharikar *et al.*, 2005; Pedrero *et al.*, 2010). The wine industry in South Africa generates approximately 1.24 billion litres of high strength wastewater every harvest season (Howell & Myburgh, 2018).

Anaerobic treatment processes have been widely-used in the past to treat wastewater from varying sources, however very little research has been conducted on a specific anaerobic digestion technique to treat winery wastewater, namely the anaerobic sequencing batch reactor (AnSBR) (Ruiz *et al.*, 2002; Mosse *et al.*, 2011). There are numerous advantages of the AnSBR technology namely; flexibility with regards to control of the process; alternating food:microorganisms (F:M) ratio (High at the beginning of cycle and lower towards end of cycle); low sludge production and generation of methane containing biogas which could be re-used (Andreottola *et al.*, 2009; Eleutheria *et al.*, 2016; Show & Lee, 2016). Limited research is available for the use of AnSBR to treat winery wastewater. Current studies have identified three important operational parameters that need to be optimised. The feeding strategy, mixing interval and operational pH need to be investigated to for the optimisation of the AnSBR technology (Laing, 2016).

Chemical oxygen demand (COD) and total suspended solids (TSS) are important parameters to monitor reactor stability and performance. The determination of these parameters are time-consuming and laborious (APHA, 2005). It is important to develop a screening method that has the capability of quantifying and classifying COD and TSS based on the concentration of the respective parameters.

Near-infrared spectroscopy is a rapid and non-destructive technique which has been used to quantify COD and TSS in wastewater of various origins (Rieger *et al.*, 2006; Innocent *et al.*, 2007; Sarraguça *et al.*, 2009; Pan *et al.*, 2012a). Winery wastewater has never been quantified or classified based on COD and TSS concentrations.

The first aim of this study was to develop calibration models for the classification and quantification of winery wastewater in terms of COD and TSS concentrations using a benchtop FT-NIR and a portable handheld NIR spectrophotometer. The second aim of this study was to investigate the efficacy of the AnSBR technology to treat winery wastewater of variable strength and to optimise the operational parameters.

Near-infrared spectroscopy in combination with multivariate data analysis techniques was used to quantify and classify winery wastewater in terms of COD concentration, irrespective of the farm of origin of the wastewater. Wastewater was collected from four farms in the Stellenbosch wine region from different locations on each farm. The samples were scanned using a benchtop FT-NIR and a handheld NIR spectrophotometer.

The benchtop FT-NIR spectrophotometer was able to predict COD concentration with a root mean square error of prediction (RMSEP) of 1 006.13 mg.L⁻¹ using orthogonal signal correction (OSC) as pre-processing and principal component regression (PCR). This means that the prediction of COD has a confidence of $\pm 1\ 006.13$ mg.L⁻¹. Orthogonal signal correction outperformed the other pre-processing techniques for which the most likely explanation is that OSC removes spectral data that is not related to the Y-response (COD concentration) (Wold *et al.*, 1998). Partial least squares regression (PLS-R) outperformed PCR for the prediction of COD concentration. The obtained RMSEP was 937.93 mg.L⁻¹ for the same reference range of COD of 102.5 – 10 570 mg.L⁻¹. This translates to an error to the range of 10.38 %. The performance of PLS-R and OSC compares favourably with previous studies which had error rates between 6 and 12 % (Innocent *et al.*, 2007; Yang *et al.*, 2009). It is possible that PLS-R outperformed PCR due to the fact that PLS-R includes the Y-response in the calculation, with OSC only using the X-variables (wavelengths) (Hemmateenejad *et al.*, 2007). Wavelength selection was manually performed using the benchtop FT-NIR. The wavelength range of 2 060 – 2 340 nm was identified as a possible region where COD could be represented due to the absorption of glucose, fructose, ethanol and tannins within that spectral range (Soukupova *et al.*, 2002; Cozzolino *et al.*, 2007). When reduced wavelengths were used, RMSEP for both PCR and PLS-R was below 900 mg.L⁻¹. Another important performance parameter to consider is standard error of prediction (SEP) / standard error of the laboratory (SEL). The SEL is the average error of the laboratory and was calculated to be 453 mg.L⁻¹. When the SEP/SEL is between 1.5 and 2.0 it can be concluded that the technique may be useful for screening purposes (Corredor *et al.*, 2015). The SEP/SEL ratio for PLS-R with OSC as pre-processing using reduced wavelengths was 1.93 which means that this model may be useful for the determination of COD of winery wastewater for screening purposes.

Discriminant analysis (DA) could accurately classify COD of winery wastewater into three different classes, namely; in (0 – 4 999 mg.L⁻¹ COD); Warning (5 000 – 6 999 mg.L⁻¹ COD) and out (above 7 000 mg.L⁻¹ COD). The linear discriminant analysis (LDA) model with OSC as pre-processing was deemed successful as the classification accuracy achieved was 90.40 % for classification into the three classes. The successful classification may be attributed to OSC being able to eliminate X-variables that are not related to the Y-response. This model does however struggle to differentiate between the warning and out classes. This may be because the classes are separated on a sliding scale of increasing strength and the classes do not have hard boundaries. Prediction of the “in” class for this model was very accurate and predict the in class with 100 % accuracy. It can be concluded that NIR may be useful in the classification of winery wastewater in terms of COD.

Quantification of COD using a portable spectrophotometer with a wavelength range of 908 – 1 651 nm was showed potential for the prediction of COD in winery wastewater. Principal component regression in combination with OSC could not predict COD to a reasonable accuracy and had a SEP/SEL of 3.40 which is unacceptable for screening. Partial least squares regression in combination with OSC had a RMSEP of 1 047.97 mg.L⁻¹, which translates to an error of ± 11.60 %. This compares favourably with previous studies that had root mean square error of cross validation (RMSECV) of 7.79 – 11.60 %. The SEP/SEL was however calculated to be 2.36 which indicates that the portable spectrophotometer shows potential for the prediction of COD in winery wastewater, but it is not sufficient at this stage to be used for screening purposes.

Linear discriminant analysis in combination with OSC could classify COD into the three classes with an 81 % overall accuracy. Quadratic discriminant analysis (QDA) showed the same overall accuracy of 81 %. The LDA model was superior due to increased precision and increased sensitivity for the “in” class. The performance of the portable spectrophotometer was inferior to the benchtop FT-NIR, likely due to reduced wavelength range of the instrument.

Total soluble solids was predicted with an RMSEP of 124.84 mg.L⁻¹ when using the benchtop FT-NIR, PCR and OSC as pre-processing. This equates to an error of 5.22 % compared to the range of reference values of 33 – 2 425 mg.L⁻¹. The SEL of the reference value was 112 mg.L⁻¹ which means that if the reference method is determined to be 1 000 mg.L⁻¹, then it can be expected that it is ± 112 mg.L⁻¹ off in both the positive and negative direction (888 – 1112 mg.L⁻¹). The SEP/SEL was 1.04 which indicates that this model predicted TSS to almost the same accuracy of the reference method. This model outperformed previous studies with errors in other studies varying between 10.0 and 21.6 % (Jeong *et al.*, 2007; Páscoa *et al.*, 2008; Melendez-Pastor *et al.*, 2013). The prediction model using PLS-R and OSC performed slightly worse than the PCR model with an RMSEP of 144.16 mg.L⁻¹ and a SEP/SEL of 1.17. While this model performs worse, it still only has an error of 6.03 %. This model outperforms previous work conducted on NIR to predict TSS and is a viable option for the prediction of TSS in winery wastewater. Wavelength selection improved the PLS-R model and slightly reduced the effectiveness of PCR. Both techniques with OSC and reduced wavelengths (1 900 – 2 500 nm) performed identically with an RMSEP of 136.94 mg.L⁻¹ and SEP/SEL of 1.07. The error of prediction for these models was 5.72 % which once again outperformed previous work performed on TSS quantification for various wastewaters. The increased performance of TSS compared to COD indicates that TSS may correlate better than COD at these wavelengths.

Classification of TSS using a benchtop FT-NIR spectrophotometer could classify TSS into two classes; high and low, with 100 % accuracy. The prediction accuracy is improved compared to COD because of a reduction in the number of classes which simplifies the prediction. Added to that is the fact that quantification of TSS was superior to that of COD and NIR may be more useful for the prediction of TSS and hence a more powerful classifier for TSS compared to COD.

Both PCR and PLS-R had exactly the same RMSEP of 311.49 mg.L⁻¹ for the prediction of TSS in winery wastewater using the handheld spectrophotometer and OSC as pre-processing. The error of prediction was

13.02 % compared to the range of the reference values. These models have a SEP/SEL of 2.85 which is above the threshold of 2.0 for an effective screening method. The reduced wavelength of 908 – 1 651 nm is the main reason for the decreased performance as wavelengths above 1 900 nm seem to be responsible for the accurate prediction of TSS in winery wastewater.

Linear discriminant analysis in combination with OSC was the optimal model for classification of TSS into the two classes with an overall accuracy of 95.00 %. Multiplicative scatter correction (MSC) in combination with Savitzky-Golay 2nd derivative as pre-processing had the same classification accuracy, however LDA and OSC had a higher overall specificity and sensitivity. Added to this is that for every other model OSC was the optimal pre-processing, so for ease of use for the operator it would be advised to use OSC as pre-processing for this model. In future NIR spectroscopy could be implemented in an AnSBR to monitor process efficiency and performance measures.

The aim of the 2nd part of the study was to investigate the performance of the AnSBR and determine the optimal operational parameters associated with the performance measures.

The AnSBR technology was able to treat winery wastewater with overall COD reduction percentages of 68.32 % with the range of reduction percentages achieved being 41.5 – 85.4 %. Low COD reduction percentages correlate with increased volatile fatty acids (VFA):Alkalinity. A VFA:Alkalinity below 0.3 is optimal for the stability of an AnSBR (Fannin, 1987). An increased ratio may hinder performance of the AnSBR and increase acidification within the reactor. The COD reduction is within the range of reported COD reduction percentages. The reduction percentage achieved in this study is inferior to some studies which reported COD reduction percentages of more than 90 % (Ruiz *et al.*, 2002; Shao *et al.*, 2008). These studies were however conducted using smaller volume reactors and winery wastewater that was of consistent strength in terms of COD for each experimental run. Polyphenol reduction percentages ranged from 13.11 – 77.69 % with a mean reduction percentage of 53.35 %. While this is lower than mean values reported in literature (63 %), the reduction percentage is still acceptable, however polyphenol content of the wastewater should be monitored as polyphenols may slow down the digestion process and decrease reactor performance (Melamane *et al.*, 2007). Overall the reactor was stable as illustrated by a mean VFA:Alkalinity of 0.23. However there were times when the VFA:Alkalinity exceeded 0.4 and reached 0.593 at its maximum. When VFA:Alkalinity exceeds 0.4 the reactor can be said to be unstable and an immediate reduction of VFA should commence (Brown & Li, 2013). Methane percentage obtained in this study ranged between 54.89 and 72.18 with a mean methane percentage of 61.81 %. This is within the acceptable range of methane percentage of the biogas previously reported. The performance measures were deemed to be stable throughout the study with an occasional decrease in performance of the reactor. Overall the reactor could be said to be stable and it could efficiently treat winery wastewater of varying quality.

Operational parameters for the AnSBR were determined by conducting a CCD experiment in a 5-level design for the three parameters: pH; feed time and mixing interval. The experimental design called for 16 experimental runs conducted in a randomised order. The data obtained was used to generate response

surface methodology (RSM) contour plots to determine optimal conditions for each of the six responses: COD reduction (%); COD ultimate reduction; TSS; VFA:Alkalinity; polyphenol reduction (%) and methane (%). Optimal conditions were selected based on the solution generated which had the highest desirability values. The optimal pH was deemed to be 7.30. An optimal feed time of 180.91 minutes was obtained. The optimal mixing interval was found to be every 84.17 minutes (for 10 seconds at a time).

5.1 Concluding remarks

This study illustrated that a benchtop FT-NIR spectrophotometer (1 000 – 2 500 nm) can be used to predict COD and TSS in winery wastewater at a level that can be said to be accurate enough to be considered as a viable screening method. This is very important as it offers an alternative to the current time-consuming and laborious methods currently in use to determine these parameters. A rapid technique can allow a reactor operator to take more frequent samples to assess the performance and stability of the reactor. These models can allow wineries to monitor the quality of the effluent more frequently which could lead to implementation of more stringent wastewater practices. The portable NIR instrument with a wavelength range of 908 – 1 651 nm could classify wastewater accurately in terms of strength for both COD and TSS. Whilst the instrument struggled to quantify these parameters, there is significant potential for this technology to be used in-line to monitor reactor stability. Classification of these parameters as either low or high strength could allow an operator to make an informed decision about the stability of the reactor, and potentially prevent reactor failure. The low cost of the portable instrument and the ease of use may make this an attractive option for in-line monitoring of winery wastewater treatment facilities in the future. Before this technology can be implemented successfully, more research needs to be conducted to optimise the COD and TSS quantification by attempting to increase the wavelength range to between 1 700 nm and 2 200 nm as this is the region that is correlated with TSS and COD. This may prove to be too expensive to manufacture, in which case, a robust benchtop instrument could be placed on-site and an operator could take measurements more frequently. Furthermore, more samples should be obtained to increase the robustness of the calibration model, which could decrease the error of prediction for both the benchtop and portable spectrophotometers.

The use of a pilot-scale AnSBR to treat winery wastewater between a COD range of 3 200 – 9 700 mg.L⁻¹ was determined to be feasible as performance parameters remained mostly stable throughout the experiment. The performance of the reactor was inferior to previous studies, although most of those studies were conducted on lab-scale reactors with wastewater that did not vary significantly in terms of composition. To increase the performance of the reactor it is possible to increase the cycle time to facilitate further degradation of organic compounds. The occasional instability illustrated by elevated VFA:Alkalinity for some of the runs highlights the potential pitfalls of this technology, however this may be overcome by increasing the hydraulic retention time (HRT) and up-scaling to potentially increase buffering capacity of the water. The design of the reactor would need to be optimised with the addition of a closed vessel instead of a floating lid to maximise biogas capture and ensure an anaerobic environment within the reactor. Gas

recirculation could be used as an alternative to mechanical mixing as it may be gentler and cause less destruction of anaerobic granules.

The optimal parameters for the operational parameters were found to be: pH of 7.3 a feeding time of 180.91 minutes and a mixing interval of every 84.17 minutes for 10 seconds at a time. These optimal parameters were very similar to a previous study conducted at the Department of Food Science at Stellenbosch University which found optimal parameters to be: pH of 7.3, feed time of 240 minutes and mixing intervals of 110 minutes (Laing, 2016). This study showed that the operational parameters remained comparable irrespective of the size of the reactor and the treatment of wastewater of variable strength. Further research should focus on the optimisation of the design of a larger AnSBR before this technology can be used for the full-scale treatment of winery wastewater.

5.2 References

- Andreottola, G., Foladori, P. & Ziglio, G. (2009). Biological treatment of winery wastewater: an overview. *Water Science and Technology*, **60**, 1117-1125.
- APHA (2005). Standard methods for the examination of water and wastewater. *American Public Health Association (APHA): Washington, DC, USA*.
- Brown, D. & Li, Y. (2013). Solid state anaerobic co-digestion of yard waste and food waste for biogas production. *Bioresource technology*, **127**, 275-280.
- Cooley, H., Ajami, N., Ha, M.-L., Srinivasan, V., Morrison, J., Donnelly, K. & Christian-Smith, J. (2014). Global water governance in the twenty-first century. In: *The world's water*. Pp. 1-18. Springer.
- Corredor, C.C., Lozano, R., Bu, X., McCann, R., Dougherty, J., Stevens, T., Both, D. & Shah, P. (2015). Analytical method quality by design for an on-line near-infrared method to monitor blend potency and uniformity. *Journal of Pharmaceutical Innovation*, **10**, 47-55.
- Cozzolino, D., Liu, L., Cynkar, W., Damberg, R., Janik, L., Colby, C. & Gishen, M. (2007). Effect of temperature variation on the visible and near infrared spectra of wine and the consequences on the partial least square calibrations developed to measure chemical composition. *Analytica chimica acta*, **588**, 224-230.
- Eleutheria, N., Maria, I., Vasiliki, T., Alexandros, E., Alexandros, A. & Vasileios, D. (2016). Energy Recovery and Treatment of Winery Wastes by a Compact Anaerobic Digester. *Waste and Biomass Valorization*, **7**, 799-805.
- Fannin, K. (1987). Start-up, operation, stability, and control. *Start-up, operation, stability, and control.*, 171-196.
- FAO (2016). South Africa. [WWW document]. http://www.fao.org/nr/water/aquastat/countries_regions/Profile_segments/ZAF-WU_eng.stm. 27/07/2017

- Hemmateenejad, B., Akhond, M. & Samari, F. (2007). A comparative study between PCR and PLS in simultaneous spectrophotometric determination of diphenylamine, aniline, and phenol: effect of wavelength selection. *Spectrochimica Acta Part A: Molecular and Biomolecular Spectroscopy*, **67**, 958-965.
- Howell, C. & Myburgh, P. (2018). Management of winery wastewater by re-using it for crop irrigation-A review. *South African Journal of Enology and Viticulture*, **39**, 116-131.
- Innocent, M.R., Morita, K. & Miyazato, Y. (2007). Rapid Estimation of Chemical Oxygen Demand of some Organic Solutions by using NIR and Chemometrics. *Journal of the Japanese Society of Agricultural Technology Management*, **14**, 107-114.
- Jeong, H.-S., Lee, S.-H. & Shin, H.-S. (2007). Feasibility of on-line measurement of sewage components using the UV absorbance and the neural network. *Environmental monitoring and assessment*, **133**, 15-24.
- Laing, M. (2016). Investigating the performance of a novel Anaerobic Sequencing Batch Reactor (AnSBR) and optimisation of operational parameters to treat synthetic winery wastewater. Stellenbosch: Stellenbosch University.
- McNabb, D.E. (2019). The population growth barrier. In: *Global Pathways to Water Sustainability*. Pp. 67-81. Springer.
- Melamane, X., Tandlich, R. & Burgess, J. (2007). Treatment of wine distillery wastewater by high rate anaerobic digestion. *Water Science and Technology*, **56**, 9-16.
- Melendez-Pastor, I., Almendro-Candel, M.B., Navarro-Pedreño, J., Gómez, I., Lillo, M.G. & Hernández, E.I. (2013). Monitoring urban wastewaters' characteristics by visible and short wave near-infrared spectroscopy. *Water*, **5**, 2026-2036.
- Moharikar, A., Purohit, H.J. & Kumar, R. (2005). Microbial population dynamics at effluent treatment plants. *Journal of Environmental Monitoring*, **7**, 552-558.
- Mosse, K., Patti, A., Christen, E. & Cavagnaro, T. (2011). Winery wastewater quality and treatment options in Australia. *Australian Journal of Grape and Wine Research*, **17**, 111-122.
- Pan, T., Chen, W.W., Huang, W.J. & Qu, R.T. (Year). Model optimization for near-infrared spectroscopy analysis of chemical oxygen demand of wastewater. In: *Key Engineering Materials*. Pp. 832-837. Month and 2012a
- Páscoa, R.N., Lopes, J.A. & Lima, J.L. (2008). In situ near infrared monitoring of activated dairy sludge wastewater treatment processes. *Journal of Near Infrared Spectroscopy*, **16**, 409-419.
- Pedrero, F., Kalavrouziotis, I., Alarcón, J.J., Koukoulakis, P. & Asano, T. (2010). Use of treated municipal wastewater in irrigated agriculture—Review of some practices in Spain and Greece. *Agricultural Water Management*, **97**, 1233-1241.
- Rieger, L., Langergraber, G. & Siegrist, H. (2006). Uncertainties of spectral in situ measurements in wastewater using different calibration approaches. *Water Science and Technology*, **53**, 187-197.

- Ruiz, C., Torrijos, M., Sousbie, P., Martinez, J.L., Moletta, R. & Delgenes, J. (2002). Treatment of winery wastewater by an anaerobic sequencing batch reactor. *Water Science and Technology*, **45**, 219-224.
- Sarraguça, M.C., Paulo, A., Alves, M.M., Dias, A.M., Lopes, J.A. & Ferreira, E.C. (2009). Quantitative monitoring of an activated sludge reactor using on-line UV-visible and near-infrared spectroscopy. *Analytical and bioanalytical chemistry*, **395**, 1159-1166.
- Shao, X., Peng, D., Teng, Z. & Ju, X. (2008). Treatment of brewery wastewater using anaerobic sequencing batch reactor (ASBR). *Bioresource technology*, **99**, 3182-3186.
- Show, K. & Lee, D. (2016). Anaerobic Treatment Versus Aerobic Treatment. *Current Developments in Biotechnology and Bioengineering: Biological Treatment of Industrial Effluents*, 205.
- Sivakumar, B. (2011). Water crisis: from conflict to cooperation—an overview. *Hydrological Sciences Journal*, **56**, 531-552.
- Soukupova, J., Rock, B. & Albrechtova, J. (2002). Spectral characteristics of lignin and soluble phenolics in the near infrared—a comparative study. *International Journal of Remote Sensing*, **23**, 3039-3055.
- Wold, S., Martens, H. & Wold, H. (1983). The multivariate calibration problem in chemistry solved by the PLS method. In: *Matrix pencils*. Pp. 286-293. Springer.
- Yang, Q., Liu, Z. & Yang, J. (2009). Simultaneous determination of chemical oxygen demand (COD) and biological oxygen demand (BOD₅) in wastewater by near-infrared spectrometry. *Journal of Water Resource and Protection*, **4**, 286-289.